MicroRNA-mediated regulation of p53 in *Drosophila*: a new role in adaptation to nutrient deprivation

Regulación de p53 por microARNs en *Drosophila*: una nueva función en la adaptación a la escasez nutricional

Lara Barrio Guerrero

Programa de Doctorado del Departamento de Genética
Facultad de Biología
Universidad de Barcelona

MicroRNA-mediated regulation of p53 in *Drosophila*: a new role in adaptation to nutrient deprivation

Regulación de p53 por microARNs en *Drosophila*: una nueva función en la adaptación a la escasez nutricional

Memoria presentada por
Lara Barrio Guerrero
para optar al grado de Doctor por la Universidad de Barcelona

Development and growth control laboratory
ICREA and Institute for Research in Biomedicine (IRB)
Parc Científic de Barcelona

Barcelona, September 2014

Marco Milán	Lara Barrio	Florenci Serras
(Director)	(Alumna)	(Tutor)

Al meu pare

tot i que potser no s'enrecordi

AGRADECIMIENTOS

Bueno, bueno, bueno…muchos pensareis…*" ¡por fin!"* o *"ya era hora…"*, y es que parece que empecé la tesis allá en los tiempos de *Maricastaña*, y no veas lo que ha llovido des de aquel día en que, como no, perdí el tren y llegué tarde a mi entrevista con mi futuro jefe. Desde entonces, y hasta el día de hoy, me considero la estudiante de doctorado más afortunada del mundo, y eso se lo debo a todos y cada uno de mis Milanos.

Marco. Como dirían los de Seguridad Social…*"las palabras se quedan cortas para decir todo lo que siento"*, Jefe. Te quiero dar las gracias por acogerme en tu laboratorio todos estos años (que no son pocos jeje) y darme la oportunidad de realizar el máster y la tesis en tu lab, ¡gracias! Por transmitirme la pasión por la ciencia, ¡gracias! Por levantarme el ánimo y ver resultados positivos dónde yo solo veía negativos, negros y grises, ¡gracias! Por creer en mí y enseñarme a creer en mí, ¡gracias! Por tratarme tan y tan bien, ¡gracias! Dicen que a lo largo de tu carrera científica te encontrarás con un mal jefe, un jefe mediocre, un buen jefe y un jefe excelente…pues vaya…menuda rabia porque eso quiere decir que ahora me va a tocar, como máximo, un buen jefe. No solo eres un jefe maravilloso, sino una persona encantadora y magnífica. Sigue así, ¡siempre! Si estás leyendo esto y dudas en venir a trabajar al laboratorio de Marco Milán, no seas tonto, no dudes y llama al 93 40….!!! ¡¡¡Gracias jefe por estos 7 años!!!

Andresito. Boludo, querido…¡¡¡*Ay mammita* que hubiera sido de mí sin ti!!! No quiero ni pensarlo vamos. Parecía que nunca iba a llegar el día en que aterrizaras en este *lab*, pero llegó, ¡¡¡y cuanto me alegro!!! Has sido mi mini-jefe, mi referente, mi *colleague*, mi amigo, mi pilar. Menudo equipo hacíamos en el *lab* :) Lo he pasado en grande trabajando y conviviendo estos años contigo…*sos un crack*, si no fuera por ti…hoy no sabría hacer ni la mitad de cosas que sé hacer. También me enseñaste a ser feliz haciendo lo que hacemos, e intentaste enseñarme a ser buena *arquera* (esto último me temo…que se quedó en el intento jeje), me enseñaste a hacer asados, y yo espero haberte enseñado algo también a ti. No me cabe duda de que te va a ir genial en tu propio *lab*…tu consigue dinero, y seguimos en contacto ;)

Héctores. ¡¡¡Tronco!!! Que te voy a decir a ti, que me acogiste en tus brazos cuando el Cuqui se nos fue a hacer las Américas. Otro jefe más que he tenido. Contigo aprendí un huevo (y parte del otro) de moscas, a ser eficiente y veloz con los cruces, nada de vírgenes, machitos a lo *dirty*, y pim-pam. Pues no lo pasamos nada mal, no. Y gracias a ti, soy quien soy: *'Pelofino'*. Aún recuerdo tu fiesta de despedida… ¡menuda borrachera! Parecía que el mundo iba a acabar sin ti en el *lab*, pero pese habitar en S'pore y ahora Copenhagen, tu espíritu sigue vivo en el *lab* ¡¡¡Aupa Aleti!!!

Fer. Cuqui! Tú has sido mi primer jefe, el que me enseñó a manipular y trabajar con las mosquitas, interacciones génicas a raudales, cientos de alitas para montar, *Mrt* pa'arriba y *Mrt* pa'abajo. Gracias guapo por tener la paciencia de aceptarme como *master student*! ¡Nos vemos por los States!

Aninhas. Bestie…eres, sin duda, de las mejores personas que conozco, que he conocido y que conoceré jamás, *seriously…I love you* Anita!!! No tan solo creo que científicamente lo vas a petar mucho, sino que a nivel personal te has convertido en mi *bestie* dentro y fuera del lab…tantas horas juntas, era eso u odio a muerte jeje Contigo he compartido muchas cosas…viajes (Lisbon, Paris, Sevilla,…y te falta venir a Lanzarote!), *meetings* con sus respectivos estreses, clases durísimas de gym (aunque amenas…*you know* ;p), cenitas, birras&gins, sonrisas y lágrimas (gracias especiales por estas últimas), cientos de *stickers* por el line, *rides* en coches alquilados y *motorbikes* supersónicas (no conduzco tan rápido… ¬¬). Sabes que solo hay una cosa de ti que me molesta….¡¡¡que te guste CR!!! Arrrrgghhh! Que suerte tiene Marco de tenerte en el *lab*, y que placer el mío por haber podido crecer todos estos años a tu lado, *muito obrigada por tudo Aninhas*!!! Nos vemos pronto…en Barna, Lisbon, SFCO, NYC,… ¡dónde sea!

Carles. El encargado de informática del *lab* y el que más sabe de genética del *wing disc*!!! Tot i que ja saps que a vegades crec que ets una mica radical…m'encantes!!! M'agrada sobretot lo friki que ets!!! Em fas sentir com si no estigués sola jeje Estic super contenta del *"team growth"* que formeu tu i l'Anita ;) de veritat!!! Ànims amb la tesi (aguro cientos de *papers* Recasens *et al*.,) i amb la vida en general!!

Marta. ¡Quilla! Qué bien que te decidiste por nuestro *lab* para el postdoc! Y que suerte que me he alargado un par de años con la tesis (:p) y hemos podido coincidir!! Ha sido un enooorme placer Martita, de veritat!! Cuando quieras, y donde quiera que esté, sabes que tendrás lugar en mi casita/mini-piso!!! A petarlo y disfrutar de BCN!

Lídia. Buuuf, cuanto tiempo llevamos aquí, ¿no? Lo pasamos bien con el *hh-project* y nuestro Deivid :) *"Research asistance & mama del lab"* debería de poner en la web. No por la edad (tienes un espíritu jovial que me encanta), sino por todo lo que sabes y ayudas a la gente cuando lo necesita. Se me hace muy raro el pensar que cuando llegue a mi nuevo *lab* no té veré ahí, al fondo, en tu PC.

Juanchi. Será verdad que nos habremos ido del *lab* y el tequila seguirá intacto!?! Juanchi, mi compi de office, medio tímido pero siempre está ahí. Han sido geniales estos 3 añitos contigo, voy a echar de menos tus camisas jeje. Mucha suerte en tu futuro, seguro que te va bien, eres de las personas más trabajadoras que he visto nunca! Por cierto…¡nos debes una cena mejicana! Tendremos que ir a México…

Mariana. Marianiiita! Gracias por estar siempre ahí, y por todos los zapatos y joyas que me has dejado para mis ocasiones especiales :p *Tenés* una perra lindísima, y dicen que todos los perros se parecen a sus amos… ;) Que la siguas disfrutando mucho en el *lab*, en bcn, *everywere*!

Najate. Salvadora, te recordaré siempre por tus dátiles jeje Nooo, es broma, te recordaré por muchas otras cosas más. Me alegro muchísimo por ti, porque hayas venido a bcn, conocido el *amour*, trabajado en el *lab*, siempre dispuesta a ayudar en todo. *You are a great person* Najate!!! *I wish you the best!!!*

Ana T. No hemos coincidido mucho, pero te dejo mi legado más importante….el *business* de la papilla…¡¡paciencia!! Creo que eres una gran incorporación para el *lab* Ana, a nivel personal y científico, creo que transmites buen rollito, y eso siempre es bueno!

Lada. Ara que marxo del *lab*…ja no crearem més confusions jeje Realment, Lada i Lara sonen molt igual!! Be, has vist que el nostre lab és molt wai, així que t'esperen 4 anys estupendíssims, disfruta'ls!

Mercedes. Dicen que detrás de un gran hombre, hay una gran mujer… ¡Y tanto que sí! Gracias por cuidar nuestras mosquitas y por tu buen humor.

Duarte. Mosquita, a pesar de que eres un poco demasiado portugués…*gosto de ti*!!! Para mí, fuiste mi hermano mayor en el *lab*, siempre ayudándome, aconsejándome, animándome, haciéndome reír… Tantas cosas compartimos juntos! Cuando te fuiste, nos dejaste un pequeño vacío Marica. A ver cuando voy a Lisbon a conocer a Paquito, y cuando queráis, mi casa es tu casa Mosqui!

Laurita. *Mon amie!!!* Menuda crack estás hecha Boulan. En serio, te admiro, en muchos aspectos. Científicamente, ni hablar, pero la manera alegre, positiva y feliz que tienes de ver la vida…me encanta! *Go for it* Laurita, sé que te vas a comer el mundo, *no doubt*. Y ahora en catalán…como no me miras…jeje Quin gran plaer haver-te conegut i emportar-me a la butxaca una amiga com tú, gràcies per tot guapa!

Isa. Eeeeehhh, Isaaaa!!! Ya hace tiempo que te fuiste del lab, pero nunca habrá una francesa tan francesa como tú. Eres una super-girl, super-científica, super-mamá, super-futbolera! Siempre que escuche *"voyage, voyage"* pensaré en ti. Gracias por ser mi *roomie* en San Diego, siempre recordaremos la visita al Zoo, eh? **Neus.** La veritat es que sempre m'he vist una mica reflectida en tu Neus, i ara et veig, a NYC, feliç menjant-te el mon i això em dona forces per aventurar-me jo també! Gràcies per escoltar-me i ajudar-me sempre que ho he necessitat. Ens veiem pels States!!! **Georgi.** No sé si et veies diferent perquè feies embrió dintre de la màfia del wing disc, però jo et veia super bé. Igual que ara et veig, nenaaaa, tota una executiva agressiva!! Em fa molta il·lusió que hagis trobat el teu camí, i qui sap qui sap, potser algun dia ens acabaràs contractant jeje **Deivid**. ¡¡Siempre serás mi primer estudiante!! Lo pasamos genial contigo en el *lab*, que si partidos de fútbol, que si birritas….y menudas paellas…mmmm!

Y esto solo ha sido la gente del *lab*…me parece que esta sección de agradecimientos va para largo!

Gràcies també al **Florenci**, perquè a més a més de ser el meu tutor, és per 'culpa' teva que avui estigui on estic (desenvolupament embrionari em va captivar!). Y también quiero agradecer a la gente del IRB/PCB. Sé que en general los Milanos somos un poco…como decirlo…rancios/asociales jeje pero en estos años por el PCB me he cruzado con mucha gente, por los pasillos, por la *flyroom*, por el *confo*, en la máquina de café,… Querría darles las gracias a **todos** por soportarme en mayor o menor grado jeje y disculparme si no os enumero uno a uno. A todos y cada uno de vosotros…gracias mil!!!

Y es que, no solo puedo agradecer al sector laboral, porque una tesis es como una aventura, te implicas tanto que todos tus grupos sociales se ven afectados, y sin el apoyo y las distracciones que estos suponen, mi tesis no habría sido posible jamás de los *jamases*!

Empezaré por mi familia. Todo empezó en segundo o tercero de carrera, una nochebuena… bueno….mentira…desde siempre he querido estudiar biología, a quien quiero engañar :p Pero volviendo a esa nochebuena…pues bien, decidí hacerles una *"poster session"* en privado…creo que les solté como media hora de rollo sobre *Hox genes* y *limb development*…desde entonces que decidieron que no entendían muy bien lo que hacía pero que me iban a apoyar hasta la muerte. Y es que quizás ellos se siente orgullosos de mi (seré la primera doctora de la familia, yupi!), pero lo que hoy os quiero decir es que soy yo la que se siente orgullosa de vosotros, de verdad…tengo una familia geniaaaaaaaaal!!! Especial, peculiar, única, divertida, inigualable, entrañable, somos una piña, somos Warriors!!!

Gracias **Yaya mama**, porque sé que se te inflas como un pollo cuando hablas de mí, y aunque a veces no compartimos el mismo punto de vista de las cosas, y aunque te vaya a ver muy poquito, te quiero enormemente Yaya**. Rubén**, mi *brother*, gracias por poner sobre la mesa siempre las cosas claras, ese aporte de racionalidad y simplicidad que a veces a mi tanto me falta, gracias por estar ahí siempre. Y **Mey**, gracias por estar con Rubén, santa paciencia!!! Menuda suerte tiene…que 'cuñada' más genial que tengo :D **Olga**, **María**, **Pablito** y **Carmen**, aunque nos vemos de uvas a peras, sé que si necesito algo, lo que sea…solo tengo que ir a Selva de Mar. **José Luís**, **Natalia**, **Gabriel**, **Helga**, gracias por ser tan únicos, juntos y por separado, creo que sois la chispa de la familia. **Bea**, **Santi**, **Alex**, **Pauli** y **Pablico**, que mala sobrina/prima he sido que he dejado abandonados a los del pueblo…¡¡lo siento!! Pero sabéis que os quiero mucho,¡¿no!? **Pablo** (grande). Aún recuerdo el día de vuestra boda ¡que nerviosa que estaba por leer! Y que contenta me sentía al ver a mama feliz a tu lado. Todos tenemos nuestros más y nuestros menos, pero tú has sido para mí mucho más que "el marido de mi madre", o que un "papa putativo", has sido el Pablo y me has hecho sentirme como una hija para ti ¡gracias! Te quiero. **Mama**. Y que le voy a decir a mi mama pato que no le haya dicho ya. Al empezar la uni te fuiste a Lanzarote, y eso me hizo madurar y ser quien soy hoy en día, aunque en verdad…sigo siendo la misma patito mareado, con dudas, maripupas, despistada e inocente. Siempre me has apoyado, aconsejado, animado, ayudado a levantarme si me he caído,... Que sería de mi sin tus mails quilométricos jeje. Gracias mama por ser tan buena mama, no veas como presumo de madre ¡que lo sepas! Muaaa (besitos de mariposa). Te quiero. **Yaya Isabel**. No sabes si estoy estudiando, si trabajo o que…solo sabes que voy a la universidad jeje No sé si algún día conseguirás que me convierta en la mujercita que a ti te gustaría que fuese, pero sé que me quieres mucho de todas formas, y yo también te quiero con locura. **Samanta**. Cuqui, no sé si he sigut gaire bon referent de germana gran, però em fa molta il·lusió que hagis escollit Bio, em fa sentir orgullosa de tu. T'estimo molt i quan torni del *postdoc*, a veure si ens posem al dia. **Carlos** y **Veronica**, que bien que nos hayamos vuelto a encontrar. **Pare**. La vida es punyetera a vegades, i a tu t'ha fet ensopegar amb una pedra, que pot ser molt gran o molt petita, depèn del punt de vista. Jo la veig petita, i m'agradaria que tú la veiesis igual. T'estimo molt pare, moltíssim, vull que ho sàpigues i que ho recordis sempre, això no se't pot oblidar, d'acord? T'estimo.

Y ahora los amigos, fiesshhhta!!!

Començaré per les ***"nenes"***. Amb el temps sembla que costa més quedar, les nostres vides es van bifurcant, unes es van casant fins i tot, però el que trobo genial es que passi el temps que passi que no ens veiem, com a mínim per mi, sembla que no hagi passat el temps! En un moment ens posem al dia fotent-nos unes bones *rises*. Durant aquests anys hem sortit de *fiestuki*, em fet quedades varies, em fet viatgets,… i només us vull dir que sou genials, i que m'agradeu molt, cada una per unes coses, però crec que tenim un gran grupito!!! **Perla**, tota una vida compartida, i conviscuda fins i tot, gràcies per estar sempre al meu costat. **Lili**, gràcies a tenir parelles compartides jeje he tingut la sort d'haver-te conegut millor, i m'ha encantat!!! **Gemela**, pues eso…com diu la peli, "Tu a Vic i jo a SFCO" jeje t'estimo Desi (amb "s" sonora!! :p) **Miralles**, ups!…Laia :p crec que ets simplement genial, de veritat. *I love you*. **Paola**, gaudeix de la vida, somriure segur que ho fas estant amb l'Angel, me'n alegro molt per vosaltres! **Anna R.**, continua lluitant pels teus somnis guapa, muaa! **Gina**, *va Gina* fes-nos tietes aviat :p no hi ha tia més directa que tu, m'agrades! **Mire**, tot i estar un poco perdida gràcies per ser com ets.

Al·lots. Com és que un dia va dir la Lili…?..."amics imposats?" Potser sou amics imposats, o de 'rebote', però si tots els 'rebotes' són així…jo firmo!!! **Mireia**, **Rubén**, **Júlia** i el que vingui **(!)**. Quina família més ferma i més maca, no falleu mai, sempre hi sou, sou genials! **Puig**, **Carme** i **Arnau**. Família de catàleg que dic jo, irradieu felicitat, felicitats pel nou vingut! **Romerito** i **Tati** (i Lizzi!) Família divertida, riallera i viva! **Urbaneja**, **Montse** i **Laia**, tot i que ens surt 'carillo' venir-vos a veure, ens encanta! **Biel**, el meu ganxo en totes les sorpreses! el que no sap en Berni es que en veritat tu i jo…jeje Merci guapo, no canviïs! **Oleguer**. O hauria de dir Colador? Quants riures hem fet junts! Ets tant important per en Berni que et considero un cunyat, i amic! (això darrer ho has aconseguit per mèrits propis). També vull agrair als Al·lots de pura raça, als ***Menorquins***!!! Moltes gràcies per totes les festes, pomades i cap d'anys *xal·lats* al vostre costat!!!

Biofrikis. Des de sempre que jo tenia clarissim que volia fer bio i no m'arrepenteixo de res, perquè no només he aconseguit fer el que volia i m'agrada, sinó que us he conegut a vosaltres!!! Tinc taaaants tants bons records de la meva època universitària que si començo….no acabo: biofestes, apalanques, zulos, biblios, pràctiques, escapades, estudis intensius,… *Briefly*...**Cris**, sé que si vull un té, consell, somriures, una espatlla,.. puc venir a casa teva, t'estimo pet!!! **Mima**, la uni, el CAP, les mosques,...mitja vida juntes, gràcies per tot, ets genial!!! **Taxu**, al teu costat em sento bé, ets indescriptible, m'encantes!!! **Bene**, un tros de pà, un gran amic, tot i que et vegi poc el pèl!!! **Lluis**, ets pura vida, i la persona més friki que he conegut mai, 愛しています!!! **Joanet**, el tio més enfeinat que mai he conegut, humil i bona persona, magnífic!!! **Laia**, una altra que no para quieta (!), bellíssima personeta i lluitadora nata. I ara, els *pipios*, que al final, també s'han guanyat la condició de biofrikis. **Pipio**, l'original (com els Werther's, que no Werchter, que també!), més tarat que ningú, més peculiar que ningú, (fiber)gran adquisició!!! **Herms**, més llest que tots els porters del Sala junts!! i si li dones la oportunitat...descobriràs una persona meravellosa també!!! **Berta**, una ànima lliure, viva, alegre, brillant com un estel amb llum i màgia pròpia!!!

Bernat. Segurament ets a la persona a qui més hauria d'agrair i podria dir-te tantes coses…que no ho faré jeje Simplement et diré que gràcies (sobretot pels darrers mesos de convivència d'aquesta tesis) i que tinc moltes ganes de San Francisco!!!

TABLE OF CONTENTS

ABSTRACT

The integration of nutrient status to metabolic homeostasis at the cellular and organismal level is a complex process performed in multicellular organisms, and the ability of an organism to respond to nutritional stress is critical for its survival. In the last few years, the tumour suppressor protein p53 has emerged as an important regulator of several metabolic pathways such as glycolysis, oxidative phosphorylation and autophagy, that triggers a cellular adaptive response to nutrient deprivation, a function that may contribute not only to tumour suppression activities of this molecule but also to its non-cancer-associated functions.

A better understanding of the molecular mechanisms underlying nutritional stress-mediated p53 activation and the potential role of p53 in organismal homeostasis is important to improve our current knowledge about p53 biology and its role in disease. In this regard, *Drosophila* is a very attractive model system whereby the physiology and the molecular mechanism that control metabolic homeostasis display significant parallels with humans. The fat body (FB), a functional analogue of vertebrate liver and adipose tissue, functions as a key sensor that couples nutrient status and energy expenditure, and the Drosophila homologue of mammalian p53 (Dp53) shares significant amino acid identity with p53 and regulates, as its mammalian counterparts, similar cellular processes upon several stress.

The results presented in this thesis reveal a fundamental role of Dp53 in the organismal adaptation to nutrient deprivation. The depletion of Dp53 activity levels specifically in FB cells accelerates the consumption of the main energy stores, reduces the levels of sugars in the animal, and compromises organismal survival upon fasting. We present evidence that the levels of fasting hormones and metabolic enzymes that mobilize these energy resources are similarly modulated by starvation in control and dp53 mutant animals and unveil a cell autonomous role of Dp53 in modulating the metabolic changes of FB cells to nutrient deprivation. We also identified the molecular mechanism by which Dp53 is activated by nutrient conditions in FB cells. We show that microRNAs (miRNAs), an abundant class of endogenous non-coding RNAs measuring 22-23 nucleotides in lenght, regulate dp53 expression by targeting its 3' UTR, and we identify miR-305 as a major regulatory element. Interestingly, two elements involved in the biogenesis of miRNAs, Drosha and Dicer, and one catalytic component of the RISC complex, Argonaute-1, are downregulated during starvation, thus alleviating miR-305-dependent targeting of the dp53-3'UTR

and contributing to organismal resistance to starvation. These results open up new avenues towards the molecular understanding of p53 activation under metabolic stress and reveal the participation of p53 in nutrient sensing and metabolic adaptation at the organismal level.

iNTRoDuCTioN

INTRODUCTION

1. *Drosophila* as a model organism

In many areas of research, less evolved organism have been shown to be useful model systems that can facilitate our general understanding of human biology. There are several different model organisms that are used in research ranging from vertebrates, such as Zebrafish (*Danio rerio*) or mouse (*Mus musculus*) to invertebrates, like the fruit fly (*Drosophila melanogaster*) or the roundworm (*Caenorhabditis elegans*), and unicellular organisms as well, such as bacteria and yeast. All of them possess their own benefits such as size, generation time, accessibility and genetics manipulation and depending on the kind of study to be performed, they are differently selected by researchers. In this work we used the fruit fly *Drosophila melanogaster* as a model.

Drosophila has been classically used for the study of cell and developmental biology, but during the last decades the fly has emerged as a powerful system to study other aspects of biology such as physiology and metabolism, stress response and cancer. Due to its long tradition and well-established knowledge [in 2000 its genome was completely sequence *(Adams, 2000)*], *Drosophila* became a very powerful model system with sophisticated genetic and molecular tools. These tools allowed to quickly generate loss-of-function mutant animals to query gene function, and epistasis experiments to query gene relationships. Techniques based on the alteration of gene expression in a particular tissue or group of cells, like the UAS/Gal4 system *(Brand and Perrimon, 1993)* or the generation of genetic mosaics, allowed the study of essential genes and in many cases to bypass lethality. Tissue specific genetic screens based on these techniques allowed the identification and characterization of new genetic loci and signalling networks. Even more interesting is the fact that the highly active '*Drosophila* community' has produced a free network to exchange information and reagents. Remarkably, *Drosophila* is a simple organism with only four pairs of chromosomes, three autosomes and the sex chromosomes, thus facilitating genetic studies. Moreover, about 75% of known human disease genes have a recognizable match in the genetic code of fruit flies *(Reiter and Bier, 2002)* and 50% of fly protein sequences have mammalian homologues. Thus, *Drosophila* has been proved as a very suitable model system.

The high fecundity rates and the short life generation time, about 10 days at 25 °C in laboratory conditions, represent another important aspect that makes the fruit fly such a good model system. The life cycle of *Drosophila* is divided into four stages (Figure 1). During the embryonic stage body axes are first established, followed by cellularization, segmentation and complex morphogenetic events leading to hatching to the larval stage. Animals go through three larval instars before metamorphosis.

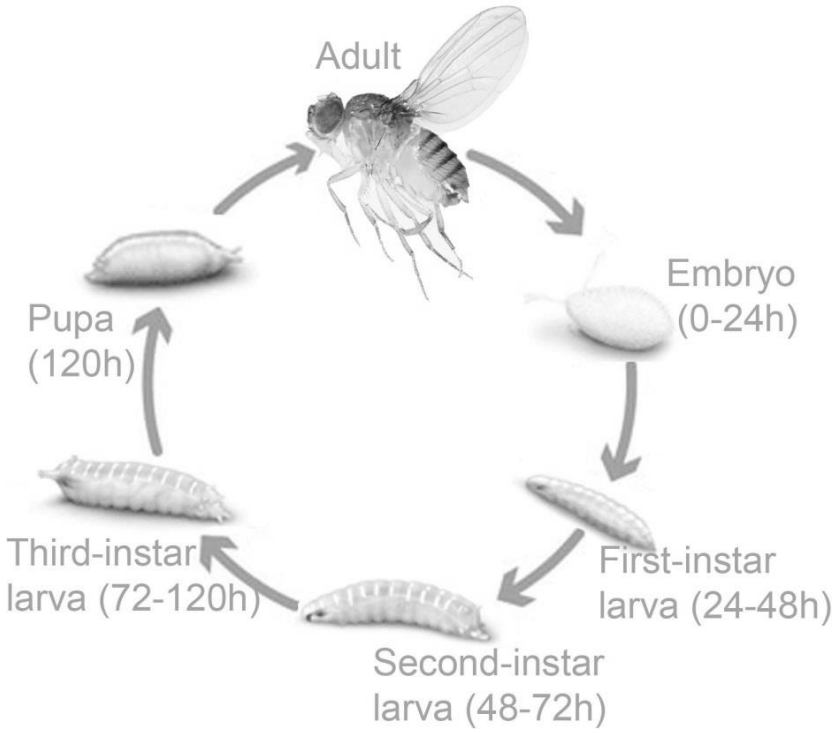

Figure 1: The life cycle of *Drosophila melanogaster*

The speed of *Drosophila melanogaster* development varies with temperature. At 25°C, it produces new adults in 10 days. The females laid the egg and embryos develop during the first 24 hours until the larva hatches. The fruit fly has three larval instars: first-instar larva (L1) which is proceed from the embryo stage and it longs about 24h; afterwards the second-instar larva (L2) hatches and will take also 24h; finally the third-instar larva (L3) stage will close the larval stage and finish with the encapsulation in the puparium. The puparium is where metamorphosis takes place, after which the adults eclose.

The larval instars are separated by an ecdysis, or molting of the cuticle, that allows animals to continuously grow. Two types of tissues are present in the larva: the endoreplicative and the proliferative tissues. Many larval tissues, such as the adipose tissue (known as the fat body), grow thanks to successive rounds of genome duplication leading to an increase in cell size without cell division. The impressive increase in body mass observed during the larval stages is mainly due to the growth of these

endoreplicative tissues. On the contrary, imaginal tissues, specified during embryogenesis, are proliferative tissues that will form the adult epidermal structures of the body (Figure 2). At the end of the third larval instar, larvae enter into pupariation. This transition marks the beginning of metamorphosis, a phase of intensive tissue remodeling and changes in the body structure ending in the hatching of an adult. During the pupal stage, larval tissues are histolyzed while imaginal tissues metamorphose to form the adult structures, and the rigid exoskeleton constrains any future increased in the body's dimensions. As a consequence, body growth is restricted to the feeding period of larval development, and the transition from larva to pupa fixes the future adult size.

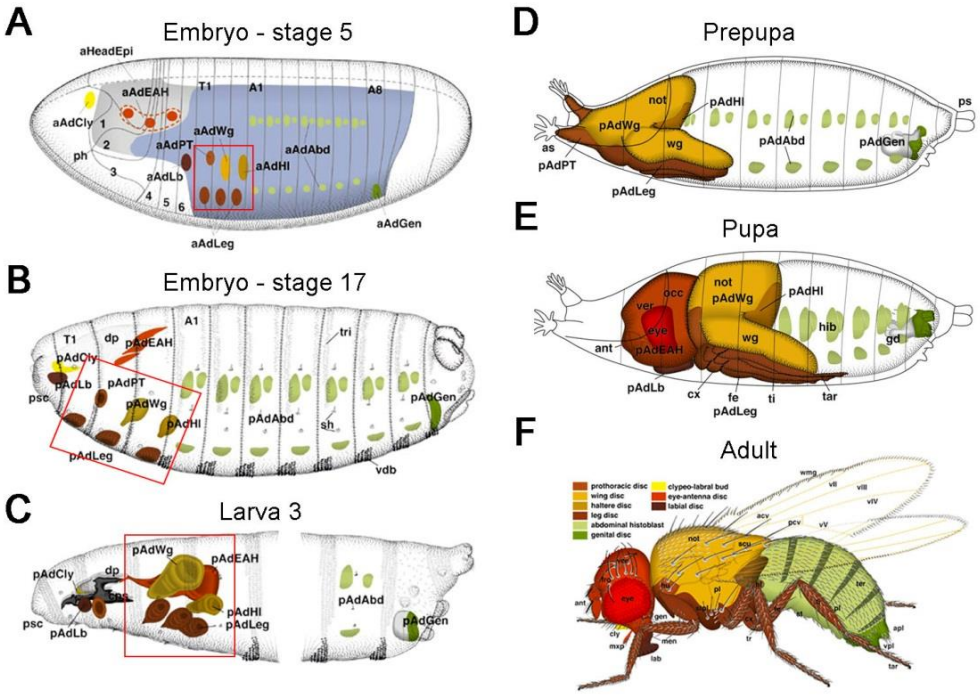

Figure 2. *Drosophila melanogaster* imaginal discs origin and their respective adult organs

The imaginal discs orginate early in development as clusters of 5 to 50 undifferentiated groups of cells in the embryonic ectoderm **(A)**. These cells start to develop inside of the embryo and are segregated from their neighbors by invagination from the ectoderm **(B)**. During larval development these groups of cells start to proliferate to give rise to a sac-like structure **(C)**. After the fly has passed through the larval stages it undergoes metamorphosis. During this process the imaginal disc extends along its proximal-distal axis by turning inside out through the lumen in a process called eversion **(D, E)**. Each imaginal disc gives rise to a specific adult structure, such as legs or wings, the body wall, eyes and head cuticle, halters, antennae or genitalia, and each of them depends on its own genetic cues **(F)**. Adapted from the Atlas of Drosophila Development by Volker Hartenstein.

In this thesis, we have mainly used the wing imaginal disc and the fat body as model tissues to study the involvement of the *Drosophila* p53 (Dp53) protein in the response to several stresses.

In order to address key important features related with Dp53 regulation and the role of Dp53 in the DNA damage response pathway, we have used the wing disc primordium. The wing imaginal disc is a sac-like structure formed by a continuous epithelial monolayer composed of two opposing layers which surround the disc lumen. One side of the imaginal disc is called the columnar epithelium (ce), a pseudostratified epithelium. The other part of the disc, the peripodial membrane (pm), is a squamous epithelium formed by flat cells (Figure 3B, C). At the end of the larval period, the wing disc is subdivided into different territories by the restricted expression of selector genes, which confer specific cell identity. These selector genes encode transcription factors and are thought to regulate genes required for cell-type-specific differentiation as well as genes that control cell interactions between territories *(Garcia-Bellido, 1975).* During embryogenesis, the wing primordium is subdivided into anterior (A) and posterior (P) regions by the activity of the Engrailed transcription factor in P cells. Early in larval development, the wing disc is subdivided again into dorsal (D) and ventral (V) territories by the localized expression of the selector gene *apterous* in D cells. Finally, the tissue is subdivided into proximal (notum) and distal (wing) regions *(Garcia-Bellido et al., 1973)*. The AP and the DV subdivisions constitute developmental compartments, groups of cells that do not mix with adjacent cells of other compartments most probably as a consequence of the compartment specific expression of adhesion molecules. At the border between two adjacent compartments, compartment boundary, specific signaling pathways, such as Hedhehog, Notch, Wingless and Decapentaplegic, are activated and play fundamental roles in wing growth and patterning *(Garcia-Bellido and Merriam, 1971; Lawrence and Struhl, 1996; Vincent, 1998)*.

In order to address the role of Dp53 in the response to nutrient stress, we have also used the *Drosophila* fat body (FB), a functional analogue of vertebrate adipose and hepatic tissues. This metabolic organ plays an essential role in energy storage and utilization. It is the central storage depot for excess nutrients. In conditions of nutrient deprivation, the FB supplies energy to the rest of the body by mobilizing stored glycogen and triacylglycerides to circulation. It functions as a key sensor that couples nutrient status and energy expenditure, thus playing a pivotal role in the metabolic homeostasis of the organism *(Arrese and Soulages, 2010)*.

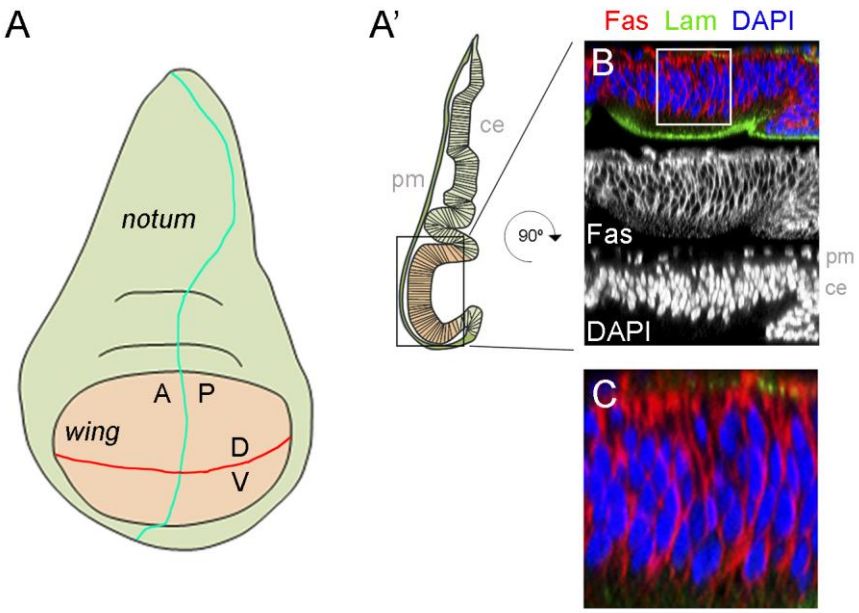

Figure 3: The wing imaginal disc: specification of territories and cellular organization

A) Cartoon depicting the wing imaginal disc. The horizontal red line corresponds to the dorsal-ventral boundary (D/V), and the perpendicular blue line to the anterior-posterior boundary (A/P). The notum region is colored in green and wing pouch in red. **(A')** Cartoon depicting a cross-section of the wing imaginal disc. The wing primordium is a cellular monolayer that forms a two-sided epithelial sac. One side of the sac forms a thin squamous sheet, the peripodial membrane (pm), whereas the apposed epithelial surface, the columnar epithelium (ce) adopts a pseudostratified columnar morphology. The apical side of both epithelia is oriented towards the lumen of the sac, while the basal side is the external surface. **(B,C)** Cross-sections of the wing primordial stained for DAPI (blue or white, labels the nuclei), Fasciclin III (red or white, labels the plasma membrane) and Laminin-γ (green, labels the basement membrane). **(C)** High magnification of the box insert in **B** to shown the nuclei organization at different levels of the pseudostratified columnar epithelium

2. p53: The Lord Of The Cell

Since its discovery in 1976, the transcription factor p53 has been well established as a key tumour suppressor protein. More than 50% of all human cancer show inactivation of p53, which can occur either by direct mutation or deletion of the *p53* gene, or by disrupting any of the pathways that regulate the p53 protein. p53 is activated in response to a myriad of stress signals, ranging from DNA damage, hypoxia, oncogene activation, etc. Depending on the context, cell and tissue type and the extent of the stress, p53 triggers adequate cellular responses including cell-cycle arrest and induction of apoptosis, thus preventing the multiplication of damaged cells and acting as "the guardian of the genome". The *Drosophila* ortholog of mammalian p53 (dp53) was discovered in 2000. Since then, Dp53 has been shown to be a useful model for studying general aspects of p53. In this chapter of the introduction, I will focus on the current knowledge about p53 biology, like the gene and protein structure, its regulation and its more relevant biological functions, and I will highlight the similarities and the differences between mammalian and *Drosophila* p53.

Gene and protein structure

Mammalian genomes contain three members of the *p53* family (*p53, p63* and *p73*) whereas in invertebrates like *Drosophila* only one member has being identified. Thus, the diversification of the *p53* gene family into three members occurred in vertebrates as a consequence of the triplication of one ancestral gene *(Belyi et al., 2010)*. The *Drosophila dp53* gene resembles more the vertebrate *p53* than the *p63* or *p73* paralogs.

The *p53* family of genes shares a complex structure with alternative splicing sites, alternative promoters and different translational initiation sites that result in multiple mRNA variants for each gene. As a result, several protein isoforms can be transcribed, but the full length protein is structured in three main functional domains: an acidic amino-terminal (N-terminal) transactivation (TA) domain; a core DNA-binding domain and a carboxy-terminal (C-terminal) oligomerization (Oligo) domain (Figure 4C). The human *p53* gene is composed of 11 exons that contain two promoters upstream of exon 1 (P1 and P1') and an alternative internal promoter (P2) in intron 4 that leads to the expression of amino-terminally truncated p53 proteins (Δ133p53). Moreover, the intron 9 can be alternatively spliced to produce three

isoforms p53, p53β and p53γ and intron 2 can also be alternatively spliced to generate a Δ40p53 isoform lacking the first 40 amino acids [Figure 4A and C *(Khoury and Bourdon, 2010; Murray-Zmijewski et al., 2006)*].

In *Drosophila*, the *dp53* gene and protein structure is significantly conserved compared to its mammalian homologue because it also contains an internal alternative promoter and encodes for three possible protein isoforms. Anecdotally, the first chronologically discovered variant correspond to an amino-terminally truncated (in this thesis Dp53, but also known as DΔNp53) isoform of 385 aa produced by the internal promoter located upstream of exon 3 (formerly designated as exon 1). It was thought to be the only *Drosophila* p53 isoform for many *years (Brodsky et al., 2000; Jin et al., 2000; Ollmann et al., 2000)*. The full-length variant encodes for a 495 aa protein (Dp53L or Dp53) with a large amino-terminal domain containing the conserved TA domain. A third carboxy-terminally truncated protein can be also produced from a splice variant of the Dp53L encoding only the first 123 aa (Dp53n or Dp53ΔC), although this last isoform has not been experimentally confirmed yet [Figure 4B and D *(Dichtel-Danjoy et al., 2013; Khoury and Bourdon, 2010; Marcel et al., 2011)*].

Thus, the human and *Drosophila* p53 proteins share a significant protein structure with three main functional domains and despite low sequence conservation, the overall structural and functional features of both proteins are conserved *(Herzog et al., 2012)*. Interestingly, the N-terminal TA domain is highly divergent among the p53/p63/p73 family members, except for conserved residues critical for MDM2 binding, and Dp53. The central DNA-binding domain is the region that shows maximum conservation between *Drosophila* and human p53. Indeed, Dp53 can bind to DNA containing p53 consensus binding sequences and activate known p53 target genes *(Jin et al., 2000; Ollmann et al., 2000)*. And finally, important conserved residues in the Ct oligomerization domain of both human and *Drosophila* p53 allow the formation of a dimer of dimers, a feature that is essential for the protein to bind to the DNA.

In this thesis, we used several transgenic flies to deplete or reduce Dp53 levels or activity. We used two different classical recessive null alleles of *dp53: dp53^{ns},* consisting of a deletion that covers the formerly exon 1 and the beginning of exon 2 (current exons 3 and 4, respectively) produced by ends-in gene targeting *(Sogame et al., 2003);* and *dp53^{5A14},* consisting of a 3.3 kb deletion of almost the whole gene produced by recombination *(Rong et al., 2002)*. We also used alleles carried on transgenic constructs: Dp53$^{H159.N}$ works as a dominant negative version and is produced by a point mutation (amino

acid replacement) in the DNA binding domain *(Ollmann et al., 2000)*, and dp53^{RNAi}, a dsRNA form against *dp53*.

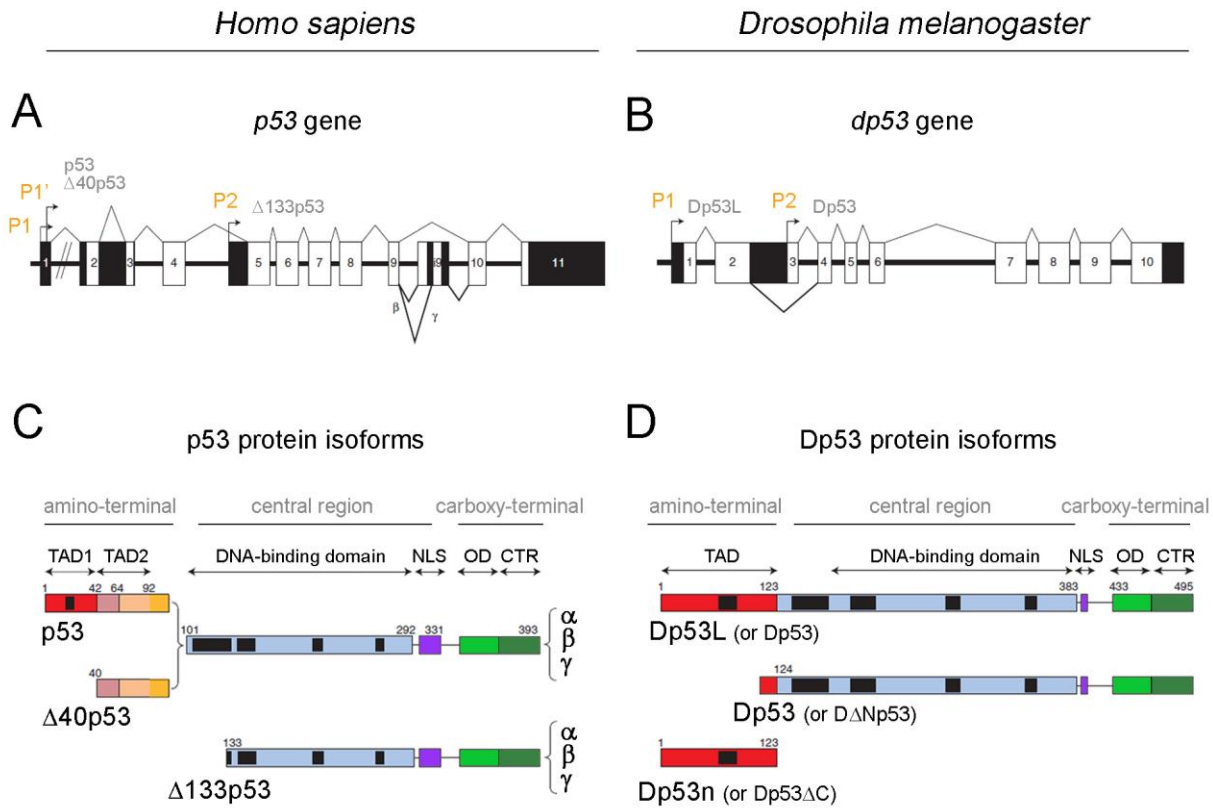

Figure 4: Gene and protein structures of the human and *Drosophila* p53

(A-B) Scheme of the *p53* gene of *Homo sapiens* **(A)** and *Drosophila melanogaster* **(B)** were exons are numbered and represented by boxes (black boxes correspond to non-coding exons) and promoters (P1, P1' and P2) are indicated with arrows. **(C-D)** Scheme of the p53 isoforms proteins in *Homo sapiens* **(C)** and *Drosophila melanogaster* **(D)** were the amino acid positions defining p53 domains are indicated. Mainly functional domains: transactivation domain (TAD, in red), DNA-binding domain (in blue), nuclear localization signal (NLS, in purple), oligomerization domain (OD, in light green) and C-terminal regulatory domain (CTR, in dark green). Internal black boxes represent regions conserved through evolution. **(D)** The full-length Dp53L/Dp53 isofrom includes a full TAD domain corresponding to the human full-length p53 isoform; the Dp53/DΔNp53 isoform is encoded by a mRNA transcibed from an internal promoter in exon 3 (P2 in B) and contains a truncated TAD thus reensembling the humans Δ133p53 and Δ40p53 isoforms; and Dp53n/Dp53ΔC lacks all the DNA-bindind domain and the oligomerization domain. Adapted from *(Khoury and Bourdon, 2010).*

Regulation

Many different stress signals converge on p53 to induce a number of distinct cell biological responses. p53, through its cell-cycle arrest and apoptotic activities, can have a strong inhibitory effect on cell growth and viability, making it essential to hold p53 function in check during normal development. To ensure a robust and precise response to different stress stimuli, p53 has to be tightly regulated, from the transcriptional to the post-transcriptional level, but mainly at the post-transcriptional level. In mammals, multiple mechanisms exist to control p53 **protein activity**, **stability** and **subcellular localization** through the action of numerous other proteins that work directly or indirectly to restrain p53 under normal conditions. These p53-regulatory proteins include enzymes involved in post-translational modification of p53 that can influence all three mechanisms of regulation, or transcriptional co-factors that can mainly modulate the transcriptional activity of p53 *(Kruse and Gu, 2009)*. Distinct signals use different pathways to activate p53 and many of these pathways are not mutually exclusive, making the system very complex. Human p53 protein harbors many conserved sites that can be regulated by a complex network of covalent post-transcriptional modifications, including phosphorylation, ubiquitination, acetylation, methylation, sumoylation and neddylation, most of them concentrated in the C-terminal regulatory domain, important for both activation or repression of p53 [Figure 5, *(Dai and Gu, 2010; Horn and Vousden, 2007)*]. There is an intricate interplay between various post-translational modifications of p53 that can compete between them for the same residues.

Important in the scenario of p53 regulation is the role of ubiquitin ligases, which promote the **ubiquitination** and subsequent degradation of p53 by the proteasome, thus controlling p53 protein stability. Ubiquitination requires the consecutive function of three enzymes: E1 ubiquitin-activating enzyme, E2 ubiquitin-conjugating enzyme and E3/E4 ubiquitin-ligating enzyme. Although a large number of E3 and E4 ubiquitin ligases have been shown to contribute to p53 regulation, an overwhelming amount of molecular and genetic evidences support the major role of Mouse double minute 2 (Mdm2) as a key negative regulator of p53. Whereas poliubiquitination promotes p53 degradation, monoubiquitiniation of p53 by Mdm2 controls the subcellular localization by promoting nuclear export. Moreover, apart from its E3 ligase activity, binding of Mdm2 into p53 target promoters can directly block the transcriptional activity of p53 *(Hock and Vousden, 2014; Shi and Gu, 2012)*. Besides the importance of this enzyme, recent studies confirmed the old hypothesis that *Drosophila* lacks an Mdm2 homolog *(Lane and Verma, 2012)*. The only identified so far E3 ubiquitin ligase acting on Dp53 is Synoviolin, an endoplasmic reticulum-associated degradation (ERAD) E3 ubiquitin ligase able to reduce Dp53 protein

levels and Dp53-dependent apoptosis in overexpression experiments using the *Drosophila* wing primordium *(Yamasaki et al., 2007)*. *Drosophila* Rad6 (*dRad6*), an E2 ubiquitin-conjugating enzyme, interacts with the N-terminal TA domain of Dp53 and regulates Dp53 turnover *in vitro*, and loss of dRad6 in S2 cells treated with DNA damaging agents enhances the Dp53-dependent apoptosis *(Chen et al., 2011)*. Mutations of the Tripartite-motif protein 24 (Trim24) homolog in *Drosophila*, *bonus*, leads to apoptosis, which can be partially rescued by Dp53-depletion, thus suggesting that in *Drosophila* tissues the member of the Polycomb group of genes, *bonus,* could function as Trim24 in mammals by targeting endogenous p53 for degradation *(Allton et al., 2009)*. In addition to ubiquitination, other ubiquitin-like modifications of p53 have been found to modulate p53 localization or transcriptional activity, such as **sumoylation**. Interestingly, Dp53 can be sumoylated on two different residues (lysine 26 and lysine 302 within the N-terminal and C-terminal region respectively) and sumoylation-defective Dp53 mutants show reduced transcriptional activity and are less efficient in inducing apoptosis both in cell culture and *in vivo (Mauri et al., 2008; Stehmeier and Muller, 2009)*. Thus, despite differences in the sumoylation sites, in *Drosophila,* as in mammals, sumoylation promotes Dp53 function. However, the gene responsible for the sumoylation of Dp53 remains to be elucidated.

Phosphorylation of serine(S)/threonine (T) sites all along p53 but specifically in the N-terminal region of the protein also mediatesp53 regulation. In response to DNA damage, a cascade of protein kinases involving Ataxia telangiectasia mutated (ATM), Ataxia telangiectasia related (ATR), Checkpoint kinase 1 (Chk1) and Checkpoint kinase 2(Chk2) phosphorylate specific residues in the N-terminal region of p53. These modifications block the interaction with Mdm2 leading to increased stability of the protein, and they also contribute to the transcriptional activation of p53 *(Dai and Gu, 2010)*. As in mammals, activation of Dp53 following DNA damage depends on the downstream kinase Mnk/Chk2, which phosphorylates Dp53 on serine 4 without changing the protein levels at all but inducing its transactivation activity *in vivo (Brodsky et al., 2004; Peters et al., 2002)*. Whether Mnk/Chk2 phosphorylates Dp53 directly or through an intermediate kinase is not known. Interestingly, unlike mammalian p53, grapes/Chk1 does not appear to regulate Dp53 in flies *(Jaklevic et al., 2006)*.

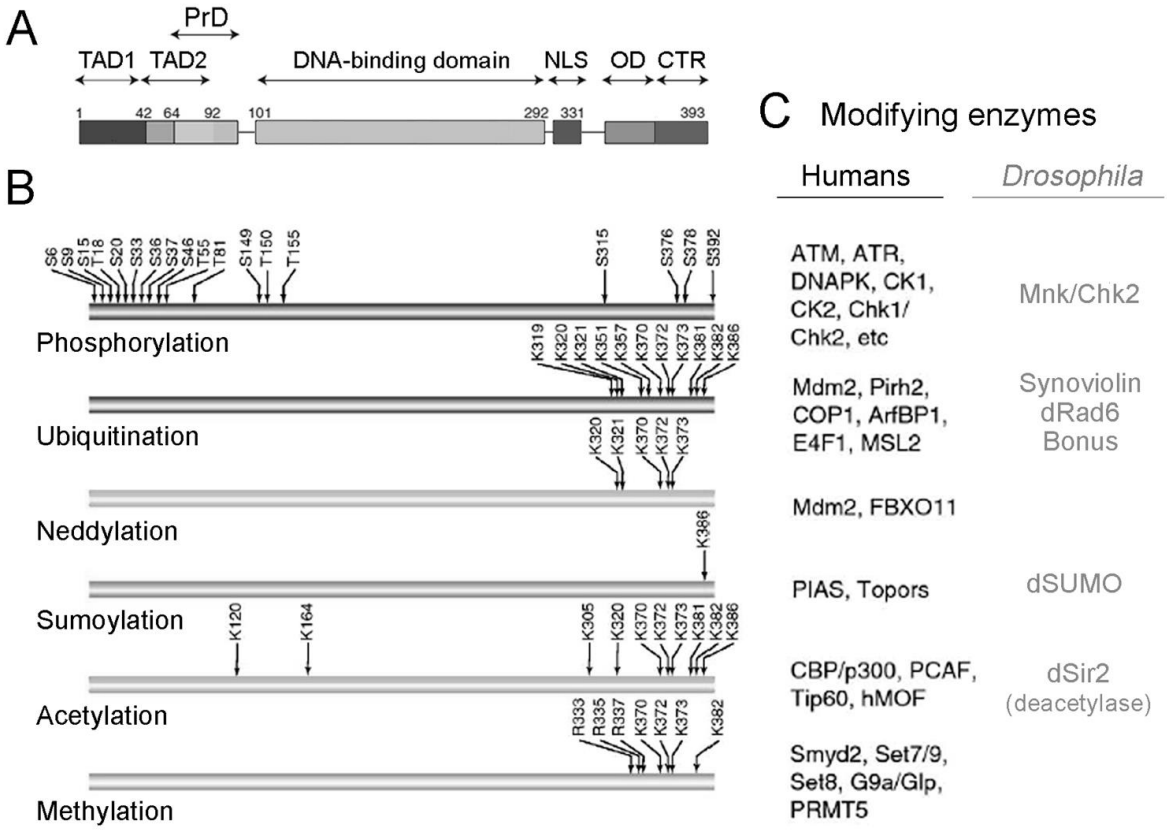

Figure 5: Overview of p53 post-translational modifications

(A) General scheme of the p53 protein with the main functional domains indicated. **(B)** The major sites for p53 phosphorylation, ubiquitination, neddylation, sumoylation, acetylation and methylation are plotted along the protein. **(C)** Enzymes responsible for each type of modification in humans (on the left), and the experimentally validated enzymes for *Drosophila* (in grey, on the right). Abreviations: TAD, transactivation domain; PRD, proline rich domain; NSL, nuclear localization signal (NLS), OD, oligomerization domain; CTR, C-terminal regulatory domain (CTR). Adapted from *(Dai and Gu, 2010)*.

Another important post-translation modification involved in p53 activation is **acetylation**. Nine acetylation sites (concentrated in the C-terminal region) and several histone acetyl transferases have been identified for p53 and are able to: promote p53 stabilization by excluding ubiquitination on the same sites, inhibit the interaction with Mdm2 or recruit cofactors essential for p53 transcriptional activity. Equilibrium in the acetylation rate of p53 is maintained by several deacetylases, such as Sirtuins (Sirt). Deaceytilation of p53 by Sirt2 has a profound negative impact on the transcriptional activity of p53. Although the regulation of Dp53 by acetylases has not been entirely elucidated, *Drosophila* Sirt2 (dSir2) physically interacts with overexpressed Dp53 and can deacetylate Dp53-derived peptides.

Moreover, these two molecules genetically interact to mediate some aspects of the life span extending effects of caloric restriction, suggesting that Dp53 is a downstream target of dSir2 *(Bauer et al., 2009)*.

As mammalian p53, Dp53 activity could be also controlled by direct binding of regulatory proteins such as Daxx-like protein (DLP), the homolog of Daxx, a known regulator of p53 transcriptional activity *(Gostissa et al., 2004)*. DLP binds to the C-terminal region of Dp53 and genetically interacts to repress some Dp53-mediated responses *(Bodai et al., 2007)*.

Interestingly, in the last few years, an additional mechanism for the regulation of p53 has been identified. MicroRNAs (miRNAs) are an abundant class of endogenous non-coding RNAs measuring 22-23 nucleotides in length that have emerged as key post-transcriptional regulators of gene expression (see chapter 4 of the introduction for more information). The first miRNA shown to be involved in the regulation of p53 was the miRNA *miR-125b.* In 2009, Le *et al.* showed that *miR-125b* was able to directly regulate p53 through its 3' UTR, thus repressing p53 protein levels and activity *(Le et al., 2009)*. Since then, vertebrate p53 has been shown to be under the control of the miRNA machinery through direct repression of p53 or its regulators *(Fan et al., 2014; Feng et al., 2011; Hu et al., 2010; Kumar et al., 2010; Takwi and Li, 2009)*.

Function

In mammals, although the two *p53*-related genes, *p63* and *p73* are able to transactivate p53-responsive genes (due to the high sequence similarity of its DNA binding domains) causing cell cycle arrest and apoptosis, each protein has its own unique functions that significantly differ from the tumour suppressor role of p53. Classically, p53 has been always involved in stress responses whereas p63 and p73 have been shown to play an important role during development. For instance, genetic experiments in mice have shown that p63 is essential for epidermal morphogenesis and limb development, and p73 plays important roles during development of the brain and kidney *(Murray-Zmijewski et al., 2006)*. The only p53 family member in *Drosophila* is more related to p53 in terms of biological functions (Figure 11), although few studies have reported a role for Dp53 in cell differentiation during eye development, thus suggesting that Dp53 could maintain certain features of mammalian p63 and p73 as well *(Fan et al., 2010)*.

Over the years, p53 has been shown to sit at the center of an increasingly complex web of incoming stress signals and outgoing effectors pathways (Figure 6). The major mechanism by which p53 functions is as a transcription factor that both positively and negatively regulates the expression of a large and disperse group of target genes involved in a variety of cellular responses. In addition, transcriptionally independent activities of p53 have been involved in the regulation of apoptosis *(Moll et al., 2005)* or autophagy *(Tasdemir et al., 2008)*. The outcome of the p53-mediated stress response depends on cell/tissue type and context as well as the extent, duration, magnitude and origin of the stress. Moreover, to complicate even more the scenario, since the discovery of the different p53 isoforms, several works have started to reveal some specific biological functions and biochemical activities for each of them in vertebrates models *(Olivares-Illana and Fåhraeus, 2010)* as well as in *Drosophila (Dichtel-Danjoy et al., 2013)*.

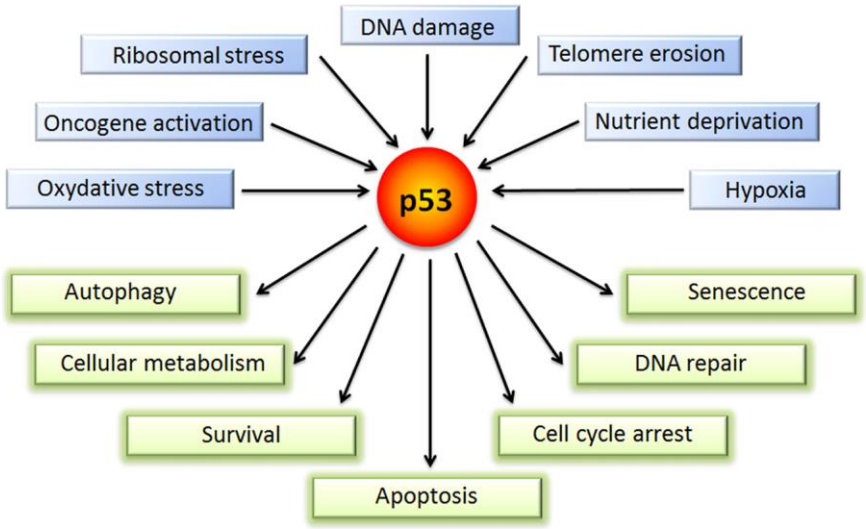

Figure 6: Activation and functions of p53

In mammals, p53 has a key role in integrating the cellular responses (green boxes) in response to different types of stress (blue boxes). The outcome of the p53-mediated stress response depends on cell/tissue type and the context as well as the extent, duration, magnitude and origin of the stress. Although the importance of these cellular responses to tumour suppression is clear and well understood, contributions of these responses can be also important to other aspect of human health and physiology. Interestingly, Dp53 seems to respond to some of these stress stimuli and is able to induce similar cellular responses (see Figure 11).

- **Apoptosis**

Induction of apoptosis or programmed cell death (PCD) is a central function of p53 in tumour suppression *(Vousden and Prives, 2009)*, a pro-apoptotic function that is well conserved in *Drosophila* (Figure 7).

In flies, in response to apoptotic stimuli, the pro-apoptotic genes *reaper* (*rpr*), *head involution defective* (hid), *grim* and *sickle* (*skl*) are necessary and sufficient to induce apoptosis through inhibition of the caspase inhibitor *Drosophila* inhibitor of apoptosis protein 1 (Diap1), which subsequently leads to activation of the initiator caspase, *Drosophila* Nedd2-like caspase (Dronc, Caspase-9-like), and two major effector caspases, *Drosophila* interleukin-1 converting enzyme (DrICE, Caspase-3-like) and death caspase-1 (Dcp-1, Caspase-7-like) [reviewed in *(Xu et al., 2009)*].

Already at the time that Dp53 was identified and characterized, overexpression of Dp53 was shown to be able to induce apoptosis, and dominant negative variants of the protein (disrupted for DNA binding activity) blocked radiation-induced apoptosis in several tissues *(Brodsky et al., 2000; Jin et al., 2000; Ollmann et al., 2000)*. In response to radiation-induced DNA damage, Dp53 transcriptionally activates *reaper* (*rpr*) to induce apoptosis due to the existence of a conserved p53 response element (p53RE, a 150 bp *cis*-element that contains a consensus binding site for p53) in its promoter region *(Brodsky et al., 2000)*. Although *rpr* is the most well characterized direct target of Dp53 in the induction of apoptosis, *hid* and *skl* are also important effectors of Dp53-induced apoptosis *in vivo (Akdemir et al., 2007; Brodsky et al., 2004; Fan et al., 2010; Sogame et al., 2003).* Besides regulating several pro-apoptotic genes, other downstream effectors have been involved in the regulation of Dp53-dependent PCD (Figure 7). The Jun-N-terminal kinase (JNK) signaling pathway induces apoptosis in response to irradiation in *Drosophila* tissues, and Dp53 is required for the activation of the JNK-dependent apoptosis in response to such genotoxic stress *(McEwen and Peifer, 2005)*. The proposed mechanism suggests that the direct binding between Dp53 and phosphorylated JNK prevents dephosphorylation of activated JNK resulting in sustained activation of the pathway and induction of apoptosis *(Gowda et al., 2012)*. Moreover, a feedback amplification loop between Dp53, JNK, the pro-apoptotic genes *hid* and *rpr* and the caspase Dronc further supports the relationship between Dp53 and the JNK pathway *(Shlevkov and Morata, 2012; Wells et al., 2006)*. Another pathway involved is the Hippo (Hpo) pathway. Under exposure to ionizing irradiation (IR), Hpo is activated by phosphorylation in a Dp53-dependent manner, and depletion of the Hpo pathway significantly reduces (although not completely) the cell death response elicited by IR or Dp53-overexpression *(Colombani et al., 2006).* Very recently, the *Drosophila* Caliban, a nuclear export

mediator factor, has been shown to be upregulated in a Dp53-dependent manner upon irradiation and to greatly contribute to Dp53-dependent apoptosis in this context *(Wang et al., 2013)*.

Interestingly, while rapid induction of apoptosis following IR-induced DNA damage (4 to 24 hours after exposure) absolutely requires Dp53, there is a late Dp53-independent but JNK-dependent second wave of apoptosis induction (24 hours onward), most probably as a consequence of DNA damage-induced aneuploidy *(Dekanty et al., 2012; McNamee and Brodsky, 2009; Wichmann et al., 2006)*. Dp53 is responsible for the induction of apoptosis in response to DNA damage caused not only by exogenous sources such as different types of *irradiation (Brodsky et al., 2000; Lee et al., 2003a; Ollmann et al., 2000; Sogame et al., 2003),* but also by endogenous sources such as telomere loss after dicentric chromosome induction in somatic cells *(Titen and Golic, 2008; Titen et al., 2014)* or under replication stress in mitotic cells *(LaRocque et al., 2007)*. Besides its role in mediating DNA-damage-induced apoptosis, Dp53 is also responsible for removing abnormal, misplaced or excessive primordial germ cells by PCD during normal germ cell development in *Drosophila* embryos *(Yamada et al., 2008)*.

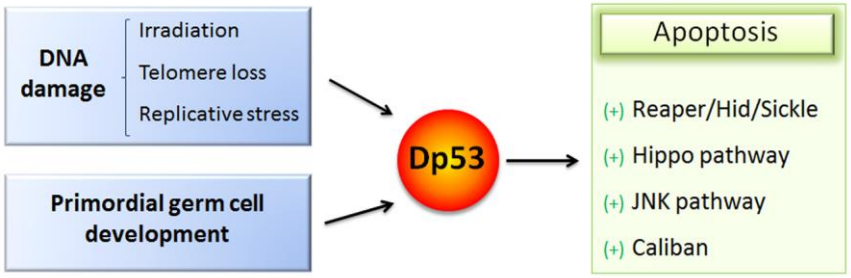

Figure 7: Pro-apoptotic function of Dp53

Induction of apoptosis or programmed cell death is a central function of p53 in tumour suppression, and this pro-apoptotic function is well conserved in *Drosophila*. Diagramme showing the incomes (blue boxes) that leads to Dp53-dependent induction of apoptosis and the pathways involved on this cellular response (green box).

- **Cell cycle arrest**

In mammals, p53 can regulate cell cycle progression through transcriptional regulation of several target genes. Whereas expression of the cyclin-dependent kinase inhibitor p21 is largely responsible for the p53-dependent G1-S arrest, repression of cdc25c, a phosphatase that promotes mitosis, induces a G2-M arrest *(Zilfou and Lowe, 2009)*.

In *Drosophila*, the capacity of Dp53 to modulate cell cycle progression is controversial: whereas Dp53 is not needed to arrest the cell cycle upon DNA damage, it is needed in response to mitochondrial dysfunction. The initial studies already contemplated this controversy by suggesting that overexpression of Dp53 affects the duration of M phase but demonstrating that Dp53 was not required for DNA damage-induced cell-cycle arrest, even though many cell-cycle regulators, including p21 and string/cdc25, are conserved in the fly genome *(Ollmann et al., 2000)*. In *Drosophila,* the DNA damage-induced cell cycle arrest and apoptosis responses are independently controlled: whereas tefu/ATM and its downstream targets Mnk/Chk2 and Dp53 regulate the immediate apoptotic response of the tissue to IR, cell cycle arrest in G2 is controlled by the activity of mei-41/ATR and its downstream target grapes/Chk1 *(Brodsky et al., 2000; Brodsky et al., 2004; Jaklevic and Su, 2004; Ollmann et al., 2000; Sogame et al., 2003)*.

However, Dp53 has been shown to induce cell cycle arrest in other biological contexts (Figure 8). Disruption of the mitochondrial electron transport chain induces a metabolic stress (low ATP levels) sensed by the AMP-activated protein kinase (AMPK) that, in turn, acts through Dp53 to activate a G1-S checkpoint *(Mandal et al., 2005)*. Dp53 induces transcriptional upregulation of the F-box protein Archipielago which contributes to the proteasomal degradation of cyclin E protein and thereby imposing cell cycle arrest upon mitochondrial dysfunction *(Mandal et al., 2005; Mandal et al., 2010)*. The same molecular mechanism involving Archipielago and cyclin E is able to mediate the tumour suppressor role of Dp53 in restraining ectopically neural stem cell formation in the *Drosophila* brain *(Ouyang et al., 2011)*. In addition, Dp53 also seems to regulate the transient cell cycle arrest (both in G1 and G2 phases) found in wing imaginal discs that contain 'undead cells' [*(Wells et al., 2006)*, see below for more information concerning 'undead cells').

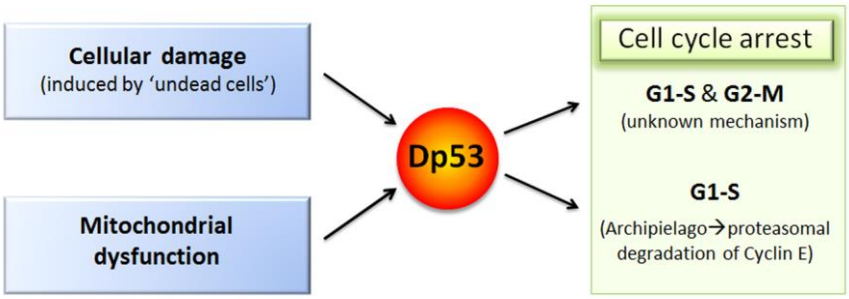

Figure 8: Regulation of the cell cycle by Dp53

Although the DNA damage-induced cell cycle arrest in *Drosophila* is Dp53-independent, other biological contexts such as mitochondrial dysfunction and cellular damaged caused by induction of 'undead cells' leads to a Dp53-dependent arrest of the cell cycle.

- **DNA repair**

The first evidences that suggest a role of Dp53 in DNA repair were found in pupal retinas, where Dp53 protects cells from undergoing apoptosis in response to UV irradiation probably by enhancing nucleotide excision repair *(Jassim et al., 2003)*. Later on, a genome-wide analysis of IR-induced transcription profile in embryos indicate that *Mre11*, *ku70* and *ku80*, genes involved in homologous recombination (HR) and non-homologous end joining (NHEJ), are been regulated by Dp53 *(Brodsky et al., 2004).* Recent studies have demonstrated that UTX is required for the transcriptional up-regulation of *ku80* by Dp53 under IR. UTX and Dp53 physically interact and are recruited in an interdependent manner to the *ku80* promoter region in *Drosophila* cultured cells *(Zhang et al., 2013)*. Finally, the persistence of phosphorylated H2Av [a marker for DNA double-strand breaks *(Madigan et al., 2002)*] in *dp53* mutant flies exposed to IR suggest that resolution of DNA repair following IR requires Dp53 *(Wells and Johnston, 2012).* Another mechanism by which Dp53 promotes DNA repair is by modulating chromatin structure. Interestingly, *dp53* mutant flies have impaired chromatin remodelling since these flies fail to induce K9 acetylation upon UV treatment and have lower levels of basal K14 acetylation of histone H3, chromatin marks typical of a more "open-state" necessary to allow the access of the DNA repair machinery to the damaged areas of the chromosomes *(Rebollar et al., 2006)*.

- **Tissue homeostasis**

The idea that p53 activation can be beneficial to tissue homeostasis has been largely shown in mammalian models and could be easily argued. On one hand, p53 directs the elimination of aberrant or

damaged cells from a tissue, thus preserving normal physiology. On the other hand, increased p53 activity under certain circumstances can promote DNA repair, enhance the antioxidant response and induce proliferation to efficiently renew tissues *(Schoppy et al., 2010)*. In *Drosophila* several studies have significantly contributed to the idea of p53 as an essential regulator of tissue homeostasis.

- Compensatory proliferation or tissue regeneration

In *Drosophila*, tissues with severe damage are capable of regeneration during development through a process of compensatory proliferation, resulting in tissues and structures with normal size and pattern. Such damage could be triggered by several insults, including irradiation, disc fragmentation or genetic manipulation, which finally leads to activation of PCD. To visualize and characterize this regenerative capacity and the different compensatory processes taking place, the *Drosophila* community has conceived the concept of 'undead cells'. 'Undead cells' can be created in developing fly tissues by activating cell death while protecting against the demise of these cells by means of expression of the baculovirus caspase inhibitor p35. Under these conditions, these 'undead cells' remain alive and acquire unexpected properties. The classical phenotypes observed by several laboratories when 'undead cells' are induced in imaginal tissues are: changes in gene expression like ectopic expression of wingless (wg) and decapentaplegic (dpp), an increase in cell proliferation, a subsequent hyperplastic overgrowth of the tissue and invasiveness behaviors between compartments *(Huh et al., 2004; Pére*(Herrera and Morata, 2014)*z-garijo et al., 2004; Ryoo et al., 2004)*. Interestingly, later on, it has been shown that in this context, Dronc induces expression of *dp53* mRNA, and that Dp53 plays a central role in the coordination of the compensatory growth response to tissue damage *(Wells et al., 2006)*. Johnston and colleagues showed that Dp53 activity is required and sufficient to promote compensatory proliferation, ectopic expression of Wg, tissue overgrowth, re-patterning, and systemic larval delay associated with disc damage as well as for the differentiation of adult structures *(Wells and Johnston, 2012; Wells et al., 2006)*. In addition, Dp53 overexpression is able to upregulate *Notch* mRNA and protein, and recent genetic interactions between *dp53* and *Notch* suggest that Dp53-induced proliferation is partially dependent on *Notch* activation *(Simón et al., 2014).* Interestingly, the role of p53 in apoptosis-induced compensatory growth seems to be conserved, since mice deficient for MDM2 in the intestinal epithelium develop intestinal hyperplasia due to the activation of the canonical Wnt and EGFR pathways in response to a p53-dependent cell death increase *(Valentin-Vega et al., 2008)*.

- Coordination of tissue growth

In mammalian cells, inhibition of the Insulin/TOR pathway, ribosomal biogenesis and protein translation leads to an increase in the activity of the tumour suppressor gene p53 *(Mayo and Donner, 2002; Zhang and Lu, 2009)*. In *Drosophila* imaginal tissues, adjacent cell populations grow in a coordinated manner during development. In a situation in which growth conditions are compromised in a specific territory, a mechanism that coordinates growth is activated in order to maintain final shape and proportions of the adult wing. In this scenario, Dp53 is activated autonomously upon growth impairment and induces cell death and cell cycle arrest, and reduces growth rates in adjacent populations *(Mesquita et al., 2010)*. These results unveil a fundamental role for Dp53 in preserving tissue integrity and homeostasis by acting in a non-autonomous manner.

♦ **Longevity**

Several mouse models also support the involvement of p53 in aging. The most accepted role of p53 in aging involves an intensity-based model: whereas physiological p53 activity protects from aging *(Matheu et al., 2007),* unrestrained and excessive p53 activation is detrimental to healthy aging due to widespread apoptosis of stem cells *(Maier et al., 2004)*.

In *Drosophila,* Dp53 is also an important mediator of longevity, and its intensity-base mode of action resembles that of mammalian p53. The effects of Dp53 in aging appear to be sex-, stage- and tissue-specific *(Biteau and Jasper, 2009; Donehower, 2009)*. On one hand, ubiquitous overexpression of Dp53 in adults flies limits life span in females but favors life span in males, whereas neuronal expression of the same construct extends life span in females and decreases life span in males *(Shen and Tower, 2010; Waskar et al., 2009)*. On the other hand, overexpression of Dp53 during larval development increases longevity similarly in both sexes, but in a dose-dependent manner. While strong expression is deleterious for life span, moderate to weak overexpression increases it *(Waskar et al., 2009)*. Most interestingly, inactivation of the *dp53* locus increases adult life span in both sexes, although in males the effect is minor and less consistent than in females *(Waskar et al., 2009)*. Similar phenotypes are observed when Dp53 activity is blocked by means of expression of dominant negative forms ($Dp53^{DN}$) via the tissue-specific GeneSwitch driver system. The effect of Dp53 in this later case also seems to be sex- and tissue-dependent. Flies expressing $Dp53^{DN}$ in the muscle or fat body have shortened life span, whereas expression of this transgene in neuronal cells, and specifically in the fourteen insulin producing cells (IPCs), extends life span through inhibition of the insulin signaling *(Bauer et al., 2005; Bauer et al.,*

2007). Indeed, Dp53 depletion in IPCs results in both reduced production of *Drosophila* insulin-like peptide 2 (Dilp2), shown by a decrease in *Dilp2* mRNA, and reduced insulin signaling in the fat body (FB, probably the major insulin-responsive organ in the fly), shown by the nuclear localization of the forkhead transcription factor FOXO in FB cells *(Bauer et al., 2007).* These results are consistent with the fact that reduced insulin signaling is well known to extend lifespan in flies and mammals *(Clancy et al., 2001)*.

The life span effects of Dp53 are closely related with calorie restriction (CR), another well-known increasing life span factor. In that sense, Bauer and colleagues proposed a model in which CR activates dSir2 by an unknown mechanism and dSir2 deacetylates and inhibits Dp53 activity, which in turn leads to lower activity of the insulin pathway, a pleiotropic pathway that regulates different signaling outputs. Interestingly, recent studies have demonstrated that although reduction of Dilp2 is a key signal for longevity regulation by Dp53, FOXO does not seem not to be required for it. Instead, downstream components of the Target of Rapamycin (TOR) signaling pathway, such as the translational inhibitor 4EBP, may be required for the life span extending effects of reduced Dp53 activity *(Bauer et al., 2010)*. Thus, Dp53 may affect life span by differentially engaging the insulin and TOR pathways, in a CR- and dSir2-dependent manner (Figure 9).

Interestingly for our work, besides extending life span, reduction of Dp53 activity in neurons selectively confers resistance to genotoxic stresses, such as oxidative stress caused by paraquat treatment. However, resistance to other kind of stresses such as starvation, are not affected by depletion of Dp53 in neurons *(Bauer et al., 2005)*.

- **Cell differentiation and stem cell biology**

Drosophila p53 incorporates functions of the two other mammalian family members, p63 and p73, in what concerns regulation of cell differentiation. Interestingly, overexpression of Dp53 in the developing eye induces massive cell death but also inhibits cellular differentiation of photoreceptor neurons and cone cells therefore disturbing ommatidial organization in the eye independently of its apoptotic function *(Fan et al., 2010)*.

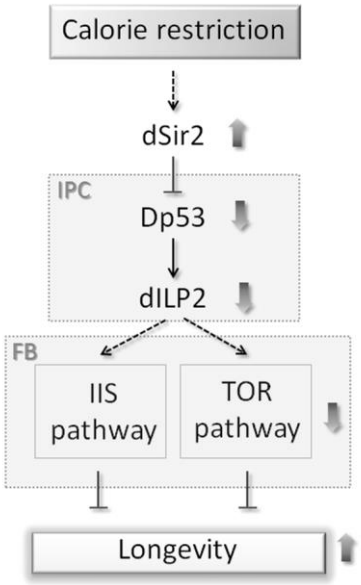

Figure 9: Calorie restriction-dependent life span extension: better without Dp53

Calorie restriction (CR) treatment of animals leads to an increase in life span. Under CR conditions the *Drosophila* Sirtuin 2 (dSir2) protein is upregulated by an unknown mechanism and is supposed to deacetylate and inhibit Dp53 activity. Decreased Dp53 activity specifically in the fourteen insulin producing cells (IPCs) results in reduced production of insulin-like peptide 2 (dILP2) which in turn triggers a reduction in insulin signaling (IIS) in the fat body, the major insulin-responsive organ in the fly.As a consequence the activity of the Target of Rapamycin (TOR) signaling pathway is also reduced. Thus, Dp53 affects life span by differentially engaging the IIS and dTOR pathways, in a CR- and Sir2-dependent manner.

Increasing evidences support the proposal that p53 may act as a barrier for pluripotency, limiting in some tissues the population of stem cells by controlling its quantity and quality *(Aloni-Grinstein et al., 2014)*. As its mammalian counterpart, Dp53 has been recently involved in stem cell biology. Ectopic neural stem cells (NSCs) in the *Drosophila* brain and the consequently tumour-like overgrowth can be rescued by overexpression of Dp53 *(Ouyang et al., 2011)*. Adult flies exposed to genotoxic stress or genome destabilizers selectively activate Dp53 in germline stem cells (GSCs) and *dp53* mutants exhibit impaired fertility and delayed re-entry into the cell cycle after irradiation *(Wylie et al., 2014).* In this report they also show that uncontrolled stem cell proliferation (caused by forced oncogene expression), failed differentiation programs or expansion of the stem cell niche, lead to Dp53 activation and suggest a potential role for Dp53 in promoting proper cell cycle progression in these stem-like tumours.

- **Cell competition**

Cell competition was originally described in *Drosophila* as a process of selection of the fittest cells (Morata and Ripoll, 1975). Cell competition occurs when, within a growing tissue, two cell populations with different growth rates confront each other resulting in growth of the stronger population ('winner' cells) at the expense of the weaker one ('loser' cells). This 'cell fate' is absolutely context dependent, it is not an intrinsic property of cells, it completely relies on cell-cell interactions, and certain parameters such as common limiting resources (nutrients, growth factors, space or survival factors) define the level of fitness of developmentally equivalent cells *(de Beco et al., 2012; Johnston, 2009; Levayer and Moreno, 2013)*. During cell competition, apoptosis is proposed to be the principal cause of the growth disadvantage of 'loser' cells and is triggered by interactions with the 'winner' cells. What signals apoptosis and *hid* induction in 'loser' cells is still unknown, but it relies on activation of the JNK stress-response pathway and JNK activation in loser cells is independent of Dp53 *(Amoyel and Bach, 2014)*. Competition can be induced playing with different genetic contexts. Classically, differences in ribosomal protein gene dosages (collectively known as *Minutes*) were used, but in the last few years many other genetic situations have been shown to induce cell competition. Among them, experiments playing with differences in the transcription factor dMyc levels have been thoroughly studied *(Cova et al., 2004; Moreno and Basler, 2004)*. Interestingly, recent findings show that Dp53 is required for the 'supercompetitor' status of cells with extra dMyc activity. In its absence, dMyc 'supercompetitor' cells no longer kill the *wild-type* surrounding cells, cannot expand as a population, have increased genomic instability and undergo catastrophic induction of apoptosis *(de la Cova et al., 2014)*.

On the contrary, in mammals, p53 seems to be activated in the 'loser' cells and mediate several aspects of cell competition. In a recent study using genetic mosaic mouse models and bone marrow chimeras, the authors were able to simulate a situation of cell competition, specific to the hematopoietic stem and progenitor cells, where p53 was involved. This competition appears to be mediated by a non-cell-autonomous induction of growth arrest and senescence-related gene expression in outcompeted cells with higher p53 activity *(Bondar and Medzhitov, 2010)*.

- **Cell metabolism**

During cancer development, the reprogramming of metabolic pathways provides cancer cells with numerous benefits, including the ability to survive under adverse conditions (such as low or variable oxygen availability), the ability to mobilize anabolic pathways to generate the macromolecules necessary to sustain highly proliferative tumour growth and the ability to limit oxidative damage *(DeBerardinis et al., 2008).* Therefore, it is not surprising that in the last decade p53 has been shown to contribute to the regulation of metabolism, a function that greatly participates on its tumour suppressor roles by counteracting many of the metabolic alterations associated with cancer development *(Jiang et al., 2013)*. Unlike the majority of normal cells, which depend on mitochondrial oxidative phosphorylation to provide energy (produces 36 ATP per molecule of glucose), most tumour cells primarily utilize glycolysis for their energy needs even under normal oxygen conditions (aerobic glycolysis or the Warburg effect). Due to the less efficient capacity of glycolysis to generate energy (only 2 ATP per molecule of glucose), tumour cells have a much higher rate of glucose uptake and produce large amounts of lactate. Despite the low efficiency of aerobic glycolysis, it provides rapid ATP generation, biosynthetic advantages and contributes to a proper control of redox balance of highly proliferative tumour cells. In addition to the Warburg effect, tumours show alterations in many other aspects of metabolism, including altered amino acid and lipid metabolism. For instance, many tumours are addicted to glutamine, a non-essential amino acid, which can be used as an alternative source for proteins synthesis and ATP generation *(Cairns et al., 2011; Hsu and Sabatini, 2008)*. In that sense, p53 plays a major tumour suppressor role by (1) repressing at multiple levels aerobic glycolysis through regulating glucose uptake, consumption and several glycolytic enzymes, and by (2) regulating glutamine metabolism [Figure 10 *(Jiang et al., 2013)*]. Moreover, p53 interacts with mammalian target of rapamycin (mTOR) and AMP-activated protein kinase (AMPK), two master regulators of cellular metabolism, thus indirectly inhibiting glycolysis and influencing, among others, many key pathways involved in carbohydrate and lipid metabolism *(Feng et al., 2007; Levine et al., 2006)*. Another important mechanism of p53 in tumour suppression is the regulation of oxidative stress. Under conditions of non- or low stress, p53 exerts an antioxidant function by reducing the intracellular ROS levels and enhancing antioxidant defense genes such as sestrins. However, in response to severe oxidative stress p53 induces the expression of several prooxidant genes which in turn, increase even more the ROS levels to promote a p53-mediated apoptosis and senescence, thus maintaining genomic integrity *(Bensaad and Vousden, 2007)*. In addition to these tumour suppressive roles, p53 also plays a critical role in maintaining the integrity of mitochondria and

promoting oxidative phosphorylation through regulation of many target genes, such as synthesis of cytochrome c oxidase 2 (SCO2, a key regulator of the mitochondrial complex IV), as well as negatively regulating lipid metabolism by promoting fatty acid oxidation and inhibiting fatty acid synthesis [Figure 10, *(Gottlieb and Vousden, 2010; Liang et al., 2013)*].

On the other side, p53 has been proposed to function in the adaptive response upon transient metabolic stresses at the cellular level by inducing metabolic remodeling and promoting cell survival. In cultured cells, in response to glucose deprivation, p53 induces Lipin-1 to promote fatty acid oxidation *(Assaily et al., 2011)* and arrests the cell cycle to promote cell survival *(Jones et al., 2005)*. Upon starvation, p53 regulates the autophagic flux within the cell according to its needs to increase cell fitness *(Scherz-Shouval et al., 2010)*. In a situation of serine deprivation, p53 preserves the anti-oxidant capacity of the cell to increase survival rates *(Maddocks et al., 2013)*.

In *Drosophila*, the connection between p53 and cellular metabolism has been so far poorly addressed. On one hand, it has been shown that Dp53 is able to sense metabolic stress signals, namely low ATP levels upon mitochondrial dysfunction. In this situation, Dp53 modulates the cell cycle progression by reducing the levels of Cyclin E, thus promoting a metabolic Dp53-dependent G1-S checkpoint *(Mandal et al., 2005; Mandal et al., 2010)*. On the other hand, a recent study in S2 cells analyzing the molecular basis of the fitness of dMyc 'supercompetitor' cells proposes that Dp53 is able to regulate glycolysis and oxidative phosphorylation, as it does in mammals. In this study, however, they found contradictory roles for Dp53 in a context dependent manner. While in normal conditions Dp53 seems to restrain glycolysis (by reducing the glucose transporters *Glut1* and *Glut3* mRNA levels) and promote oxidative phosphorylation (by inducing ScoX mRNA levels, the *Drosophila* homolog of the mammalian SCO2), in dMyc 'supercompetitor' cells Dp53 promotes glycolysis *(de la Cova et al., 2014)*.

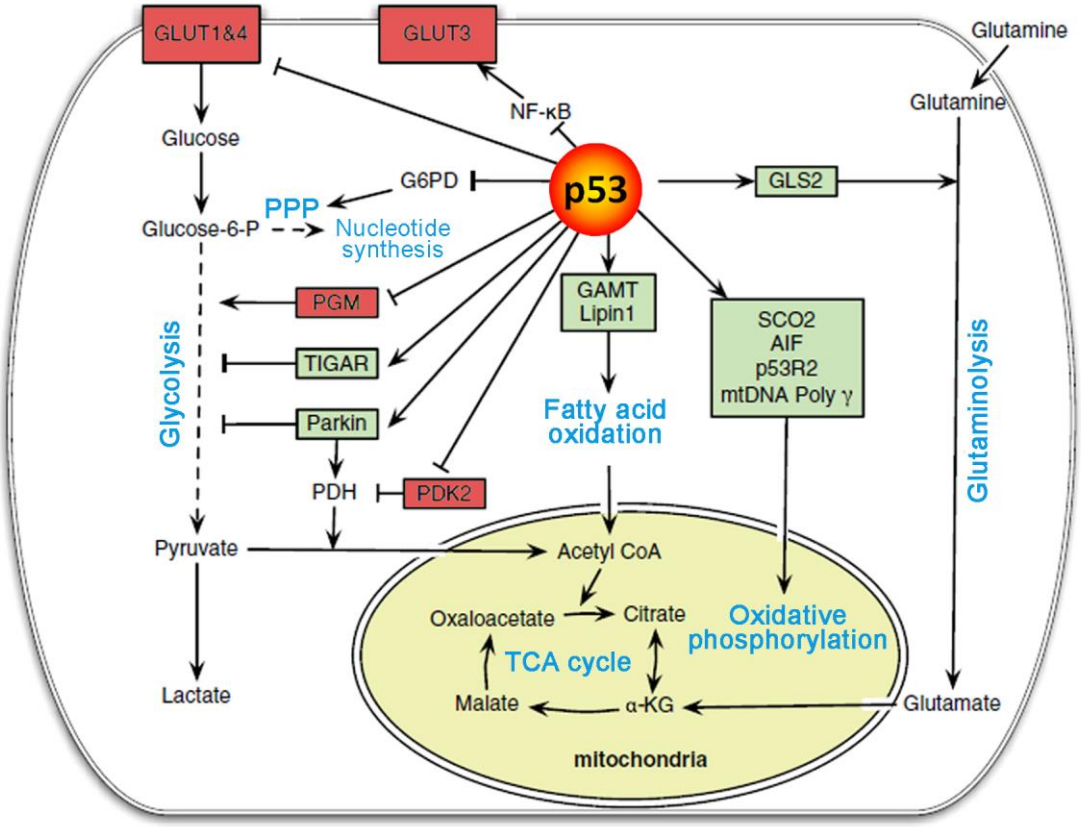

Figure 10: The regulation of cellular metabolism by p53

p53 has emerged as a key regulator of cellular metabolism, including mitochondrial oxidative phosphorilation, glycolysis, glutaminolysis and fatty acid oxidation. Elements positively regulated (directly or indirectly) by p53 are shown in green boxes and those negatively regulated in red boxes. p53 play a major role in antagonizing the Warburg effect by: (1) reducing glucose uptake, through direct repression of glucose transporters (Glut) Glut1 and Glut4, and indirect repression of the Glut3, (2) by lowering the glycolytic rates through upregulation of the expression levels of TIGAR (TP53-induced glycolysis and apoptosis regulator) and Parkin, and by lowering the levels of PGM (phosphoglycerate mutase) and (3) by promoting oxidative phosphorilation. Several p53 target genes that mediate the role of p53 in maintaining mitochondrial integrity and promoting oxidative phosphorylation have been identified, including SCO2 (synthesis of cytochrome oxidase c 2), AIF (apoptosis-inducing factor), Parkin, p53R2 and PDK2 (pyruvate dehydrogenase kinase-2). Moreover, p53 induces the expression of GLS2 (glutaminase 2), which catalyzes the hydrolysis of glutamine to glutamate that can be converted to α-KG (α-ketoglutarate) and promote the TCA cycle. In addition, p53 induces the expression of GAMT (guanidinoacetate methyltransferase) and Lipin1 to promote fatty acid oxidation. Lastly, p53 physically interacts with glucose-6-P inhibiting its function, thereby downregulating PPP (pentose phosphate pathway), critical for nucleotide synthesis and production of NADPH, a reducing agent required for anabolic and antioxidant pathways. Adapted from *(Liang et al., 2013)*.

- **Autophagy**

Autophagy is an evolutionary conserved mechanism for the degradation of long-lived proteins and organelles. Depending on the physiological and pathological conditions, autophagy has been shown to act as a pro-survival or as a pro-death mechanism in the cell. During autophagy, cytoplasmic components are sequestered into double membrane structures called autophagosomes, which then fuse to lysosomes to form autophagolysosomes, where degradation takes place *(Xie and Klionsky, 2007)*. Degraded products are then recycled for energy production or other metabolic processes, which justify the importance of the autophagic induction in conditions of nutrient deprivation *(Kuma and Mizushima, 2010)*. Moreover, autophagy is also used for the removal of damaged macromolecules and dysfunctional organelles such as mitochondria. Thus, autophagy works as a cytoprotective mechanism able to modulate aging and influence cancer survival *(Rubinsztein et al., 2011)*. Because of the biological nature of the processes in which autophagy plays a role, it is easy to believe that p53 is involved in the regulation of such an important cellular process. Indeed, in mammals, p53 has a dual function in the control of autophagy, it can either activate or repress it. On one hand, nuclear p53 can induce autophagy through transcriptional up-regulation of targets genes such as AMPK, PTEN and Sestrins, thus activating autophagy mainly through inhibition of mTOR. On the other hand, cytoplasmatic p53 has been shown to repress autophagy through an unknown mechanism *(Balaburski et al., 2010; Levine and Abrams, 2008; Tasdemir et al., 2008).* Recent evidences suggest that the ability to enhance or suppress autophagy (by regulating autophagy protein LC3) allows p53 signaling to provide the most appropriate cell survival strategy during nutrient deprivation depending on the autophagic rate of the cell *(Scherz-Shouval et al., 2010)*.

In Drosophila, it is still an open question whether Dp53 is able or not to modulate autophagy.

- **Senescence**

Senescence represents a stress response in which cells withdraw from the cell cycle and no longer have the capability to proliferate in response to growth factors or mitogens. In other words, it is an irreversible cell-cycle arrest. The senescence pathway can be activated by multiple mechanisms such as replicative stress and telomeres shortening, by persistent oncogenic signaling (to prevent cellular transformation) or by accumulation of oxidative damage. In these conditions, p53 plays an important role in triggering cellular senescence. Several targets and pathways have been involved in the p53-mediated senescence such as: the cell cycle control, through its target p21 (responsible for G1 cell cycle

arrest) and E2F7 (pivotal in repression of mitotic genes); the regulation of ROS generation and oxidative stress, as well as the regulation of autophagy and mTOR pathways through different means *(Rufini et al., 2013)*. Moreover, the link between senescence cells and its contribution to aging phenotypes is clear. Due to the involvement of Dp53 in regulating longevity in *Drosophila*, one could expect that cellular senescence may mediate some aspects of the Dp53-dependent regulation of life span and play a role in the so called 'functional senescence', defined as the intrinsic age-related decline in functional cell and tissue status *(Shen et al., 2009)*. However, nothing is known about the molecular mechanism that could mediate the role of Dp53 in cellular senescence.

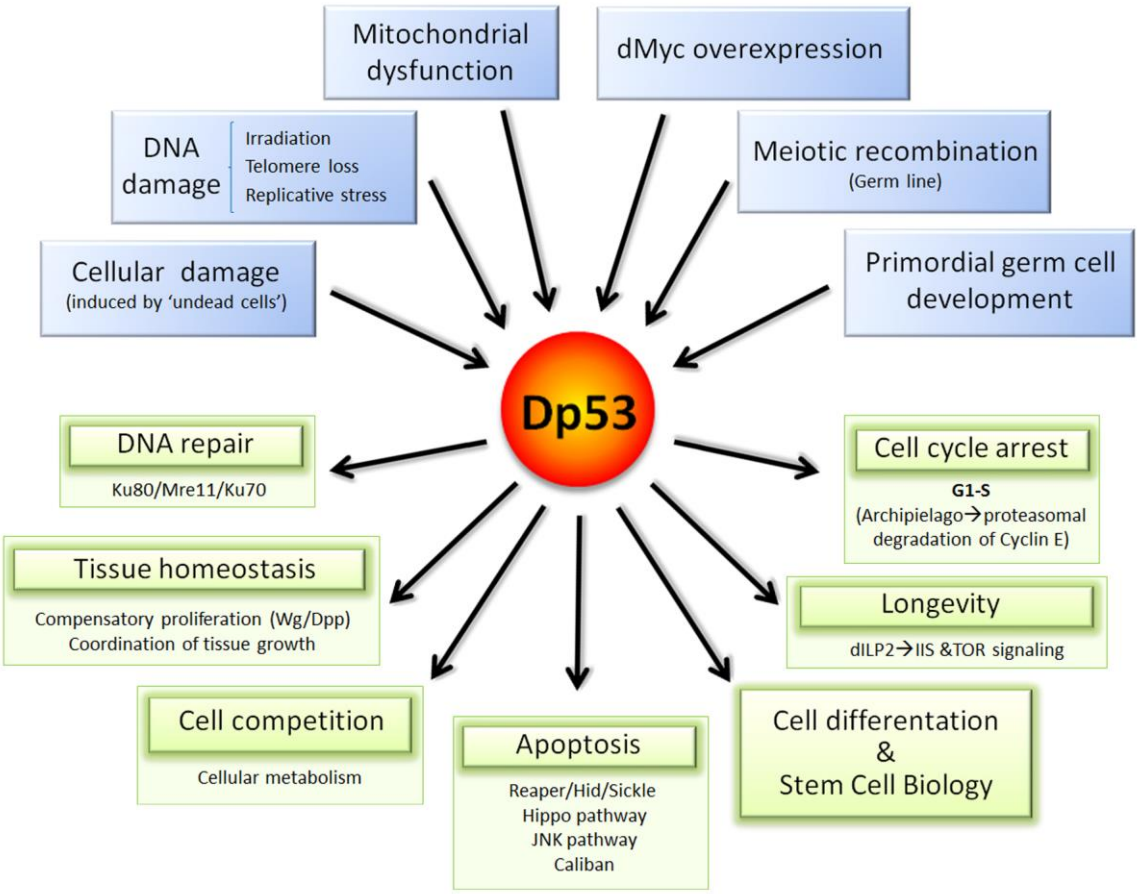

Figure 11: Dp53 best known inputs and outputs

In *Drosophila*, as in mammals, p53 has a key role in integrating different types of stresses and few developmental clues (blue boxes) with several cellular responses (green boxes) through the regulation of several target genes that coordinate different pathway.

3. **Metabolic homeostasis in *Drosophila***

Homeostasis, from the Greek words for 'same' and 'steady', is one of the most remarkable properties of complex systems that permit organisms to maintain a stable internal atmosphere despite environmental perturbations (including temperature, salinity, acidity and nutrients). Nutrition is one of the most important environmental factors influencing the life of any living being. Organisms have to adapt to rapid fluctuations in nutrient intake to efficiently utilize and store resources whenever available and tune down energy-consuming cellular processes during times of fasting. There is a constant flux in the nutritional supply and in the energy needs of an organism. Hence, strategies that maintain a steady state under varying nutritional conditions are crucial for the healthy functioning of an individual. Inability to efficiently maintain energy homeostasis results in the development of metabolic disorders such as obesity and diabetes. These complex metabolic disorders and their associated risks of cardiovascular diseases affect more than 34% of the adult population in certain countries like USA, thus highlighting the importance of the study of the molecular mechanisms underlying energy homeostasis.

The short life cycle and the ease of genetic manipulation has come to the establishment of *Drosophila* as one of the prime models for research in cell and developmental biology, greatly contributing to our general understanding of fundamental components of signaling pathways. Furthermore, in the past decade, *Drosophila* has emerged as an important model organism for the study of energy metabolism and metabolic homeostasis. Plenty of parallels exist between *Drosophila* and human physiology, ranging from the functionality of the different organ systems to the existence of ortholog genes involved in energy homeostasis in both organisms *(Leopold and Perrimon, 2007)*.

Organs involved in energy homeostasis in *Drosophila*

Despite the clear differences between humans and flies, *Drosophila* shares an organ composition comparable with that of mammals. In that sense, organs relevant for metabolic control and the flow of nutrients to storage organs share similar function and architecture (Figure 12).

- **Gut**

As in mammals, the first-line metabolic organ in *Drosophila* is the gut (Figure 12). Based on morphological and functional characteristics, the gut of the fly presents an anterior-posterior regionalization: ingested food passes through the foregut to be stored temporarily in the crop; it then moves to the midgut, where digestion and absorption takes places (thus combining functions of the mamamilan intestine and stomach); after that, it transits through the hindgut and rectum, where water and electrolytes are exchanged, and finally reaches the anus for excretion. In addition to its role as the organ of digestion and absorption, the midgut of *Drosophila* also functions as a very dynamic storage organ for fat *(Hoffmann et al., 2013)*. Two additional organs are part of the energy storage system in the fly: the oenocytes and the fat body, being the last one the most important one.

- **Fat body**

The insect fat body (FB) plays an essential role in energy storage and utilization. It integrates and emits signals involved in the regulation of growth and metabolism according to the nutritional status of the animal (Figure 12). The FB has no exact homologue in vertebrates, but it shares numerous similarities with the vertebrate white adipose and hepatic tissues, as it stores lipids (in form of triglycerides) and carbohydrates (in form of glycogen), respectively, and respond to energy demands liberating both diacylglycerides and trehalose (a disaccharide of glucose) into circulation. Flies have an open circulatory system (called hemolymph), rather than a vascular blood system, where nutrients and other molecules are transported. The FB is a loose organ organized in a lobular structure, mostly attached to the cuticle and bathed by the hemolymph distributed throughout the insect body. In larvae, it is made of two main large lobes, whereas in adults it is mainly organized in smaller patches of cells. In addition to its role in storage and utilization of nutrients, the fat body is a multifunctional organ able to produce the majority of proteins found in the hemolymph, participating in the immune response, in the detoxification of nitrogen metabolism as well as functioning as an endocrine organ *(Arrese and Soulages, 2010)*. The basic cell of the fat body is the adipocyte, characterized by the presence of numerous lipid droplets, intracellular cytoplasmic compartments specialized in the accumulation of neutral lipids *(Kühnlein, 2011)*.

Many of these functions are hormonally regulated, and thus the fat body is the target organ of several hormones such as the *Drosophila* insulin-like peptides (Dilp) and the adipokinetic hormone (Akh). These two hormones are produced in neurosecretory cells located in the brain and in the ring gland

respectively (together forming a bipartite '*Drosophila* pancreas') and secreted into the open hemolymph (the '*Drosophila* blood').

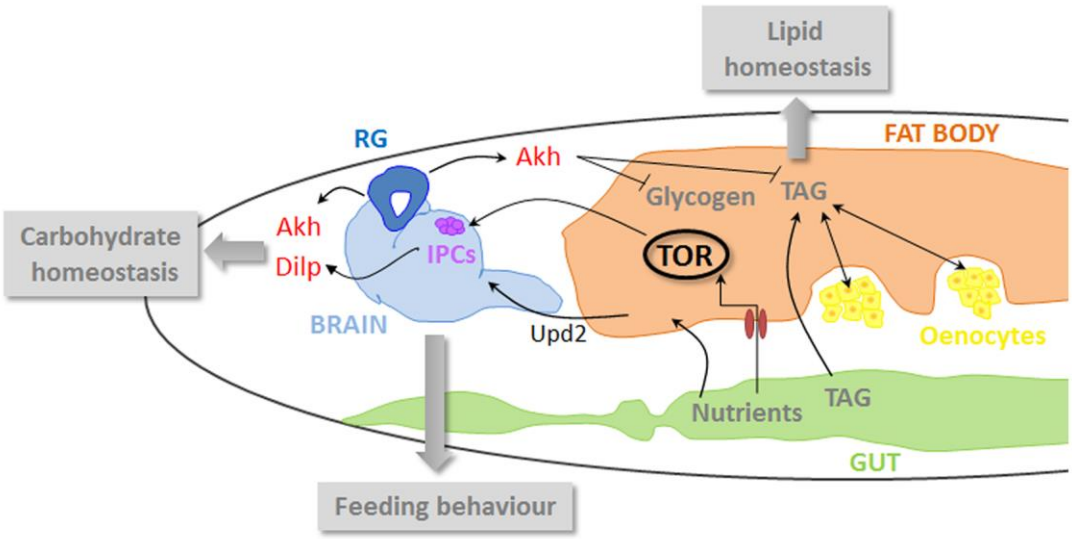

Figure 12: A general view of interactions regulating metabolic homeostasis in *Drosophila*

Sugar levels are maintained by the combinatorial effect of two key hormones, *Drosophila* insulin-like peptides (Dilps) and adipokinetic hormone (Akh, the insect glucagon) that are produced in neurosecretory cells located in the brain and in the ring gland (together forming a bipartite '*Drosophila* pancreas') respectively and secreted into the open hemolymph (the '*Drosophila* blood'). The fat body (the '*Drosophila* liver and white fat') is an important reservoir organ for glycogen and tryglicerides and functions as a key metabolic sensor able to couple nutrient status and energy expenditure of the entire animal. The conserved TOR pathway in fat body cells functions as an energy sensor that influences by a remote control the IIS pathway. Oenocytes ('*Drosophila* hepatocytes') form part of the energy cycling and lipid storage system in flies.

- **Brain and Ring gland**

Insulin producing cells (IPCs) are located in the median neurosecretory region of the fly brain and are essential for systemic control of carbohydrate metabolism through the release of several Dilps (Dilp 2, 3 and 5) into circulating hemolymph, similar to mammalian pancreatic β cells *(Rulifson et al., 2002)*. On the other hand, corpora cardiaca cells located in the ring gland (a neuroendocrine organ) secrete Akh (a polypeptide with glucagon-like functions) and are reminiscent of pancreatic α cells *(Kim and Rulifson, 2004)*. The antagonistic activities of these hormones control metabolic homeostasis in mammals and in *Drosophila*. While insulin promotes the uptake of sugar from the hemolymph by the different tissues and

its storage as glycogen and fats, Akh is secreted during starvation conditions to break down these energy storages (Figure 12).

- **Oenocytes**

A third organ composed of cells called oenocytes has been shown to specifically contribute to energy shuttling and fat storage. Oenocytes are organized in segmental rows of very large cells close to the fat body and directly attached to the cuticle of the animal (Figure 12). Oenocytes are believed to have similar functions to mammalian hepatocytes *(Gutierrez et al., 2007)*. Under normal feeding conditions, oenocytes are devoid of stored lipids and fat is primarily stored in the fat body and also in the intestine. Upon starvation, the intestine transfers to the fat body all the stored lipids, and oenocytes start to take it up. These cells are apparently required to modify lipids, making them available for other tissues, thus reminiscent of the mammalian hepatocytes. However, in contrast to hepatocytes, the oenocytes are not involved in glycogen catabolism, a role that is merely taken by the fat body (Figure 12).

Lipid and carbohydrate metabolism in *Drosophila*

- **Lipid metabolism**

We have seen that *Drosophila* shares with mammals a comparable anatomy of organs and cell types involved in lipid metabolism and homeostasis. Storage lipids in form of triacylglycerol (TAG) are mainly accumulated in the fat body, and to a less extent in the gut, in specialized organelles called lipid droplets. Besides that, oenocytes may have a role in lipid mobilization during starvation. At the ultrastructural level, lipid droplets have been found to be evolutionary conserved. Functionally, lipid droplets are dynamic organelles serving a central role in fat and energy metabolism. Structurally, they consist of a core of neutral lipids surrounded by a monolayer of phospholipids and cholesterol, into which specific proteins associate *(Kühnlein, 2012)*. Perilipin is the best characterized lipid droplet protein in mammals, and in *Drosophila* the lipid storage droplet 1 and 2 (Lsd-1 and 2) play relevant functions in lipid homeostasis and share homologies with vertebrate perilipins *(Beller et al., 2010; Grönke et al., 2003)*. Besides the similarities exhibited by organs/cells, the basic metabolic pathways and signaling pathways involved in lipid metabolism are likewise evolutionarily and functionally conserved. Thus, *Drosophila* has a full set of lipogenic enzymes involved in TAG and fatty acid biosynthesis and several

lipases involved in the mobilization of lipid reserves. Among these lipases, Brummer, the homolog of mammalian adipose triglyceride lipase (ATGL), is of central importance although is not the only enzyme involved in the mobilization of lipids in the fly *(Grönke et al., 2005)*. Lipases are responsible for catalyzing the hydrolysis of triglycerides into free fatty acids, which in turn, can be metabolized by several pathways. Most importantly, they undergo β-oxidation in the mitochondria to generate large amounts of energy (ATP). During the whole life cycle of *Drosophila,* mobilization of lipids are used as a source of energy to, among others, support embryonic development, adult flight and starvation periods *(Liu and Huang, 2013)*.

- **Carbohydrate metabolism**

Proper regulation of carbohydrate homeostasis is critical to maintain normal physiology. The two primary forms of circulating carbohydrates in *Drosophila* are glucose and trehalose (a disaccharide of glucose), the latter representing the most important one. These sugars serve a variety of purposes like being (1) an essential energy source, (2) substrates for biosynthetic reactions and (3) a way to store energy. Most carbohydrates in the fly are stored in a polymeric hydrated form, as glycogen, which provides a large and accessible energy source as a glycolytic fuel during times of fasting and intense activity. The most important reservoirs for glycogen in flies are the fat body and the muscle. Glycogen is synthesized from UDP-glucose mainly derived from dietary carbohydrates or amino acids. This UDP-glucose can be used for the synthesis of either glycogen or trehalose. In response to energy needs, the fat body is the main responsible for the production of circulating sugars from the breakdown of glycogen *(Tick et al., 1999)*. Interestingly, the vast majority of the enzymes involved in carbohydrate metabolic pathways, such as glycogen synthesis and breakdown or glycolysis, display significant parallelisms between mammals and insects, as well as the hormonal regulation responsible for the maintenance of glucose homeostasis *(Reyes-delatorre et al., 2012).*

Systemic metabolic responses in metabolism: the antagonistic functions of Insulin and Akh

The major hormonal pathways controlling metabolism in vertebrates are conserved in *Drosophila*. Thus, the molecular mechanisms by which vertebrates and flies regulate the storage and release of fuel molecules at the systemic level display significant parallels. The fasting hormone Adipokinetic hormone (Akh), the functional analogue of the vertebrate glucagon, plays a key role in mobilizing energy resources

during fasting, whereas *Drosophila* insulin-like peptides (Dilps), the hormone of feast, promote energy storage in normal feeding conditions, recapitulating the role of the vertebrate insulin pathway.

Akh hormone is produced and released by the corpora cardiac cells located in the ring gland (Figure 12). Akh receptors (AkhR) are present in the fat body membrane, where they transmit the effects of the hormone allowing both lipid and carbohydrate mobilization from this organ *(Bharucha et al., 2008).* Consistent with this role in mobilizing the main energy sources, ablation of Akh-producing cells or mutations affecting AkhR lead to: (1) abnormal accumulation of lipids and carbohydrates (shown by increased TAG and glycogen levels in total body and by the presence of larger fat body cells with huge lipid droplets) both in fed and starved conditions; (2) reduced sugar concentration (mainly trehalose) in the hemolymph both in fed and starved animals; (3) loss of the normal hyperlocomotor response to starvation for seeking food, and (4) increased starvation *resistance (Bharucha et al., 2008; Isabel et al., 2005; Kim and Rulifson, 2004; Lee and Park, 2004).* Although little is known about the downstream signaling components through which Akh signaling acts, it has been proposed that it is specifically required to mobilize glycogen in the fat body, predominantly via activation of glycogen phosphorylase. Interestingly, Tobi (target of brain insulin), an evolutionary conserved α-glucosidase, has been shown to be regulated by both insulin- and Akh- signaling responding oppositely to dietary protein and sugar, and to contribute to breakdown of glycogen in the absence of sugar *(Buch et al., 2008)*. On the other hand, Akh seems to form part of a dual lipolytic-signaling system together with the action of the Brummer lipase (ATGL in mammals). A very simple type of control sensitive to glucose/trehalose levels in the hemolypmh ensures that Akh is released only if required. Under low sugar levels, a calcium-mediated release of Akh is promoted by activation of the AMP-activated protein kinase (AMPK), the universal energy sensor *(Braco et al., 2012)*. Besides its role during starvation, Akh is also essential during energy-requiring activities, such as flight and locomotion.

The other molecular pathway involved in the systemic regulation of metabolic homeostasis is the insulin signaling. This point is developed in the next part of this introduction dedicated to the nutrient sensing pathways.

The Insulin and TOR signaling pathways: the nutrient sensing pathways

The Insulin/IGF (IIS) and the TOR signaling pathways are two highly conserved pathways that sense energetic and nutrient status in animals from flies to humans. These pathways are the main players in

sensing and relaying nutritional information in order to coordinate growth and metabolism with nutrient availability. Information about the nutritional status is directly sensed at the level of individual cells via the TOR pathway, while the systemic response is carried out by the hormonal action of insulin.

- **The insulin signaling pathway**

Insects only possess a single insulin-like system that combines the metabolic functions of the insulin pathway and the growth promoting functions of the insulin-like growth factor (IGF) pathway in mammals *(Wu and Brown, 2006)*.

There are eight *dilp* genes in the *Drosophila* genome that encode for eight peptides with similarities both at the amino acid level as well as at the functional level, but with diverse temporal and spatial expression patterns during development. Pertinent for this thesis are three of them (Dilp 2, 3 and 5) that are expressed in two symmetric clusters of seven neurosecretory cells in the brain in a nutrient-dependent manner *(Rulifson et al., 2002)*. These neurons, called IPCs, release Dilps into the hemolymph were they act systemically on remote target tissues by activating a single insulin-like receptor (InR), and a downstream intracellular signaling cascade consisting of kinases (Figure 13). Activation of the InR by its ligand leads to the recruitment of the adaptor protein Insulin receptor substrate (IRS), named Chico in *Drosophila*. Then, the activated InR-chico complex recruits and activates phosphoinositide 3-kinase (PI3K), a complex formed by the catalytic Dp110 and regulatory Dp60 subunits. Activated PI3K phosphorylates phosphatidylinositol-4,5-diphosphate (PIP2) on the plasma membrane to produce phosphatidylinositol-triphosphate (PIP3). This stimulation is reversed by the action of phosphatase and tensin homolog (PTEN), a negative regulator of the pathway known to act as a tumour suppressor in mammals (Figure 13). Accumulation of PIP3 induces the recruitment of two kinases, PDK1 and Akt (a proto-oncogene also known as PKB, protein kinase B) to the plasma membrane and its subsequent activation by phosphorylation. Then, Akt phosphorylates and regulates several target proteins including the Forkhead Box O (FOXO) transcription factor, a central catabolic regulator that counteracts the anabolic effects of the insulin signaling pathway [review in *(Garofalo, 2002; Hietakangas and Cohen, 2009; Teleman, 2010)]*. Phosphorylation of FOXO by Akt leads to its retention in the cytoplasm, inhibiting its nuclear transcriptional activity *(Puig et al., 2003)*. Moreover, Akt can also regulate FOXO activity indirectly by modulating its deacetylation via a module consisting in the Ser/Thr kinase SIK3 and the class IIa deacetylase HDAC4 *(Wang et al., 2011)*.

The metabolic functions of the insulin pathway have been confirmed by the different metabolic phenotypes reported for many components of the pathway. For instance, ablation of IPCs, mild reduction in InR levels or mutants for *chico* produced elevated circulating sugar levels and high levels of stored glycogen and lipids, analogous to the effects seen in diabetic patients with generalized insulin resistance. Conversely, PTEN mutants flies have reduced levels of stored glycogen and lipids *(Teleman, 2010).*

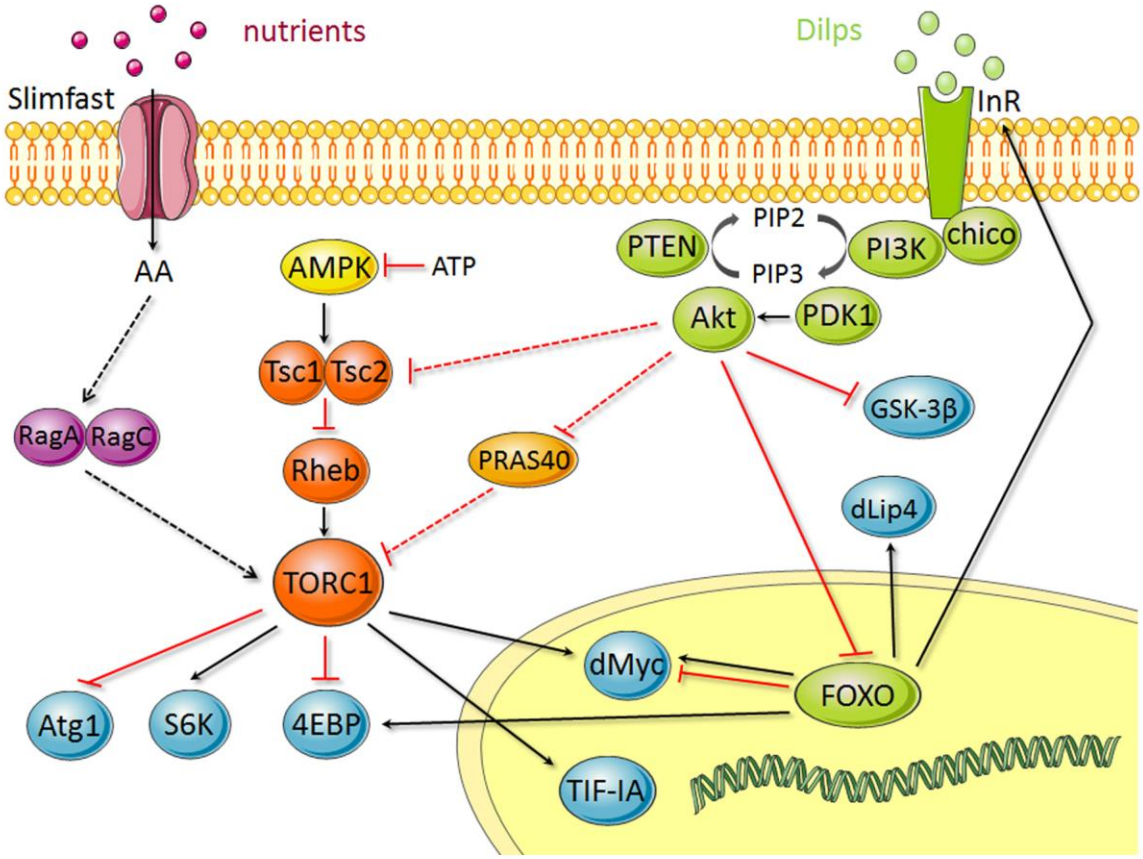

Figure 13: The Insulin/TOR signaling pathway

A schematic diagram showing the main elements of the conserved Insulin/TOR signaling pathway in green and orange respectively, as well as the input signals controlling this nutrient sensing pathway. In blue are shown some of the most important metabolic outputs and downstream effectors. Black arrows indicate positive regulation and red bar-ended lines indicate inhibitory interactions. Broken lines indicate indirect interactions or interactions requiring further study. Details of each interaction are described in the main text.

♦ **Remote control of Dilps**

The regulation of *dilp* expression or Dilp secretion in the IPCs is a complex process that involves the interplay between multiple tissues and elements and varies depending on the developmental stage of the animal (Figure 14). Several molecules, including neuropeptides [sNPF, short neuropeptide F), GTPases [NS3, nucleostemin family GTPase 3, *(Kaplan et al., 2008)*], histone deacetylases and microRNAs [*miR-14*, *(Varghese et al., 2010)* and *miR-278 (Teleman et al., 2006)*] are able to regulate *dilp* expression in the IPCs during development in an autocrine or paracrine way (Figure 14). How insulin signaling is controlled by the nutrient status of the animal is of crucial importance for this thesis.

The expression, secretion and activity of Dilps are also under control of humoral factors that adjust their circulating levels in response to nutrient availability (Figure 14). Upon starvation, expression levels of *dilp3* and *dilp5*, but not *dilp2* are reduced [Figure 14, (Ikeya et al., 2002)]. The histone deacetylase dSir2 has been shown to modulate *dilp2* and *dilp5* expression. Activation of this molecule specifically in the fat body seems to be responsible, in part, of the decrease in *dilp5* expression observed during starvation *(Banerjee et al., 2012)*. Moreover, it was demonstrated that a regulatory mechanism exists to control the release of Dilps rather than the expression *(Géminard et al., 2009)*. In this study, the authors elegantly demonstrated by *ex vivo* tissue co-culture experiments that the fat body regulates the secretion of Dilp2 and Dilp5 by a hormonal signal that involves TOR signaling. Recently, the leptin-like adipokine unpaired 2 (Upd2) has been found to be produced by fat cells in response to high-fat and high-sugar diets. Then, Upd2 can remotely activate JAK/STAT signaling in intermediate GABAergic neurons and promote insulin release from brain IPCs *(Rajan and Perrimon, 2012)*. Interestingly, whereas Upd2 expression drops when adults flies are subjected to extended starvation, it increases on acute amino acid restriction, thus suggesting that different signals are expected to mediate the sensing of distinct nutrients that at the end converge on the release of brain Dilps to control growth and metabolic homeostasis. For instance, Dilp6 acts as a hormone produced by the fat body in times of starvation or during pupariation to enable growth during these nonfeeding states through modulation of circulating Dilp2 levels *(Bai et al., 2012)*.

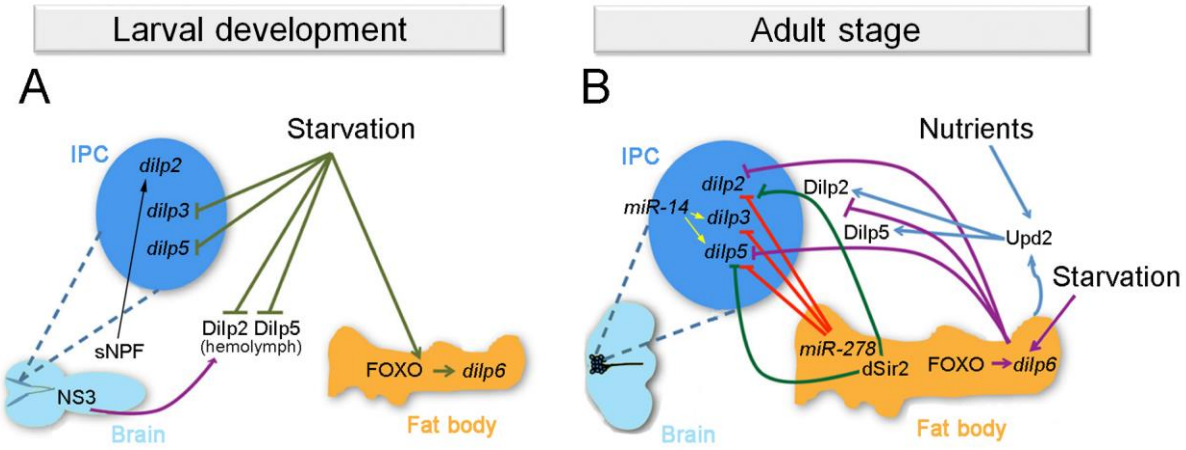

Figure 14: Regulation of *dilp* expression and circulating Dilp levels during larval development and adulthood

Squeme representing some of the players that have been involved in the regulation of *dilp* expression in the insulin producing cells (IPCs) or in controling ciculating Dilp levels during larval development **(A)** and in the adult stage **(B)** in response to nutrient status, transciptional factors, neuropeptides and microRNAs. Interestingly, starvation represses *dilp3* and *dilp5* expression and induces *dilp6* expression through FOXO in the fat body whereas circulating Dilp2 and Dilp5 levels in the hemolymph are reduced **(A, B)**. While *dilp6* negatively regulates *dilp2* and *dilp5* expression and Dilp2 secretion in starved adult animals, Upd2 induces secretion of Dilp2 and Dilp5 in response to sugar and fat diets. Dilp, *Drosophila* insulin-like peptides; NS3, a nucleostemin family GTPase; sNPF, short neuropeptide F; dSir2, a histone deacetylase. Adapted from *(Kannan and Fridell, 2013)*.

- **The TOR signaling pathway**

The role of the protein kinase TOR in mediating nutrient sensing and regulating growth and metabolism at the cellular level is conserved from yeast to mammals (De Virgilio and Loewith, 2006). The TOR kinase is found in two complexes, TORC1 and TORC2 *(Loewith et al., 2002)*. TORC1 is the primary mediator of energy and amino acid sensing, coupling growth cues to cellular metabolism *(Wullschleger et al., 2006)*. TORC1 activity is positively controlled by the small GTPase Rheb [Figure 13, *(Saucedo et al., 2003; Stocker et al., 2003)*]. The tumour suppressors TSC1 and TSC2 (Tuberous Sclerosis Complex genes 1 and 2) act together in a complex to inhibit Rheb activity [Figure 13, *(Inoki et al., 2003a; Tapon et al., 2001; Tee et al., 2003; Zhang et al., 2003)*]. TOR receives information from cellular amino acid and energy levels. It acts as a central regulator of cellular metabolism (promoting anabolism) and growth (which could be considered as a metabolic process *per se*) by regulating a variety of downstream targets, such as the initiation factor 4E binding protein (4EBP), and processes, such as protein bioshynthesis (Figure 13 and next section).

The amino acid-dependent activation of TORC1 occurs downstream of the TSC1/2 complex and is mediated by Rag GTPase proteins (Figure 13). The Rag complex is required for the translocation of TORC1 to the lysosomal surface, a crucial step for TOR activation *(Kim et al., 2008; Sancak et al., 2008; Sancak et al., 2010).* Another study in *Drosophila* proposed that the MAP4K3 kinase could also be involved in the regulation of Rag complex activity by amino acids *(Bryk et al., 2010)*. TORC1-mediated cell growth is also under control of an energy sensing-mechanism that depends on AMP-activated protein kinase (AMPK, Figure 13). AMPK activity monitors the immediately available energy by measuring the cellular ATP levels *(Hardie, 2007)* as well as reserve energy stores in the form of glycogen *(McBride et al., 2009)*. Thus, AMPK signaling is able to negatively regulate growth by phosphorylating and activating TSC2, which results in TORC1 inhibition *(Inoki et al., 2003b).* However, further studies confirming the regulation of TORC1 by AMPK in *Drosophila* need to be done.

- **Crosstalk between the two branches of the Insulin/TOR signaling**

The crosstalk between IIS and TORC1 constitutes a connection between the systemic and the cell intrinsic nutrient-sensing modules. Yet, this connection has been a matter of debate. In human and *Drosophila* cultured cells, treatment with insulin leads to rapid TORC1 activation as a result of TSC1/2 direct phosphorylation and inhibition by Akt [Figure 13, *(Inoki et al., 2002; Potter et al., 2002)*]. However, *in vivo* studies in *Drosophila* have challenged the idea that this link is functionally relevant under physiological conditions. Removal of the Akt phosphorylation sites on Tsc1 and Tsc2 leads to no defects in TOR activation *(Dong and Pan, 2004; Schleich and Teleman, 2009)*. Recently, the protein PRAS40 (Proline-rich AKT substrate 40) has been proposed to link IIS to TORC1 *in vitro (Sancak et al., 2007; Vander Haar et al., 2007).* PRAS40 binds to TORC1 and inhibits its interaction with substrates. Phosphorylation by Akt on a single site relieves this inhibition and is necessary for insulin-induced activation of TORC1 (Figure 13). In *Drosophila*, consistent with an inhibition of TORC1, the overexpression of dPRAS40 reduces tissue growth in an autonomous manner by reducing cell size. While changes in TORC1 activity strongly affect body size, *PRAS40* null mutant flies are viable and present no obvious alterations of cell and body growth, suggesting that *PRAS40* does not regulate TORC1 activity during the growth period in *Drosophila*. Yet, further analysis of adult *PRAS40* mutant females revealed that PRAS40 represses TORC1 in ovaries but not in the rest of the body *(Pallares-Cartes et al., 2012)*. Thus, IIS and TORC1 seem to be linked only in specific tissues, and the activity of PRAS40 mediates this tissue-specific crosstalk.

If the direct interplay between TOR and insulin pathway through Akt has been recently challenged, their functional interaction remains at the center of responses to the nutritional status. A genomic approach allowed to identify dMyc, a transcription factor that promotes protein synthesis via the regulation of ribosome biogenesis *(Grewal et al., 2005)*, as a common target of TOR and insulin signaling *(Teleman et al., 2008).* FOXO directly regulates *dMyc* transcription, while TOR activates dMyc at a post-transcriptional level. These interactions are crucial to mediate the effects of FOXO and TOR upon nutrient deprivation. Another important crosstalk between the two branches is the downstream regulation of the translation inhibitor 4EBP. Whereas TOR activity phosphorylates and inhibits 4EBP, the transcription factor FOXO positively regulates 4EBP transcription *(Junger et al., 2003; Puig et al., 2003)*.

A second conserved member of the FoxO subfamily of transcription factor, the Drosophila FoxA ortholog Forkhead (FKH), has been shown to regulate cellular and organismal size downstream of TOR and nutrient status, thus functionality linking the FoxO family of proteins to the Insulin/TOR signaling, through FOXO and FKH respectively *(Bülow et al., 2010)*.

- **Metabolic functions and key downstream targets of the Insulin and TOR signaling**

Cellular protein biosynthesis

When nutrient levels are low, protein biosynthesis is reduced because it is one of the primary energy-consuming process in the cell. Indeed, this is one of the most important branches that the Insulin and TOR signaling pathways modulate at many different levels. The Insulin and TOR pathways can directly regulate the rate of translation or indirectly through modulation of ribosomal biogenesis.

TORC1 promotes general protein translation through the regulation of the two translational regulators S6K (ribosomal protein kinase 6) and 4EBP (Figure 13). TORC1-mediated inhibition of 4EBP and activation of S6K enable the assembly of the translation pre-initiation complex and stimulate peptide chain elongation, thus enhancing protein synthesis *(Holz et al., 2005; Wang et al., 2001)*. Moreover, the control of RNA polymerase III (Pol III)-dependent transcription, which is responsible for the synthesis of small non-coding RNAs that are essential for mRNA translation, is another essential target of TORC1 in *Drosophila (Marshall et al., 2012)*. Furthermore, TORC1 also regulates ribosome biogenesis by controlling the production of both components of the ribosome: ribosomal proteins and ribosomal RNAs (rRNAs). The control of rRNAs transcription by TORC1 in a nutrition-dependent manner is mediated by promoting

the function of the conserved Pol I transcription factor TIF-1A [transcriptional intermediary factor-1A, Figure 13, *(Grewal et al., 2007)*]. The transcription factor dMyc can control the expression of ribosome synthesis genes *(Grewal et al., 2005)*, and both Insulin and TOR pathways appear to function through dMyc to regulate ribosomal biogenesis. On one hand, dMyc mRNA transcript levels are regulated by FOXO, and TORC1, on the other hand, regulates dMyc protein levels and its localization at gene promoters (Teleman et al., 2008).

Carbohydrate and lipid metabolism

The Insulin and TOR signaling pathways in *Drosophila* have a clear impact on cellular metabolism by regulating lipid and carbohydrate biosynthesis and breakdown. Using a combination of genetics and expression profiling, FOXO was found as an important mediator of the transcriptional response during starvation *(Teleman et al., 2008).* However, the outputs of the Insulin and TOR signaling pathways and the molecular mechanisms downstream regulating lipid and carbohydrate metabolism are not clearly defined*,* although some metabolic enzymes, including regulators of gluconeogenesis such as the phosphoenolpyruvate carboxykinase (PEPCK) and regulators of lipolysis such as the *Drosophila* lipase 4 (dLip4*),* have been experimentally validated *(Gershman et al., 2007; Teleman, 2010; Teleman et al., 2008; Vihervaara and Puig, 2008).* In addition, 4EBP strongly affects fat metabolism working as a 'metabolic brake' that is activated under conditions of environmental stress such as nutrient starvation, most probably through the regulation of overall cellular translation *(Teleman et al., 2005)*. In mammals, activation of Akt increases cell energy supply by promoting the uptake of glucose through the insertion of glucose transporters into the membrane, and by promoting glycogen synthesis through inhibition of glycogen synthase kinase 3β (GSK-3β) *(Taniguchi et al., 2006)*. Whereas GSK-3β (or Shaggy in *Drosophila)* is a target of Akt in flies *(Papadopoulou et al., 2004)*, the relation between insulin signaling and glucose uptake is still unclear in *Drosophila (Ceddia et al., 2003)*.

Autophagy

Autophagy is a conserved starvation response in which cells degrade and recycle their cytoplasm and organelles to maintain amino acid and nutrient levels. In *Drosophila*, strong reduction of TORC1 activity in the adipose tissue induces autophagy even in nutrient rich conditions and its activation is sufficient to suppress starvation-induced autophagy *(Scott et al., 2004)*. Although the molecular mechanism is not completely understood, genetic studies indicate that the activity of the conserved autophagy protein kinase Atg1, one key player sufficient to induce autophagy, is inhibited by TORC1

(Scott et al., 2007). Interestingly, autophagy has been shown to play an important role in lipid mobilization *(Singh et al., 2009; Weidberg et al., 2009)* providing another mechanism by which TORC1 regulates metabolism. Thus, during starvation when Insulin and TOR signaling is low, translation must be repressed (via 4EBP) and autophagy activated (via Atg1) in order to both limit protein synthesis and cell growth and maintain essential nutrient and energy levels required for survival.

Endocytosis

In a genetic screen for modifiers of TOR function, Hsc70, a regulator of clathrin-coated vesicles, was identified. This study opens up new avenues towards the identification of a role for endocytosis in TOR signaling. Authors found that TOR signaling stimulates bulk endocytic uptake while specifically inhibits the endocytic degradation of the amino acid transporter Slimfast, thus maintaining levels of amino acid import required for cellular protein synthesis and growth *(Hennig et al., 2006)*.

Feeding behavior

Both Insulin and TOR signaling are responsible for controlling feeding behavior. For instance, overexpression of FOXO during the first larval periods suppresses the growth and drastically alters feeding behavior by inducing a premature wandering-like behavior and a starvation type response even with adequate food supply *(Kramer and Davidge, 2003).* In what concerns the other branch, besides its cell-autonomous effect on mRNA translation, S6K in a subset of brain cells has also been shown to regulate the feeding behavior of *Drosophila* larvae. Interference with S6K in the IPCs mimics starvation responses, increases the feeding rate and decreases the food selectivity of larvae, while constitutively active S6K partially suppresses starvation-induced changes in feeding behavior *(Wu et al., 2005)*.

4. **The miRNA machinery**

During the last decades, gene regulation has been shown to have a huge importance in many aspects of biology. Regardless of the importance of the gene regulation at the transcriptional level in development, the relevance of post-transcriptional regulation has considerably increased during the last years. It is known that small RNAs (sRNA) regulate gene expression in various organisms. The three main classes of regulatory sRNAs include: microRNAs (miRNAs), short interfering RNAs (siRNAs) and piwi-interacting RNAs (piRNAs). Three aspects separate piRNAs from the other two classes: (1) while the distribution of the miRNAs and siRNAs is broad in both phylogenetic and physiological terms, piRNAs are only found in animals and act typically in the germline, although emerging evidences point to a more widespread role in other tissues; (2) piRNAs appear from single-stranded precursors while the other two classes are preceded from double-stranded antecedents; (3) piRNAs associate with Piwi effector proteins, whereas miRNAs and siRNAs bind to Argonaute (Ago) proteins *(Ishizu et al., 2012; Malone and Hannon, 2009).* What distinguish miRNAs from siRNAs subsist in three aspects, most of them concerning their biogenesis: (1) miRNAs are endogenous products derived from the genome of the own organism, whereas siRNAs are thought to be exogenous, derived from viruses, transposons or transgenes; (2) miRNAs are processed from stem-loop precursors with incomplete double-stranded character, while siRNAs are excised twice, by the same enzyme, from long and fully complementary double-stranded RNAs (dsRNAs); (3) miRNAs interact with Ago-1 and bind to the target by imperfect complementarity at multiple sites, whereas siRNAs are loaded into Ago-2 and habitually form a perfect duplex with their targets at only one site *(Carthew and Sontheimer, 2009; Gomes et al., 2013; Tomari and Zamore, 2005).*

miRNA are short (~20-23 nt long), endogenous, single-stranded, non-coding RNAs that typically inhibit gene expression by base-pairing to partially complementary sites on target messenger RNA (mRNA). In the 1990s, miRNAs were first discovered in the nematode *Caenorhabditis elegans* by the identification of two mutations affecting the *lin-4* and *let-7* genes responsible for disorders in timing of larva development *(Lee et al., 1993; Reinhart et al., 2000)*. Since then, thousands of putative miRNAs have been identified and a huge effort has been made in order to understand their biogenesis, mode of action, regulation and function. In *Drosophila*, the first miRNA reported in 2003 was *bantam*, working as a growth promoting and anti-apoptotic gene *(Brennecke et al., 2003).*

Biogenesis

In insects, as in mammals, the production of miRNAs follows a canonical multistep process that starts in the nucleus and ends in the cytoplasm, and is composed of four main events: transcription of the miRNA loci, cropping, nuclear export and dicing. Finally the mature miRNA is loaded into the miRNA-RNA induced silencing complex (miRISC) to regulate target gene expression *(Kim et al., 2009)*.

The biogenesis of miRNAs starts with the production of the primary miRNA transcript (pri-miRNA) that can measure up to several thousands of nucleotides and are characterized by containing stem-loop structures (Figure 15A). These pri-miRNAs are, for the largest part, transcribed by RNA polymerase II, although a minor group of miRNA located within repetitive sequences are transcribed by RNA polymerase III *(Borchert et al., 2006; Lee et al., 2004b)*, and retain mRNA features such as the 5' cap structure and 3' poly(A) tail. While the majority of miRNAs are derived from intergenic regions quite distant from other annotated genes and found as independent transcription units, a few miRNAs are instead considered intragenic, since they are found in intronic or exonic regions of coding or non-coding host genes. Furthermore, mature miRNAs can arise from monocistronic, bicistronic or polycistronic miRNAs transcripts depending on the degree of clustering *(Lee et al., 2002).*

Still in the nucleus, miRNA maduration starts with the crop of the synthesized pri-miRNA by the Microprocessor complex to produce a ~70 nt pre-miRNA (Figure 15A). In *Drosophila*, the ~500 kDa Microprocessor complex is formed by an RNase III-type enzyme, Drosha, and its dsRNA binding cofactor, Pasha [DiGeorge syndrome critical region gene 8 (DGCR8) in mammals and *C. elegans (Landthaler et al., 2004)*). A typical pri-miRNA consists of ~30 bp stem structure, a terminal loop and flanking ssRNA segments. Pasha/DGCR8 interacts with the pri-miRNA through the ssRNA flanking segments and the stem structure, and assists Drosha to cleave the substrate at the stem of the hairpin structure, ~11 bp away from the ssRNA-dsRNA junction, thus creating an imperfect stem-loop pre-miRNA *(Gregory et al., 2004; Lee et al., 2003b).* It should be noted that intronic pri-miRNA, also known as miRtron, can bypass the Microprocessor step and use classic splicing machinery instead of Drosha cleavage *(Berezikov et al., 2007)*.

The next step implicates Exportin-5, a Ran-GTP dependent nucleo/cytoplasmatic cargo transporter that exports pre-miRNAs out of the nucleus, through nuclear pore complexes, into the cytoplasm *(Lund et al., 2004)*. In the cytoplasm, the terminal loop structure of the pre-miRNA is cleaved by another RNase III-type enzyme, Dicer-1 (Dcr-1), relieving a ~22 nt miRNA-miRNA* duplex (Figure 15A). The *Drosophila*

genome encodes two Dicer enzymes, Dcr-1 and Dcr-2, each with a specialized function in the miRNA and the siRNA pathways, respectively *(Lee et al., 2004a)*. Like Drosha, Dcr-1 also requires a dsRNA binding domain protein partner, Loquacious (Loqs), and together they form the pre-miRNA processing complex *(Saito et al., 2005)*.

After Dcr-1 cleavage, the miRNA-miRNA* duplex is incorporated into the miRISC (microRNA-induced silencing complex) whose core component is the miRNA binding protein Argonaute-1 (Ago1) protein. One strand of the duplex remains in Ago1 as a mature miRNA (guide strand or miRNA), while the other (passenger strand or miRNA*) is degraded (Figure 15A). The *Drosophila* genome encodes five distinct Ago proteins categorized into two sub-clades: Ago and Piwi. The Ago sub-clade comprises Ago-1 and Ago-2, which are largely known to bind miRNAs and siRNAs, respectively, although several studies suggest that certain characteristics of the miRNA-miRNA* duplex influence strand selection and partitioning between Ago proteins *(Okamura et al., 2004; Okamura et al., 2009; Smibert et al., 2011; Yang and Lai, 2011).* For the majority of *Drosophila* miRNAs, the miRNA-Ago complex is ready to perform its action on target sequences, however, some miRNAs require additional processing after Ago loading *(Han et al., 2011)*.

It is important to note, that although the canonical miRNA biogenesis pathway driven by the RNase III enzymes Dcr-1 and Drosha generates the majority of animal miRNAs [Figure 15A, *(Carthew and Sontheimer, 2009; Kim et al., 2009; Ruby et al., 2007)*], a variety of alternative mechanisms that generate functional miRNAs have emerged recently [Figure 15B, C, reviewed in *(Kim et al., 2009; Tétreault and De Guire, 2013; Yang and Lai, 2011)*].

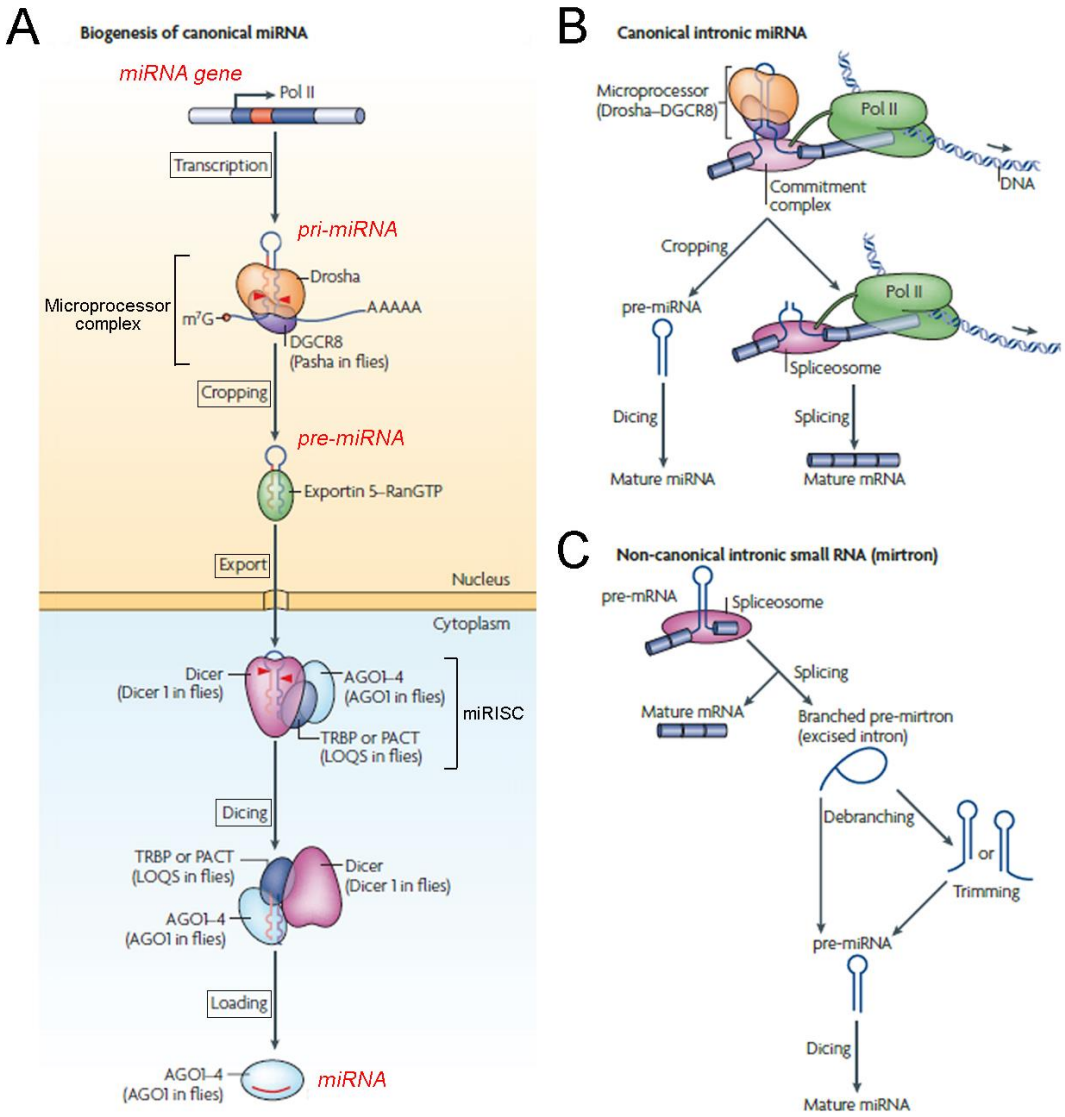

Figure 15: miRNA biogenesis pathways

Cartoon depicting the canonical and major alternative miRNA biogenesis pathways in animals (with the *Drosophila* components in brakets) adapted from *(Kim et al., 2009)*. Briefly, canonical miRNA genes **(A)** are transcribed by RNA polymerase II to generate the primary transcripts (pri-miRNAs) in the nucleus were the Microprocessor complex formed by Drosha/Pasha will crop it to generate the pre-miRNA. This will be exported into the cytoplasm by the nuclear export factor Exportin 5 were Dicer (Dcr) will perform a second cleaveage to produce the miRNA duplex. Then, in *Drosophila*, Dcr-1/Argonaute 1/Loquacious will form the miRISC and one strand of the duplex will remain on the Ago protein as the mature miRNA. **(B)** Canonical intronic miRNA are processed co-transcriptionally before splicing by the Drosha/Pasha complex. **(C)** Non-canonical intronic small RNAs (miRtrons) can bypass the Drosha-processing step and are produced from spliced introns and debranching.

Mode of action

Typically, within the miRISC, the mature miRNAs guide Ago proteins to fully or partially complementary mRNA targets, which are then silenced post-transcriptionally. Most miRNAs base-pair imperfectly with a sequence in the 3' untranslated region (3' UTR) of target mRNAs via a sequence between their 2nd and 8th nt of their 5' extreme known as the 'seed region' *(Lewis et al., 2005)*. However, emerging evidence for functional binding sites of miRNAs in the 5' UTR and in Open Reading Frames of mRNAs have been also identified *(Forman and Coller, 2010; Lytle et al., 2007)*. The regulatory mechanism by which miRNAs regulate gene expression is a complex process that involves both translational inhibition and/or mRNA degradation *(Pillai et al., 2007)*. The choice between these two mechanisms depends on specific features of the structure formed by the miRNA-mRNA duplex, such as the total number of miRNA binding sites or their position within the 3' UTR, as well as the predisposition of certain complementally proteins associated with a given mRNA *target (Eulalio et al., 2007a; Grimson et al., 2007)*. Although miRNAs have long been thought only to downregulate protein synthesis, miRNAs are also capable, under certain conditions, of activating translation *(Vasudevan et al., 2007*).

In animals, miRNA-mediated translational repression can occur either before or after translation initiation. Translation requires numerous factors that are involved in the recruitment of the ribosomal subunits to mRNAs. These mRNAs have to possess a 5' cap structure and a 3' poly(A) in order to form the characteristic mRNA closed loop to be efficiently translated and protected to degradation once all the translational machinery is recruited. Translational repression by miRNA has been proposed to occur in four distinct ways: inhibition of translational initiation, inhibition of translational elongation, co-translational protein degradation and premature termination of translation through several molecular mechanisms summarized in Figure 16 *(Carthew and Sontheimer, 2009; Eulalio et al., 2008; Huntzinger and Izaurralde, 2011)*. In addition to translational repression, miRNAs can induce significant degradation of mRNA targets. The mechanism of miRNA-mediated targeted degradation can occur in two different ways. As it happens in plants, full complementarity of animal miRNA to its target may lead to cleavage by Ago proteins. However, in most of the circumstances, mRNA degradation in animals occurs through the general mRNA decay pathway, where miRNAs have been shown to accelerate deadenylation and

decapping of their targets [Figure 16 *(Eulalio et al., 2008; Filipowicz et al., 2008; Huntzinger and Izaurralde, 2011; Pillai et al., 2007)*]. The importance of the intracellular cytoplasmatic domains called P-bodies, where mRNAs aggregate for either storage or degradation, has been shown to play crucial roles

in miRNA-mediated silencing functions *(Bhattacharyya et al., 2006; Eulalio et al., 2007b; Rehwinkel et al., 2005).*

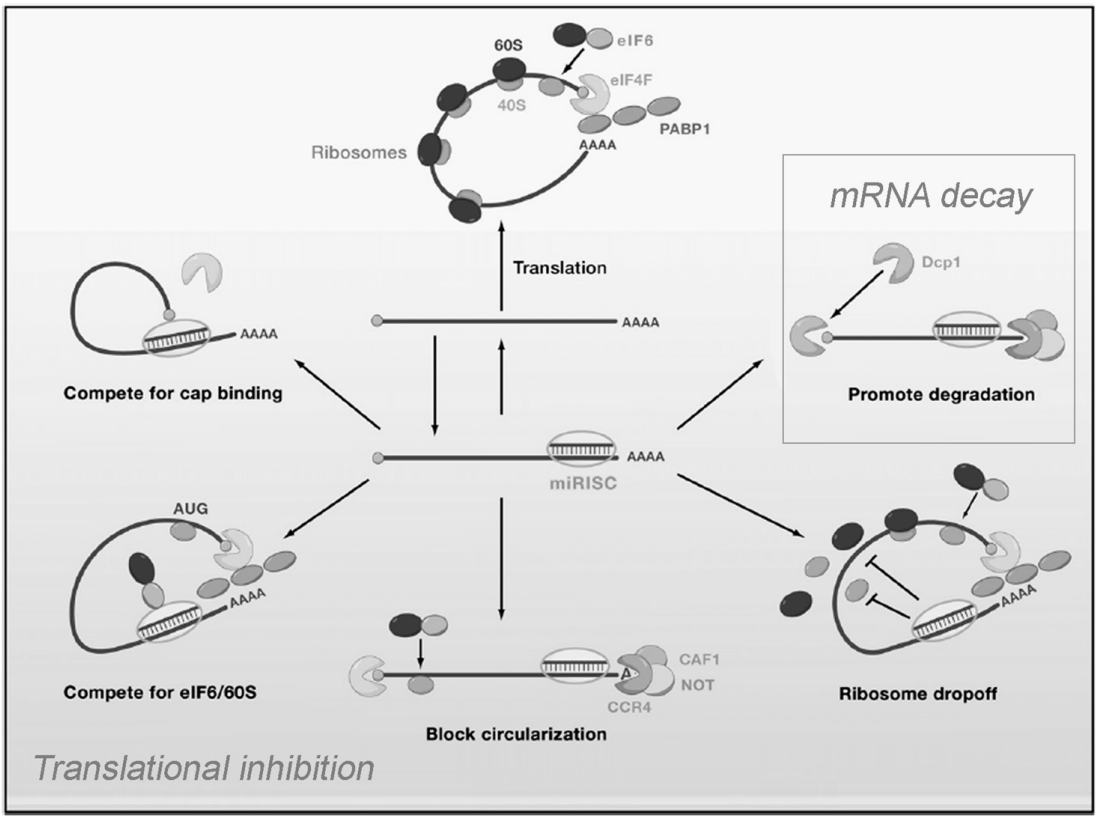

Figure 16: Possible miRNA-mediated repression mechanism

Non-repressed mRNAs recruit initiation factors and ribosomal subunits and form circularized structures to enhance translation (top). When miRISCs bind to mRNAs target, they can repress initiation at the cap recognition step (upper left) or the 60S recruitment stage (lower left). Alternatively, they can induce deadenylation of the mRNA thus inhibiting circularization of the mRNA (bottom). MicroRNAs can also repress a post-initiation stage of translation by inducing ribosomes to drop off (lower right) or by slowing the elongation. Finally, they can promote mRNA degradation by inducing deadenylation followed by decapping (upper right). Adapted from *(Carthew and Sontheimer, 2009)*.

Functions

Since their discovery in *C. elegans,* more than 900 mammalian miRNAs have been experimentally validated and up to 2000 predicted in humans *(Friedman et al., 2009)*. These numbers are still increasing in mammals, as well as in *Drosophila.* It is accepted that miRNAs account for ~1% of all predicted genes

in humans, nematodes and *Drosophila* and therefore make-up one of the major families of gene regulatory molecules *(Lai et al., 2003; Lim et al., 2003a; Lim et al., 2003b)*. The limited complementarity between a miRNA and its target was first considered as a weak-point. However, this property allows a single miRNA to inhibit simultaneously the expression of hundreds of different mRNAs. In addition, one gene can be regulated by multiple microRNAs, thus opening a large combinatorial power to these molecules. Therefore, miRNAs have emerged as very potent regulators of gene expression that have been found to regulate over 30% of mRNAs in a cell. In the last decade, functional analysis have recognized miRNAs as mayor players in almost every biological process, such as apoptosis, cell proliferation, cell growth, cell differentiation, energy homeostasis and metabolism, behavior and heterochromatin regulation, among *others (Ambros, 2003; Chivukula and Mendell, 2008; Dumortier et al., 2013; Ge et al., 2012; Jaubert et al., 2007; Krützfeldt and Stoffel, 2006; Lucas and Raikhel, 2013; Ruby et al., 2007)*. Also, they have been shown to perform important roles during development *(Hornstein and Shomron, 2006; Jones and Newbury, 2010)*, stress *response (De Lella Ezcurra et al., 2012; Leung and Sharp, 2007; Leung and Sharp, 2010; Simone et al., 2009; Wang and Taniguchi, 2013),* immune response *(Fullaondo and Lee, 2012)*, aging *(Garg and Cohen, 2014; Smith-Vikos and Slack, 2012)* and, of course, in cancer and other diseases *(Di Leva et al., 2014; van Kouwenhove et al., 2011)*.

In many cases, a single miRNA affects multiple biological processes through different targets (Table 1). For instance, besides its role in cell death, *miR-14* is involved in fat metabolism by regulating the level of triacylglycerols and diacylglycerols *(Xu et al., 2003)*. Another clear example is the conserved miRNA *miR-8*. Originally, *miR-8* was involved in some aspects of neural development. It is able to prevent neurodegeneration by reducing the levels of Atrophin in the brain, thus preventing premature cell death *(Karres et al., 2007)*. It also controls synapse structure by repressing the actin regulator Enable *(Loya et al., 2014). miR-8* acts as negative regulator of the Wingless signaling pathway in the developing eye *(Kennell et al., 2008).* Moreover, *miR-8* has been involved in growth control and tumourogensis through inhibition of the Notch ligand Serrate *(Vallejo et al., 2011)*. It also affects the regulation of body size in response to ecdysone signaling by affecting insulin signaling in the larval fat *body (Hyun et al., 2009; Jin et al., 2012)*. Finally, *miR-8* has been shown to contribute to immune homeostasis through the regulation of several targets in the fat body *(Lee and Hyun, 2014)*.

One possibility to address the role of miRNAs is by disrupting enzymes involved in the miRNA biogenesis pathway and, as such, several reports have used mutations in *dcr-1*. For instance, loss of dcr-1 causes defects in *Drosophila* stem cell maintenance *(Jin and Xie, 2007)* or reduced cell and tissue growth

(Herranz et al., 2010). However, it is essential to identify the specific miRNAs involved as well as their biologically relevant targets to fully understand the molecular mechanism. In Table 1, there is a summary of examples of experimentally verified targets of miRNA in *Drosophila*.

miRNA	Target gene	Function/mechanism affected	References
bantam	Hid	Apoptosis	(Brennecke et al., 2003)
	Clock	Circadian rhythm	*(Kadener et al., 2009)*
	optomotor-blind (omb)	Optic lobe development	*(Li and Padgett, 2012)*
	enable	Actin cytoskeleton	*(Becam et al., 2011)*
	Socs36E	Growth control	(Herranz et al., 2012b)
	(?)	Ecdyson singaling/systemic growth	*(Boulan et al., 2013)*
let-7	abrupt	Metamorphosis	*(Caygill and Johnston, 2008)*
	IGF-II mRNA-binding protein (Imp)	Stem cell behavior	*(Toledano et al., 2012)*
miR-iab4	Ultrabithorax	Wing development	*(Ronshaugen et al., 2005)*
miR-1	Delta	Cardiogenesis	*(Kwon et al., 2005)*
miR-6	Rpr,hid,grim, skl	Apoptosis	*(Ge et al., 2012)*
miR-7	Yan	Photoreceptor differentation	*(Li and Carthew, 2005)*
	Bag-of-marbles	Germline differentation	*(Pek et al., 2009)*
miR-8	Atrophin	Apoptosis/neurodegeneration	*(Karres et al., 2007)*
	Wingless/TCF/CG32767	Wingless singaniling pathway	*(Kennell et al., 2008)*
	U-shaped	Insulin signaling/growth	*(Hyun et al., 2009)*
	Serrate	Notch signaling/growth	*(Vallejo et al., 2011)*
	Toll/dorsal	Immune response	*(Lee and Hyun, 2014)*
miR-9a	senseless	Neuronal development	*(Li et al., 2006)*
	dLMO	Apoptosis	*(Bejarano et al., 2010)*
miR-11	reaper,hid,grim, sickle	Apoptosis	*(Ge et al., 2012)*
miR-14	(?)	Apoptosis/Fat metabolism	*(Xu et al., 2003)*
	Ecdyson receptor	Ecdyson signaling	*(Varghese and Cohen, 2007)*
	sugarbabe	Insulin signaling/metabolism	*(Varghese et al., 2010)*
miR-124	anachronism	Neuronal development	*(Weng and Cohen, 2012)*
miR-184	saxophone	Germline differentation	*(Iovino et al., 2009)*
	tramtrack	Embryonic patterning	*(Iovino et al., 2009)*
miR-278	expanded	Insulin signaling/metabolism	*(Teleman and Cohen, 2006)*
miR-279	nerfin-1	Neuronal olfactory development	*(Cayirlioglu et al., 2008)*

Table 1: *Drosophila* miRNA

Table compiling a summary of examples of experimentally validated target genes and functions of several *Drosophila* miRNAs.

5. **Project and objectives**

The p53 tumour suppressor protein is a vital regulator of several stress responses and plays a fundamental role during cancer development. Induction of apoptosis and cell cycle arrest are well-understood functions of p53 and are traditionally accepted as the major mechanisms by which p53 promotes genomic stability and prevents tumour formation. In the last few years, p53 has emerged as an important regulator of several metabolic pathways able to trigger a cellular adaptive response to nutrient deprivation. This function of p53 may contribute not only to tumour suppression, but also to the ability of normal cells to adapt to starvation.

The major objetives of this thesis can be summarized as follows:

- To analyze and confirm the classical roles of Dp53 as a tumour suppressor protein in *Drosophila* epithelial tissues.

- To characterize the potential role of Dp53 in organismal homeostasis in a situation of nutritional stress.

- To identify the molecular mechanism by which Dp53 activity is regulated in *Drosophila.*

- To define the physiological relevance of this molecular mechanism regulating Dp53 under different stress conditions.

ReSuLTS

RESULTS

1. Classical roles of *Drosophila* p53 as a tumour suppressor protein

As described in the introduction of this thesis, the *Drosophila* homologue of p53 (Dp53) shares significant amino acid identity with the mammalian p53, including specific residues frequently associated with human cancer. The core DNA binding domain has the greatest sequence similarity, while the N- and C-terminal domains show little sequence conservation but retain similar structural and functional features *(Brodsky et al., 2000; Jin et al., 2000; Ollmann et al., 2000; Rutkowski et al., 2010)*. The tumour suppressor protein p53 acts as a central regulator of the stress response and a wide variety of stress signals converge on p53 to induce different cellular responses.

In the following sections we will analyze in detail the classical roles of Dp53 as a tumour suppressor protein, meaning apoptosis, cell cycle arrest and DNA repair. For that, we will perform two different approaches: (1) analyze the capacity of Dp53 to induce programmed cell death and arrest the cell cycle when overexpressed and (2) dissect the function of Dp53 upon DNA damage by blocking its activity after exposure to ionizing radiation (IR).

Dp53 is able to induce apoptosis and cell cycle arrest when overexpressed

To investigate the potential capacity of Dp53 in inducing programmed cell death (PCD, also known as apoptosis) and cell cycle arrest we decided to overexpress a wild-type form of Dp53 in a temporally and spatially controlled manner by combining the UAS/Gal4 system *(Brand and Perrimon, 1993)* with the thermosensitive version of Gal80 [Gal80^{ts}, *(McGuire et al., 2004)*], a repressor of Gal4 protein activity (see Materials and Methods for more details). By using the *engrailed* (*en*)-*gal4* driver we promoted Dp53 expression in the posterior (P) compartment of the disc and the anterior (A) compartment was used as a control.

Dp53 transcriptionally activates the pro-apoptotic gene *reaper* (*rpr*) to induce apoptosis due to the existence of a conserved response element in its promoter region *(Brodsky et al., 2000)*. Consistently,

overexpression of Dp53 (24 hours of transgene expression) induces up-regulation of the *rpr* mRNA levels (compare Figure 1A and 1B) and a clear apoptotic response as shown by positive staining for activated caspases (using an antibody against the cleaved form of human Caspase-3, which is a marker of Caspase-9-like Dronc activity in *Drosophila*, Caspase-3*, Figure 1C) and by the presence of TUNEL positive cells (that labels DNA strand breaks, Figure 1D) in the basal side of the epithelia were apoptotic cells accumulate. Moreover, overexpression of Dp53 also induces activation of the Jun-N-terminal kinase (JNK) signaling pathway (visualized by the expression of *puckered-lacZ* reporter, a transcriptional target gene of JNK signaling, Figure 1E), a well-known stress pathway that plays a prominent role in inducing apoptosis *(McEwen and Peifer, 2005; Shlevkov and Morata, 2012)*.

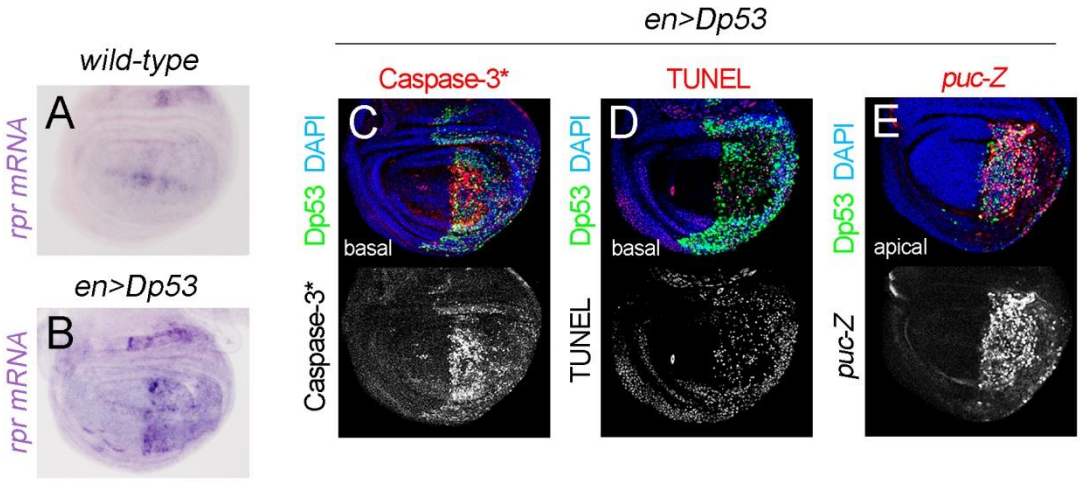

Figure 1: Dp53 overexpression is able to induce apoptosis

(A-E) Wing primordia from *wild-type* larvae (A) or larvae expressing a wild-type form of Dp53 under the control of a temperature sensitive *en-Gal*^{80ts} driver for a period of 24 hours (*en>Dp53,* B-E) labeled to visualize *reaper (rpr)* mRNA levels (A, B); DAPI (blue, C-E), Dp53 protein (green, C-E), activated Caspase-3 (red or grey, C), TUNEL-positive cells (red or grey, D) or *puckered* activity (*puc-Z*, red or grey, E). *en-Gal*^{80ts} drive transgene expression in the posterior compartment. X-Y sections of the basal and apical sides of the wing epithelia are shown. Note that almost all the *engrailed* population of cells activate *rpr* expression, JNK and caspases upon Dp53 overexpression which leads to a massive induction of apoptosis.

While all the studies, and our results, agree with the capacity to induce programmed cell death, the ability of Dp53 to modulate cell cycle progression is hotly debated. Therefore, we investigated the capacity of Dp53 to regulate the cell cycle by carefully analyzing several cell cycle markers upon Dp53 overexpression. In order to avoid massive apoptosis and prevent the loss of the tissue, we overexpressed a wild-type form of Dp53 in the P compartment under the control of the*en-Gal*^{80ts} driver for a shorter

period of time (12 hours). In this condition, we monitored several cell cycle regulators involved in both G_1-S (Cyclin E, E2F and Dacapo) and G_2-M (Cyclin B and String) transitions as well as BrdU incorporation to visualize cells in the S phase. Overexpression of Dp53 induced a clear reduction in BrdU incorporation and a strong accumulation of Cyclin E protein levels (CycE, Figure 2A-B) indicating that these cells are arrested in G_1 and cannot go through the S phase. CycE/CDK1 activity can be regulated by several different mechanisms. (1) The *Drosophila* E2F1 transcription factor (together with its co-factor DP) induces the transcription of "S-phase genes" such as CycE *(Dynlacht et al., 1994)*. (2) Dacapo (Dap) is a *Drosophila* member of the p21/p27 family of CDK inhibitors that inhibits CycE/CDK1 *(Lane et al., 1996)*, and it is know that p21 is a transcriptional target of p53 largely responsible for the p53-dependent G_1-S arrest in mammals *(Deng et al., 1995)*, and finally, (3) Archipielago (Ago) is a F-box protein and a direct downstream target of Dp53 that contributes to the proteosomal degradation of CycE under mitochondrial dysfuntion *(Mandal et al., 2010)*. To elucidate whether the effects on CycE and G_1-S progression seen upon Dp53 overexpression relay on any of these mechanisms, we measured E2F1 activity [visualized by the expression of the E2F1-responsive reporter ORC1-GFP, E2F sensor in Figure 2C, *(Asano and Wharton, 1999)*], Dacapo (Figure 2D) and Archipielago (Figure 2E) protein levels. Upon Dp53 overexpression we found that none of them was affected. In what concern the G_2-M transition, we observed an increase in the Cyclin B protein levels (Figure 2F) and a strong decrease in *string* mRNA levels [a phosphatase that acts as a critical regulator of the activity of CycA-B/CDK2 dimers responsible for driving cells into mitosis *(Milán et al., 1996)* (Figure 2G and H)] after Dp53 overexpression, suggesting that those cells might be arrested in G_2 as well.

Altogether, our overexpression experiments confirm the evolutionary conserved role of Dp53 in autonomously inducing programmed cell death and show that Dp53 is able to stop the cell cycle.

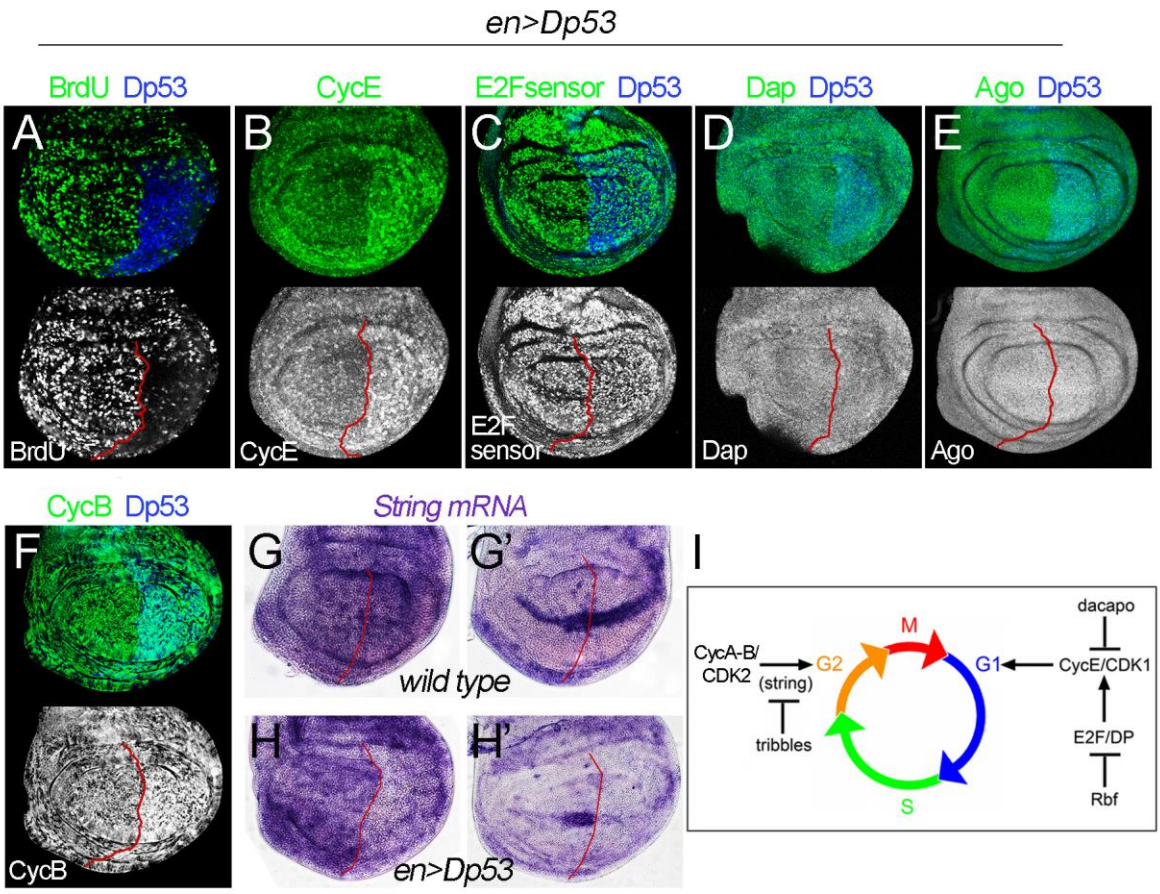

Figure 2: Dp53 overexpression is able to compromise G_1-S and G_2-M transitions

(A-F) Wing primordia expressing a *wild-type* form of Dp53 for a period of 12 hours under the control of a temperature sensitive *en-Gal*^{80ts} driver and labeled to visualize Dp53 protein levels (blue in A, C-F), BrdU incorporation (green or grey in A), Cyclin E (green or grey in B), E2F1 activity (green or grey in C), Dacapo (green or grey in D), Archipielago (green or grey in E) and Cyclin B (green or grey in F) protein levels. **(G-H)** *wild-type* (G-G') and *en>Dp53* (H-H') wing discs in two different time points of development (mid L3 (120 hours) in G and H and late L3 (144 hours) in G' and H') labeled to visualze *string* mRNA levels. *en-Gal*^{80ts} drive transgene expression in the posterior compartment (red line marks the anterior-posterior boundary). Note that Dp53 overexpression in the posterior compartment induces a decrease in BrdU incorporation and *string* mRNA levels, and accumulation of Cyclin E and Cyclin B protein levels. **(I)** Squeme showing a simple representation of the cell cylce regulation in *Drosophila.*

Dp53 functions upon ionizing radiation-induced DNA damage

One of the known signals that trigger p53 activation is DNA damage. When exposed to DNA-damaging agents, components of the DNA damage response (DDR) pathway phosphorylate, stabilize and activate p53 that acts as a major downstream effector driving apoptosis, cell cycle arrest and DNA repair

in mammals *(Lane and Levine, 2010; Jackson and Bartek, 2009)*. We then revisited the role of Dp53 in inducing these three effects upon DNA damage.

- **No doubt: Dp53 is able to induce apoptosis**

Like its mammalian counterparts, Dp53 has been shown to PCD in response to ionizing radiation (IR)-induced DNA damage [Figure 3I, *(Brodsky et al., 2000; Jin et al., 2000; Ollmann et al., 2000; Sogame et al., 2003; Lee et al., 2003)*]. Cell death is almost absent in *Drosophila* developing wing primordia [Figure 3A, *(Milán et al., 1997*)] but when *wild-type* larvae are exposed to high doses of IR, the wing primordia exhibit massive apoptotic cell death *(Haynie and Bryant, 1976)* as shown by positive staining for activated caspases (Caspase-3*, Figure 3C) and TUNEL staining (Figure 3A'-A'''').

The Jun-N-terminal kinase (JNK) signaling pathway induces apoptosis in response to IR in *Drosophila* tissues *(McEwen and Peifer, 2005)*. Consistently, JNK signaling is activated following IR (visualized by the expression of *puckered-lacZ* reporter, *puc-Z*, Figure 3E). In contrast, in the absence of Dp53, IR-induced JNK activation and apoptosis is reverted (Figure 3B, D, F, G-H). We analyzed *puc-Z* expression and apoptosis in wing primordia of *dp53* mutant larvae, $dp53^{ns}$ (Figure 3B , D), a null allele consisting in a deletion that covers the formerly first exon and the beginning of the second intron *(Sogame et al., 2003)* or wing primordia with reduced Dp53 activity. In the latter case, $dp53^{H159.N}$ (Figure 3F, H), a dominant negative version of Dp53 carrying a point mutation in the DNA binding domain *(Ollmann et al., 2000)]*, or $dp53^{RNAi}$ (Figure 3G, a dsRNA form against *dp53*) were expressed in the posterior (P) compartment of wing primordia using the *engrailed-gal4 (en-gal4)* driver. In all cases, exposure to IR neither activated JNK nor induced apoptosis (Fig 3B, D, F, G-H) thus confirming the central role of Dp53 in connecting the DNA damage signaling pathway to the core of the apoptotic machinery.

While the fast induction of apoptosis following IR required Dp53, there was a late Dp53-independent and JNK-dependent wave of apoptosis induction that started 24 hours after exposure to IR (Figure 1B''-B''''). This late apoptotic response is most probably due to DNA damage-induced aneuploidy *(McNamee and Brodsky, 2009; Dekanty et al., 2012)*.

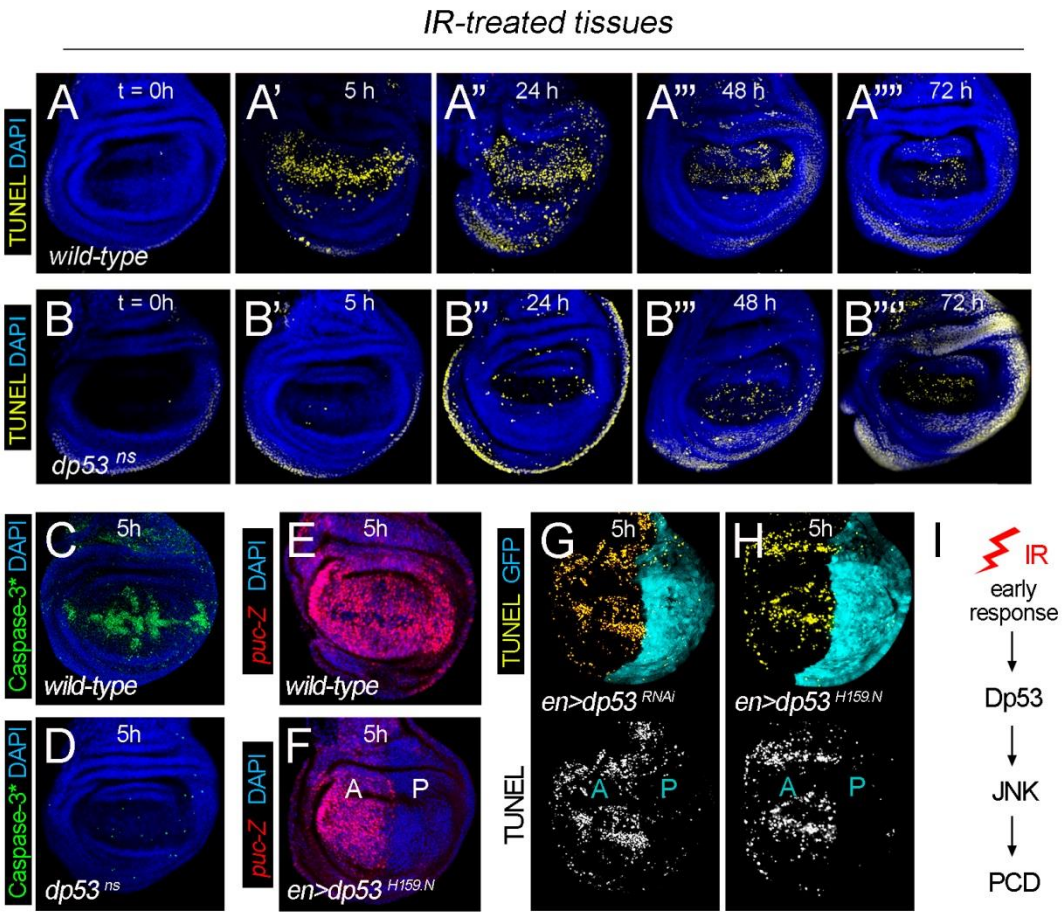

Figure 3: DNA damage-induced activation of Dp53 is able to trigger early apoptosis

(A-E) Wing primordia from *wild-type* (A-A'''', C, E) or $dp53^{ns}$ (B-B'''', D) larvae subjected to a high dose of ionizing-radiation (IR, 4000 R) at the indicated time points before dissection, and labeled to visualize DAPI (blue), TUNEL-positive cells (yellow), activated Caspase-3 (green) and *puckered* activity (*puc-Z*, red). **(F-H)** Wing primordia dissected 5 hours after exposure to IR expressing GFP (cyan in G-H) and $dp53^{H159.N}$ (a dominant negative form of dp53, in F, H) or $dp53^{RNAi}$ (in G) under the *en-gal4* driver and stained to visualize DAPI (blue, F), TUNEL-positive cells (yellow or grey, G-H) and *puckered* activity (*puc-Z*, red, F). *en-gal4* (F-H) drives transgene expression in the posterior (P) compartment. Anterior (A) and posterior (P) compartments are indicated. X-Y sections of the basal (A-D and G-H) and apical (E-F) sides of the wing epithelia are shown. **(I)** Squeme showing the main elements involved in the early apoptotic response to IR.

- **The controversy: is Dp53 able to induce cell cycle arrest and DNA repair?**

Whereas apoptosis induction by Dp53 is clearly conserved between *Drosophila* and vertebrates, the ability of Dp53 to regulate cell cycle and DNA repair upon DNA damage remains controversial. A number of studies support the hypothesis that Dp53 is only required for DNA damage-induced apoptosis *(Brodsky et al., 2000; Jin et al., 2000; Ollmann et al., 2000; Sogame et al., 2003; Jaklevic and Su, 2004;*

Titen and Golic, 2008). However, other studies claim that Dp53 may also play a role in DNA repair after genotoxic challenge *(Jassim et al., 2003; Brodsky et al., 2004; Akdemir et al., 2007; Wells and Johnston, 2012)*. Finally, the consensus is that Dp53 is not required for IR-induced cell cycle arrest, with only one single exception found in the literature *(Akdemir et al., 2007)*].

To address the role of Dp53 in cell cycle arrest we visualized mitotic cells by stainning against a phosphorylated form of histone H3 (PH3). *Drosophila* imaginal discs proliferate by mitotic divisions during development, and cells that undergo M phase are random and homogeneously distributed along the epithelia [Figure 3A, *(Milán et al., 1996)*]. In response to DNA lesions, Tefu (the Ataxia Telangiectasia–mutated, ATM, ortholog) and Mei-41 (the Ataxia Telangiectasia–related, ATR, ortholog) kinases are rapidly activated and phosphorylate many substrates including the downstream kinases Mnk (the Chk2 ortholog) and grapes (Grp, the Chk1 ortholog) respectively [Figure 3I, *(Brodsky et al., 2004; Jaklevic and Su, 2004)*]. Whereas Mnk is known to activate Dp53 and then induce apoptosis, Mei-41 and Grapes promote cell cycle arrest after DNA damage. Consistently, down-regulation of *grapes* (by expressing a dsRNA form against *grapes* under the control of the *ci-gal4* driver) allowed the cells to undergo through G_2-M and maintained the wild-type number of mitotic cells despite the IR treatment (Figure 4C see also Figure 4A-B). Conversely, down-regulation of Dp53 (by expressing $dp53^{H159.N}$ under the control of the *en-gal4* driver) did not affect cell cycle arrest upon IR (Figure 4D).

To study the contribution of Dp53 in DNA repair upon IR we analyzed the levels of phosphorylated H2Av (pH2Av), the functional homolog of H2AX in *Drosophila*, that mark DNA double-strand breaks (Madigan et al., 2002). *Wild-type* wing discs subjected to IR and dissected 24 hours later showed elevated levels of pH2Av (compare Figure 4E with 3F). Interestingly, reduction of okra [the *Drosophila* homolog of Rad54, a DEAD-like helicase involved in homologous recombination *(Kooistra et al., 1997)*] or Dp53 activity in the posterior compartment showed higher pH2Av levels after IR when compared to the *wild-type* anterior domain (labeled by Ci in red).

Altogether, our results reinforce the proposal that Dp53 contributes to DNA repair upon IR and confirm that DNA damage-induced cell cycle arrest is Dp53 independent in *Drosophila* wing imaginal discs. However, overexpressed Dp53 is able to regulate cell cycle progression, suggesting that low Dp53 activation levels (IR-induction) does not arrest the cell cycle whereas high levels do. Alternatively, this could also directly depend on the origin and type of the stress, as Dp53 is able to induce a G_1-S arrest in epithelial cells upon mitochondrial dysfunction *(Mandal et al., 2010)*.

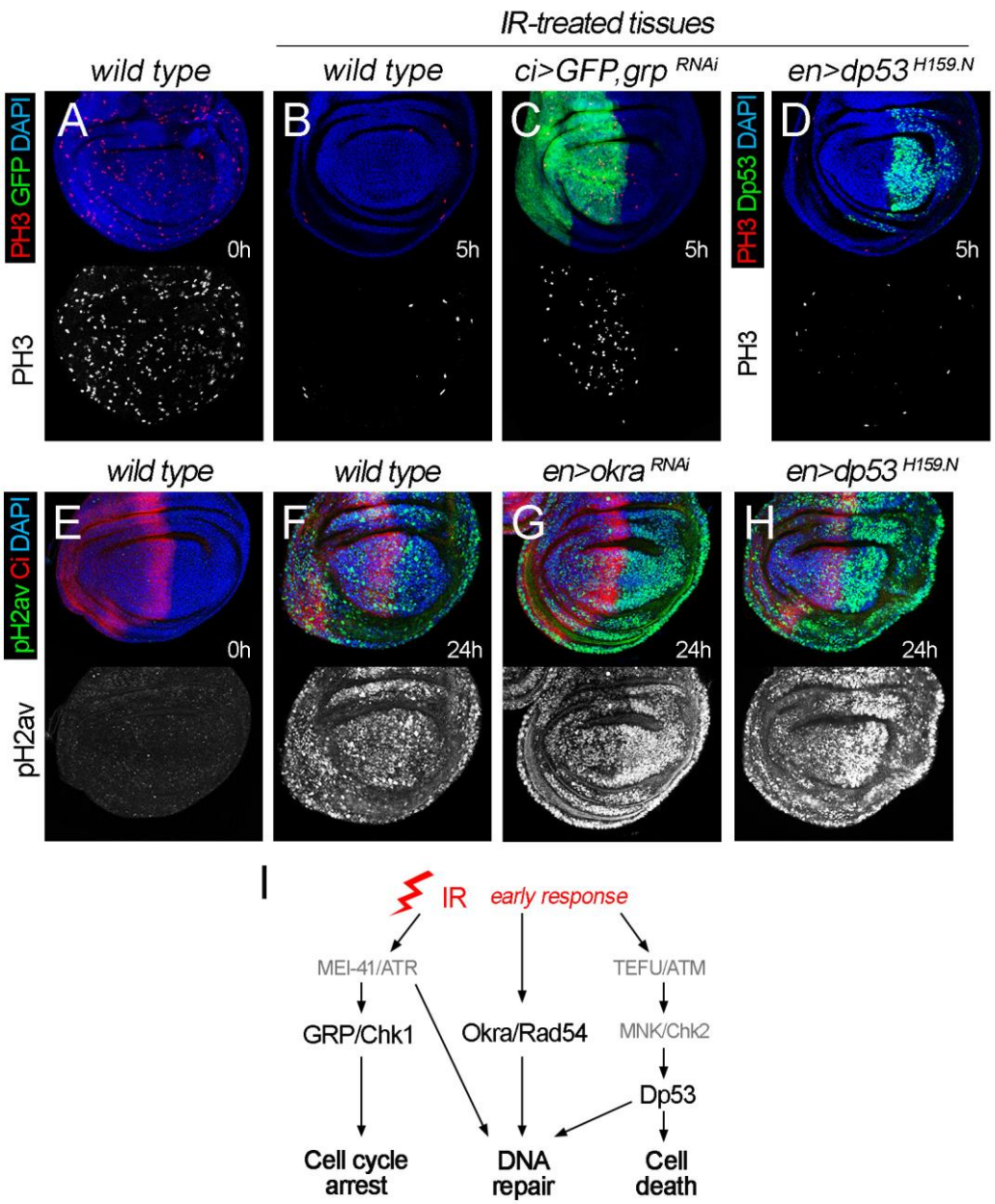

Figure 4: Dp53 activation under IR contributes to the DNA repair but does not affect cell cycle arrest

(A-D) Wing primordia from *wild-type* (A-B), *ci>GFP,grp*^{RNAi} (C) and *en>dp53*$^{H159.N}$ larvae subjected to a high dose of ionizing-radiation (IR, 4000 R) at the indicated time points before dissection, and labeled to visualize mitotic cells through PH3 staining (red or grey), DAPI (blue) and GFP (green in C) or Dp53 protein levels (green in D). Note that Dp53 depleted cells stil undergo G2 cell cycle arrest. **(E-H)** Wing primordia from *wild-type* (E-F), *en>okra*^{RNAi} (G) and *en>dp53*$^{H159.N}$ (H) larvae subjected to a high dose of IR at the indicated time points before dissection, and labeled to visualize DNA damage through phosphorylated H2av (pH2av, green or grey), Ci (red) and DAPI (blue). Downregulation of both okra and Dp53 increase pH2av levels. *en-gal4* (D,G-H) and *ci-gal4* (C) drive transgene expression in the posterior and the anterior compartment respectively. **(I)** Squeme showing the main elements involved in the DNA damage response pathway in *Drosophila*.

2. A new role for Dp53 in regulating the metabolic adaptation to nutrient deprivation

Dp53 contributes to the metabolic adaptation to nutrient deprivation

Apoptosis, cell cycle arrest, DNA repair and senescence are well-understood functions of p53, and are traditionally accepted as the major mechanisms by which p53 promotes genomic stability and prevents tumour formation. Interestingly, recent discoveries indicate that the tumour suppressor activity of p53 also relies on its capacity to regulate cellular metabolism. p53 has emerged as a key regulator of metabolic homeostasis through the transcriptional regulation of target genes involved in glycolysis, lipid metabolism, mitochondrial oxidative phosphorylation, glutaminolysis, autophagy and regulators of the anti-oxidant response (review in *Berkers et al., 2013; Liang et al., 2013; Maddocks and Vousden, 2011*). Furthermore, p53 has also been proposed to function in the adaptive response to nutrient deprivation at a cellular level. In cultured cells, p53 induces cell cycle arrest and promotes cell survival in response to transient glucose deprivation *(Jones et al., 2005)* and regulates autophagic flux and increases cell fitness upon starvation *(Scherz-Shouval et al., 2010)*. It has also been shown that p53 preserves the anti-oxidant capacity of the cell and increases survival rates upon serine deprivation *(Maddocks et al., 2013)*. All these evidences supporting a function of p53 in regulation of cellular metabolism come from experiments that have been done mainly in cancer cell lines with a special focus in understanding cancer biology. However, one could expect that the metabolic function of p53 could be also important in normal physiology and at the organismal level. To address this question, we took advantage of *Drosophila*, a very attractive model system whereby the physiology and the molecular mechanism that control metabolic homeostasis display significant parallels with vertebrates.

- ***dp53* mutants show sensitivity to different conditions of nutrient deprivation**

To study whether Dp53 is involved in nutrient sensing and in regulating metabolism at the organismal level, we tested the ability of *dp53* mutant flies to survive under different restricted nutritional conditions. Animals mutants for *dp53* are viable and with no apparent developmental defects besides a modest reduction in the apoptosis of primordial germ cells *(Sogame et al., 2003; Yamada et al., 2008)*. Moreover, flies lacking *dp53* show increased life span under normal food conditions *(Waskar et al., 2009)*. As a first step towards assessing possible metabolic functions of *dp53,* we exposed young

adult flies (1- to 2-day old) to acute starvation [2% agar, 1% sucrose; *(Géminard et al., 2009)*] and compared the survival rates of *dp53* mutant and *control* animals. For these experiments we used two null alleles of *dp53*: $dp53^{ns}$ and $dp53^{5A14}$ (see introduction for more details), both of them backcrossed six times into the w^{1118} genetic background to isogenize the strains and minimize possible genetic background effects on survival rates. Interestingly, we observed a clear reduction in the survival rates of *dp53* mutant adult flies when compared to *controls* in both males (Figure 5A, C) and females (Figure 5B, D) (statistical analysis are summarized in Table 1).

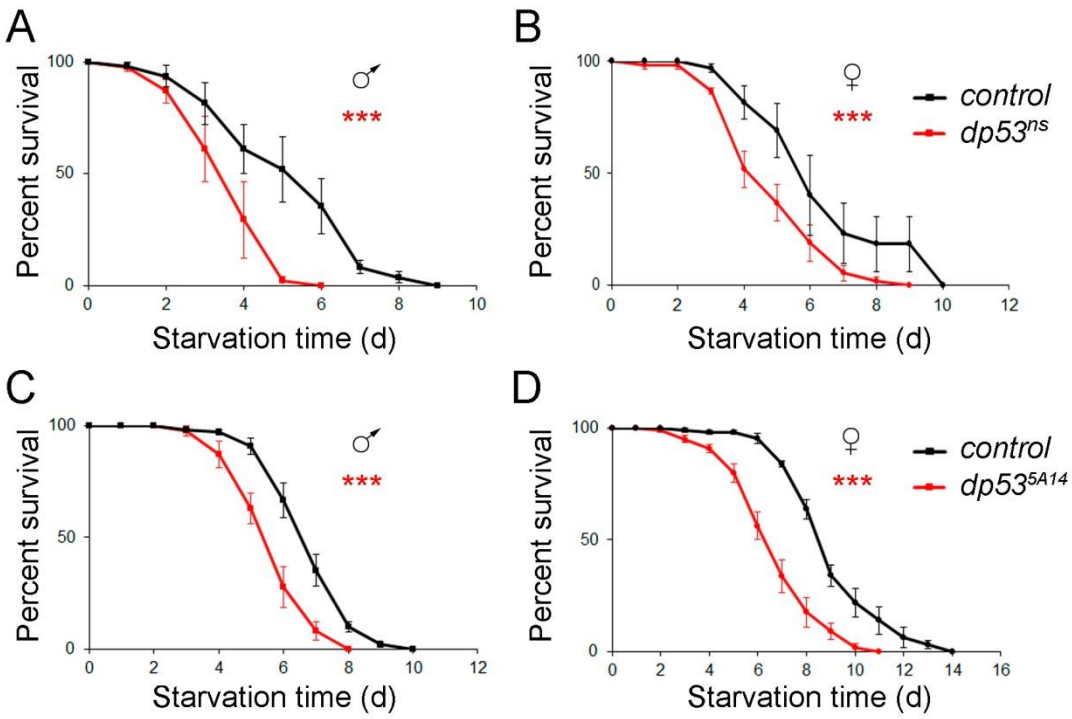

Figure 5: *dp53* mutant adult flies are sensitive to acute starvation

(A-D) Survival rates to acute starvation (2% of agar, 1% sucrose) of 1- to 2-days old adult *dp53* mutant [$dp53^{ns}$ (A, B) and $dp53^{5A14}$ (C, D) in red] and control (w^{1118} in black) flies. Both males (A, C) and females (B, D) are shown. See Table 1 for n, p, median and maximum survival values. Error bars represent SEM. *** p<0.001. Note that *dp53* mutant flies die faster upon fasting.

To discard possible effects of fat-body remodeling during metamorphosis and young adult flies, we also used 5- to 7-days old flies and similar results were observed (Figure 6A, B). Although we believe that 1% sucrose implies an important sugar deprivation for the animal, we analyzed in young adult flies (Figure 6C) or early second instar larvae (Figure 6D) the effect of complete nutrient deprivation (2% agar 0% sucrose, in the case of adults, and PBS soaked paper in the case of larvae, see Materials and Methods for details) on survival rates of *dp53* mutant animals. Even though the time scale of the experiment was highly reduced by the absence of sugar in the medium, the survival rates of *dp53* mutant animals were significantly reduced compared with *control* animals (statistical analysis are summarized in Table 1). We also investigated the possible role of *dp53* in a long-term effect of chronic starvation during the development of the animal by raising larvae immediately after eclosion on either standard food (Std food) or diluted food (0.2X). For that, we measured survival rates as the percent of individuals entering pupariation (Figure 6E) or giving rise to adult flies (Figure 6F) and we observed that *dp53* mutant animals were more sensitive than *controls*.

To summarize, we have shown that under restricted nutrient conditions (ranging from complete starvation to a less severe situation) *dp53* mutant animals showed reduced survival rates when compared to *control* flies. This high sensitivity of *dp53* mutants to nutrient deprivation was observed in two developmental stages, larvae and adult flies. These results suggest a main contribution of Dp53 to the adaptive response of the animal upon a nutrient challenge.

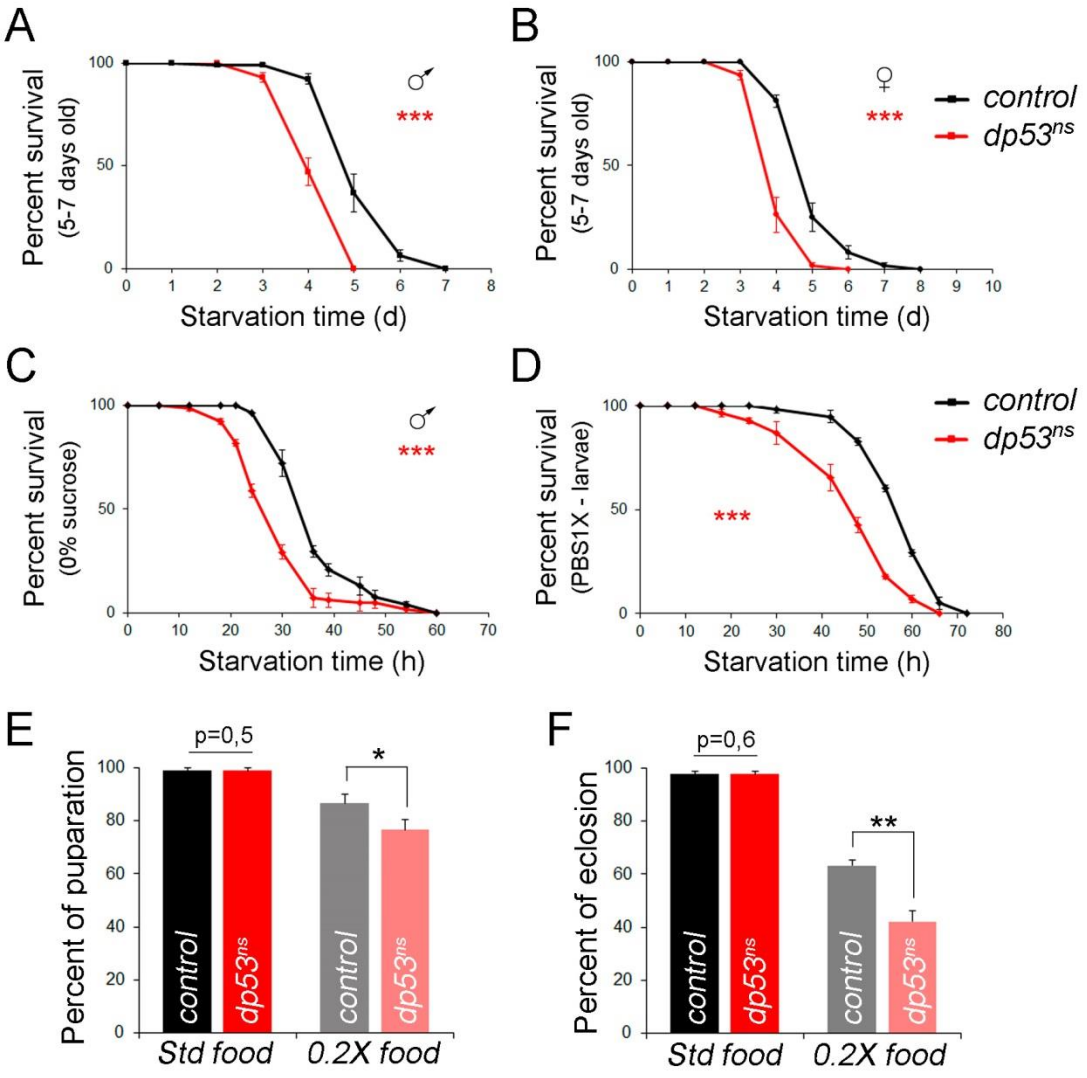

Figure 6: *dp53* mutant animals have compromised survival rates in different restricted nutritional conditions

(A, B) Survival rates to acute starvation (2% agar, 1% sucrose) of 5- to 7-days-old *dp53* mutant (*dp53*^{ns} in red) and control (*w*^{1118} in black) adult flies. Both males (A) and females (B) are shown. **(C)** Survival rates to complete nutrient deprivation (2% agar, 0% sucrose) of 1-2-day-old *dp53* mutant (*dp53*^{ns} in red) and control (*w*^{1118} in black) adult males. **(D)** Survival rates to complete nutrient deprivation (PBS1X soaked paper) of *dp53* mutant (*dp53*^{ns} in red) and control (*w*^{1118} in black) early second instar larvae. See Table 1 for n, p, median and maximum survival values. **(E, F)** Histograms plotting percent of pupariation (E) and eclosion (F) of control (*w*^{1118} in black) and *dp53* mutant (*dp53*^{ns} in red) larvae raised immediately after haching in standard food (Std food) or in diluted food (0.2X food). Data were represented as a percent of the fed values for each genotype. Error bars represent SEM, upper brackets indicate the genotypes that are compared, *** p<0.001, ** p<0.01 and * p<0.05. Note that under different conditions of nutrient deprivation, *dp53* mutant animals show a clear sensitivity to starvtion, in both adult and larval stages.

adult males	n	Mantel-Cox test	Median surv	Maximum surv
control w^{1118}	130		6	9
$p53^{ns}$	120	p < 0,0001	4 (-33%)	6 (-33%)
adult females	**n**	**Mantel-Cox test**	**Median surv**	**Maximum surv**
control w^{1118}	136		6	10
$p53^{ns}$	132	p < 0,0001	4 (-33%)	9 (-10%)
adult males	**n**	**Mantel-Cox test**	**Median surv**	**Maximum surv**
control w^{1118}	107		7	10
$p53^{5A14}$	101	p < 0,0001	6 (-15%)	8 (-20%)
adult females	**n**	**Mantel-Cox test**	**Median surv**	**Maximum surv**
control w^{1118}	112		9	14
$p53^{5A14}$	103	p < 0,0001	7 (-22%)	11 (-21%)
adult males (5-7 d old)	**n**	**Mantel-Cox test**	**Median surv**	**Maximum surv**
control w^{1118}	127		5	7
$p53^{ns}$	145	p < 0,0001	4 (-20%)	5 (-28%)
adult females (5-7 d old)	**n**	**Mantel-Cox test**	**Median surv**	**Maximum surv**
control w^{1118}	107		5	8
$p53^{ns}$	101	p < 0,0001	4 (-20%)	6 (-25%)
adult males (0% sucrose)	**n**	**Mantel-Cox test**	**Median surv**	**Maximum surv**
control w^{1118}	156		36 h	60 h
$p53^{ns}$	155	p < 0,0001	30 h (-17%)	60 h (=)
larvae (PBS1X)	**n**	**Mantel-Cox test**	**Median surv**	**Maximum surv**
control w^{1118}	116		60 h	72 h
$p53^{ns}$	118	p < 0,0001	48 h (-20%)	66 h (-10%)

Table 1: Statistical analysis of survival to nutrient deprivation in *dp53* mutants

Table compiling the number of individuals analyzed (n), p-values for the survival distributions according to the Mantel-cox test, median survival values (in days or otherwise specified) and maximum survival values (in days or otherwise specified) corresponding to *dp53* mutant (*dp53*^{ns} or *dp53*^{5A14}*) and control (w*^{1118}*)* animals of the experiments of survival to nutrient deprivation shown in Figures 5 and 6. One- to 2-days old adult animals (or otherwise specified) were grown under identical conditions and exposed to acute starvation in 2% of agar, 1% sucrose (or otherwise specified). Control animals were always analyzed in parallel in each experimental condition. The change (in percentage) with respect to control values is shown in brackets.

- **Dp53 modulates the consumption of the main energy storage upon fasting**

In order to identify possible causes for the starvation sensitivity of *dp53* mutant animals we measured glycogen and triglycerides (TAG) levels. The response of an organism to a period of nutrient deprivation is largely dependent on its capacity to obtain energy from stored reserves and in *Drosophila*, animals store sugars in form of glycogen, and lipids in form of TAG. In starvation, these resources are mobilize to support the energetic demand of the organism *(Arrese and Soulages, 2010)*. Our question was whether Dp53 could be involved in this process. To address this question we measured glycogen and TAG levels in *dp53* mutant and *control* animals that were either fed or starved (2% agar, 1% sucrose) for

1 day (for glycogen measurements) or for 3 days (in case of TAG measurements). Given the importance of the growth conditions for metabolic studies, both *dp53* mutant and *control* flies were grown under identical conditions and aged 5 days prior to the starvation experiments (see Materials and Methods). The first thing that we noticed was that the levels of both metabolites did not change significantly in fed *control* and *dp53* mutant flies (Figure 7A, C), consistent with the normal developmental progression of *dp53* mutant animals and suggesting that these animals do not have feeding-behavior defects. Under nutrient deprivation, however, glycogen and TAG levels were significantly lower in fasted *dp53* mutant animals (Figure 7B, D).

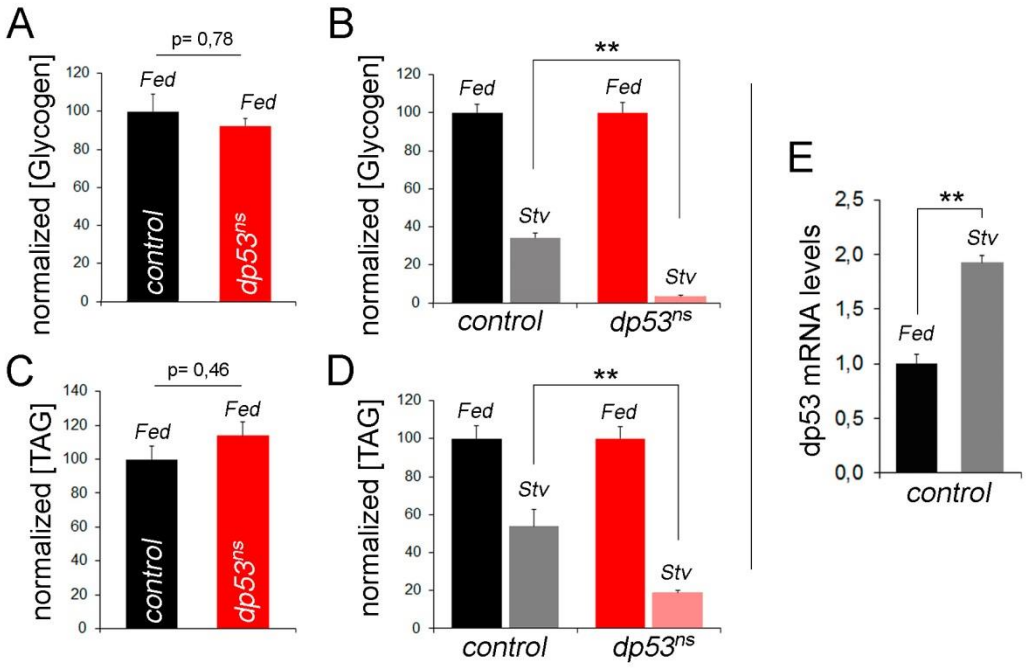

Figure 7: *dp53* modulates the consumption of the main energy storage upon fasting

(A-D) Histograms plotting glycogen (A, B) and tryglycerides (TAG, C, D) levels from *dp53* mutant ($dp53^{ns}$) and control (w^{1118}) adult males under fed or starved conditions. Data were normalized to protein concentration and represented as a percentage of the control fed values (A, C) or as a percentage of the fed values for each genotype (B, D). In all the cases animals were grown under identical conditions and aged for 5 days prior to exposion to fasting conditions (2% agar, 1% sucrose) for 1 day in B or for 3 days in D. While TAG and glycogen levels are not significantly different in *dp53* mutant and control animals at the beginning of the starvation procedure (A, C), they are consumed at higher rates in fasted *dp53*-mutant animals. **(E)** Histogram plotting *dp53* mRNA levels in control (w^{1118}) flies subjected to fed or starved (Stv) conditions for 72 hours. Results are expressed as fold induction with respect to fed conditions. Error bars represent SEM, upper brackets indicate the genotypes that are compared, ** $p<0.01$.

These results suggest that *dp53* mutant flies consume their metabolites at higher rates and deplete their energetic reserves faster than *control* animals, which in turn might contribute to their poor survival rates in fasting conditions. Altogether, our results show that Dp53 plays an important role in the adaptive response to nutritional stress at the level of the organism. To check if this adaptive response to nutritional stress in *control* flies involved an up-regulation of *dp53* expression levels, we measured, by quantitative real-time reverse transcription PCR (qRT-PCR), its mRNA levels in adult flies under fed and starving conditions. Interestingly, an increase in *dp53* mRNA levels was observed upon nutrient deprivation (Figure 7E) thereby supporting the requirement of Dp53 in this stress condition.

- **The impact of Dp53 in energy balance is independent off the regulation of the fasting hormones**

In complex organisms, adaptation to changing dietary conditions is critical to maintain metabolic homeostasis. This adaptation has to occur at the cellular and systemic levels and involves the adjustment of processes that control nutrient uptake, metabolite storage and energetic consumption. The molecular mechanisms by which vertebrates and flies regulate the storage and release of fuel molecules at the systemic level display significant parallels *(Hietakangas and Cohen, 2009)*. The Adipokinetic Hormone (Akh), the functional analogue of the vertebrate glucagon, plays a key role in mobilizing energy resources during fasting, whereas *Drosophila* insulin-like peptides (Dilps) promote energy storage in normal feeding conditions, recapitulating the role of the vertebrate insulin pathway *(Bharucha et al., 2008; Kim and Rulifson, 2004; Rulifson et al., 2002)*. To analyze if the accelerated consumption of energy resources and the starvation sensitivity observed in *dp53* loss-of-function animals was due to an aberrant regulation of these hormones we monitored AKH and insulin signaling by different means. We exposed 5-days-old adult males either to normal food (Fed) or acute starvation (Stv) for 24 hours and measured by quantitative real-time PCR (qRT-PCR) the mRNA levels of *Akh*, *Drosophila* insulin receptor (*dInR)* and *4EBP* [these two last genes are known targets of the FOXO transcription factor and then regatively regulated by insulin signaling *(Puig et al., 2003; Teleman et al., 2005)*]. Interestingly, despite the accelerated consumption of energy resources observed in starved *dp53* mutant animals when compared to *control* individuals, *Akh* production was increased (Figure 8A, B) and Insulin signaling was reduced (Figure 8 C-F), in a similar manner in both genotypes upon fasting. We noticed that the levels of *Akh*, *dInR* and *4EBP* mRNA did not change significantly in fed *control* and *dp53* mutant flies (Figure 8 A, C, E).

Brain Insulin Producing Cells (IPCs) secrete Dilps in response to nutrition and accumulate Dilps under nutrient deprivation *(Géminard et al., 2009)*. Thus, we decided to analyze the dynamics of Dilp2 secretion and we observed a strong accumulation of Dilp2 protein levels in IPCs of both *control* and *dp53*^{ns} mutant animals upon fasting (Figure 8G, H). Consistent with the life-expanding role of Dp53 in the IPCs *(Bauer et al., 2005; Bauer et al., 2007)*, we noticed slightly more Dilp2 fluorescence levels in *dp53*^{ns} mutant than in control animals in fed conditions.

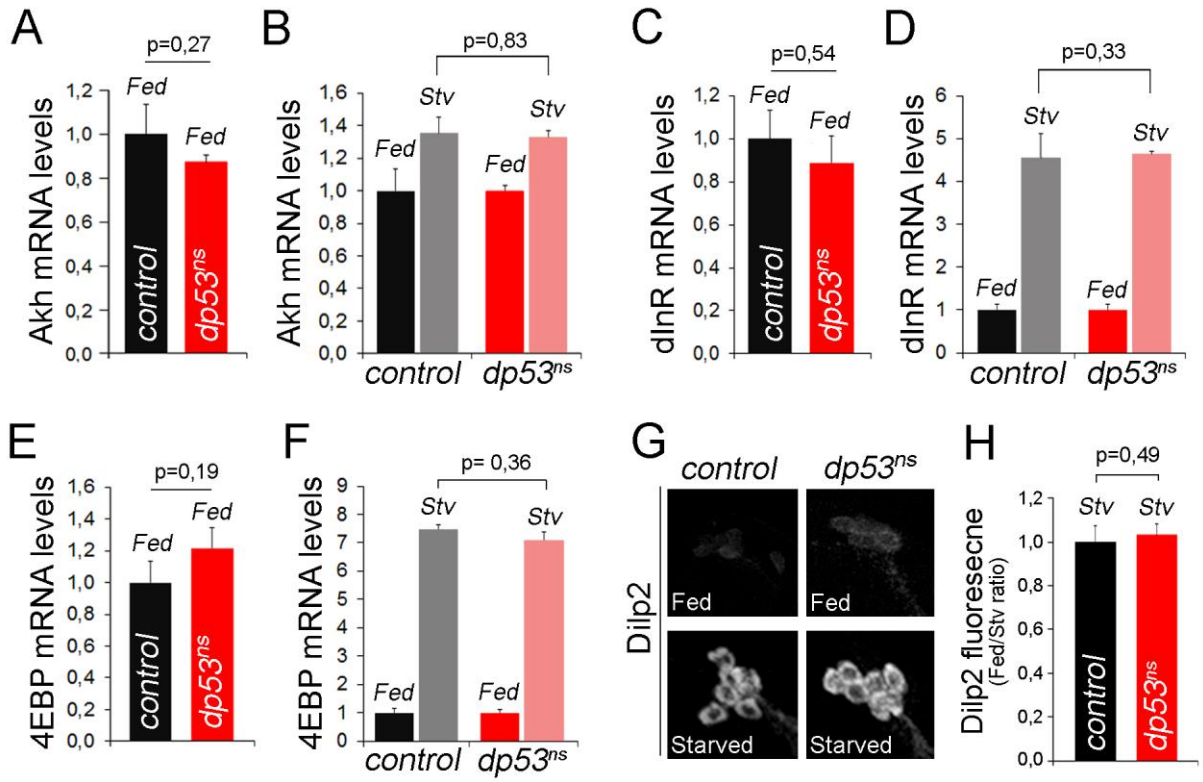

Figure 8: Dp53 activity does not regulate *Akh* expression, Dilp secretion and dInR signaling during nutrient deprivation

(A-F) Histograms plotting Adipokinetic Hormone (Akh in A, B), *Drosophila* insulin receptor (dInR in C, D) and 4EBP (E, F) mRNA levels from 5-days-old adult males *dp53* mutant (*dp53*^{ns}) and control (*w*^{1118}) flies subjected to fed (Fed) or starved (Stv) conditions for 24 hours. Results are expressed as fold induction with respect to control animals in A, C and E, and with respect to fed conditions for each genotype in B, D and F. Heads were used in A and B, and decapited bodies in C-F. **(G)** Brain Insulin Producing Cells, IPCs, stained to visualize Dilp2 (grey) protein levels in *dp53* mutant (*dp53*^{ns}) and control (*w*^{1118}) animals under fed or starved conditions. **(H)** Histogram plotting mean Dilp2 fluorescence intensity as a Fed/Stv ratio of IPCs shown in G. Results were normalized to control flies. Dilp2 protein levels are strongly accumulated in a similar manner in both genotypes upon nutrient deprivation. Error bars represent SEM, upper brackets indicate the genotypes that are compared.

All together, these results indicate that Dp53 has an impact on energy balance upon fasting that cannot be explained merely by a failure in the regulation of Akh production and dInR signaling.

Dp53 is specifically required in the fat body for animal resistance to nutrient deprivation

We have shown that depletion of Dp53 in the whole animal is essential for the organismal adaptation to nutrient deprivation. The next question we wanted to address was if there was a tissue-specific requirement of Dp53.

- **Dp53 reduction in the FB compromises organismal survival upon nutrient deprivation**

The fat body (FB) of insects functions as a key sensor well know to couple nutrient status and energy expenditure and serves as a repository for both TAGs and glycogen, combining the energy storage and endocrine functions of vertebrate adipose and hepatic tissues, respectively *(Arrese and Soulages, 2010; Canavoso et al., 2001)*. We then took advantage of the Gal4-UAS binary system to specifically analyze whether Dp53 plays a role in this key organ during starvation. To reduced Dp53 activity we used two different UAS-transgenes: *UAS-dp53*$^{H159.N}$, a dominant negative version of Dp53 carrying a point mutation in the DNA binding domain *(Ollmann et al., 2000)*, and *UAS-dp53*^{RNAi}, a dsRNA form against *dp53*. We combined these two transgenes with three Gal-4 drivers expressed in the larval and adult FB (*ppl-gal4* and *cg-gal4)* or just in the adult FB *(yolk-gal4*) to reduce Dp53 activity or levels in the FB. When we exposed adult flies to acute starvation (2% agar, 1% sucrose), in all cases, depletion of Dp53 activity or levels in the FB reduced survival rates upon fasting when compared to control flies expressing GFP under the control of the same Gal4 drivers (Figure 9A-D, F; statistical analysis are summarized in Table 2). Once again, we obtained the same results in both males and females. It is important to notice that the *yolk-gal4* driver is only expressed in FB cells of adult females *(JM Reichhard, personal communication to Flybase)*.

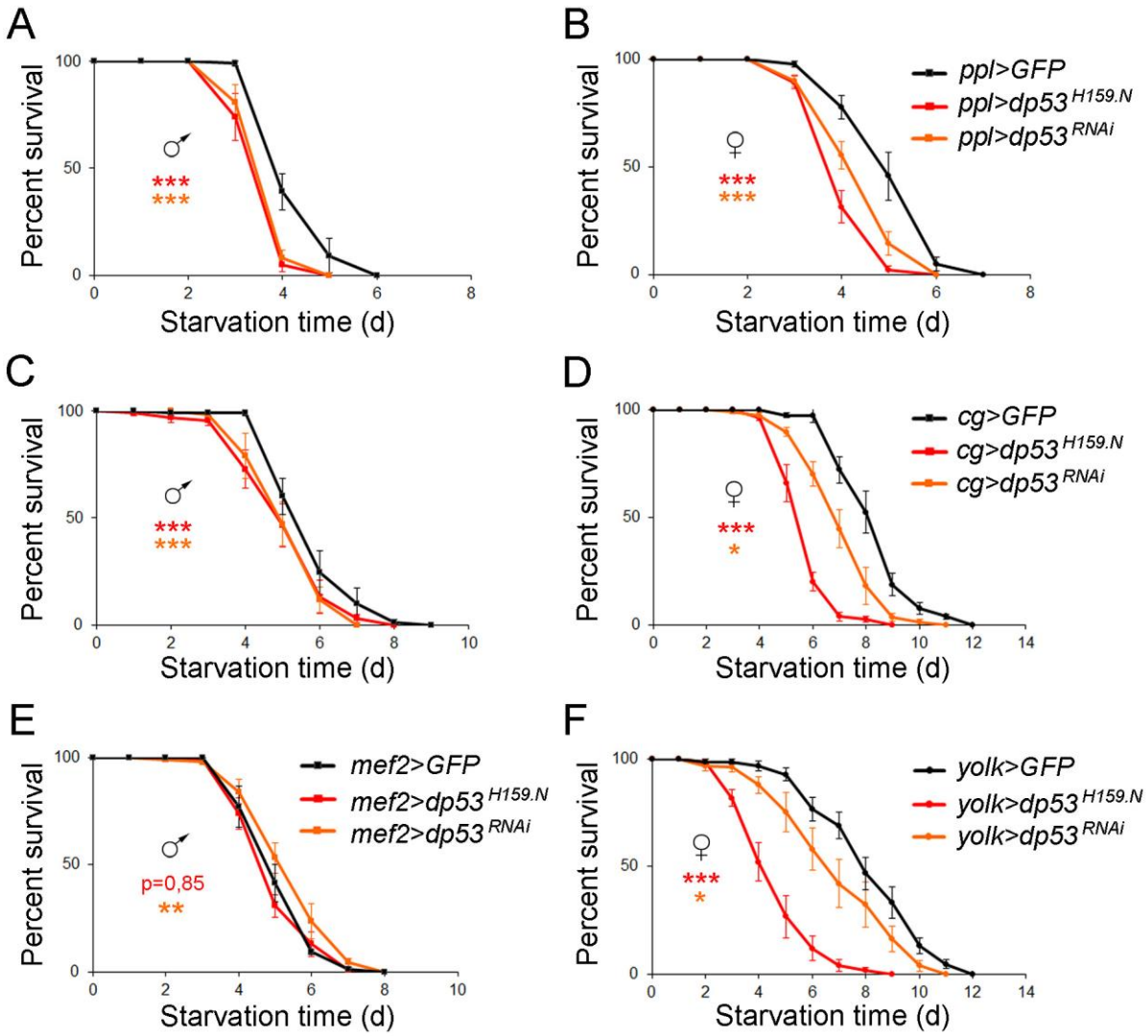

Figure 9: Reduction of Dp53 activity in the fat body, and not in the muscles, reduces survival rates upon fasting

(A-F) Survival rates to nutrient deprivation (2% agar, 1% sucrose) of 1- to 2-days-old adult flies expressing *GFP* (as a control, in black), *Dp53*$^{H159.N}$ (a dominant negative version of Dp53, in red) and *UAS-dp53*^{RNAi} (a dsRNA form against *dp53*, in orange) in FB cells (A-D, F) or muscle cells (E) under the control of the *ppl-gal4* (A, B), *cg-gal4* (C, D), *mef2-gal4* (E) and *yolk-gal4* (F) drivers. Both males (A, C, E) and females (B, D, F) are shown. *yolk-gal4* is expressed only in females. See Table 2 for n, p, median and maximum survival values. Error bars represent SEM. *** p<0.001, ** p<0.01 and * p<0.05.

Moreover, we analyzed the effects on survival rates in flies exposed to complete nutrient deprivation (2% agar, 0% sucrose) and we also observed a clear sensitivity to starvation upon depletion of Dp53 activity using the *ppl-gal4* and the *yolk-gal4* drivers (Figure 10A, B; statistical analysis are summarized in Table 2). As a control, the three parental UAS lines (*UAS-GFP*, *UAS-dp53$^{H159.N}$* and *UAS-dp53^{RNAi}*) backcrossed into the *w^{1118}* genetic background showed similar survival rates (Figure 10C; statistical analysis are summarized in Table 2).

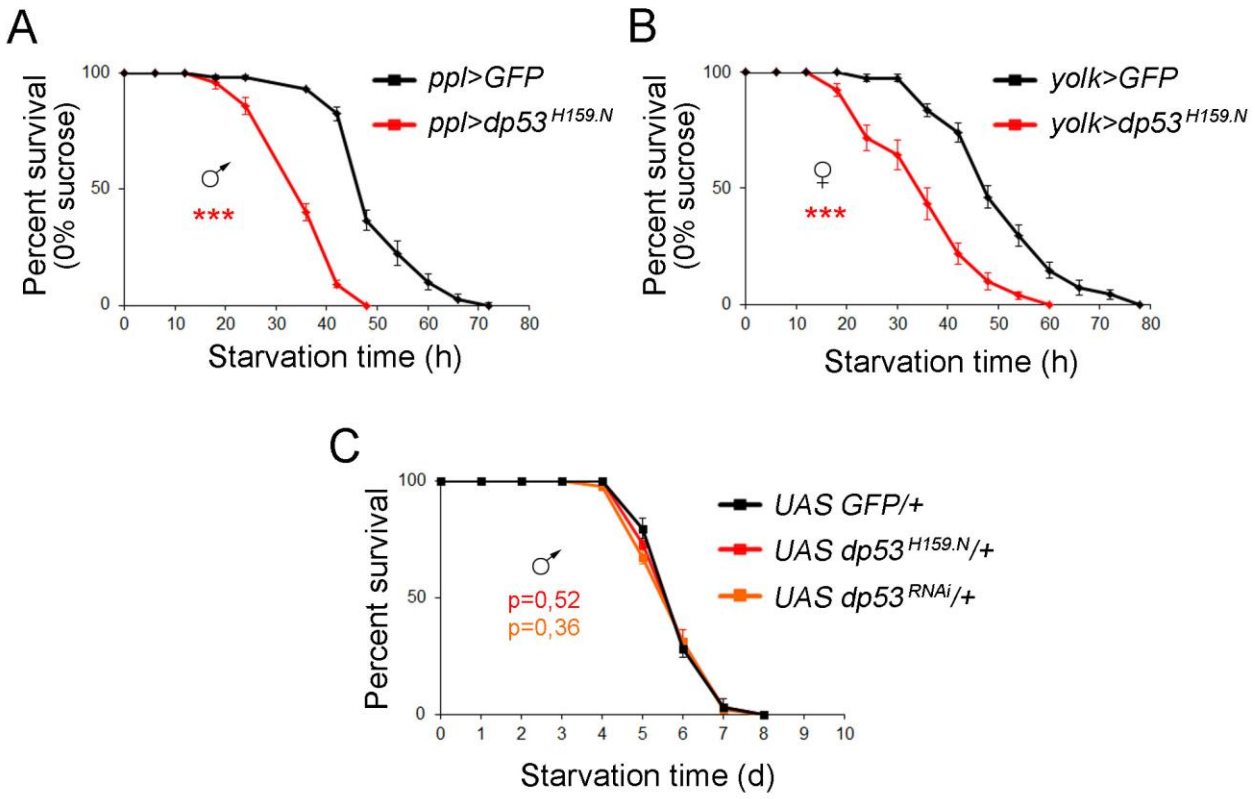

Figure 10: Survival rates upon complete starvation in FB-specific depleted Dp53 animals and control parental lines.

(A-B) Survival rates to complete starvation (2% agar, 0% sucrose) of 1- to 2-days-old adult flies expressing *GFP* (as a control, in black) and *Dp53$^{H159.N}$* (a dominant negative version of Dp53, in red) in FB cells under the control of the *ppl-gal4* (A) and *yolk-gal4* (B) drivers. Adult males were used in A and females in B (*yolk-gal4* is expressed only in females). Note that depletion of Dp53 in the FB induces a clear reduction in both median and maximum survival values when compared with GFP expressing flies. **(C)** Survival rates to nutrient deprivation (2% agar, 1% sucrose) of young adult flies of the following genotypes: *UAS-GFP/+*, *UAS Dp53$^{H159.N}$ /+* and *UAS Dp53^{RNAi}*/+. No significant differences were observed between any of the parental UAS transgenic lines. See Table 2 for n, p, median and maximum survival values. Error bars represent SEM. *** p<0.001.

Interestingly, we noticed that depletion of Dp53 activity with the *cg- and yolk-gal4* drivers reduced the survival rates by a magnitude similar to that seen in the whole animal mutant, suggesting that most of the Dp53 effect is FB-specific. To further support this proposal, muscle-specific depletion of Dp53 activity [using the *mef2-gal4* driver *(Demontis and Perrimon, 2010; Ranganayakulu et al., 1995)*] did not have any impact on the survival rates upon fasting (Figure 9E and Table 2). To really confirm the requirement of Dp53 in the FB we carried out a rescue experiment by overexpressing a wild-type form of Dp53 specifically in the FB of *dp53* homozygous mutant flies. First, we monitored whether overexpression of Dp53 *per se* in the FB leads to a starvation resistance. Since overexpression of wild-type Dp53 ($dp53^{2.1}$) with the *ppl* and *cg-gal4* caused larval lethality (data not shown) we used the *yolk-gal4* line to drive expression of Dp53 in FB cells only during the adult stages. As shown in Figure 11A, overexpression of Dp53 in FB increased the starvation resistance of adult flies when compared to control flies expressing GFP. Interestingly, FB-specific overexpression of Dp53 was able to rescue the survival rates of starved *dp53* mutant animals (Figure 11B, statistical analysis are summarized in Table 2).

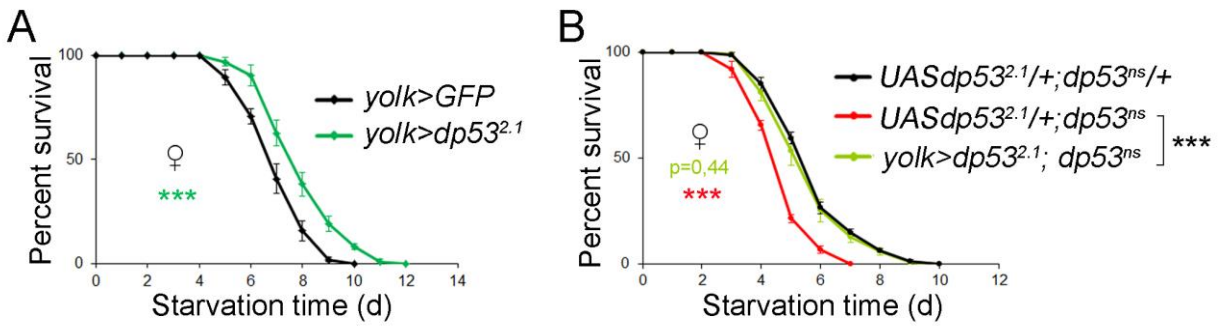

Figure 11: FB-specific overexpression of Dp53 lead to starvation resistance

(A) Survival rates to acute starvation (2% agar, 0% sucrose) of 1- to 2-days-old adult females expressing *GFP* (as a control, in black) and $dp53^{2.1}$ (a *wild-type* form of Dp53, in green) in FB cells under the control of the *yolk-gal4* driver. **(B)** Survival rates to acute starvation (2% agar, 0% sucrose) of 1- to 2-days-old adult females of the following genotypes: *UAS-*$dp53^{2.1}$ */+; *$dp53^{ns}$*/+* ('control' animals, in black), *UAS-*$dp53^{2.1}$ */+; *$dp53^{ns}$ ('mutant' animals, in red), yolk>$dp53^{2.1}$ */+; *$dp53^{ns}$ (the 'rescue' experiment, in light green). Note that FB-specific overexpression of Dp53 leads to starvation resistance and rescues the survival rates of $dp53^{ns}$ mutant flies under nutrient deprivation. See Table 2 for n, p, median and maximum survival values. Error bars represent SEM. *** p<0.001.

adult males	n	Mantel-Cox test	Median surv	Maximum surv
ppl>GFP (control)	102		4	6
ppl>dp53 $^{H159.N}$	100	p < 0,0001	4 (=)	5 (-17%)
ppl>dp53 ^{RNAi}	100	p < 0,0001	4 (=)	5 (-17%)
adult females	**n**	**Mantel-Cox test**	**Median surv**	**Maximum surv**
ppl>GFP (control)	100		5	7
ppl>dp53 $^{H159.N}$	105	p < 0,0001	4 (-20%)	6 (-14%)
ppl>dp53 ^{RNAi}	101	p < 0,0001	5 (=)	6 (-14%)
adult males (0% sucrose)	**n**	**Mantel-Cox test**	**Median surv**	**Maximum surv**
ppl>GFP (control)	120		48 h	72 h
ppl>dp53 $^{H159.N}$	118	p < 0,0001	33 h (-31%)	48 h (-33%)
adult males	**n**	**Mantel-Cox test**	**Median surv**	**Maximum surv**
cg>GFP (control)	100		6	9
cg>dp53 $^{H159.N}$	105	p = 0,0004	5 (-17%)	8 (-11%)
cg>dp53 ^{RNAi}	113	p < 0,0001	5 (-17%)	7 (-22%)
adult females	**n**	**Mantel-Cox test**	**Median surv**	**Maximum surv**
cg>GFP (control)	100		9	12
cg>dp53 $^{H159.N}$	105	p < 0,0001	7 (-22%)	9 (-25%)
cg>dp53 ^{RNAi}	101	p = 0,0303	8 (-12%)	11 (-8%)
adult males	**n**	**Mantel-Cox test**	**Median surv**	**Maximum surv**
mef2>GFP (control)	101		5	8
mef2>dp53 $^{H159.N}$	100	p = 0,8484	5 (=)	8 (=)
mef2>dp53 ^{RNAi}	116	p = 0,007	5 (=)	8 (=)
adult females	**n**	**Mantel-Cox test**	**Median surv**	**Maximum surv**
yolk>GFP (control)	103		8	12
yolk>dp53 $^{H159.N}$	100	p < 0,0001	5 (-37%)	9 (-25%)
yolk>dp53 ^{RNAi}	101	p = 0,0321	7 (-12%)	11 (-8%)
adult females	**n**	**Mantel-Cox test**	**Median surv**	**Maximum surv**
yolk>GFP (control)	107		7	10
yolk>dp53 $^{2.1}$	101	p < 0,0001	8 (+14%)	12 (+20%)
adult females	**n**	**Mantel-Cox test**	**Median surv**	**Maximum surv**
UASdp53 $^{2.1}$/+;dp53 ^{ns}/+ (control)	103		6	10
yolk>UASdp53 $^{2.1}$; p53 ^{ns}	122	p=0,44	6 (=)	10 (=)
UASdp53 $^{2.1}$/+;dp53 ^{ns}	143	p<0,0001 (*ctrl*)	5 (-16%)	7 (-30%)
		p<0,0001 (*overexp*)		
adult females (0% sucrose)	**n**	**Mantel-Cox test**	**Median surv**	**Maximum surv**
yolk>GFP (control)	110		48 h	78 h
yolk>dp53 $^{H159.N}$	115	p < 0,0001	35 h (-27%)	60 h (-23%)
adult males	**n**	**Mantel-Cox test**	**Median surv**	**Maximum surv**
UAS GFP/+ (control)	108		6	8
UAS dp53 $^{H159.N}$/+	104	p = 0,516	6 (=)	8 (=)
UAS dp53 ^{RNAi}/+	101	p = 0,3649	6 (=)	8 (=)

Table 2: Statistical analysis of survival to nutrient deprivation in FB- or muscle-depleted Dp53 animals

Table compiling the number of individuals analyzed (n), p-values according to the Mantel-cox test, median survival values (in days or otherwise specified) and maximum survival values (in days or otherwise specified) corresponding to the different genotypes used in the experiments of survival to nutrient deprivation shown in Figures 9, 10 and 11. One- to 2-days old adult animals were grown under identical conditions and exposed to acute starvation in 2% of agar, 1% sucrose (or otherwise specified). Control animals were always analyzed in parallel in each experimental condition. The change (in percentage) with respect to control values is shown in brackets.

- **Dp53 reduction in the FB causes accelerated depletion of energy storages**

In accordance with the reduced viability upon fasting caused by targeted reduction of Dp53 in FB cells, the total levels of TAG, glycogen and sugars were further reduced in *ppl>dp53*$^{H159.N}$ and *ppl>dp53*^{RNAi} animals when compared to *ppl>GFP* control individuals (Figure 12B, D, F). Remarkably, the levels of circulating sugars were similarly reduced upon fasting in *control* and Dp53 depleted animals (Figure 12H). This result is consistent with the fact that starvation-induced reduction in Dilp release and increase in Akh transcription, hormones involved in the tight regulation of sugars in circulation, were unaffected by Dp53 depletion (Figure 8). Because the levels of all these metabolites were not consistently affected in *dp53*-depleted animals at the beginning of the starvation procedure (Figure 12A, C, E) we proposed that it is the accelerated consumption of energy storage what compromises the survival rates of Dp53-depleted animals upon fasting conditions. Altogether, our results unravel a previously uncharacterized FB-specific role of Dp53 in the metabolic adaptation to nutrient deprivation.

(next page) **Figure 12: Knock-down of Dp53 activity in the FB accelerates the consumption of the main energy storages under nutrient deprivation**

(A-H) Histograms plotting whole body glycogen (A, B), tryglycerides (TAG, C, D), total glucose+trehalose (E, F) or hemolymph glucose+trehalose (G, H) levels from *ppl>GFP*; *ppl>dp53*$^{H159.N}$ and *ppl>dp53*^{RNAi} adult males under fed (Fed) or starved (Stv) conditions. Data were normalized to protein concentration and represented as a percentage of the control fed values (A, C, E, G) or as a percentage of the fed values for each genotype (B, D, F, H). In all the cases animals were grown under identical conditions and aged for 5 days prior to exposion to fasting conditions (2% agar, 1% sucrose) for 1 day (B, F, H) or for 3 days (D). Error bars represent SEM, upper brackets indicate the genotypes that are compared, ** $p<0.01$ and * $p<0.05$.

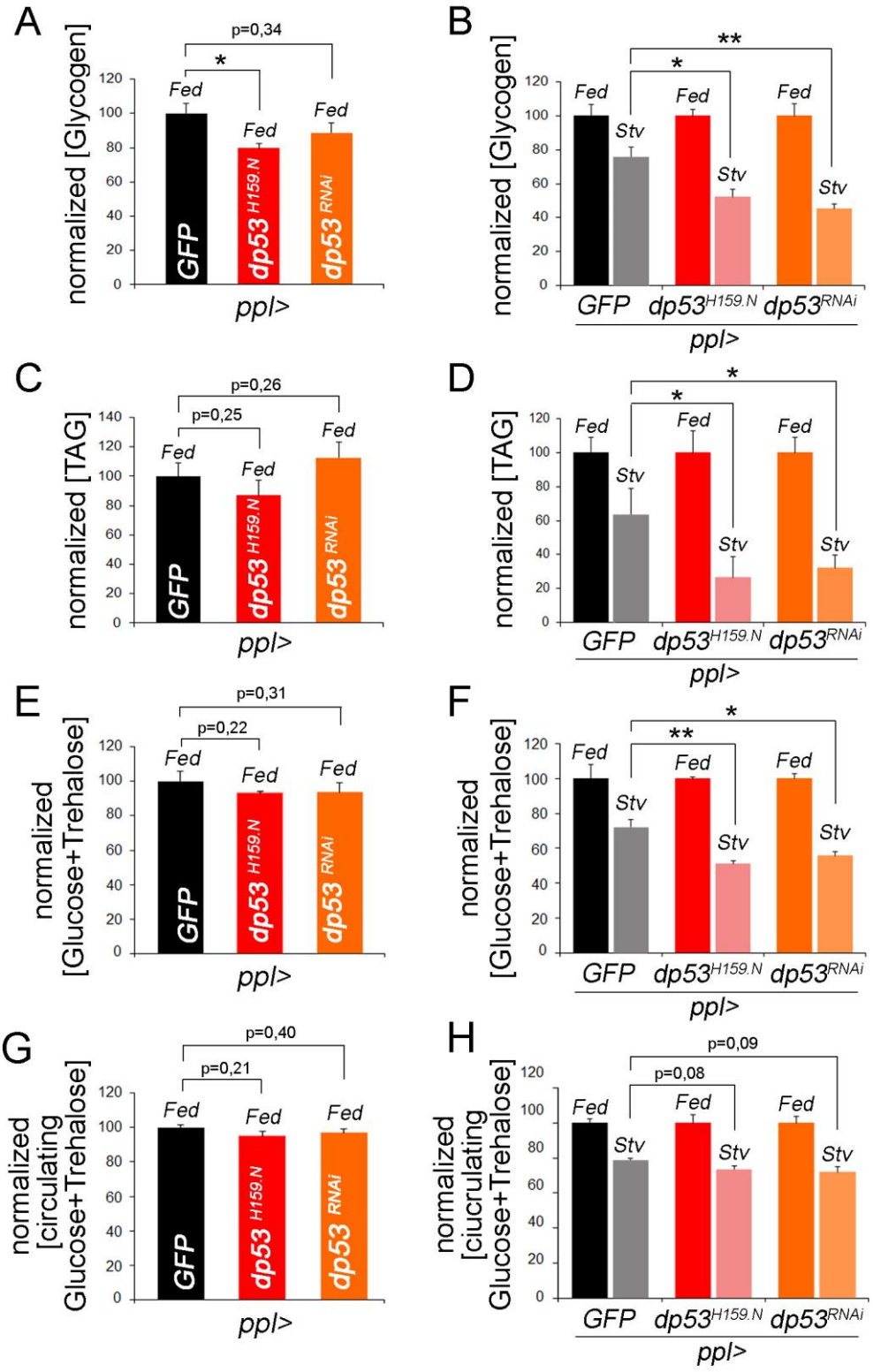

Figure 12 (legend in previous page)

- **Dp53 plays a cell-autonomous and FB-specific role in the metabolic changes upon nutrient deprivation**

Our previous results show that Dp53 is required in the fat body under nutrient deprivation to regulate the consumption of the main energy resources and promote organismal survival; and that *dp53* mRNA levels were upregulated upon starvation. We then examined Dp53 activity in FB cells upon starvation. For this purpose, we used a reporter of Dp53 activity that places a nuclear GFP (GFPnls) under the control of an enhancer of the *reaper* (rpr) locus that includes a Dp53 consensus binding site (Figure 13A). This reporter has been used as a Dp53 biosensor in different cellular contexts to monitor Dp53 activity *(Lu et al., 2010; Wylie et al., 2014)*. When we analyzed the Dp53 reporter (*dp53R-GFPnls*) in FB cells of fed and starved animals we found a clear rise in nuclear GFP expression upon the starvation treatment (Figure 13B, C). This result reinforces our proposal that Dp53 is induced in FB cells upon nutrient deprivation.

To further characterize the molecular and cellular mechanism underlying Dp53 function in the FB, we analyzed lipid content, autophagic induction and metabolic enzymes in FB cells of both *control* and Dp53 depleted animals.

Lipids are the main fat body component, and more than 90% of the lipids are stored as triglyceride (TAG). Intracellular TAG storage occurs in specialized cytoplasmic compartments called lipid droplets, dynamic organelles that play a central role in fat and energy metabolism *(Arrese and Soulages, 2010; Liu and Huang, 2013).* Consistent with the accelerated TAG consumption observed in starved *dp53* mutant flies, specific depletion of Dp53 in single FB cells (marked by the expression of GFP using the flip-out technique to express $dp53^{RNAi}$, see Materials and Methods for more details) caused smaller lipid droplets (labelled by Nile red staining) than in *wild-type* cells upon fasting (Figure 14B). Interestingly, no major change in lipid droplet size was observed in well-fed FB cells depleted for Dp53 activity (Figure 14A). This observation points to a cell-autonomous role of Dp53 in starved FB cells.

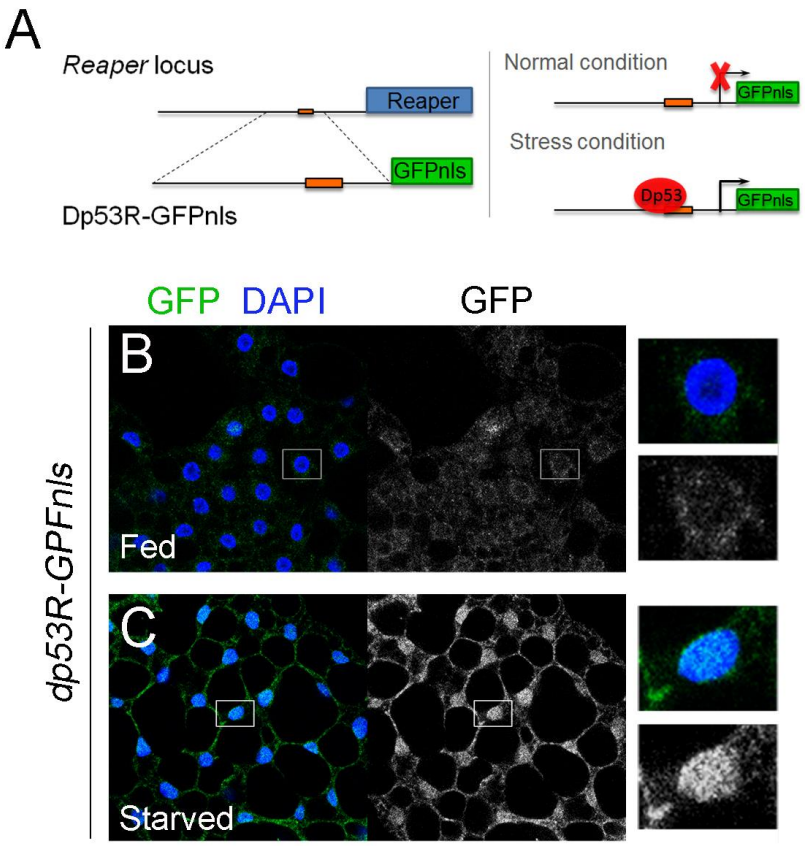

Figure 13: Dp53 is activated in FB cells upon starvation

(A) Carton depicting the Dp53 activity reporter construct and its mode of action adapted from *(Wylie et al., 2014)*. A 150-bp fragment containing a well-characterized p53 consensus binding site (orange box), conserved from flies to humans, upstream of the *reaper* locus *(Brodsky et al., 2000)* was placed upstream of GFP with a nuclear localization signal (*Dp53R-GFPnls*). Stimuli that trigger Dp53 activation induces GFP expression. **(B-C)** FB cells of fed (B) or starved (C) animals labeled to visualized the GFP levels (green or grey) of the Dp53R-GFPnls and DAPI (blue). Animals were starved for 48 hour in 2% agar, 1% sugar. Note increased levels of the *Dp53R-GFPnls* activity reporter in response to starvation.

In response to starvation, eukaryotic cells recover energy and nutrients through autophagy, a lysosomal-mediated process of cytoplasmic degradation *(Levine et al., 2004)*. Since this catabolic process has been shown to be under the control of p53 *(Levine and Abrams, 2008)*, we decided to assess the possible contribution of Dp53 in the regulation of starvation-induced autophagy.

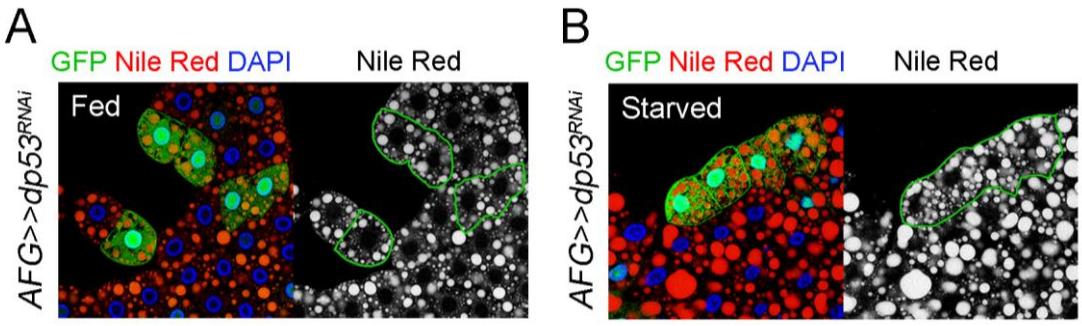

Figure 14: Reduction of Dp53 in single FB cells causes smaller lipid droplets in fasting conditions

(A-B) Lipid droplets, visualized by Nile red staining (in red or white), in FB cells of fed (A) and starved (for 24 hours in 2% agar 1% sucrose, B) animals expressing in individual FB cells *dp53*^{RNAi} (marked by the expression of GFP, in green). Starved FB cells expressing *dp53*^{RNAi} (marked by the expression of GFP, in green) showed smaller lipid droplets that the neighboring *wild- type* cells. DAPI (in blue) labels FB nuclei.

To monitor autophagic induction we follow the intracellular localization of a fluorescent tagged mCherry-Atg8a, an Atg8/LC3 orthologue that specifically labels autophagic vesicles known as autophagosomes *(Scott et al., 2004)*. This autophagic marker mobilized from an evenly dispersed and uniform localization in fed animals (Figure 15A) to a punctate pattern of dots in response to starvation (Figure 15B). Expression of *dp53*$^{H159.N}$ under the control of the *cg-gal4* driver did not affect the vague and homogeneous mCherry-Atg8a distribution in FB cells of fed animals (Figure 15C). However, in FB cells from starved individuals, targeted reduction of Dp53 (in *cg>dp53*$^{H159.N}$ animals) showed a consistent blockage of the punctate localization of mCherry-Atg8a when compared to *cg>GFP* control animals (Figure 15D, D'). These results argue for a positive role of Dp53 in controlling autophagy in FB cells subject to starvation. Although inhibition of starvation-induced autophagy do not account for the accelerated consumption of energy resources observed in Dp53 depleted animals, it could affect/block the recycling of essential intracellular components thus contributing to the poor survival of these animals in starvation.

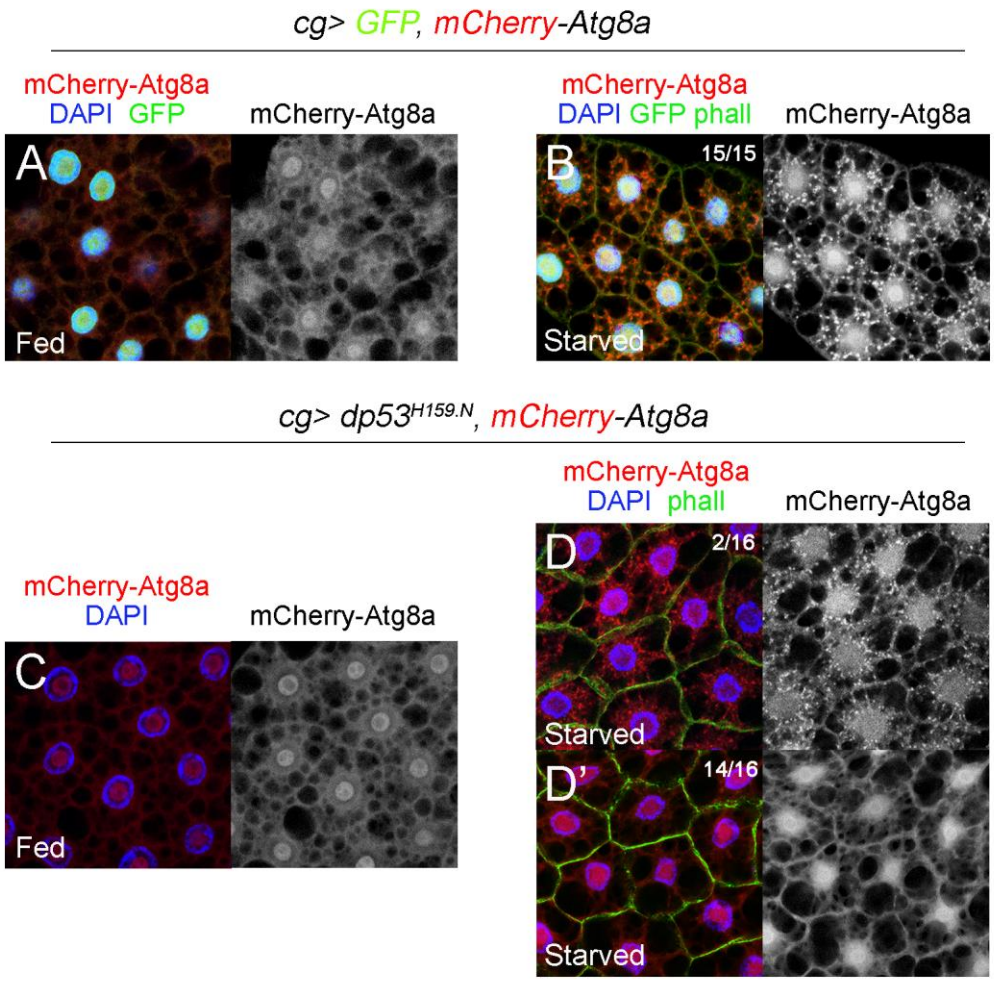

Figure 15: Starvation-induced autophagy is compromised in Dp53 depleted cells

(A-D) FB cells of fed (A, C) or starved (B, D, D') *cg>GFP* (A, B) and *cg>dp53*$^{H159.N}$ (C, D, D') animals that express mCherry-Atg8a (red or grey) as a marker for autophagic vesicles labelled to visualized FB nuclei (DAPI, in blue) and extracellular membranes (phalloidin, in green, B, D, D'). Note that reduction of Dp53 activity block in a high frequency of samples the punctate localization of mCherry-Atg8a in FB cells of starved animals. Animals were starved for 5 hours in PBS-soaked paper in B, D and D'.

Since we have seen that Dp53 activity modulates the levels of energy store breakdown and the amount of stored fat in individual cells, it is likely to operate via the regulation of cellular metabolism. We thus measured mRNA levels, by quantitative real-time-PCR (qRT-PCR), of a panel of fifteen key metabolic enzymes in fed and starved individuals (Figure 16A, B). In conditions of nutrient deprivation, the FB supplies energy to the rest of the body by mobilizing stored resources (glycogen and TAGs) to

circulation in the form of trehalose and diacylglycerides (DAGs), respectively *(Arrese and Soulages, 2010)*. Consistently, a pronounced increase in the expression levels of the Brummer lipase [Bmm, the homolog of the mammalian adipose triglyceride lipase *(Grönke et al., 2005)*], and the CG5966 lipase, both important to the mobilization of stored TAGs in the FB *(Kühnlein, 2012),* was observed in *control* animals upon fasting (Figure 16B). Conversely, a clear reduction in the expression levels of lipogenic enzymes, such as Fatty acid synthase (FAS) and Midway (Mdy) was observed (Figure 16B). These animals also had a drastic reduction in the expression levels of metabolic enzymes involved in: glucose catabolism such as Hexokinase C (HexC), Pyruvate kinase (Pyk) and Phosphoglucose mutase (PGM); cellular respiration (Pyruvate dehydrogenase, PDH) and fatty-acid oxidation such as Acyl CoA Thiolase (AcoT) and Cytocrome C Oxidase (SCOX). These changes might reflect reduced rates of glucose and fatty acid catabolism in starved FB cells, and a preferential use of these metabolites for the supply of sugars and lipids to be consumed by peripheral tissues during fasting periods.

To elucidate the possible molecular mechanism downstream of Dp53 involved in the regulation of cellular metabolism we compared the mRNA levels of the same metabolic enzymes in $dp5^{s}$ mutant and *control* animals by analyzing the Fed/Stv ratio. First we noticed that the mRNA levels of these enzymes before the starvation treatment (fed conditions) were very similar in *dp53* and *control* animals (Figure 16A). Second , we found that Dp53 activity did not appear to directly modulate the levels of those enzymes involved in mobilizing lipids during starvation (Figure 16B) since *Drosophila* Lipin (dLpin), a central regulator of adipose tissue development that promotes survival to *starvation (Ugrankar et al., 2011),* and the lipases Bmm and CG5966 were also similarly upregulated in *control* and *dp53* mutant flies. Finally, we observed that the expression levels of 2 enzymes involved in the catabolism of glucose were altered in *dp53* mutant flies. Interestingly, Hex-C, an enzyme that catalyzes the first step of glycolysis, and PGM, an enzyme that convert glucose-1-P (the first product of the breakdown of glycogen) to glucose-6-P which is used for glycolysis, remained unchanged in *dp53* mutant (similar to the levels obtained in fed conditions) while in *control* flies were clearly decreased upon starvation (Figure 16B). These differences suggest an active glycolytic pathway in starved *dp53* mutant flies which is consistent with the reduced amount of sugars under nutrient deprivation (Figure 12F). In turn, this reduction might contribute to their poor survival rates and to the accelerate rate of TAG and glycogen consumption. Consistent with this proposal, an increase in sugar concentration in the starvation treatment (2% agar, 10% sucrose) rescued the survival sensitivity of starved Dp53 depleted animals (Figure 17A) and the consumption of the energy resources (Figure 17B, C).

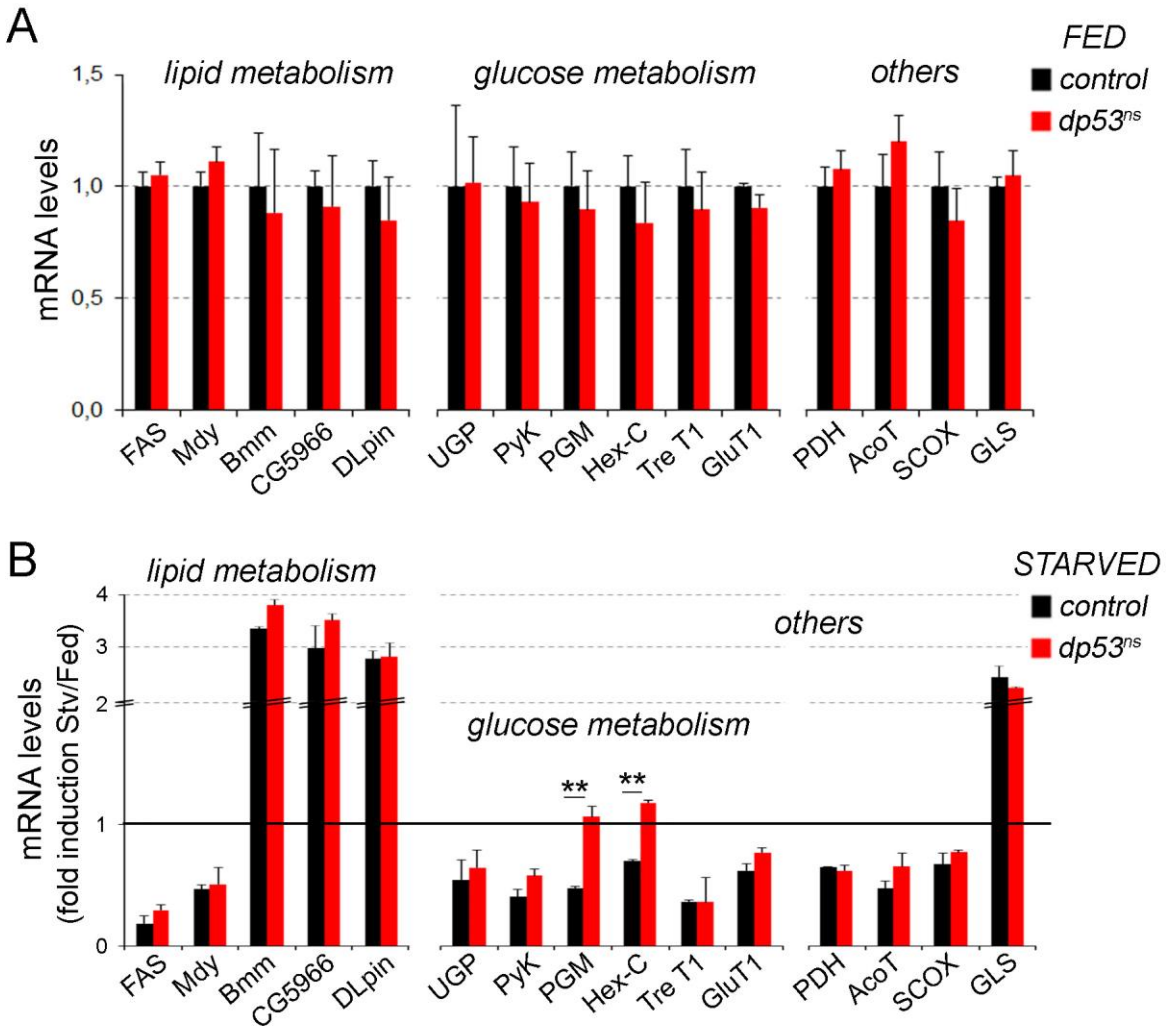

Figure 16: Dp53 activity in fat body cells reduces the levels of glucose catabolic enzymes in fasting periods

(A-B) Histograms plotting mRNA levels of a collection of fifteen key metabolic enzymes from adult males of *dp53* mutant (*dp53*^{ns}) and control (*w*^{1118}) flies under well-fed conditions (A) and subjected to 24 hours of acute starvation (B). Results are expressed as fold induction with respect to control animals in A and with respect to fed conditions for each genotype in B. Animals were grown under identical conditions, aged for 5 days and starved in 2% agar, 1% sucrose. Note that the levels of the glycolytic enzyme Hexokinase-C (HexC) and Phosphoglucose mutase (PGM) remained unchanged in dp53 mutant flies. Error bars represent SEM, upper brackets indicate the genotypes that are compared, ** $p<0.01$.

These results point to a role of Dp53 in metabolic adaptation to nutrient deprivation of FB cells and suggest that reduced survival rates of fasted *dp53* mutant animals are most probably a consequence of deregulated consumption of sugars and faster depletion of energy resources. In addition, our results also suggest a possible role of Dp53 in the induction of autophagy. Thus, a blockade of this important recycling system could affect cellular homeostasis and contribute to the poor survival of *dp53* mutant

animals in starvation as well. We propose that the metabolic function of p53 is important not only to suppress tumour initiation and/or progression *(Jiang et al., 2013)* but also to maintain animal homeostasis.

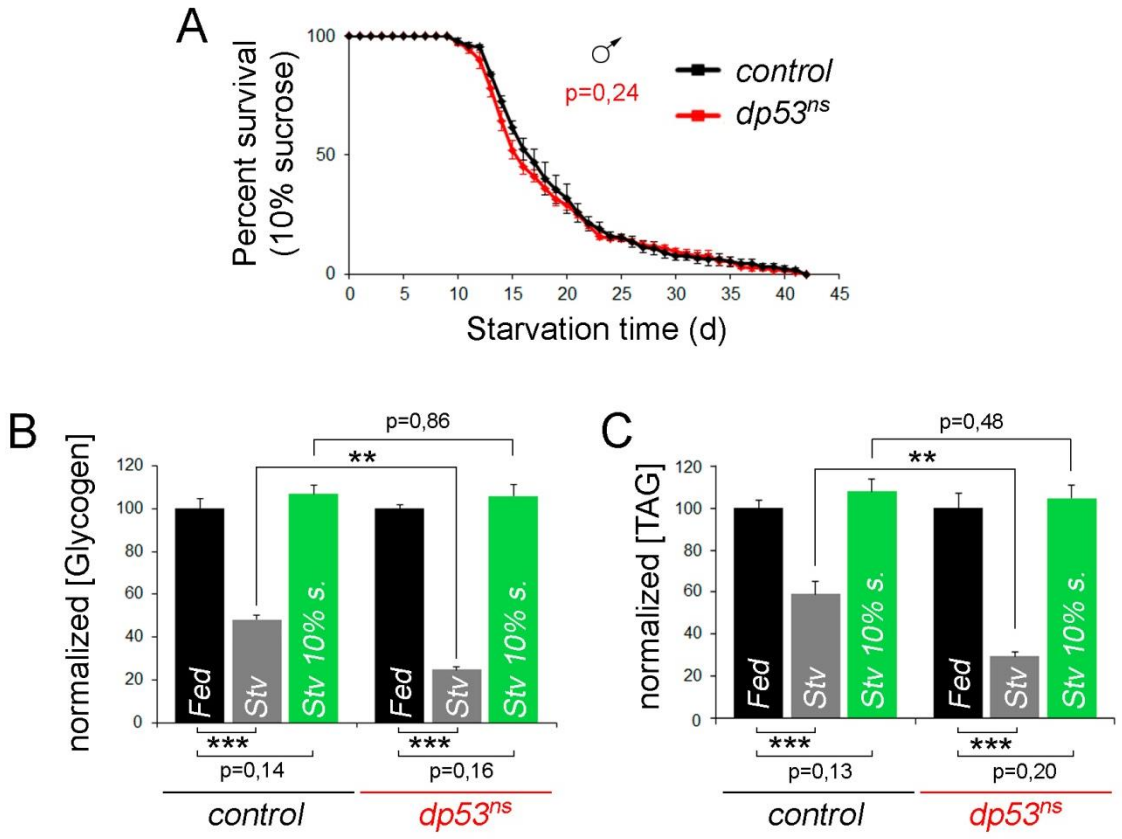

Figure 17: Reduced survival rates of fasted dp53 mutant animals are most probably a consequence of reduced amounts of sugars

(A) Survival rates to nutrient deprivation (2% agar, 10% sucrose) of 1-2-day-old dp53 mutant (*dp53*^{ns}) and control (*w*^{1118}) adult males. **(B-C)** Histograms plotting glycogen (B) and TAG (C) levels from *dp53* mutant (*dp53*^{ns}) and control (*w*^{1118}) adult males in fed conditions (black bars), starved in 2% agar, 1% sucrose (grey bars) or starved in 2% agar, 10% sucrose (green bars). Data were normalized to protein concentration and represented as a percentage of the fed values for each genotype. In all the cases animals were grown under identical conditions and aged for 5 days prior to exposion to the corresponding fasting conditions for 1 day in B or for 3 days in C. Note that increasing the amount of sugar in the medium is enough to rescue the differents between *control* and *dp53* mutant animals. Error bars represent SEM, brackets indicate the genotypes that are compared, *** p<0.001, ** p<0.01 and * p<0.05.

3. The miRNA machinery as a novel layer of post-transcriptional regulation of Dp53 in *Drosophila* tissues

In the previous section we described a novel and previously uncharacterized role of Dp53 in the metabolic adaptation to nutrient deprivation at the level of a living organism. Since p53 is a key tumour suppressor and a central regulator of the stress response, a tight regulation at different levels is essential to ensure a robust and precise response to cellular signals. In unstressed cells, p53 has to be maintained at low physiological levels to prevent its deleterious effects on living organism. In mammals, a complex array of post-translational modifications regulates the stability, localization, conformation and transcriptional activity of p53 in healthy cells. Although the most critical step is the regulation of p53 by ubiquitin ligases such as Mdm2 *(Foulkes, 2007; Gu and Zhu, 2012)*, recent studies confirmed the old hypothesis that *Drosophila* lacks Mdm2 *(Lane and Verma, 2012)*. In the last few years, the expression and activity of vertebrate p53 has been shown to be under the control of microRNAs [miRNAs,*(Hermeking, 2007; Hermeking, 2012; Le et al., 2009)*], thus prompting us to analyze whether the miRNA machinery is involved in the regulation of Dp53 in *Drosophila*.

Depletion of the miRNA machinery induces Dp53-dependent apoptotic cell death

- ***dcr-1* depleted cells showed increased Dp53 protein levels**

Previous studies in our laboratory showed that clones of cells mutant for *dicer-1* (*dcr-1*), a double-stranded RNAse III essential for miRNA biogenesis, are on average smaller than *wild-type* clones and most of them are eliminated from the wing epithelium by apoptosis *(Herranz et al., 2010).* These observations, together with the fact that Dp53 is able to induce apoptosis (Figure 2), raised the hypothesis that Dp53 might be negatively regulated by the miRNA machinery. Therefore, we decided to look for changes in Dp53 mRNA and protein levels in a situation where the miRNA machinery is downregulated. To decrease the miRNA machinery we expressed a dsRNA against dcr-1 (*dcr-1*^{RNAi}) under the *patched-gal4* (*ptc-gal4*) driver, which drives transgene expression at very high levels in the A-P boundary of the wing primordia. Depletion of the miRNA machinery reduced the protein levels of the dMyc proto-oncogene *(Herranz et al., 2010)* and interestingly, increased Dp53 protein levels (Figure 18A). In this way, our preliminary hypothesis about the capacity of the miRNA machinery to

downregulate Dp53 is confirmed. However, we were not able to detect an increase in *dp53* mRNA levels upon dcr-1 reduction by *in situ* hybridization with a specific probe against Dp53 (Figure 18B). By driving expression of Dp53 in the posterior compartment, up-regulation of *dp53* mRNA levels was detected with the same probe (Figure 18C). These results open the possibility that the miRNA machinery modulates the rate of Dp53 translation and not *dp53* mRNA degradation and/or stability.

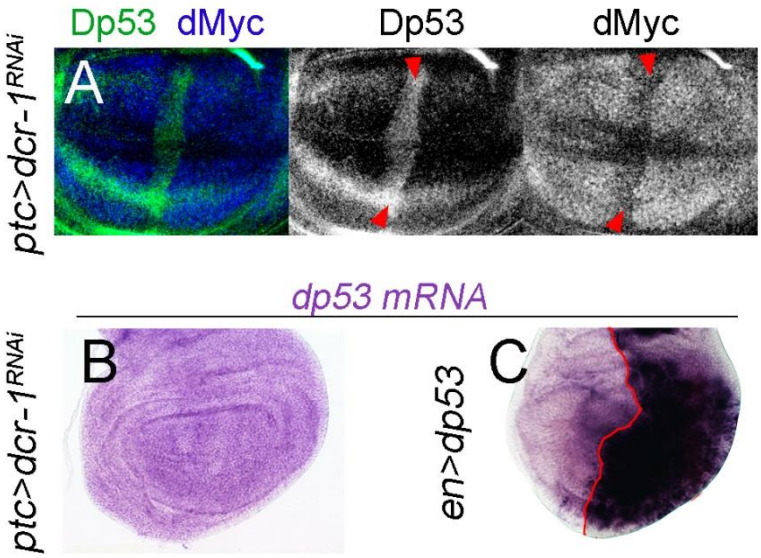

Figure 18: dcr-1 reduction show increased Dp53 protein levels but not mRNA levels

(A-B) Wing primordia expressing dsRNA form of dcr-1 (*dcr-1*^{RNAi}) under the control of the *ptc-gal4* driver and labeled to visualize Dp53 (green in A) and dMyc (blue in A) protein levels or *dp53* mRNA levels (B). *ptc-gal4* drives transgene expression in the anterior-posterior comparment boundary, indicated by red arrow heads. Note that down-regulation of dcr-1 induces an increase in Dp53 protein levels but doesn't affect dp53 mRNA levels. **(C)** Wing primordia expressing a wild-type form of Dp53 in the posterior comparment (red line marks the anterior-posterior boundary) with the *en-Gal*$^{80t.s}$ driver and labeled to visualize *dp53* mRNA levels as a possitive control.

- **Dp53 activity contributes to the apoptotic cell death and poor cell survival of dcr-1 depleted cells**

The observation that *dcr-1* depleted cells show increased Dp53 protein levels raised the possibility that the increase in Dp53 activity might contribute to the loss of *dcr-1* mutant cells by apoptosis. To tackle this question, we used the MARCM mosaic technique to analyze the size of *dcr-1* null mutant (*dcr-*

1^{Q1147X}) clones in which Dp53 activity was depleted by expressing the dominant negative form of Dp53 (Dp53$^{H159.N}$). Since *dcr-1* mutant clones are usually fragmented, the mutant tissue was positively labelled by the expression of GFP and the ratio of the mutant cell population to the total wing pouch area was measured in the different experimental conditions. This ratio was normalized to the ratio obtained with wild type clones and presented as a percent. Ratios were measured for clones induced 48, 72 and 96 hours before visualization. As shown in Figure 19, depletion of Dp53 activity was able to totally rescue the size of 48 hours old clones mutant for *dcr-1*^{Q1147X} (compare Figure 19B and C upper panel, see also Figure 19E for quantification). Similar results were obtained by expressing the baculovirus protein p35, which binds and inhibits the effector apoptotic Caspases DrIce and Dcp-1 *(Hay et al., 1994)* (compare Figure 19B and D, see also Figure 19E for quantification). We noticed that the capacity of *dp53*$^{H159.N}$ to rescue the size of older clones was diminished, whereas *p35* was able to rescue, to a larger extent but not completely, the size of 72 and 96 hours old *dcr-1*^{Q1147X} mutant clones (compare Figure 19C and D middle and lower panels, see also Figure 19E for quantification). These results indicate that Dp53 activity contributes, in part, to the loss of *dcr-1* mutant tissue and suggest that *dcr-1* mutant cells are eliminated from the tissue by both Dp53 dependent and independent mechanisms. Consistent with this proposal, *dcr-1*^{Q1147X} mutant clones expressing *dp53*$^{H159.N}$ were still positive for TUNEL staining, (Figure 20B-B'') suggesting that *dcr-1* mutant cells are still eliminated by apoptosis. However, we noticed that the fraction of mutant dying cells expressing *dp53*$^{H159.N}$, which are located on the basal side of the epithelium, was largely reduced when compared to *dcr-1*^{Q1147X} mutant clones expressing only GFP (compare Figure 20A'-A'' and B'-B'').

In order to better quantify the contribution of Dp53 activity to the apoptosis induced by *dcr-1* depletion, we measured and compared the total number of TUNEL positive cells in wing primordia expressing *dcr-1*^{RNAi} together with GFP (Figure 20C) or *dp53*$^{H159.N}$ (Figure 20D) under the control of the *nub-gal4* driver. As shown in Figure 20E, *dp53*$^{H159.N}$ expression reduced almost 40% the number of TUNEL positive cells caused by reduction of *dcr-1.*

Altogether, these results indicate that Dp53 contributes to the apoptotic cell death and poor cell survival caused by depletion of the miRNA machinery and reinforce the proposal that Dp53 is been negatively regulated by the miRNA machinery, thereby establishing the miRNA machinery as novel layer of post-transcriptional regulation of Dp53.

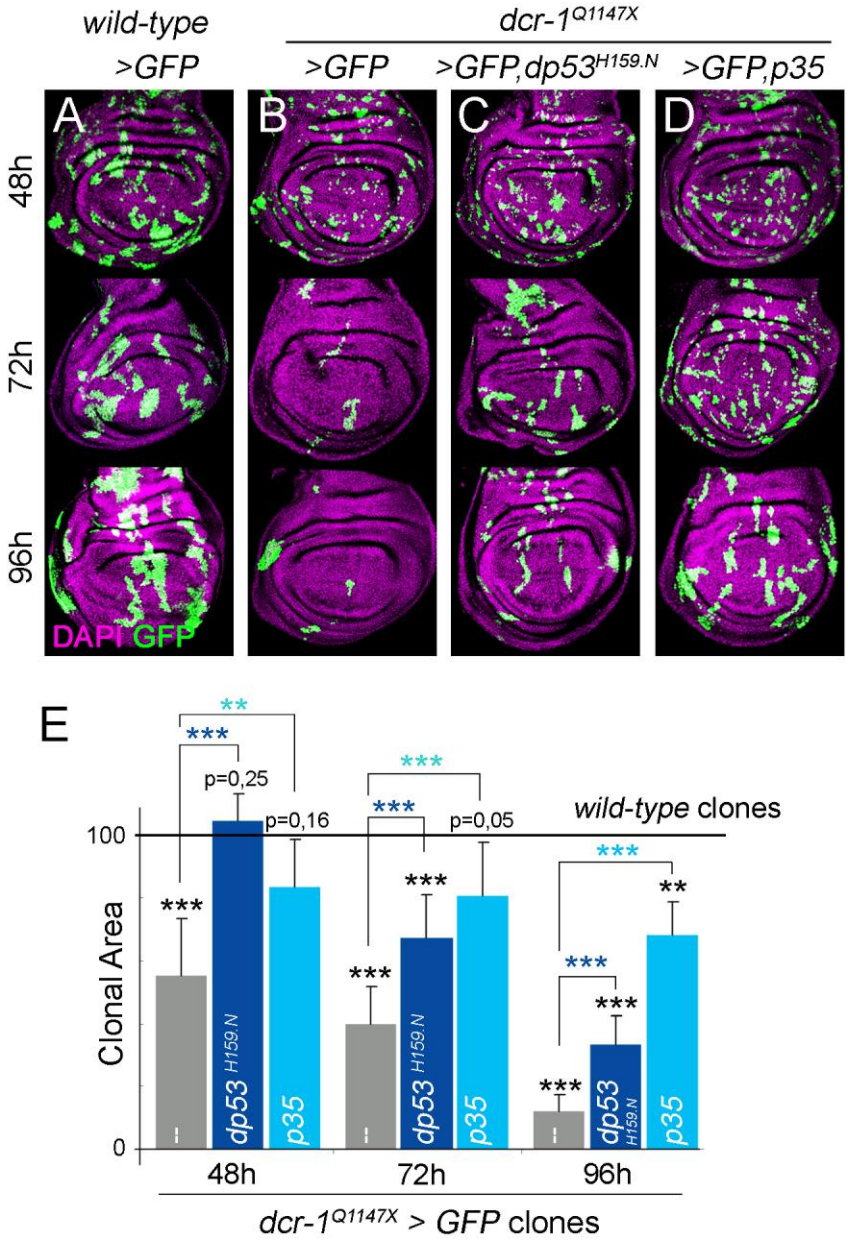

Figure 19: Dp53 activity contributes to the poor cell survival of *dcr-1*^{Q1147X} mutant cells

(A-D) Wing discs with clones of *wild-type* cells (A) or cells lacking Dcr-1 activity (homozygous for a null allele of *dcr-1*, *dcr-1*^{Q1147X} in B-D) and expressing the indicated transgenes. Clones were analized 48, 72 and 96 h after induction and visualized by GFP (green) expression. Wing discs were stained for DAPI (pink). Note that *dcr-1*^{Q1147X} mutant clones tend to be eliminated from the tissue, and expression of *p35* or *dp53*$^{H159.N}$ largely rescues this lost. **(E)** Histogram plotting the resulting clonal areas (as the ratio of GFP-mutant cell population to the total wing pouch area) of the different genotypes shown in A-D. Clonal areas were normalized as a percent of the *wild-type* ones. Note that the clonal area of the *dcr-1* mutant tissue is partially rescued when expressing *p35* or *dp53*$^{H159.N}$. Asterisc and p-values in black indicate comparisons between each genotype and the *wild-type* control clones, and upper brackets indicate comparisons between *dcr-1*^{Q1147X} mutant clones (grey) and the corresponding rescues with *dp53*$^{H159.N}$ (dark blue) or *p35* (light blue). Error bars represent SEM. *** p<0,001 and ** p<0,01.

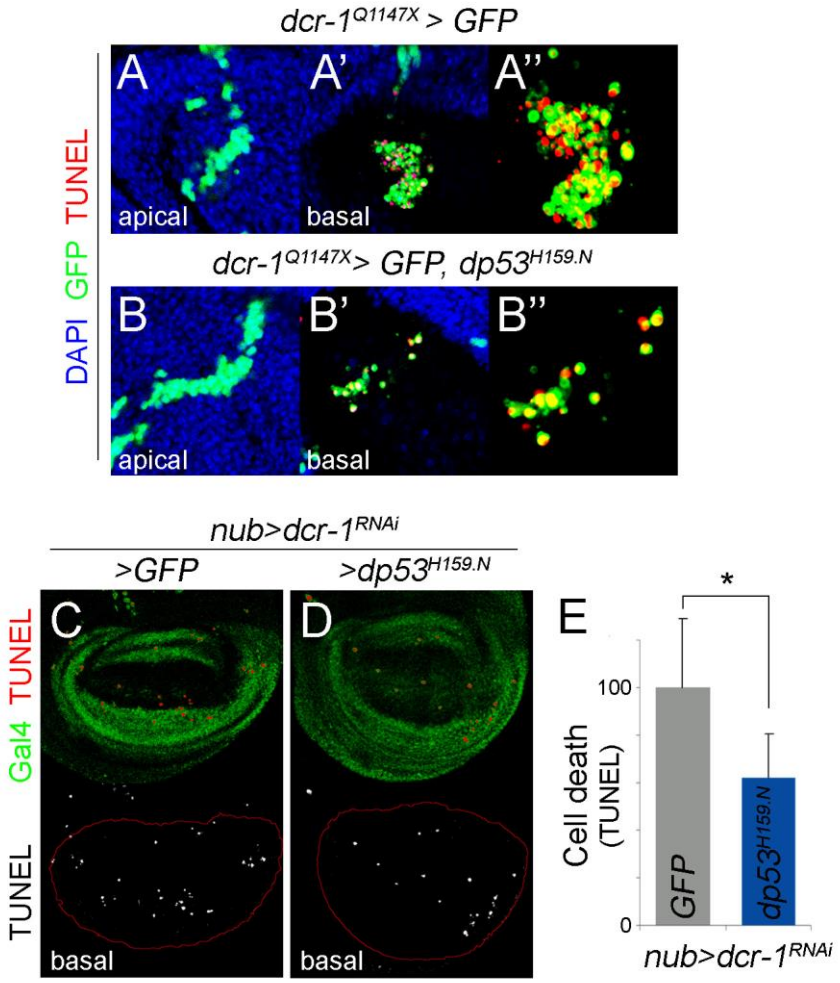

Figure 20: Dp53 activity contributes to the apoptotic cell death caused by reduction of the miRNA machinery

(A-B) Clones of cells homozygous mutant for Dcr-1 (*dcr-1*^{Q1147X}), expressing GFP (green) alone (A-A'') or together with *dp53*$^{H159.N}$ (B-B'') to decrease Dp53 activity at the same time, and labeled by TUNEL staining (red) to visualize apoptotic cell death and DAPI (blue). Apical and basal views of the epithelium are shown. Note that the fraction of dying basal cells is largely rescued when expressing *dp53*$^{H159.N}$. **(C-D)** Wing discs expressing *dcr-1*^{RNAi} either with *GFP* (C) or with *dp53*$^{H159.N}$ (D) under the control of the *nub-gal4* driver (that is expressed in the wing pouch) and labeled by TUNEL staining (red or grey) to visualize apoptotic cell death and Gal4 protein (green). Note reduced number of apoptotic cells in *dp53*$^{H159.N}$ expressing wing discs. **(E)** Histogram plotting the number of apoptotic cells per wing pouch (Gal4-positive cells) of the genotypes shown in C and D. Numbers were normalized as a percent of the GFP expressing wing discs, error bars represent SEM and * p<0,05.

Depletion of the miRNA machinery compromises tissue growth as a consequence of the reduction in the protein levels of the *dMyc* proto-oncogene [Figure 21A, *(Herranz et al., 2010)*]. TRIM32, the mouse

ortholog of Drosophila Mei-P26 *(Page et al., 2000)*, is able to display Ubiquitin Ligase activity, bind c-Myc and target it for degradation *(Schwamborn et al., 2009)*. In *Drosophila*, the miRNA machinery targets directly the *mei-P26* 3'UTR thus positively regulating dMyc protein levels, and as a consequence tissue growth *(Herranz et al., 2010)*. The observation that *dcr-1* depleted cells show increased Dp53 protein and activity levels prompted us to analyze whether Dp53 also contribute to the tissue growth defects of *dcr-1* depleted cells. Interestingly, expression of $dp53^{H159.N}$ did not have any effect on the increased levels of Mei-P26 and reduced levels of dMyc protein caused by dcr-1 depletion in $ptc>dcr\text{-}1^{RNAi}$ wing discs (Figure 21A, B). Similarly, the reduction of the posterior domain caused by $dcr\text{-}1^{RNAi}$ expression under the *en-gal4* was unaffected by co-expression of $dp53^{H159.N}$ or p35 (Figure 21C). Altogether, these results indicate that Dp53 activity caused by depletion of the miRNA machinery does not contribute to the tissue size defects and suggest that reduced tissue growth is not a consequence of increased apoptosis.

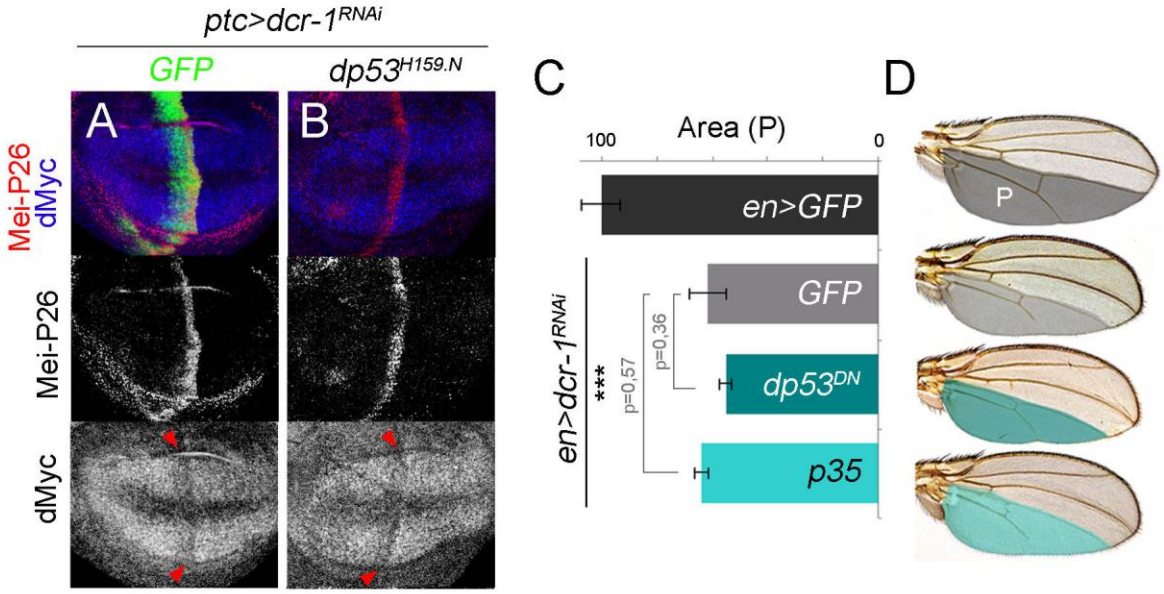

Figure 21: Dp53 activity does not contribute to the tissue size defects caused by reduction of the miRNA machinery

(A-B) Wing primordia expressing $dcr\text{-}1^{RNAi}$ and GFP (A) or $dp53^{H159.N}$ (B) under the control of the *ptc-gal4* driver and labeled to visualize Mei-P26 (red or white) and dMyc (blue or white) protein levels. *ptc-gal4* drives transgene expression in the anterior-posterior comparment boundary, indicated by red arrow heads. **(C-D)** Cuticle preparations of adult wings (D) and histogram plotting the correspondent size value (C) of the posterior (P) domains expresing the indicated transgenes under the control of the *en-gal4* driver.*3* mRNA levels as a possitive control. Values were normalized as a percent of the GFP expressing wings, error bars represent SEM and *** p<0,001. Only adult wing males were analyzed. Note that expression of $dp53^{H159.N}$ did not have any effect on the increased Mei-P26 or the reduced dMyc protein levels and in the tissue size reduction caused by *dcr-1* depletion.

dp53 is a direct target of the miRNA machinery

Our previous results indicate that in *Drosophila* epithelial cells Dp53 is activated upon depletion of the miRNA machinery. But, is Dp53 a direct target of the miRNA machinery? To address this question, we constructed a *dp53* 3'UTR sensor transgene (*dp53-sensor)* consisting of the 3'UTR of *dp53*, which is shared by the three alternative spliced forms, cloned into a tubulin-promoter-EGFP reporter plasmid (Figure 22A). A control EGFP sensor (*control-sensor*) carrying the 3' UTR of the P element in CaSpeR4 was also used *(Brennecke et al., 2003)*. When the EGFP expression levels of the two transgenes was compared using the same settings on the confocal microscope, it was apparent that the *control-sensor* (Figure 22B) was expressed at much higher levels than the *dp53-sensor* (two independent insertion lines were quantified, compare Figure 22B and C or D, see also E for quantification). The difference in the overall EGFP signal between the *control-* and the *dp53-sensors* was confirmed by Western blotting samples from full larvae (Figure 22F).

MicroRNA-mediated targeting of the *dp53* 3'UTR is expected to maintain EGFP expression levels of the *dp53-sensor* low under normal physiological conditions. Thus, the difference in the levels of *control-* and *dp53-sensors* suggested that the 3'UTR of *dp53* could be directly targeted by the miRNA machinery. Indeed, expression of *dcr-1*^{RNAi} either with an ubiquitous *actin-gal4* driver (*act-gal4*, Figure 23B, see C for quantification) or with different region-specific drivers: *hedgehog (hh-gal4,* Figure 23D), *apterous* (ap-*gal4*, Figure 23E) and *patched (ptc-gal4*, Figure 23F) Gal4 drivers (which drive transgene expression in the posterior (P) compartment, the dorsal (D) compartment and in a stripe of anterior cells adjacent to the A-P compartment boundary respectively) notably increased the EGFP expression levels of the *dp53-sensor* in wing cells. Moreover, clones of cells homozygous mutant for *dcr-1* (marked by the absence of β-gal) also showed increased EGFP expression levels of the *dp53-sensor* when compared to the surrounding heterozygous tissue (Figure 23G, red arrows).

Taken together, these results indicate that the miRNA machinery is directly targeting *dp53* in the wing epithelium.

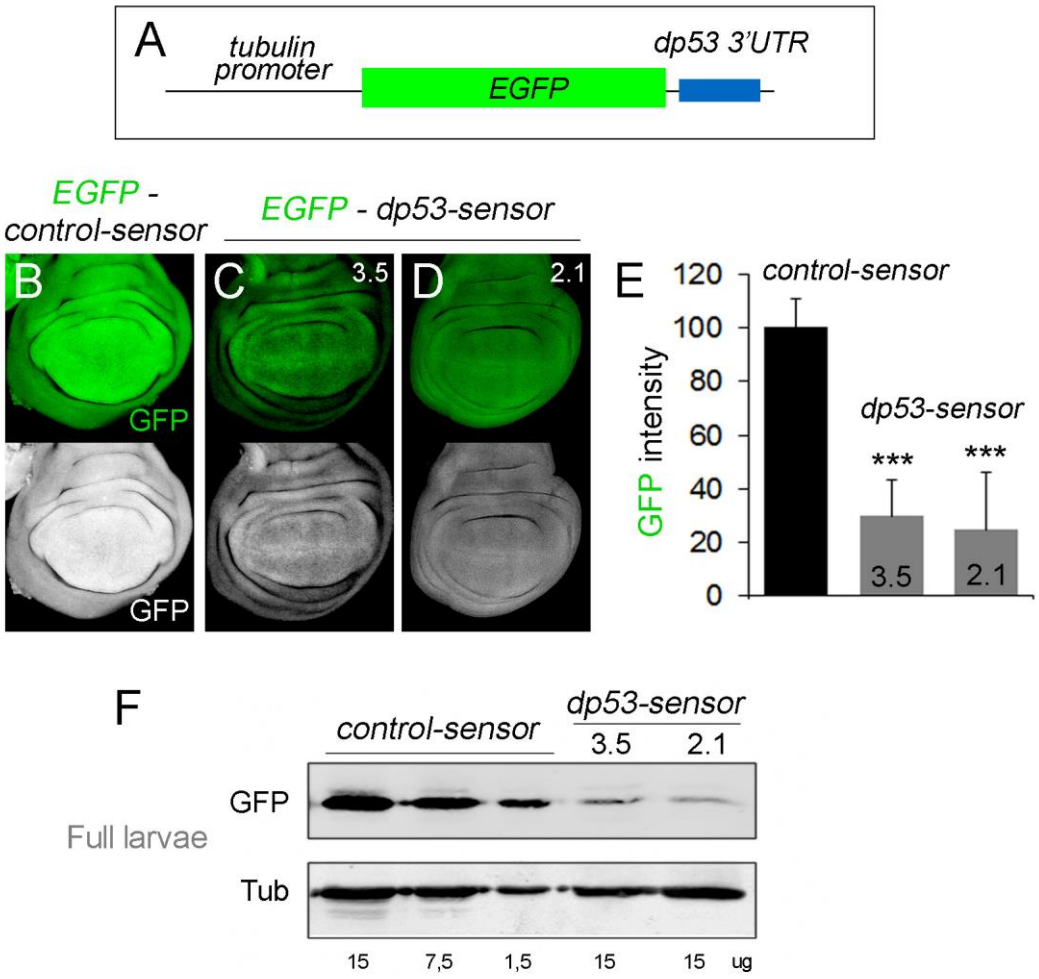

Figure 22: The dp53-sensor is expressed at lower levels than a control-sensor

(A) Cartoon depicting the *dp53-sensor* consisting of the tubulin-EGFP transgene carrying the 3' UTR of *dp53* (blue box). **(B-D)** Representative examples of wing discs carrying either the *control-sensor* (B) or two independent insertion lines of the *dp53-sensor* (C, D) stained to visualized GFP protein expression (green or grey). All the wing disc shown are imaged under identical confocal microscope settings and conditions and the images were processed identically to allow direct comparison. **(E)** Histogram plotting GFP expression levels of the wing discs shown in B-D. Results are normalized as a percent of the *control-sensor* values. Error bars represent SEM. *** p<0,001. **(F)** Western Blot showing the amount of GFP protein of full larvae carrying either the *control-sensor* (three rails to the left) or two independent insertion lines of the *dp53-sensor* (to the right). Extracts from the same number of larvae were extracted and serial dilutions (15, 7.5 and 1,5 μg) of total protein were loaded for the *control-sensor* and 15 μg of total protein were loaded for the *dp53-sensors*. β-tubulin serves as a loading control. Note the drastically reduction of GFP protein levels in tissues carrying the *dp53-sensor* when compared to tissues carrying the *control-sensor*.

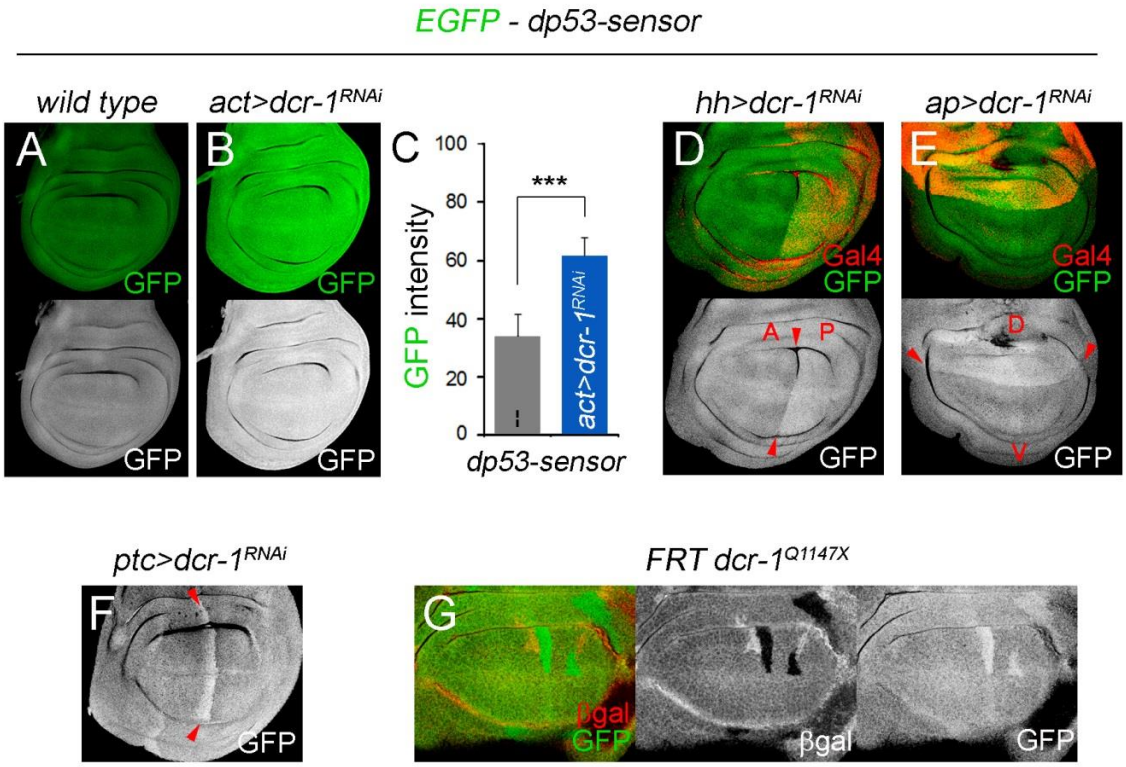

Figure 23: dcr-1 depletion induces an increase in the EGFP levels of the dp53-sensor

(A, B) Representative examples of wing discs *act-gal4; +* (*wild-type*, A) or *act-gal4; UAS-dcr-1*^{RNAi} (B) carrying the *dp53-sensor* and stained to visualize GFP protein expression (green and grey). All the wing disc shown are imaged under identical confocal microscope settings and conditions and the images were processed identically to allow direct comparison. **(C)** Histogram plotting GFP expression levels of the wing discs shown in A and B. Results are normalized as a percent of the *wild-type* condition. Error bars represent SEM. *** p<0,001. **(D-F)** Wing discs expressing *dcr-1*^{RNAi} under the control of the *hh-gal4* (D), *ap-gal4* (E) or *ptc-gal4* (F) drivers carrying the *dp53-sensor* and labeled to visualized GFP (green or grey) and Gal4 (red, D and E) protein expression. *hh-Gal4*, *ap-Gal4* and *ptc-gal4* drive transgene expression in the posterior (P) compartment, the dorsal (D) compartment and in a stripe of anterior cells adjacent to the A-P boundary respectively. Red arrowheads depict the A-P boundary in D and F, and the D-V boundary in E. Note that upon expression of *dcr-1*^{RNAi} the EGFP expression levels of the *dp-53 sensor* are largely increased. **(G)** *dcr-1*^{Q1147X} homozygous clones (marked by the absence of *β-gal*, in red or grey) showing expression of the *dp53-sensor* (green or grey). Note increased levels of EGFP in *dcr-1*-depleted cells (red arrows).

The microRNA *miR-305* is an essential regulator of dp53

To further characterize the regulation of *dp53* by the miRNA machinery, we searched for potential miRNA-binding sites in its 3'UTR by computational analysis. Searches by TargetScanFly *(Kheradpour et al., 2007; Ruby et al., 2007)* and MicroCosm Target *(Griffiths-Jones et al., 2008)* revealed a list of ten putative miRNAs predicted to target the 3'UTR of *dp53* (Figure 24A, B).

A

#	MicroRNA	MicroCosm	TargetScan
1	miR-279	Yes	No
2	miR-219	Yes	Yes
3	miR-1015	Yes	Yes
4	miR-283	No	Yes
5	miR-985	No	Yes
6	miR-iab-4as	Yes	Yes
7	miR-305	No	Yes
8	miR-1014	Yes	Yes
9	miR-10/1006	No	Yes
10	miR-190	No	Yes

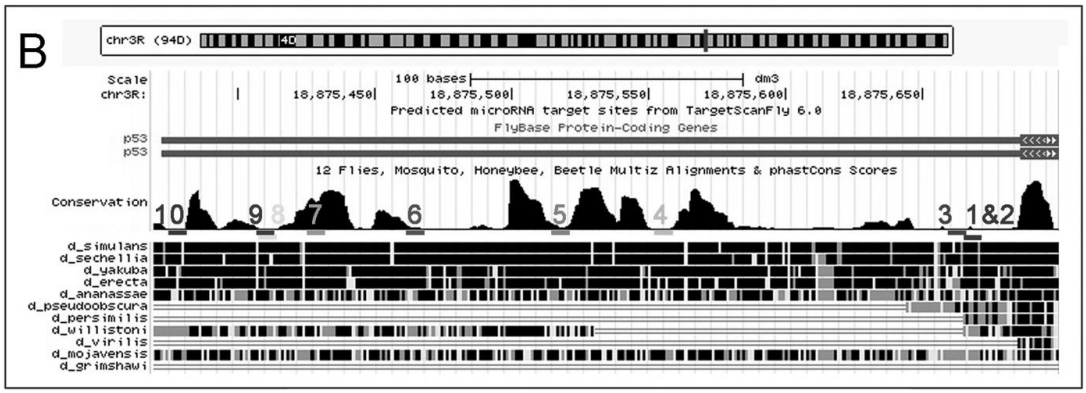

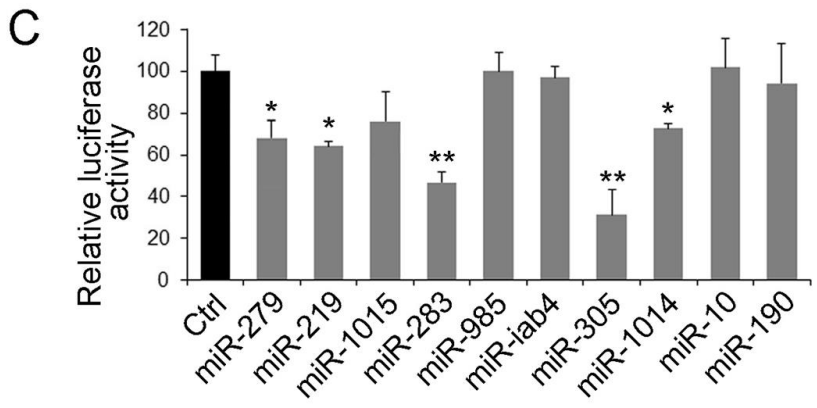

Figure 24: Bioinformatic predictions and luciferase assays of the ten putative miRNA predicted to target the 3'UTR of dp53

(A-B) List of predicted miRNA binding sites in the *dp53* 3'UTR obtained by using MicroCosm and TargetScan softwares (A) and a GenomeBrowser view of the corresponding predicted locations in the 3'UTR of *dp53* (B). **(C)** Luciferase assays in S2 cells co-transfected with the *dp53*-luciferase reporter and individual miRNAs overexpressing plasmids (see Materials and Methods). Results are normalized as a percent of the RLuc transfection control. A representative experiment from three independent replicates is shown. Luciferase expression was significantly reduced by the overexpression of *miR-279*, *miR-219*, *miR-283*, *miR-305* and *miR-1014*. Error bars represent SEM. ** p<0,01 and * p<0,05.

We first assessed the capacity of these miRNAs to reduce the activity of a *dp53* 3' UTR-luciferase reporter in S2 cells and we found that five miRNAs (*miR-279*, *miR-219*, *miR-283*, *miR-305* and *miR-1014*) reduced the activity of the *dp53* 3'UTR-luciferase reporter when overexpressed in S2 cells (Figure 24C). From these five candidates, only overexpression of three of them (*miR-219*, *miR-283* and *miR-305*) under the *ap-gal4* driver was able to reduce the EGFP expression levels of the *dp53-sensor* in wing disc cells (Figure 25). Among these three miRNAs, we decided to follow up studying the *miR-305* for several reasons: (1) the predicted *miR-305* binding site in the 3' UTR region of *dp53* is highly conserved among the members of the *melanogaster* subgroup of *Drosophila* that diverged over 10 million years ago (Figure 24B and 26A, B); (2) *miR-305* showed high expression values in a large-scale sequencing of small RNAs in *Drosophila*, while *miR-219* and *miR-283* were under-represented *(Ruby et al., 2007)*; and (3) using quantitative RT-PCR, we confirmed that *miR-305* was indeed highly enriched in FB cells in comparison with the other two (data not shown).

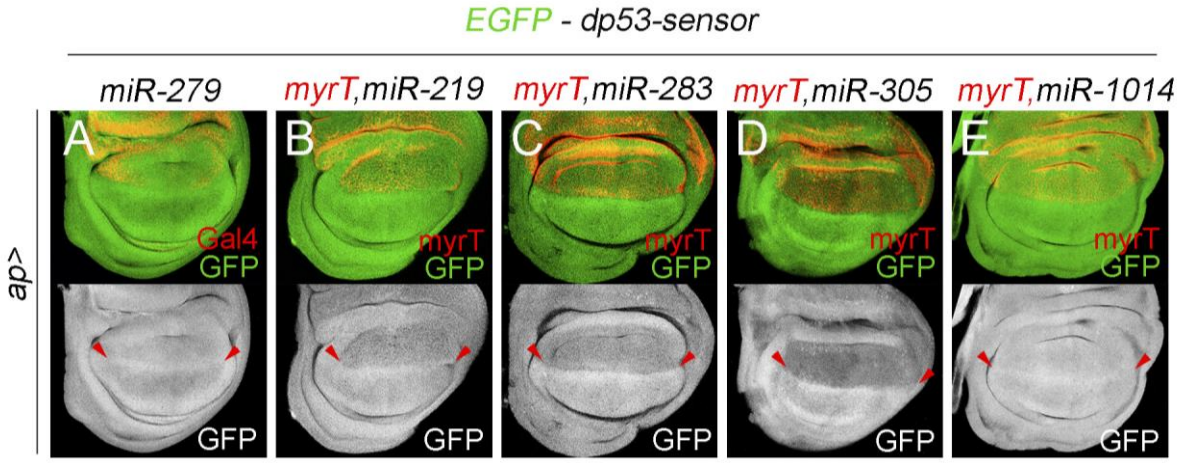

Figure 25: In vivo validation of the five candidate miRNA found in the luciferase assay

(A-E) Wing discs overexpressing *miR-279* (A), *miR-219* (B), *miR-283* (C), *miR-305* (D) and *miR-1014* (E) together with myrTomato (myrT,red in B-E) under the control of the *ap-gal4* driver carrying the *dp53-sensor* and labeled to visualized GFP (green or grey) and Gal4 (red, A) protein expression. *ap-gal4* drive transgene expression in the dorsal compartment. Red arrowheads depict the D-V boundary. Note that upon overexpression of *miR-219*, *miR-283* and *miR-305* the EGFP expression levels of the *dp53-sensor* are reduced.

To better characterize the role of *miR-305* in regulating *dp53*, we generated an EGFP sensor carrying the *dp53* 3' UTR lacking the predicted *miR-305* binding site (*dp53-Δ305-sensor*, Figure 26C).

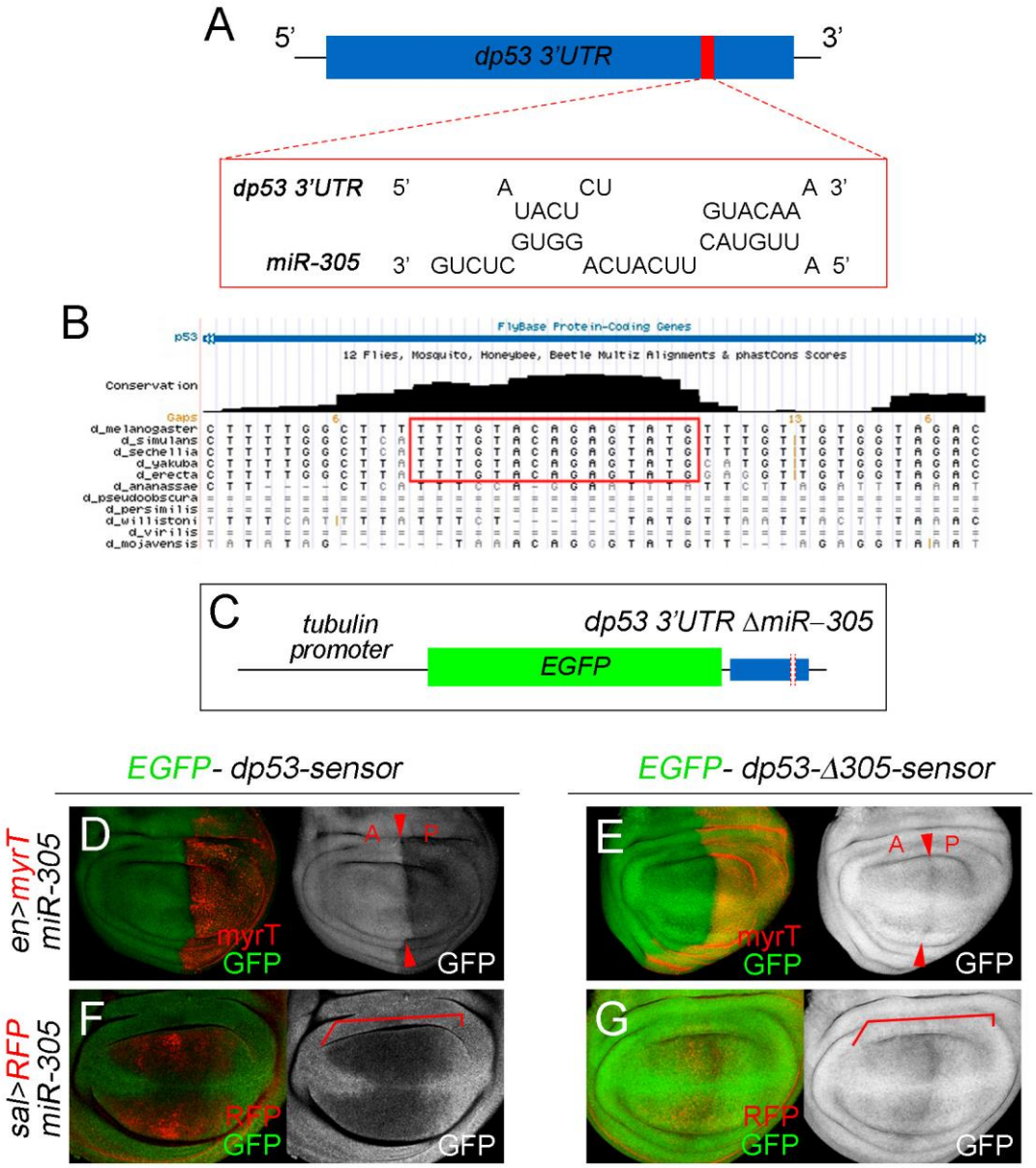

Figure 26: The predicted binding site is critical for the direct and specific binding of *miR-305 to the dp53* 3' UTR

(A) Representation of the predicted alignment between *miR-305* and the 3'UTR of *dp53 u*sing the RNAhybrid software. **(B)** GenomeBrowse view of the putative binding site of *miR-305* in the *3'UTR* of *dp53*. Note highly conservation among the members of the *melanogaster* subgroup of *Drosophila* (red box). **(C)** Cartoon depicting the tubulin-EGFP transgene carrying the 3'UTR of *dp53* with a deletion covering the miR-305 seed region (*dp53-Δ305-sensor*). **(D-G)** Wing discs carrying the *dp53-sensor* (D, F) or the *dp53-Δ305-sensor* (E, G) and stained to visualize GFP (green or grey) protein expression. Wing discs overexpressing *miR-305* and myrTomato (myrT, red) under the control of the *en-gal4* driver (D-E) or *miR-305* and RFP (red) under the control of the *spalt-Gal4* driver (*sal-gal4,* F-G). Note reduced levels of the *dp53-sensor* but not the *dp53-Δ305-sensor* in *miR-305* overexpressing cells. Red arrowheads depict the A-P boundary in D and E, and red brackets the distal zone were *sal-gal4* drives transgene expression.

miR-305 overexpression under the control of the *en-gal4* (Figure 26D, E) or the *spalt-gal4* (*sal-gal4*, Figure 26F, G) was not able to reduce the EGFP levels of the *dp53-Δ305-sensor* whereas it did it for the full *dp53-sensor* (compare Figures 26D and E, or F and G), thereby indicating that regulation of the *dp53* 3'UTR by this miRNA depends on the presence of the predicted *miR-305* binding site.

Interestingly, we noticed that in wing discs imaged under identical conditions, the EGFP expression levels of the *dp53-Δ305-sensor* were consistently higher than those in the *dp53-sensor* carrying the intact 3'UTR (Figure 27A, see B for quantification). This finding thus suggests that *miR-305* has an active role in targeting *dp53* 3'UTR under normal physiological conditions. Consistent with this proposal, clones of cells (marked by the absence of β-gal) homozygous for a small deficiency covering the *miR-305* locus (*Df-miR-305*, for details see Materials and Methods) showed increased EGFP levels of the *dp53-sensor* (Figure 27C, red arrows). Remarkably, the resulting *wild-type* twin clones (marked by two copies of β-gal) showed reduced levels of the *dp53-sensor* when compared to the surrounding heterozygous tissue (Figure 27C, yellow arrows). Thus, regulation of the *dp53* 3'UTR appears to be highly sensitive to *miR-305* doses. According with the functionality of the predicted binding site, no apparent differences in the *dp53-Δ305-sensor* were observed in clones of cells lacking *miR-305* (Figure 27D, red arrows).

These results indicate that endogenous levels of *miR-305* significantly contribute to the regulation of *dp53* and that this regulation depends on the presence of the predicted *miR-305* binding site. We found that the increase in EGFP expression levels caused by *miR-305* depletion was slightly milder than the one observed in clones of cells mutant for *dcr-1* (compare Figures 26C and 22G). Thus, other miRNAs might contribute to the regulation of Dp53 levels in the wing disc. Consistently, clones of cells mutant for *dcr-1 (dcr-1^{Q1147X})* still showed increased EGFP expression levels of the *dp53-Δ305-sensor* (Figure 27E).

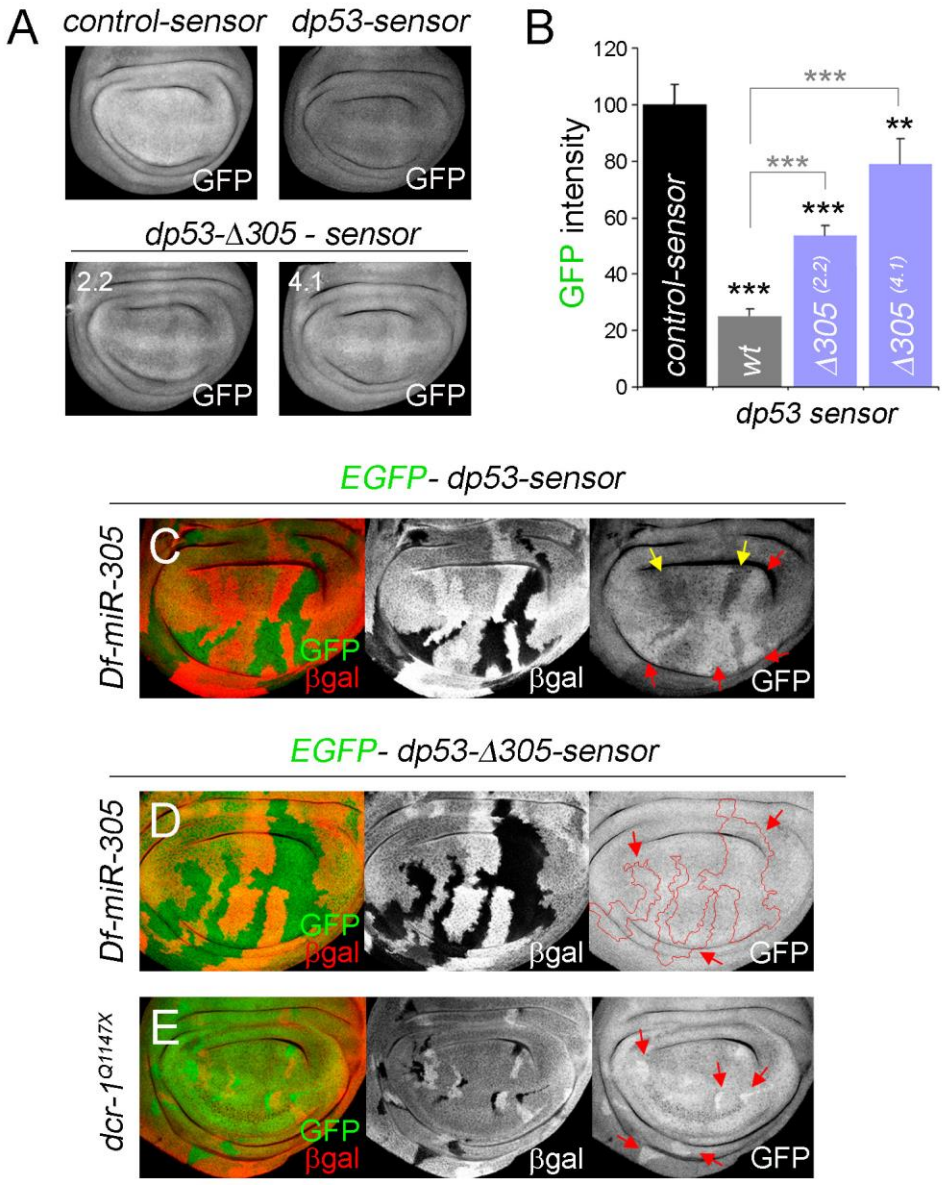

Figure 27: *miR-305* has an active role in targeting *dp53* in vivo

(A) Representative examples of wing discs carrying either the *control-sensor*, the *dp53-sensor* or two independent insertion lines of the *dp53-Δ305-sensor* stained to visualized GFP (grey) protein expression. All the wing discs shown were imaged under identical confocal microscope settings and conditions and processed identically to allow direct comparison. **(B)** Histogram plotting GFP expression levels of the wing discs shown in A. Results are normalized as a percent of the *control-sensor* values. Error bars represent SEM. *** p<0,001. **(C-D)** *Df(miR-305)* homozygous clones (marked by the absence of β-gal in red or grey) showing expression of the *dp53-sensor* (C) or *dp53-Δ305-sensor* (D) in green or grey. Note increased levels of the *dp53-sensor* but not the *dp53-Δ305-sensor* in *Df(miR-305)* cells (red arrows). Also note in C decreased EGFP levels in twin clones with two *wild-type* copies of *miR-305* (yellow arrows). **(E)** *dcr-1*^{Q1147X} homozygous clones (marked by the absence of β-gal in red or grey) showing expression of the *dp53-Δ305-sensor* in green or grey. Note that the *dp53-Δ305-sensor* is still increased in *dcr-1*^{Q1147X} mutant cells (red arrows).

4. **Physiological relevance of the miRNA-mediated regulation of Dp53**

Our results have established the miRNA machinery as a novel layer in the regulation of Dp53. We have shown that in normal physiological conditions the miRNA machinery, specifically the *miR-305*, contributes to the repression of Dp53. But, which is the physiological relevance of this regulation? In which biological context the miRNA-mediated regulation of Dp53 is crucial? Under which situations the release of this regulation plays a functional role in Dp53 activation? To address these questions, we decided to analyze the contribution of the miRNA-mediated regulation of Dp53 in the two biological contexts in which we know that Dp53 plays an important role: in response to IR and upon nutrient deprivation.

Dp53 activation upon DNA-damage appears to be independent of the miRNA-mediated regulation

Since few mechanisms have been reported that lead to IR-induced activation of Dp53 *(Brodsky et al., 2004; Mauri et al., 2008)*, we decided to monitor the possible contribution of the miRNA-mediated regulation of Dp53 in response IR.

- **Depletion of the miRNA machinery enhances the Dp53-dependent apoptotic response to IR**

To address the contribution of the miRNA-mediated regulation of Dp53 in response to DNA damaging agents, such as IR, we analyzed its early requirement in induction of apoptosis and JNK activation upon IR. As we have shown previously, wing primordia cells with reduced Dp53 activity and subjected to IR showed reduced levels of JNK activity (Figure 1F/Figure 28G) and fewer apoptotic cells (Figure 1H/Figure 28B). Interestingly, whereas the amount of cell death and JNK activation observed upon reduction of the miRNA machinery (by expressing *dcr-1*^{RNAi}) was rather mild in non-irradiated tissues (Figure 28E, J), it highly increased the amount of IR-induced programmed cell death and JNK activation (Figure 28C, H). And remarkably, both increases caused by *dcr-1*^{RNAi} were completely blocked upon depletion of Dp53 at the same time (Figure 28D, I).

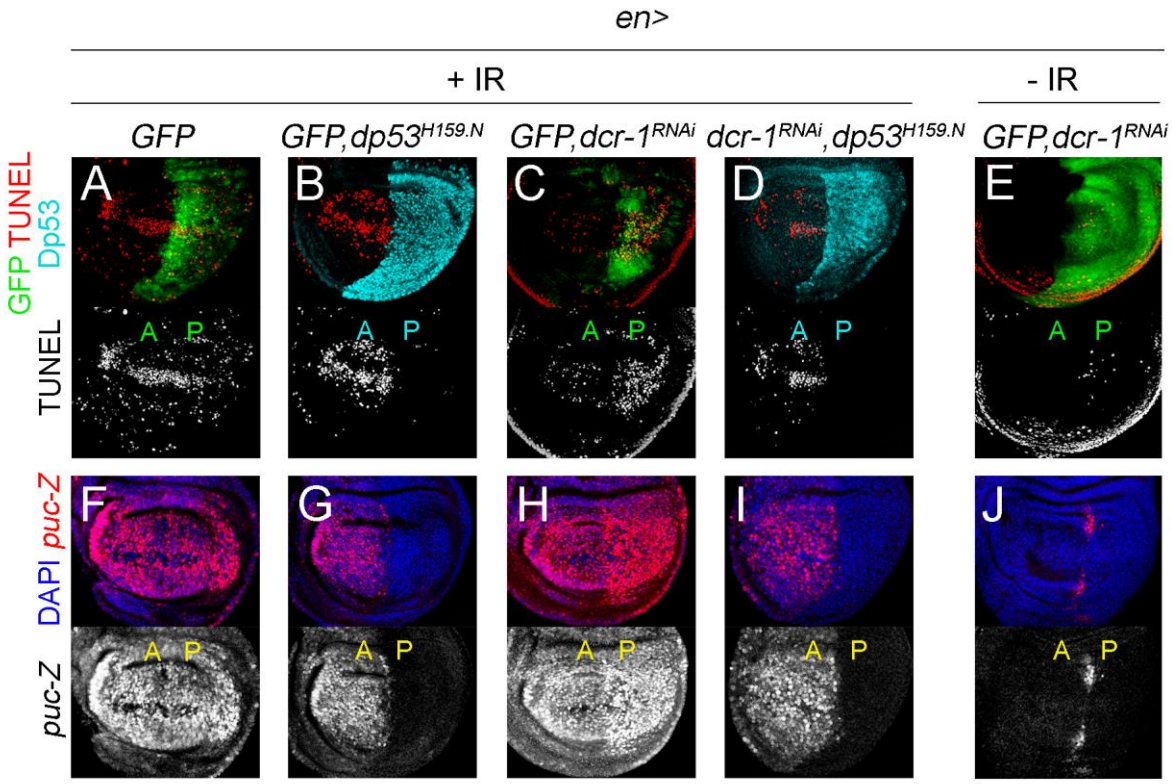

Figure 28: IR-induced apoptosis and JNK activation is increased by depletion of the miRNA machinery in a Dp53-dependent manner

(A-J) Wing primordia expressing the indicated transgenes under the control of the *en-gal4* driver, dissected in normal physiological conditions (- IR, E and J) or 5 hours after exposure to a high dose of ionizing radiation (+ IR, 4000 R, A-D, F-I), and labeled for TUNEL staining (red or grey in A-E) to visualize apoptotic cells and *puckered-lacZ* expression (*pucZ*, antibody against β-gal, red or grey in F-J) to visualize JNK activation. Wing discs were also stained for GFP (green in A, C, E), Dp53 (cyan in B, D) protein expression and DAPI (blue in F-J). *en-gal4* drives transgene expression in the posterior (P) compartment. Anterior (A) and posterior (P) compartments are indicated. Note increased levels for TUNEL staining and *pucZ* expression upon depletion of the miRNA machinery, in a dp53-dependent manner.

At least two different scenarios can explain these observations: (1) de-repression of Dp53 by reducing the levels of *dcr-1* sensitizes the tissue to IR-induced JNK activation and PCD or (2) the miRNA machinery is being targeted by the IR-stress and contributes to Dp53 activation under these circumstances.

♦ **The activity of the miRNA machinery does not change upon IR-induced DNA damage**

Our previous results support the proposed pro-survival function of miRNAs after irradiation *(Kraemer et al., 2011; Maes et al., 2008; Simone et al., 2009)* and the contribution of the miRNA machinery in targeting Dp53.

Interestingly, when we measured the expression levels of the *dp53-sensor* in the *Drosophila* wing primordia upon IR we were not able to see any major differences (Figure 29B and B', see also Figure 29C for quantification). The only thing that we observed upon IR was a salt-and-pepper increase in some cells along the dorso-ventral boundary, which also was seen in the *control-sensor* (Figure 29A', B'), thus strongly suggesting that miRNA-mediated regulation of Dp53 activity is not affected by IR. Indeed, *dcr-1* depletion still led to an increase in the expression levels of the *dp53-sensor* after IR (Figure 29E) and overexpression of *miR-305* was still able to target the 3'UTR of *dp53* in wing primordia subject to IR (Figure 29D).

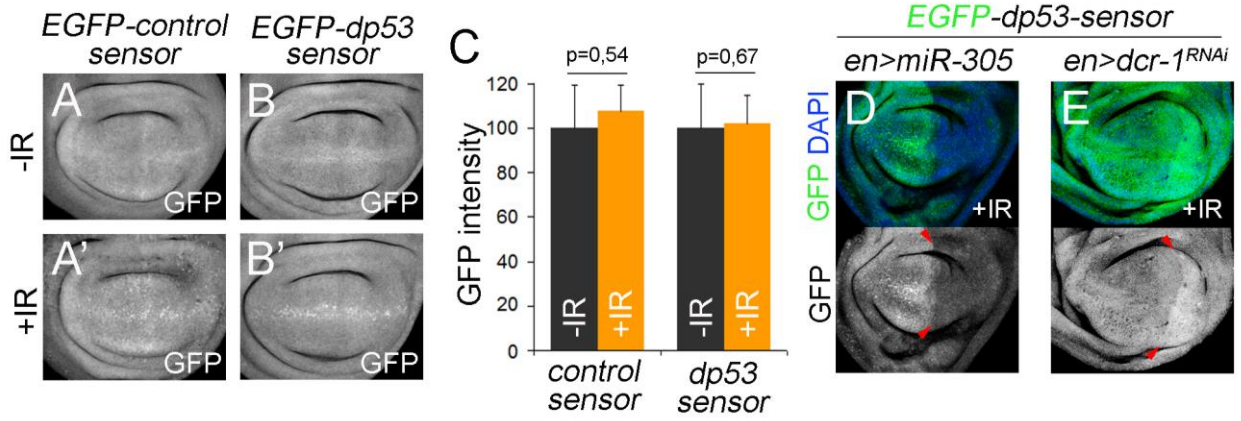

Figure 29: miRNA-dependent regulation of *dp53* is not affected by IR

(A-B) Representative examples of wing discs carrying either the *control-sensor* (A, A') or the *dp53-sensor* (B-B') dissected in normal physiological conditions (-IR, A, B) or after 5 hours of expossion to a high dose or IR (+IR, A', B') and stained to visualized EGFP (white) protein expression. For each sensor, images were taken under identical confocal microscope settings and conditions and processed identically to allow direct comparison between non-irradiated and irradiated tissues. (**C**) Histogram plotting GFP expression levels of the wing discs shown in A-B'. Results are normalized as a percent of the non-irradiated values for each sensor. Error bars represent SEM. **(D, E)** Wing disc from larvae expossed to a high dose of IR and dissected 5 hours later, expressing *miR-305* (D) or *dcr-1*^{RNAi} under the control of the *en-gal4* driver, carrying the *dp53-sensor* and labeled to visualized GFP (green or white) protein expression and DAPI (blue). *en-gal4* drives transgene expression in the posterior compartment of the wing disc, and red arrowheads point to the A-P compartment boundary. Note that overexpresson of *miR-305* and expression of *dcr-1*^{RNAi} are still able to modulate the levels of the *dp53-sensor* after irradiation.

Remarkably, this regulation not only affected the levels of the *dp53-sensor* but also the Dp53 protein levels upon IR. First of all, we noticed that Dp53 activation upon IR was correlated with an increase in Dp53 protein levels (compare Figure 30A and B), and, most interestingly, this increase was not only clearly restored upon expression of a dsRNA form against dp53 (*dp53*^{RNAi}) but also partially restored upon expression of *miR-305* (Figure 30C, D, quantification in 30E).

Altogether, these results suggest that the activity of the microRNA machinery is not affected upon IR and indicate that the activation of Dp53 upon IR does not depend on the de-regulation of the miRNA-mediated targeting of *dp53.*

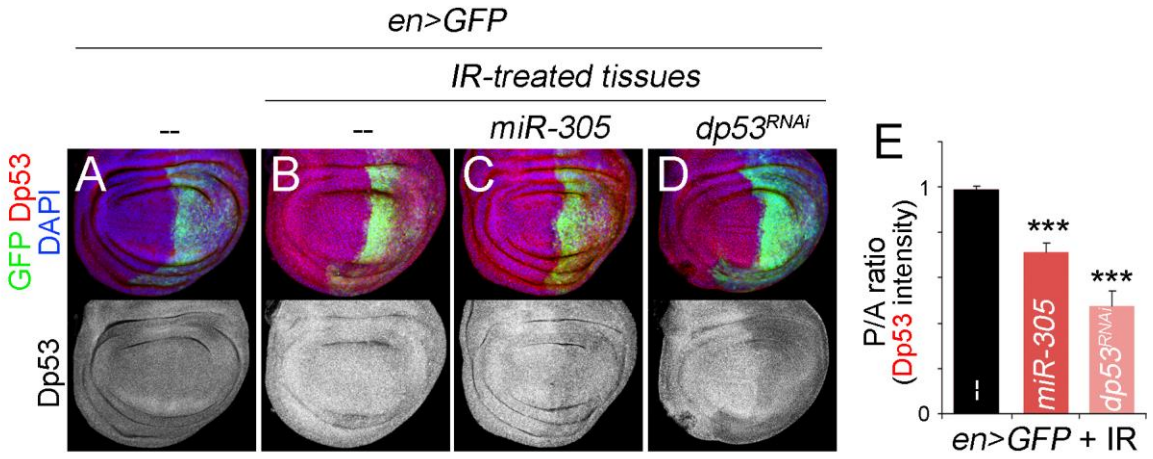

Figure 30: DNA damage-induced Dp53 is repressed by ectopic *miR-305*

(A-D) Wing disc expressing GFP alone (A, B) or together with *miR-305* (C) or a dsRNA against dp53 (*dp53*^{RNAi}, D) under the control of the *en-gal4* driver, dissected in normal physiological conditions (A) or 5 hours after a high dose of IR (B-D), labeled for Dp53 (red or grey) and GFP (green) protein expression and DAPI (blue). All images were taken under identical confocal microscope settings and conditions and processed identically to allow direct comparison **(E)** Histogram plotting the A/P Dp53 intensity levels ratio of wing disc shown in B-D. Error bars represent SEM. *** p<0,001. Note that the increase of Dp53 protein levels upon IR is significantly rescued by *miR-305* targeted expression.

Upon nutrient deprivation, miRNA-mediated regulation of Dp53 is crucial for organismal survival

Since miRNA-mediated regulation of Dp53 is not affected by IR, we next focused on the contribution of the miRNA machinery in regulating Dp53 under nutrient deprivation. Since the requirement of Dp53 under nutrient deprivation is FB-specific, we first decided to address whether the

regulation of *dp53* by the miRNA machinery also takes place in FB cells. To modulate the levels of *dcr-1* or *miR-305* in individual FB cells, we used the Flp-Out technique. We found that expression of *dcr-1*^{RNAi} (marked by the absence of CD2) results in increased EGFP levels of the *dp53-sensor* (Figure 31A). On the contrary, FB cells overexpressing *miR-305* (positively marked by RFP expression) showed a reduction in the *dp53-sensor* (Figure 31B). These results confirmed that Dp53 is indeed a target of the miRNA machinery in FB cells as well as in wing imaginal cells.

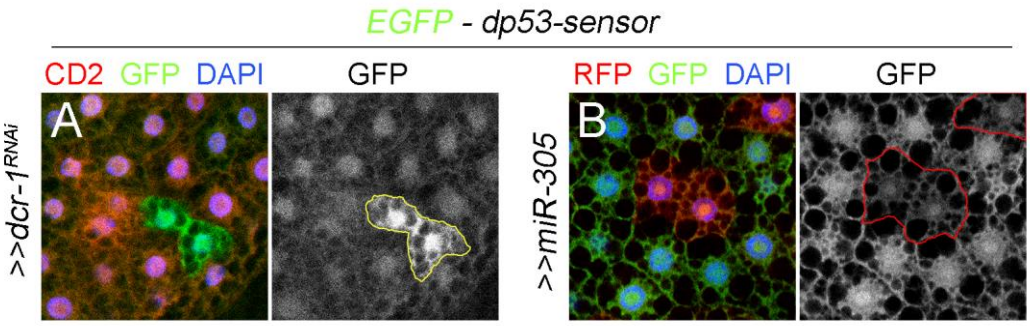

Figure 31: miRNA-mediated regulation of Dp53 takes places in fat body cells

(A-B) FB cells of well-fed animals expressing *dcr-1*^{RNAi} (marked by the absence of CD2, A in red) or overexpressing *miR-305* and RFP (red, B) carrying the *dp53-sensor* and stained to visualized GFP (green or grey) and CD2 (red, A) protein expression, and DAPI (blue). Note increased EGFP levels in *dcr-1*^{RNAi} expressing cells and reduced EGFP levels upon *miR-305* overexpression.

- ***miR-305* dependent regulation of Dp53 is modulated by nutrition**

In order to address the potential modulation of this regulation by the nutritional status of the animal, we measured the EGFP levels of the *dp53-sensor* in FB cells of starved and non-starved animals. When the EGFP levels were compared using the same settings on the confocal microscope we observed that the *dp53-sensor* was expressed in FB cells at much higher levels in starved than in normally fed individuals (Figure 32B, B' and quantification in D). This modulation is Dp53-specific since the EGFP levels of the *control-sensor* were mildly reduced upon starvation, most probably as a consequence of the decrease in whole-animal metabolism (Figure 32A, A' and quantification in D). Interestingly, the impact of nutritional conditions on the *dp53-sensor* depended on the presence of the *miR-305* binding site, as no significant changes in the EGFP expression levels were observed in FB cells carrying the *dp53-Δ305-sensor* and subjected to starvation (Figure 32C, C' and quantification in D).

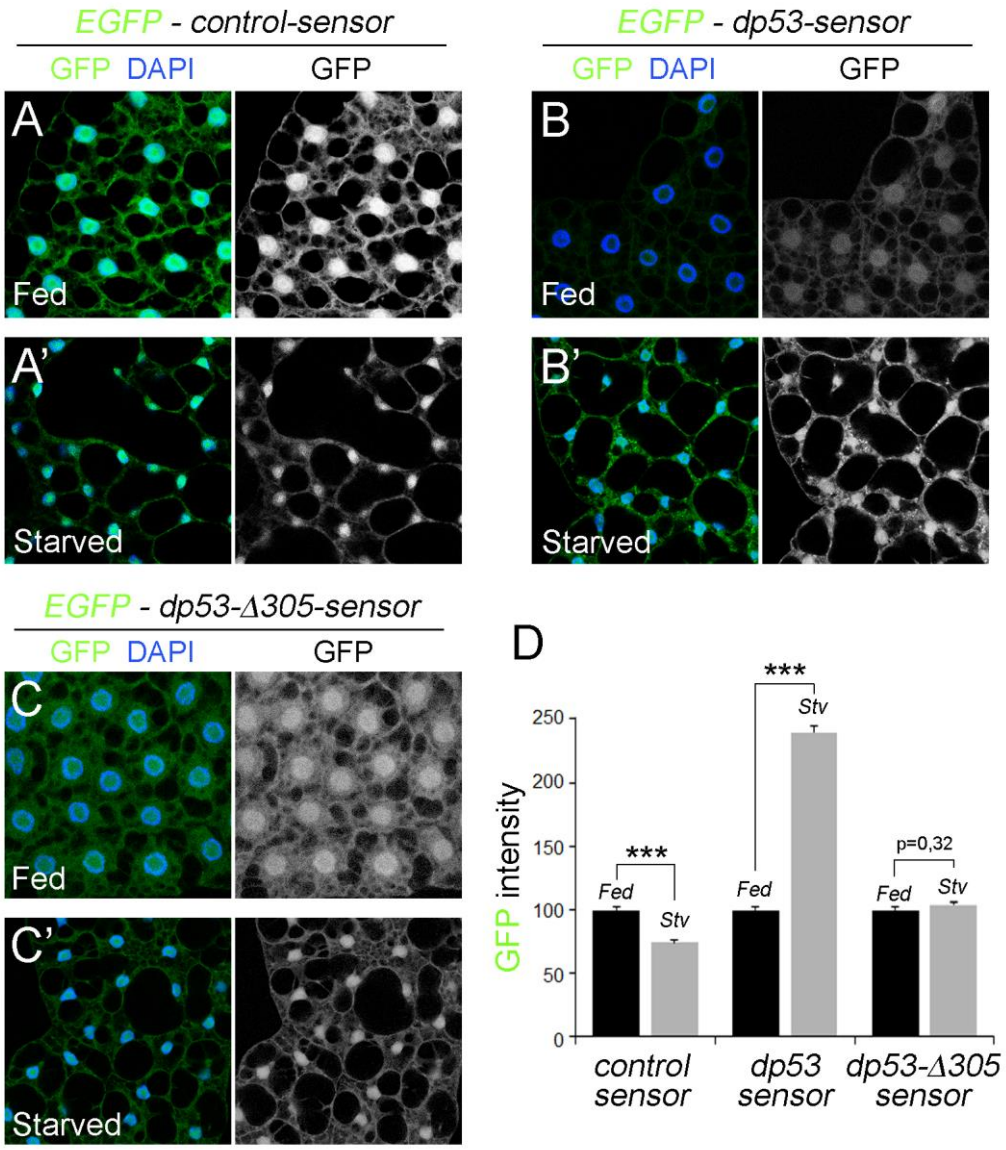

Figure 32: *miR-305* targets *dp53* in FB cells in a nutrient dependent manner

(A-C) Representative exemples of FB cells carrying the *control-sensor* (A, A'), *dp53-sensor* (B, B') or *dp53-Δ305-sensor* (C, C') in fed (A, B, C) or starved for 48 h in 2% agar, 1% sucrose (A', B', C') animals and labeled to visualized GFP (green or grey) protein levels and DAPI (blue). **(D)** Histogram plotting GFP expresion levels of FB cells shown in A-C. Results ara normalized to the fed condition for each genotype. Error bars represent SEM. *** p<0,001. Note increased levels of the *dp53-sensor* under starvation but not of the *control-sensor* nor the *dp53-Δ305-sensor*.

Collectively, these results support a major contribution of *miR-305* in targeting Dp53 in FB cells and imply that the regulation of Dp53 by the miRNA machinery is modulated by the nutritional status of the animal. Next, we characterized the molecular mechanism downstream of nutrients that regulates Dp53 in FB cells.

The major nutritional signal sensed by FB cells is amino acid (AA) availability, and down-regulation of the amino acid transporter Slimfast (Slif) in FB cells phenocopies AA deprivation *(Colombani et al., 2003)*. TOR, an essential regulator of cell and tissue growth, is regulated in response to AA availability and functions as the main nutritional sensor of a cell by coupling nutrient status to metabolic activity *(Grewal, 2009; Hietakangas and Cohen, 2009)*. We then examined whether genetic modulation of Slif or TOR activities in FB cells was able to modulate the EGFP levels of the *dp53-sensor*. Well-fed animals showed a clear increase in the EGFP expression levels of the *dp53-sensor* in FB cells expressing a RNA anti-sense form of *slif* [$slif^{Anti}$, marked by RFP expression in Figure 33A, *(Colombani et al., 2003)*] or a dominant negative version of TOR [a truncated form of TOR corresponding to a 754 amino acid central region described as "toxic effector domain", TOR^{TED}, marked by RFP expression in Figure 33B, *(Hennig and Neufeld, 2002)*], mimicking what happens during starvation. In contrast, activation of TOR (by expressing the GTPase Rheb, a positive regulator of TOR complex 1) in otherwise starved animals is expected to genetically mimic feeding conditions. Consistently, Rheb overexpression in FB cells (marked by RFP expression) strongly reduced the capacity of nutrient deprivation to up-regulate the EGFP expression levels of the *dp53-sensor* (Figure 33C). Taken together, these results indicate that modulation of the *dp53-sensor* in FB cells is a cell-autonomous process that depends on TOR activity and support the notion that Dp53 is activated in FB cells by nutrient deprivation. Interestingly, the impact of TOR on the *dp53-sensor* depended on the presence of the *miR-305* binding site, as no increase in the EGFP levels was observed in FB cells expressing TOR^{TED} and carrying the *dp53-Δ305-sensor* (Figure 33D, compare with B). On the contrary, EGFP expression levels were mildly reduced, most probably due to the reduction in translation in these cells caused by the strong depletion of TOR activity. These results reinforce the proposal that TOR signaling affects Dp53 activity levels through *miR-305*.

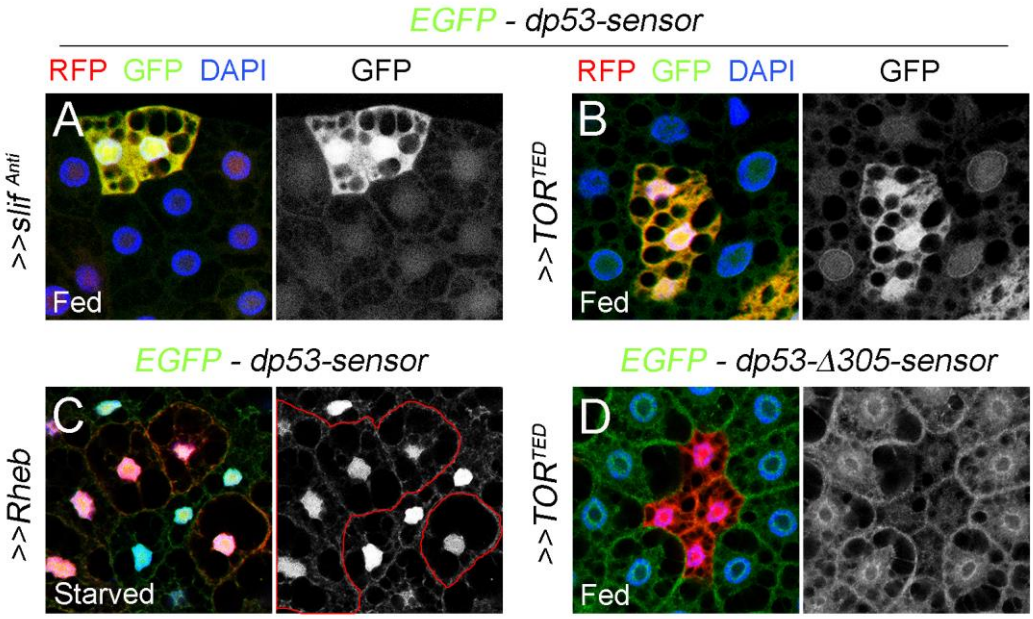

Figure 33: *miR-305* dependent regulation of *dp53* in FB cells is modulated by AA availability and TOR signaling

(A, B, D) FB cells of well-fed animals expressing RFP (red) and $slif^{Anti}$ (A) or TOR^{TED} (B, D) carrying the *dp53-sensor* (A-C) or the *dp53-Δ305-sensor* (D) and stained to visualized GFP (green or grey) protein expression, and DAPI (blue). (C) FB cells of starved animals expressing RFP (red) and Rheb carrying the *dp53-sensor* and stained to visualize GFP (green or grey) protein expression and DAPI (blue). Note increased EGFP levels in starved FB cells and reduced levels upon Rheb overexpression (enlarged cells delimited by red lines).

- **The miRNA machinery is regulated by nutrition and the TOR signaling pathway**

Our previous results show that nutrient conditions, through Slif and TOR signaling, can modulate the capacity of *miR-305* to target *dp53*, thus raising the possibility that *miR-305* levels *per se* are directly regulated by the nutritional status of the animal. In order to address this possibility, we subjected adult flies to starvation and determined the levels of mature *miR-305* and seven other miRNAs by quantitative RT-PCR. Remarkably, the levels of six miRNAs, including *miR-305*, were reduced upon starvation (Figure 34A), suggesting a general rather than specific down-regulation of miRNAs upon starvation. Moreover, when we measured the levels of hairpin primary miRNAs (pri-miRNA) transcripts in fed and starved conditions, we found that starvation did not cause a general reduction in pri-miRNAs transcripts levels (Figure 34B), thus opening up the possibility that nutrient deprivation is affecting the general processing of miRNAs. Emerging data have provided evidence that the whole miRNA machinery can be targeted

under several stress conditions *(Gibbings et al., 2012; Ho et al., 2012),* opening the possibility that starvation is targeting the miRNA machinery itself in FB cells.

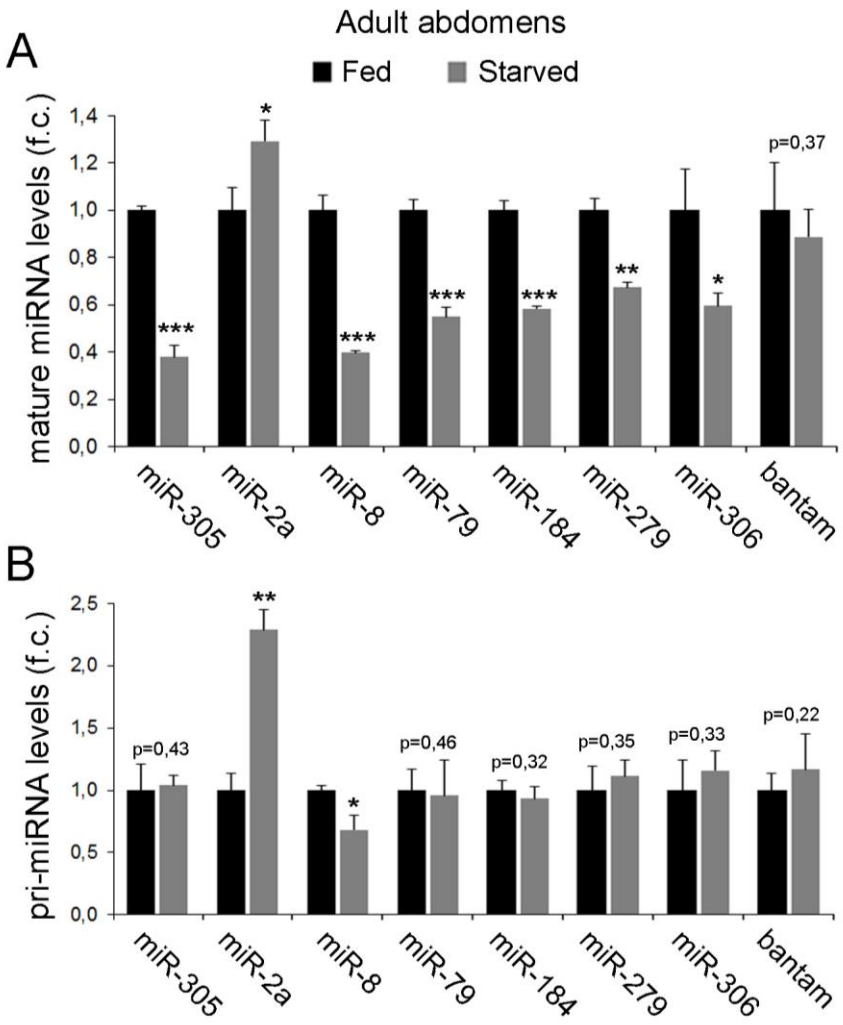

Figure 34: General downregulation of mature miRNAs in starvation

(A-B) Histograms plotting mature miRNAs levels (A) or hairpin primary miRNA (pri-miRNA) transcript levels measured by quantitative RT-PCR of adult abdomens of fed (black bars) or starved (grey bars) *control* animals. Results are expressed as fold induction with respect to fed conditions. Error bars represent SEM. *** $p<0.001$, ** $p<0.01$ and * $p<0.05$. Note that starvation conditions reduced the levels of most of the mature miRNAs, including *miR-305*, whereas pri-miRNA levels remain almost unchanged.

Consistent with this proposal, the mRNA expression levels of *dicer-1* and *drosha*, enzymes involved in miRNA processing, and *Argonaute-1* (*Ago-1*), a catalytic component of the RNA-induced silencing complex *(Huntzinger and Izaurralde, 2011)*, were reduced both in starved adult flies and starved larval FB (Figure 35A, B). The same results were observed in larval FB cells genetically deprived of AA in *ppl>slif*^{Anti} compared to control *ppl>GFP* animals (Figure 35C). These results indicate that nutrient deprivation reduces the expression levels of central elements of the miRNA machinery pathway and, consequently, alleviates *miR305*-mediated targeting of Dp53 in FB cells. Consistent with this proposal, overexpression of *miR-305* in individual FB cells of starved animals was unable to reduce the EGFP levels of the *dp53-sensor* (Figure 35D) whereas it was able to do so in well-fed animals (Figure 31B). Furthermore, the levels of mature *miR-305* were reduced in starved animals that overexpressed *miR-305* in FB cells (*ppl>miR-305*) when compared to normally fed animals of the same genotype, as shown by the decrease of the mature *miR-305/pri-miR-305* ratio (Figure 35E). Altogether, these results reinforce the hypothesis that upon nutrient deprivation the miRNA machinery is targeted and, as such, processing of *miR-305* is compromised.

- **Increased starvation resistance upon FB-specific depletion of the miRNA machinery**

Our proposal implies that in a situation of nutrient deprivation the miRNA pathway is downregulated in order to raise the levels of Dp53 which plays an important role in the metabolic adaptation to this stress situation at the organismal level. We then determined whether depletion of the miRNA machinery increased the survival rates of adult flies subjected to starvation. Halving the doses of the *dicer-1* gene (*dcr-1*^{Q1147X}*/+* flies), or having the doses of the *miR-305* locus (*Df-miR-305/+* flies) increased the survival rates of both males and female adult flies subjected to nutrient starvation when compared to *control* flies (Figure 36A-E, statistical analysis are summarized in Table 3).

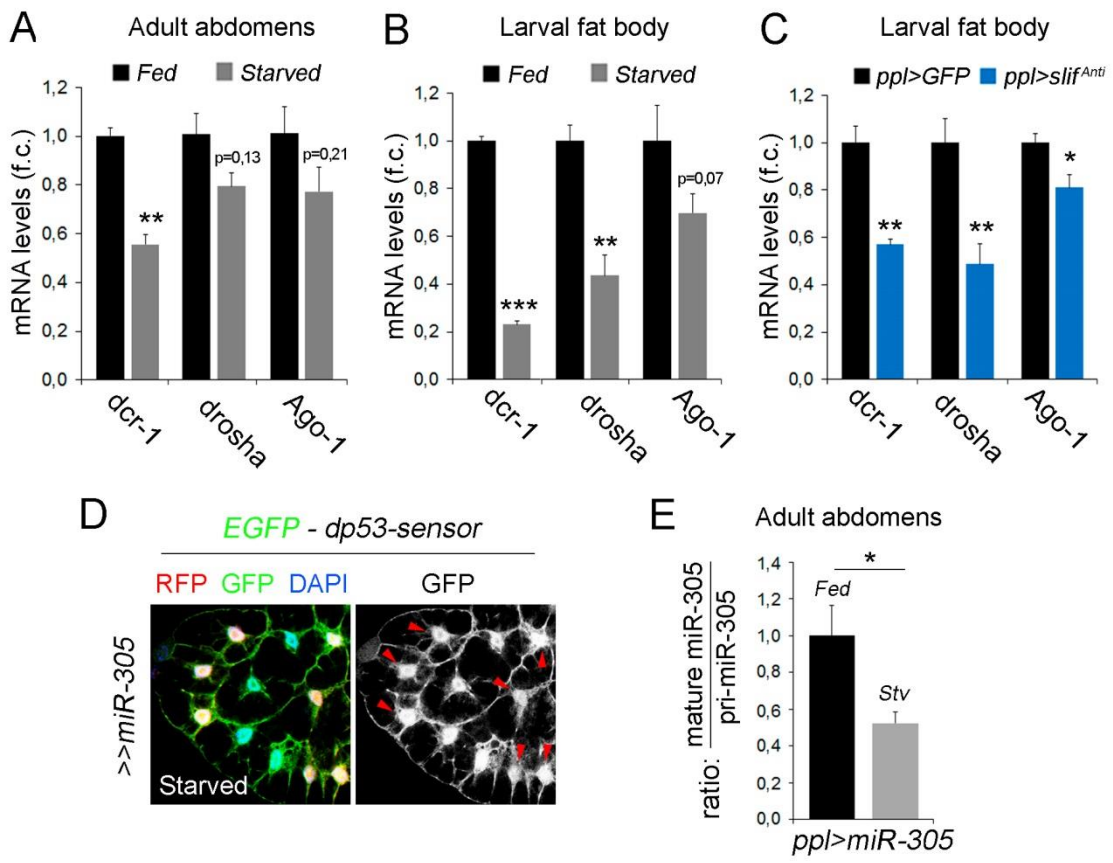

Figure 35: Reduced activity of the miRNA machinery induced by nutrient deprivation

(A-C) Histograms plotting *dicer-1* (*dcr-1*), *drosha*, and *Argonaute-1* (*Ago-1*) expression levels measured by quantitative RT-PCR of adult abdomens (A) or larval FBs of fed (black bars) and starved (grey bars) *control* animals (B) or larval FBs of *ppl>GFP* (black bars) and *ppl>slif*^{Anti} (blue bars) fed animals (C). Results are expressed as fold induction with respect to fed conditions. **(D)** FB cells of starved animals over-expressing RFP and miR-305, carrying the *dp53-sensor* and stained to visualize GFP (green or white) protein expression and DAPI. Note that miR-305 overexpression is not able to reduce GFP levels under starvation. **(E)** Histograms plotting the ratio between mature and primary *miR-305* levels measured by quantitative RT-PCR of adult abdomens of fed (black bar) or starved (grey bar) animals overexpressing *miR-305* in the FB (*ppl>miR-305*). Results are expressed as fold induction with respect to fed conditions. Error bars represent SEM. *** p<0.001, ** p<0.01 and * p<0.05.

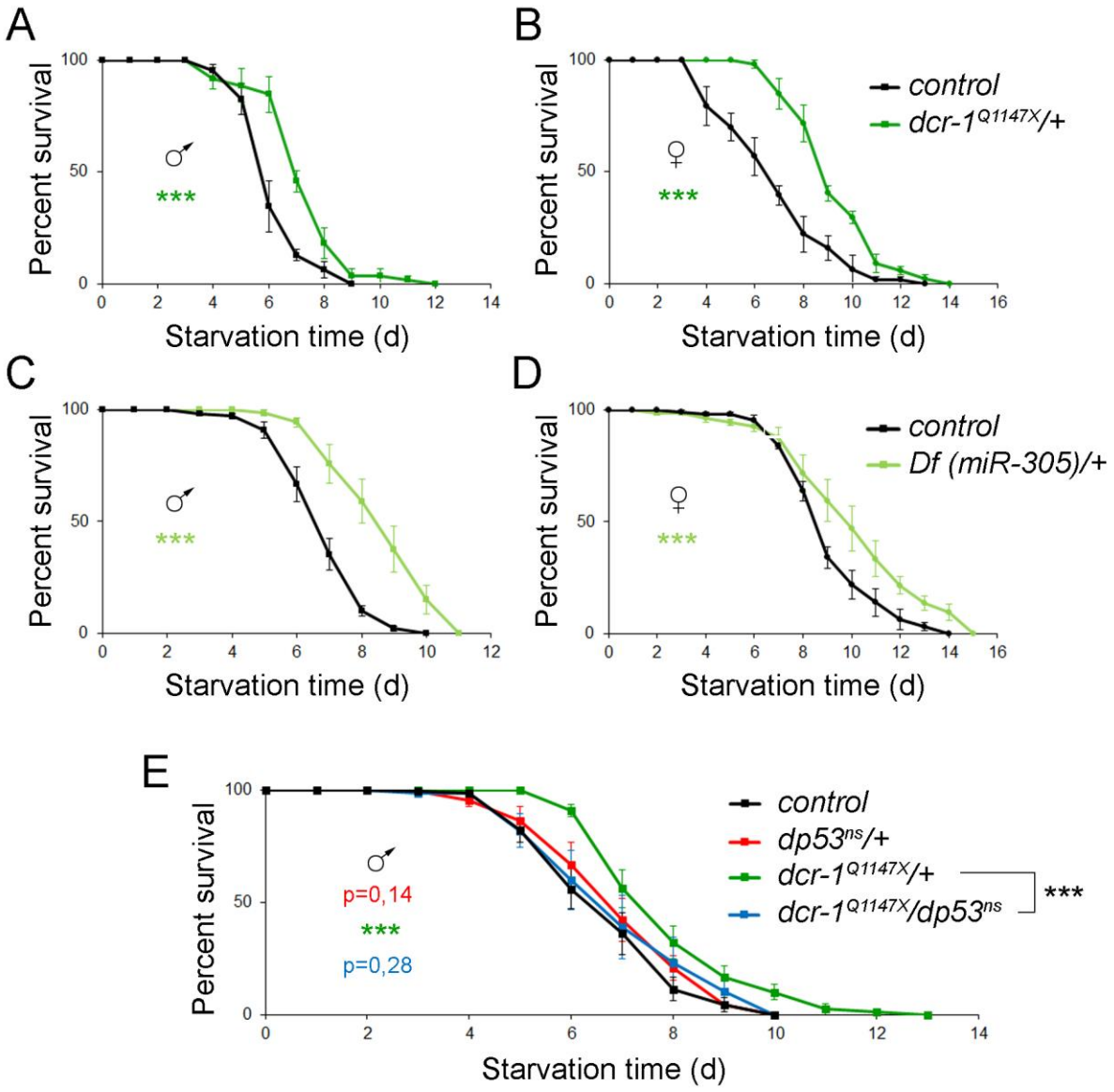

Figure 36: Reduction of the miRNA machinery increases the survival rates in a Dp53-dependent manner upon starvation

(A-E) Survival rates to acute starvation (2% of agar, 1% sucrose) of 1- to 2-days old adult flies of the following genotypes: *dcr-1*^{Q1147X}*/+,* (A, B, E), *Df(miR-305)/+* (C, D), and *dcr-1*^{Q1147X}*/ dp53*^{ns} (E), compared to *control* flies (black lines) of the following genotypes: *FRT82B ry*^{506}*/+* (A, B) and *w*^{1118} (C-E) and subjected to the same procedure. Both males (A, C, E) and females (B, D) are shown. Note that halving the dosis of *dp53* alone does not have any impact in the survival rates upon starvation but is sufficient to reduce the extended survival of *dcr-1* heterozygous flies. See Table 3 for n, p, median and maximum survival values. Error bars represent SEM. *** p<0.001.

Interestingly, when we measured the levels of TAGs and glycogen in *dcr-1*^{Q1147X}*/+* and *Df-miR-305/+* flies we found that in both genotypes just before the beginning of the starvation procedure the levels of both energy resources were consistently increased and the consumption of TAG and glycogen during starvation was delayed in time (Figure 37A-D). This is most probably a consequence of increased Dp53 activity in this animals and the proposed role of Dp53 in reducing glycolysis in FB cells, since we found that halving the doses of the *dp53* gene was able to reduce the enhanced survival rates of *dcr-1* heterozygous flies towards the ones of *control* animals (*dcr-1*^{Q1147X}*/dp53*^{ns} flies, Figure 36E).

Remarkably, similar results were obtained by reducing the levels of the miRNA machinery in a FB-specific manner. Targeted expression of a dsRNA form against *dcr-1* in FB cells (*ppl>dcr-1*^{RNAi} flies) also increased starvation resistance in both males and females (Figure 38A, B, statistical analysis are summarized in Table 3). The extended survival rates were completely reverted upon co-expression of a dominant negative version of Dp53 (*ppl> dcr-1*^{RNAi}*, dp53*$^{H159.N}$ flies, Figure 38C, D, statistical analysis are summarized in Table 3). As a control, the three parental UAS lines (*UAS-GFP*, *UAS-dcr-1*^{RNAi} alone, and the double *UAS-dcr-1*^{RNAi} *UAS-dp53*$^{H159.N}$) backcrossed into the *w*^{1118} genetic background showed similar survival rates (Figure 38E; statistical analysis are summarized in Table 3).

Collectively, these results indicate that depletion of nutrients reduces the activity of the miRNA machinery in FB cells, and as a consequence alleviates *miR-305*-mediated targeting of *dp53*, which eventually contributes to organismal resistance to nutrient deprivation.

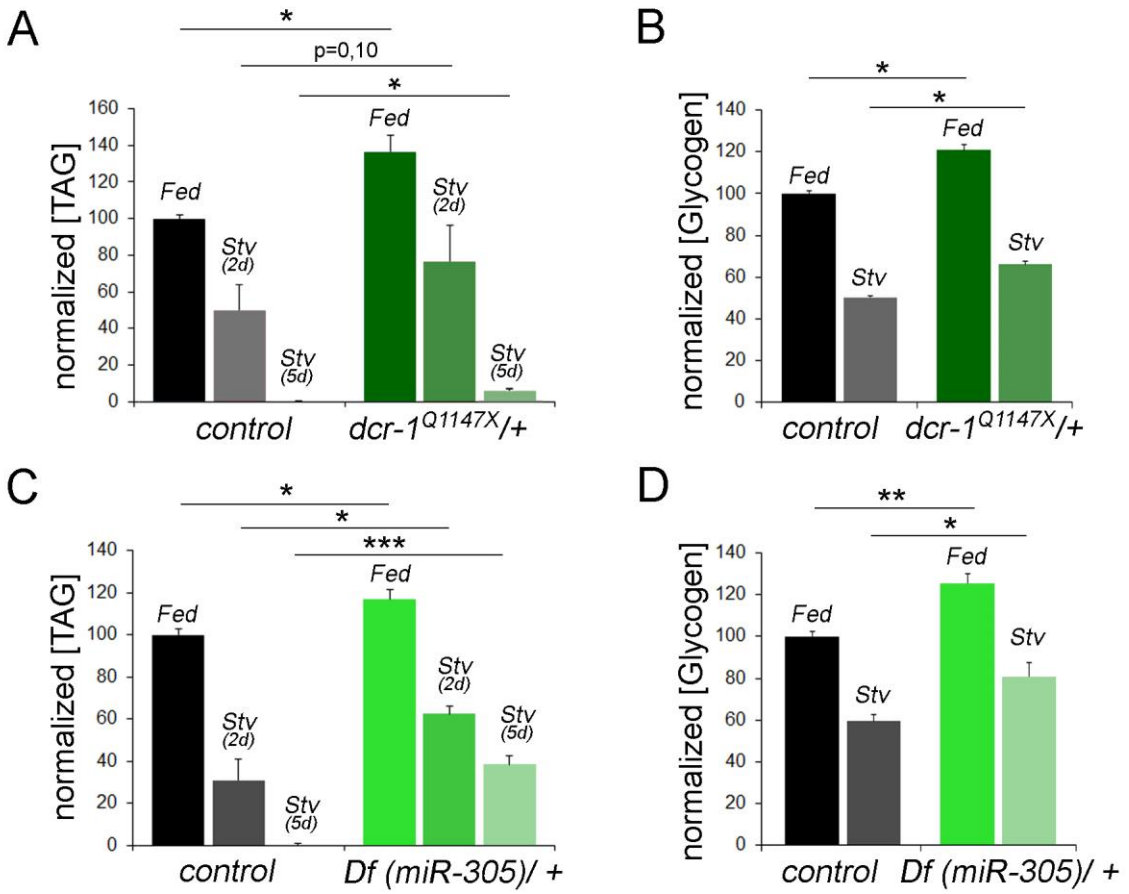

Figure 37: Main energy storages in flies with reduced activity of the miRNA machinery in well-fed and under nutrient deprivation

(A-D) Histograms plotting TAG (A, C) and glycogen (B, D) levels from *dcr-1*^{Q1147X}*/+* (A, B) or *Df(miR-305)/+* (C, D) flies and its corresponding *control* animals in well-fed conditions or starved in 2% agar, 1% sucrose for 1 day in B and D or for 2 and 5 days in A and C. Data were normalized to protein concentration and represented as a percentage of the fed values of the *control* flies. In all the cases animals were grown under identical conditions and aged for 5 days prior to exposion to the corresponding fasting. Note that in both genotypes, the levels of TAG and glycogen are much more higher at the beginning of the starvation treatments and the consumption of energy resourses is delay in time. Error bars represent SEM, brackets indicate the genotypes that are compared, *** p<0.001, ** p<0.01 and * p<0.05.

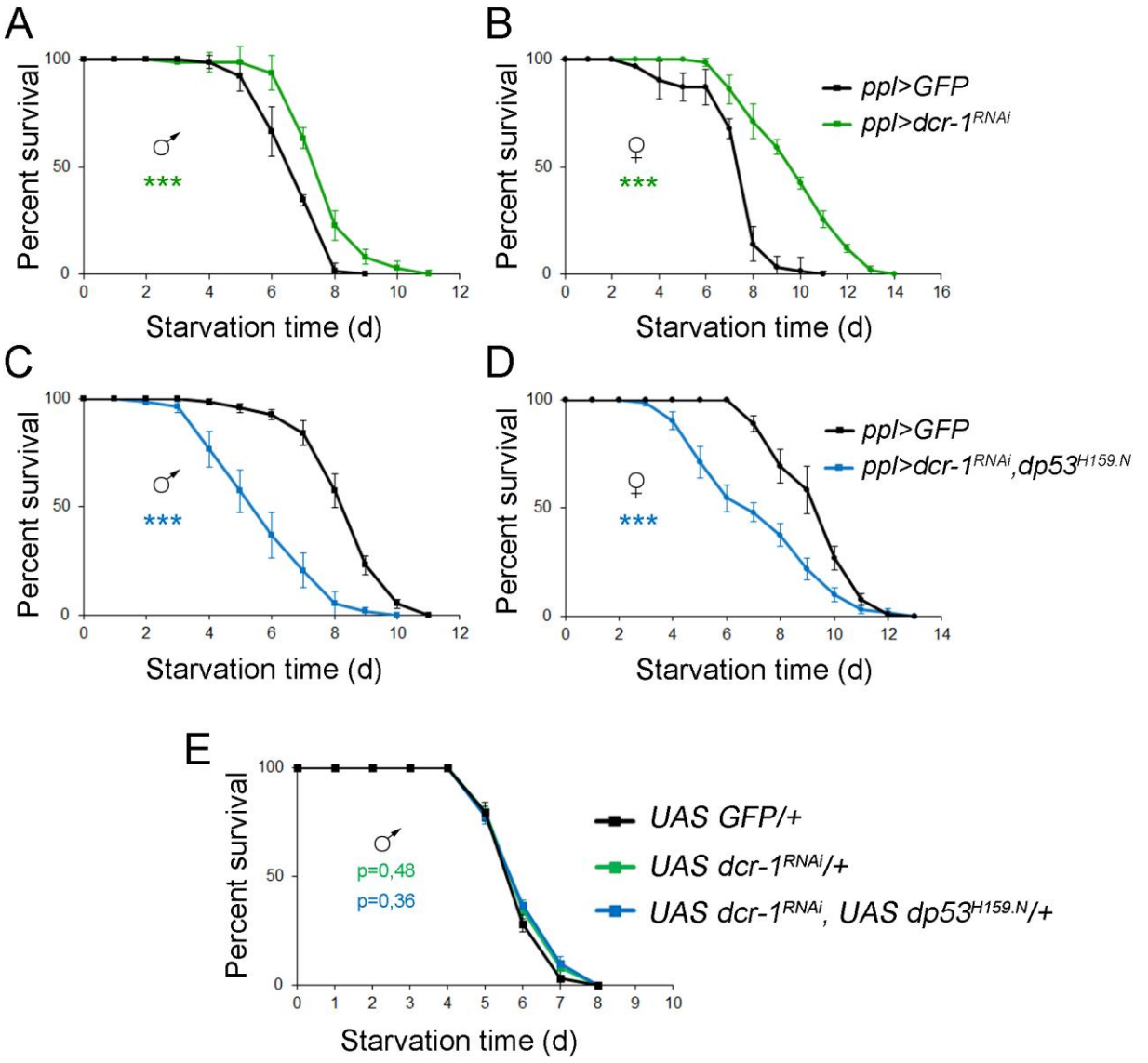

Figure 38: The enhanced survival in fasting conditions caused by FB-specific depletion of *dicer-1* is reverted by reducing the Dp53 activity levels

(A-D) Survival rates to acute starvation (2% agar, 1% sucrose) of 1- to 2-days-old adult flies expressing *GFP* (as a control, in black) and *dcr-1*^{RNAi} alone (in green, A, B) or together with *Dp53*$^{H159.N}$ (in blue, C, D) in FB cells under the control of the *ppl-gal4* driver. Both males (A, C) and females (B, D) are shown. Note that reduction of Dp53 activity in FB cells revert the extended surival rates of FB-specific depletion of the miRNA machinery observed upon nutrient deprivation. **(E)** Survival rates to nutrient deprivation (2% agar, 1% sucrose) of young adult flies of the following genotypes: *UAS-GFP/+*, *UAS dcr-1*^{RNAi}/+ and *UAS dcr-1*^{RNAi}/+,*UAS Dp53*$^{H159.N}$ /+. No significant differences were observed between any of the parental UAS transgenic lines. See Table 3 for n, p, median and maximum survival values. Error bars represent SEM. *** p<0.001.

adult females	n	Mantel-Cox test	Median surv	Maximum surv
control F82B ry^{506} /+	103		7	13
F82B dcr-1^{Q1147X}/+	104	p < 0,0001	9 (+28%)	14 (+8%)
adult males	**n**	**Mantel-Cox test**	**Median surv**	**Maximum surv**
control w^{1118}	107		7	10
Df (miR-305)/+	100	p< 0,0001	9 (+28%)	11 (+10%)
adult females	**n**	**Mantel-Cox test**	**Median surv**	**Maximum surv**
control w^{1118}	112		9	14
Df (miR-305)/+	105	p< 0,0001	10 (+11%)	15 (+7%)
adult males	**n**	**Mantel-Cox test**	**Median surv**	**Maximum surv**
control w^{1118}	116		7	10
dp53^{ns}/+	142	p=0,1375	7 (=)	10 (=)
dcr-1^{Q1147X}/+	105	p< 0,0001	8 (+14%)	13 (+30%)
dcr-1^{Q1147X}/dp53^{ns}	115	p=0,2812 (*ctrl w^{1118}*)	7 (=)	10 (=)
		p< 0,001 (*dcr-1^{Q1147X}*)		
adult males	**n**	**Mantel-Cox test**	**Median surv**	**Maximum surv**
ppl>GFP (control)	108		7	9
ppl>dcr-1^{RNAi}	105	p = 0,0005	8 (+14%)	11 (+22%)
adult females	**n**	**Mantel-Cox test**	**Median surv**	**Maximum surv**
ppl>GFP (control)	100		8	11
ppl>dcr-1^{RNAi}	100	p < 0,0001	10 (+25%)	14 (+27%)
adult males	**n**	**Mantel-Cox test**	**Median surv**	**Maximum surv**
ppl>GFP (control)	106		9	11
ppl>dcr-1^{RNAi},dp53$^{H159.N}$	105	p < 0,0001	6 (-33%)	10 (-9%)
adult females	**n**	**Mantel-Cox test**	**Median surv**	**Maximum surv**
ppl>GFP (control)	101		10	13
ppl>dcr-1^{RNAi},dp53$^{H159.N}$	103	p < 0,0001	7 (-30%)	13 (=)
adult males	**n**	**Mantel-Cox test**	**Median surv**	**Maximum surv**
UAS GFP/+ (control)	108		6	8
UAS dp53$^{H159.N}$/+	104	p = 0,516	6 (=)	8 (=)
UAS dp53^{RNAi}/+	101	p = 0,3649	6 (=)	8 (=)
UAS dcr-1^{RNAi}/+	106	p = 0,475	6 (=)	8 (=)
UAS dcr-1^{RNAi},dp53$^{H159.N}$/+	100	p = 0,356	6 (=)	8 (=)

Table 3: Statistical analysis of survival to nutrient deprivation upon depletion of the miRNA machinery

Table compiling the number of individuals analyzed (n), p-values according to the Mantel-cox test, median survival values (in days) and maximum survival values (in days) corresponding to the different genotypes used in the experiments of survival to nutrient deprivation shown in Figures 35 and 37. One- to 2-days old adult animals were grown under identical conditions and exposed to acute starvation in 2% of agar, 1% sucrose. Control animals were always analyzed in parallel in each experimental condition. The change (in percentage) with respect to control values is shown in brackets.

DiSCuSSioN

DISCUSSION

The p53 tumour suppressor protein is an important regulator of several stress responses and plays a fundamental role during cancer development. Induction of apoptosis, cell cycle arrest and DNA repair are well-understood functions of p53, and are traditionally accepted as the major mechanisms by which p53 prevents tumour formation. In the last few years, p53 has emerged as an important regulator of several metabolic pathways able to trigger a cellular adaptive response to nutrient deprivation, a function that may contribute not only to tumour suppression activities of this molecule but also to its non-cancer-associated functions.

In this thesis, we analyzed the capacity of *Drosophila* p53 (Dp53) to exert the classical tumour suppressor functions of this protein in response to DNA damage, and unraveled a fundamental role of Dp53 in organismal adaptation to nutrient deprivation.

1. Classical functions of Dp53 as a tumour suppressor protein

The controversial prospective found in the literature about the capacity of Dp53 to induce cell cycle arrest and DNA repair under stress conditions lead us to analyze in detail the classical roles of Dp53 as a tumour suppressor protein. By using two different approaches, (a) Dp53 overexpression experiments in normal conditions and (b) Dp53 loss-of-function experiments upon induction of DNA damage, we presented evidence showing that Dp53 conserved the capacity to induce apoptosis, stop the cell cycle and repair the DNA as it mammalian counterpart. However, our results demonstrated that, upon ionizing radiation (IR)-induced DNA damage, Dp53 is responsible for the fast induction of apoptosis and contributes to DNA repair, but is not able to arrest cell cycle.

Cells and tissues are continuously exposed to extrinsic and intrinsic insults that generate DNA damage and the main components of the DNA damage checkpoint are highly conserved from yeast to human, including *Drosophila (Wahl and Carr, 2001)*. In mammalian cells, p53 is a major downstream effector of the DNA damage response (DDR) pathway. p53 is phosphorylated by both ATM/Chk2 and ATR/Chk1 cascades of kinases and plays a critical role in driving cell cycle arrest, apoptosis and DNA

repair upon DNA damage [Figure 1, *(Lakin and Jackson, 1999; Lane and Levine, 2010)]*. In *Drosophila,* the DNA damage-induced cell cycle arrest and apoptosis responses are independently controlled, and as we have seen, Dp53 is only required for the immediate apoptotic response and contributes to DNA repair [Figure 1, *(Brodsky et al., 2000; Brodsky et al., 2004; Jaklevic and Su, 2004; Ollmann et al., 2000; Sogame et al., 2003)].* Interestingly, our results also present evidence of a second wave of apoptosis induction in *dp53* mutant animals upon IR. These observations are consistent with the proposal that DNA-damage is able to induce aneuploidy and that the elimination of aneuploid cells is independent of Dp53 *(McNamee and Brodsky, 2009; Dekanty et al., 2012),* as opposed to mammalian cells. Thus, although the major components of the DDR machinery have been conserved during evolution, certain characteristics in the mode of action of those components have evolved differently.

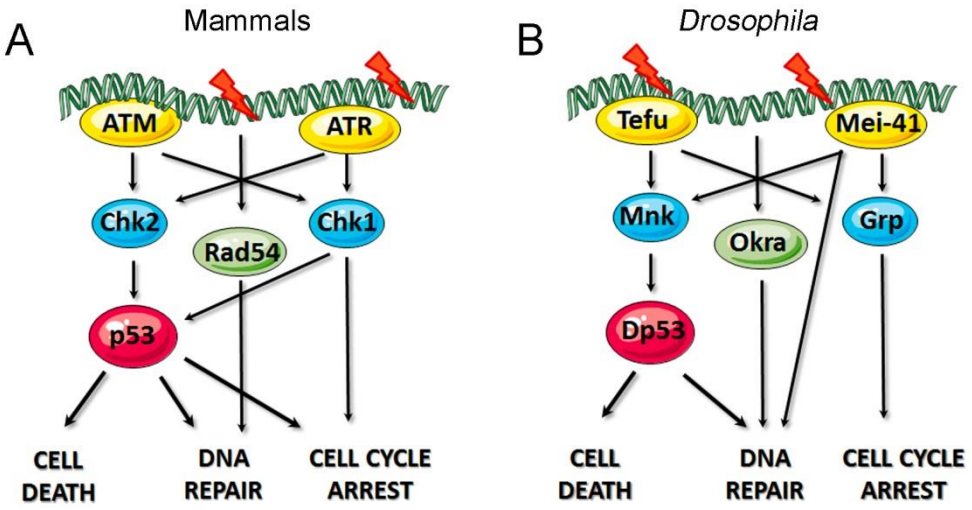

Figure 1: DNA damage checkpoint pathways in mammals and Drosophila

A schematic representation of the DNA damage response pathways in mammals (A) and in *Drosophila* (B). The main components of the DNA damage checkpoint machinery are conserved in both species. In *Drosophila* in response to DNA lesions, Tefu (the Ataxia Telangiectasia–mutated, ATM, ortholog) and Mei-41 (the Ataxia Telangiectasia–related, ATR, ortholog) kinases are rapidly activated and phosphorylate many substrates including the downstream kinases Mnk (the Chk2 ortholog) and grapes (Grp, the Chk1 ortholog) respectively *(Brodsky et al., 2004; Jaklevic and Su, 2004)*]. Whereas Mnk is known to activate Dp53 and then induce apoptosis, Mei-41 and Grapes promote cell cycle arrest after DNA damage. Finally, Okra [the *Drosophila* homolog of Rad54, a DEAD-like helicase involved in homologous recombination *(Kooistra et al., 1997)* together with Dp53 contribute to DNA repair.

Whereas Dp53 is not required for DNA damage-induced cell-cycle arrest, our overexpression experiments revealed that Dp53 has maintained the capacity to modulate cell cycle progression. We found that Dp53 induces a clear reduction in BrdU incorporation (an analog of thymidine used as a

marker for proliferating cells) and *string* mRNA levels (a phosphatase that controls the entry into and progression through mitosis), and strong accumulation of Cyclin E and Cyclin B (Cyclins required for the transition from G_1 to S and G_2 to M phase, respectively). The failure in incorporating BrdU and the absence of *string* mRNA certainly supports that high levels of Dp53 activation blocks cell proliferation *in vivo*. Although additional experiments might be required to further characterize the molecular mechanism by which Dp53 blocks cell proliferation when overexpressed, our results are consistent with the proposed role of Dp53 in arresting cell cycle in response to mitochondrial dysfunction *(Mandal et al., 2005; Mandal et al., 2010)*.

So the question is: why Dp53 is not able to arrest the cell cycle in response to ionizing radiation-induced DNA damage? It might be a matter of levels. Whereas low Dp53 levels (IR-induction) might not be enough to arrest the cell cycle, high levels of Dp53 may do it. Alternatively, the final outcome of the Dp53-mediated stress response could depend on the context and on the cell type, as well as on the extent, duration, and origin of the stress, as it happens in mammals *(Vousden and Prives, 2009)*.

2. A fundamental role of Dp53 in organismal adaptation to nutrient deprivation

Nutrient availability is a dynamic variable in natural environments, and all organisms should maintain metabolic homeostasis despite food variability. Environmental variations in food cause a series of physiological responses that require the coordination of cellular mechanisms and hormonal signaling to produce differential effects in a variety of tissues to maintain energetic homeostasis. Thus, modulation of metabolic homeostasis is a complex process and its deregulation can lead to several metabolic disorders including obesity and diabetes, as well as can have a major impact on cancer progression. The tumour suppressor gene p53 has been reported to mediate metabolic changes in cells through the regulation of several metabolic pathways and to promote cell survival upon nutrient deprivation *(Berkers et al., 2013; Vousden and Prives, 2009)*.

The results presented in this PhD thesis unravel a new role for Dp53 in organismal homeostasis and show that Dp53 is activated under nutrient deprivation to modulate cellular metabolism. Since the major

metabolic, energy-sensing and endocrine signaling networks of vertebrate systems are also conserved in flies *(Owusu-ansah and Perrimon, 2014),* we consider that these are really important achievements that shed light into the consequences of p53 mutations for animal physiology. We showed that the absence of Dp53 reduces the ability of adult flies to survive under metabolic stress, whereas in normal conditions it has been shown to increase adult life span *(Waskar et al., 2009)*. Moreover, the increased starvation sensitivity of Dp53 depleted animals occurs during larval development and in adult stages, suggesting that the adaptive role of Dp53 to nutrient deprivation is crucial throughout the life cycle.

Interestingly, we found that Dp53 requirement was tissue specific. In particular, Dp53 is required in the fat body (FB), a key sensor well known to couple nutrient status and energy expenditure and the most important reservoir for both triglycerides (TAG) and glycogen *(Arrese and Soulages, 2010)*. Several evidences support our hypothesis. First, depletion of Dp53 specifically in the FB, using three different Gal4 drivers, reduces animal survival in fasting conditions. Second, depletion of Dp53 in muscles, another tissue able to store glycogen and recently proposed to be involved in metabolic homeostasis *(Demontis and Perrimon, 2010)*, does not have any impact on survival rates in starved animals. Finally, overexpression of Dp53 in the FB increases organismal survival upon nutrient deprivation and is able to rescue the survival rates of *dp53* mutant animals.

Why does Dp53 depletion reduce resistance to starvation?

The response of an organism to metabolic stress, such as starvation, is largely dependent on its capacity to derive energy from stored reserves like TAGs and glycogen *(Leopold and Perrimon, 2007)*. Interestingly, we found that the starvation sensitivity of *dp53* mutant flies or flies with reduced Dp53 activity in the FB correlated with an accelerated consumption of the main energy resources (glycogen and TAG). In *Drosophila,* energy homeostasis is maintained by the combined action of insulin-like peptides (Dilp) and adipokinetic hormone (Akh). In well-fed animals, insulin signaling promotes energy storage, whereas Akh and reduced levels of circulating Dilps contribute to the mobilization of energy resources upon fasting *(Bharucha et al., 2008; Géminard et al., 2009; Kim and Rulifson, 2004; Rulifson et al., 2002)*. Besides the known role of Dp53 in the insulin producing cells to promote insulin signaling in life span experiments *(Bauer et al., 2005; Bauer et al., 2007)*, we found that the changes in insulin signaling and Akh expression levels caused by nutrient deprivation were very similar in Dp53 depleted and control animals. These results indicate that Dp53 has an impact on energy balance independently on the regulation of the endocrine signaling network involved in metabolic homeostasis. Indeed, specific

depletion of Dp53 in individual fat body cells subjected to starvation caused smaller lipid droplets thus revealing a cell-autonomous role of Dp53 in FB cells.

Unfortunately, the detailed molecular mechanism within the cell by which Dp53 might impact the rates of energy resources breakdown and promote organismal survival upon nutrient deprivation remains to be elucidated, but we can speculate a number of possibilities in this direction. One possibility could be that Dp53 is involved in a buffering system coordinating at the cellular level energy consumption versus expenditure. In our scenario, Dp53 could act as a 'metabolic brake' similarly to 4EBP *(Teleman et al., 2005)* in charge of slowing-down the rate of consumption of energy resources. By modulating the retention of fuel molecules, Dp53 might provide an adaptive survival benefit during periods of decreased food availability, thus prolonging long-term survival when flies are challenged with food deprivation.

Another possibility could be autophagy. In mammals, p53 has been shown to both induce and promote autophagy *(Levine and Abrams, 2008).* Autophagy is an evolutionary conserved self-eating mechanism by which intracellular cytoplasmatic portions and organelles are delivered to the lysosome for degradation. In fasting conditions, this intracellular catabolic process has a fundamental role providing energy and nutrients *(Singh and Cuervo, 2011)*. In Drosophila, the fat body engages an important autophagic response to allow and maintain adequate hemolymph nutrient levels during fasting periods. Accordingly, blocking autophagy specifically in the fat body makes the animals unable to tolerate starvation and suffer reduced viability under nutrient deprivation *(Scott et al., 2004)*. In our experiments, we observed in control (cg>GFP) animals that the localization of Atg8-mcherry (a specific marker for autophagic vesicles) changed from a diffuse cytoplasmic pattern to a punctate autophagosomal membrane-bound pattern in starvation. However, more than 80% of fat bodies analyzed in Dp53 depleted animals (cg>dp53$^{H159.N}$) failed to change the localization of Atg8-mcherry in starving conditions, suggesting that Dp53 play a positive role in the induction of autophagy under nutrient deprivation. Nevertheless, the inhibition of starvation-induced autophagy observed in Dp53-depleted cells might not account for the accelerated depletion of the energy resources. In fact, it should be the other way around, e.g. mice knocked out for an essential autophagy gene in liver (Atg7) show increased TAG levels than control animals in starvation *(Singh et al., 2009)*. Thus, we hypothesized that the effect on energy stores consumption in FB-Dp53-depleted animals might be a consequence of the active glycolytic pathway in FB cells (something that we will discuss in the next step). Besides the role of

starvation-induced autophagy in energy production by the degradation of lipid and glycogen stores, which, as a matter of fact, occurs primarily in the cytosol by the action of cytosolic lipases and glycogen phosphorylase respectively, it also contributes to the recycling of certain components. For instance, amino acids produced by autophagic degradation of long-lived proteins and organelles are important to synthesize proteins (de novo) needed for adaptation to starvation *(Mizushima and Komatsu, 2011)*. Indeed, autophagy is one of the most immediate cellular responses to starvation. Thus, the potential role of Dp53 as a positive regulator of autophagy could still confer increased survival in the face of chronic starvation, but obviously further experiments checking this hypothesis as well as the epistasis between these two elements should be done.

Finally, the idea that Dp53 may be part of a metabolic reprograming that allows cells to adapt to depletion of nutrients becomes more likely. Our expression profile analysis suggested that the accelerated consumption of energy resources observed in starved Dp53-depleted animals did not appear to be a consequence of altered changes in metabolic enzymes involved in mobilizing these resources, such as the Brummer lipase [the homolog of the mammalian adipose triglyceride lipase *(Grönke et al., 2005)*]. Interestingly, we observed that fasting also induced a decrease in the levels of enzymes involved in glycolysis and fatty acid β-oxidation. Reduced rates of glucose and fatty acid catabolism specifically in starved fat body cells might reflect a preferential use of these metabolites for the production of circulating sugars and lipids to be used by peripheral tissues upon starvation *(Arrese and Soulages, 2010)*. Interestingly, Hexokinase C (Hex-C), an enzyme that catalyzes the first step of glycolysis, and Phosphoglucose mutase (PGM), an enzyme that converts glucose-1-P (the first product of the breakdown of glycogen) to glucose-6-P (which is used for glycolysis), remained unchanged in Dp53 depleted animals while in control flies were clearly decreased upon starvation. These differences suggest an active glycolytic pathway in starved Dp53 mutant flies, which was consistent with the reduced amount of sugars observed in those flies under nutrient deprivation. These results most probably reflect a defective functional specialization of *dp53* mutant FB cells towards the production of sugars in fasting conditions and support a role of Dp53 in metabolic adaptation to nutrient deprivation. Thus, our most convincing working hypothesis is that under nutrient deprivation, FB cells have to switch its metabolism in order to inhibit glucose consumption and reduce the glycolytic rate, to preferentially derive the use of this metabolite by the rest of the tissues in the animal. In this scenario, we will like to propose Dp53 as an important player in the functional specialization of fat body cells upon nutrient deprivation. In Dp53 depleted animals therefore, the active glycolytic pathway may compromise the amount of sugars in the animal, and this reduction might contribute to their poor survival rates, as an increase in the

concentration of sugar in the medium (2% agar, 10% sucrose) rescued the survival rates of starved Dp53 depleted animals.

A role of p53 in metabolism: a conserved and ancestral function

In the last decade, regulation of cellular metabolism has been added to the repertoire of anti-tumourigenic activities of p53 *(Jiang et al., 2013; Liang et al., 2013)*. A recent study has shown that serine deprivation induces p53 in mammalian cell lines and that this activation is required to sustain growth and survival in the absence of serine. Interestingly, cancer cells become addictive to serine and depletion of p53 drastically reduces growth and survival of cancer cells under amino acids deprivation *(Maddocks et al., 2013)*. In this thesis we wanted to analyze whether these new outcomes of p53 are not only crucial for restraining cancer development but could also profoundly influence other aspects during normal physiology of the animal. The results presented in this thesis support the proposal that in Drosophila, Dp53 plays an important role in organismal adaptation to nutrient deprivation by modulating cellular metabolism of fat body cells. In our work, we measured a panel of more than twenty key metabolic enzymes involved in lipid and glucose metabolism, oxidative phosphorylation, mitochondrial respiration and glutaminolysis, in control and Dp53 depleted animals in both fed and starved conditions. As discussed in the previous section, we found different dynamics in the expression levels of two enzymes involved in glucose catabolism: Phosphoglucose mutase (PGM) and Hexokinase C (Hex-C). These enzymes were downregulated in control animals, but in Dp53 depleted animals remained unchained, suggesting that under nutrient deprivation Dp53 is able to block glycolysis in FB cells, which is consistent with the results found in S2 cells by *(de la Cova et al., 2014)*. However, their results and ours differ in several aspects. First, the proposed target genes that Dp53 is able to regulate in order to modulate glycolysis are different. They proposed that Dp53 was able to block the glycolytic flux by inhibiting glucose uptake through downregulation of the expression levels of glucose transporters Glut-1 and Glut-3, whereas we didn't see any effect in glucose transporters (data not shown). Second, in *(de la Cova et al., 2014)*, the expression levels of the target genes were affected when transfecting S2 cells with $dp53^{RNAi}$ in standard medium. However, in our case, the effects seen in PCG and Hex-C were observed only in starvation conditions, never in standard nutritional conditions. Finally, they observed context-dependent outputs of Dp53 in cellular metabolism. While Dp53 seemed to restrain glycolysis in normal

conditions, in dMyc 'supercompetitor' cells Dp53 was able to promote it. On the basis of their results and ours, we propose a conserved role of p53 in regulating glycolysis in vertebrate and invertebrate tissues.

In mammals, p53 is able to modulate autophagy. Indeed, it has a dual function; Dp53 can either activate or repress autophagy. On one hand, nuclear p53 can induce autophagy directly, through transcriptional upregulation of targets involved in the autophagy pathway such as the lysosomal protein DRAM *(Crighton et al., 2006)*, or indirectly, through transcriptionally activation of negative regulators of mTOR (a negative master regulator of autophagy) such as AMPK, PTEN, TSC-2 and sestrins *(Balaburski et al., 2010; Feng et al., 2007)*. On the other hand, cytoplasmatic p53 has been shown to repress autophagy through an unknown mechanism *(Balaburski et al., 2010; Levine and Abrams, 2008; Tasdemir et al., 2008)*. In addition to its pro-survival roles in metabolic stress, under certain conditions, autophagy has been shown to act as a cell death mechanism in cell lines where caspases or classical regulators of the apoptotic machinery are impaired. Interestingly, this anti-survival role has also been linked to p53. Indeed, p53-dependent autophagy is induced by genotoxic stress *(Budanov and Karin, 2008)*. Although we only have one experiment supporting the role of Dp53 as a positive regulator of autophagy, this is, to our knowledge, the first time that Dp53 has been shown to influence autophagy in Drosophila. Since in mammals, the role of p53 in modulating autophagy has been well established, we hypothesize that this function could be one of the ancient functions of p53, a function that could play important roles during normal development and physiology as well as in stress response. Thus, our results open a new avenue towards the involvement of Dp53 in the regulation of autophagy downstream of both nutrient stress and genotoxic stress.

As p53 is found in primitive organisms, and cancer is unlikely to have significantly influenced evolution, suppressing tumour formation was almost certainly not the original function of this gene. Therefore, prevention of cancer is likely to have evolved as a side effect derived from more ancient functions of this protein. In the last few years, a link between p53 and metabolic homeostasis has been uncovered, and together with our results, we will like to speculate that regulation of cellular metabolism could be one of the primary functions of p53. Regulation of stem cell growth and behavior has been proposed as another candidate for the ancestral function for p53 as well *(Wylie et al., 2014)*. However, considering the fact that some ancestral organism doesn't seem to have stem cells, we hypothesized that regulation of cellular metabolism is a truly good candidate for the ancestral role of p53.

3. **Connecting p53 and the miRNA world**

MicroRNA (miRNA), an abundant class of endogenous non-coding RNAs, approximately 20-23 nucleotides long, typically regulate negatively gene expression by base-pairing to partially complementary sites on the 3 'UTR region of target mRNAs and are involved in many biological processes *(Tétreault and De Guire, 2013)*. In the last years, p53 has entered the miRNA word, in both directions: p53 is regulated by, and regulates, miRNAs *(Takwi and Li, 2009)*. Thus, miRNAs are an important component of the p53 network signaling, and as such its conservation through evolution will further support this idea.

MicorRNA-mediated regulation of p53, a conserved system from humans to flies

MicroRNA-mediated inhibition of p53 activity involves direct and indirect regulatory mechanisms. On one hand, several miRNAs including *miR-125b*, *miR-504*, *miR-33* and *miR-1285*, contribute to the tight control of *p53* expression and activity by directly interacting with the 3 'UTR of *p53* mRNA *(Hu et al., 2010; Kumar et al., 2010; Le et al., 2009).* On the other hand, p53 can be regulated by miRNAs via downregulation of upstream regulators of p53 including p53-modyfing enzymes such as MDM2 *(Hermeking, 2012).*

In this thesis we analyzed the involvement of the miRNA machinery in targeting *dp53* in normal physiological conditions and upon genotoxic or nutritional stresses. We first used the wing epithelium as model system, since it has proven to be a very suitable system to underscore the molecular elements underlying the role of miRNAs in cell proliferation and survival *(Brennecke et al., 2003; Herranz et al., 2010; Herranz et al., 2012a; Nolo et al., 2006)*. First of all, we showed that generalized depletion of miRNAs, by targeting Dicer-1 (Dcr-1) a double-stranded RNAse III essential for miRNA biogenesis, increased Dp53 protein levels and that Dp53 activity contributed to the apoptotic cell death and poor cell survival of Dcr-1 depleted cells. Second, by designing specific *dp53* 3' UTR-sensors, we presented evidence that the miRNA machinery was able to directly target the *dp53* 3'UTR. Finally, we identified the miRNA *miR-305* as the major regulatory element and we experimentally proved the specific binding site on the 3' UTR of *dp53* by which *miR-305* exerted its negative regulatory action.

Although the *miR-305* ortholog in human has not yet been identified, we noticed that predictions for the human *miR-22 (h-miR-22)* in the *dp53* 3'UTR overlaped with those for the *Drosophila miR-305 (d-*

miR-305). Considering this observation, we propose that *h-miR-22* might be a functional analog of the *d-miR-305*. Analysis of conservation between the seed region of both miRNAs and further investigation would therefore be necessary to determine whether *d-miR-305* could have a functional ortholog in humans.

Interestingly, we found that, besides *miR-305,* two other miRNAs (*miR-283* and *miR-219)* were able to down-regulate the *dp53-sensor in vivo* when overexpressed. Consistently, clones of cells mutant for *dcr-1* still showed increased levels of the *dp53-Δ305-sensor* (a sensor unable to respond to *miR-305*). The physiological meaning of Dp53 regulation by this two miRNAs remains to be elucidated. Thus, although we focused on *miR-305* because it showed higher expression values in the fat body*,* our results suggest that other miRNAs might contribute to Dp53 regulation in different *Drosophila* tissues to ensure low levels of activity of this key molecule in unstressed cells.

On the basis of our findings, we want to speculate that the miRNA-mediated regulation is an important and conserved process involved p53 regulation both in vertebrates and invertebrates. The activity of p53 is tightly regulated and immediately diminishes in the absence of critical stress to avoid unwanted consequences. Mdm2 and Mdm4 have long been identified as relevant negative regulators of p53, and their essential role in the regulation of p53 expression has been demonstrated in a variety of genetic mouse models *(Horn and Vousden, 2007)*. However, *Drosophila* has no ortholog of Mdm2 or Mdm4 *(Lane and Verma, 2012)*, the master regulators of p53. Moreover, the evidences supporting the role of several regulatory proteins in *Drosophila,* like Synoviolin and Bonus, are rather scarce, without complete dissection of the molecular mechanism sometimes and only based in genetic interactions *(Allton et al., 2009; Yamasaki et al., 2007)*. Our discovery of the role of the miRNA machinery, and in concrete *miR-305*, in regulating Dp53 revealed an evolutionary conserved mechanism of controlling endogenous Dp53 levels.

Context dependent roles and regulation of the miRNA machinery (and Dp53)

The results presented in this thesis support a generalized role of the miRNA machinery in targeting *dp53* in several *Drosophila* tissues.

In epithelial cells, the miRNA machinery targets directly Mei-P26, which is able to target dMyc for degradation by the ubiquitin proteasomal system, thus positively regulating dMyc protein levels, and as a consequence tissue growth [Figure 2A, *(Herranz et al., 2010)*]. In addition, we found that the miRNA

machinery was also able to restrict endogenous Dp53 protein levels and activity to prevent its deleterious effects. While Dp53 contributed to the apoptotic cell death and poor cell survival caused by depletion of Dcr-1, it did not contribute to the tissue size defects or the reduced dMyc protein in those cells. These results could explain the partial rescue in cell survival observed upon Dp53 depletion in *dcr-1* mutant clones. Total blockage of apoptosis (by expressing the baculovirus protein p35) in *dcr-1* mutant cells was able to rescue to a larger extent cell survival than Dp53 depletion, but still the rescue didn't reach the control values. These results indicate that depletion of the miRNA machinery activates both Dp53 dependent and independent cell death mechanisms and that the reduced tissue growth is not a consequence of increased apoptosis. Thus, in normal physiological conditions, the miRNA machinery promotes tissue growth and prevents apoptosis by independent targets (Figure XA).

Our findings also established the miRNA machinery as a transducer of nutrient availability and the TOR signaling pathway in fat body cells, being essential for Dp53 activation upon nutrient deprivation. Cells that encounter low nutrient conditions often respond by arresting cell division in a p53-dependent manner *(Jones et al., 2005)*. Interestingly, we found that Dp53 was required in fat body cells upon nutrient deprivation. The FB is an endoreplicative tissue that does not divide mitotically, suggesting that the role of Dp53 upon nutrient deprivation cannot be merely arrest the cell cycle. Indeed, our results unravel a new role for Dp53 in organismal adaptation to nutrient deprivation by modulating cellular metabolism (e.g. inhibition of glycolysis and/or activation of autophagy, this issue have been previously discussed) of fat body cells. Thus, Dp53 might play different roles depending on the context, including cell type and nature of the stress.

Another difference between the mechanism that operates in epithelial cells and fat body cells relies in the contribution of the miRNA-mediated regulation of Dp53 in response to genotoxic or nutrient stress. Whereas treatment with DNA damage agents induce downregulation of *miR-125b,* among others, which helps to increase p53 protein levels in mamals *(Le et al., 2009)*, our results suggested that the activity of the miRNA machinery might not be affected upon ionizing radiation-induced DNA damage (genotoxic stress), and indicated that the activation of Dp53 upon DNA damage does not depend on the de-regulation of the miRNA-mediated targeting of *dp53.* In contrast, we showed that the miRNA machinery plays a crucial role in the regulation of Dp53 under metabolic stress. Under nutrient deprivation, we found that several elements of the miRNA machinery pathway were transcriptionally

downregulated in FB cells, and as a consequence the *miR-305*-mediated targeting of *dp53* was alleviated, contributing to modulate cellular metabolism and organismal resistance to nutrient deprivation.

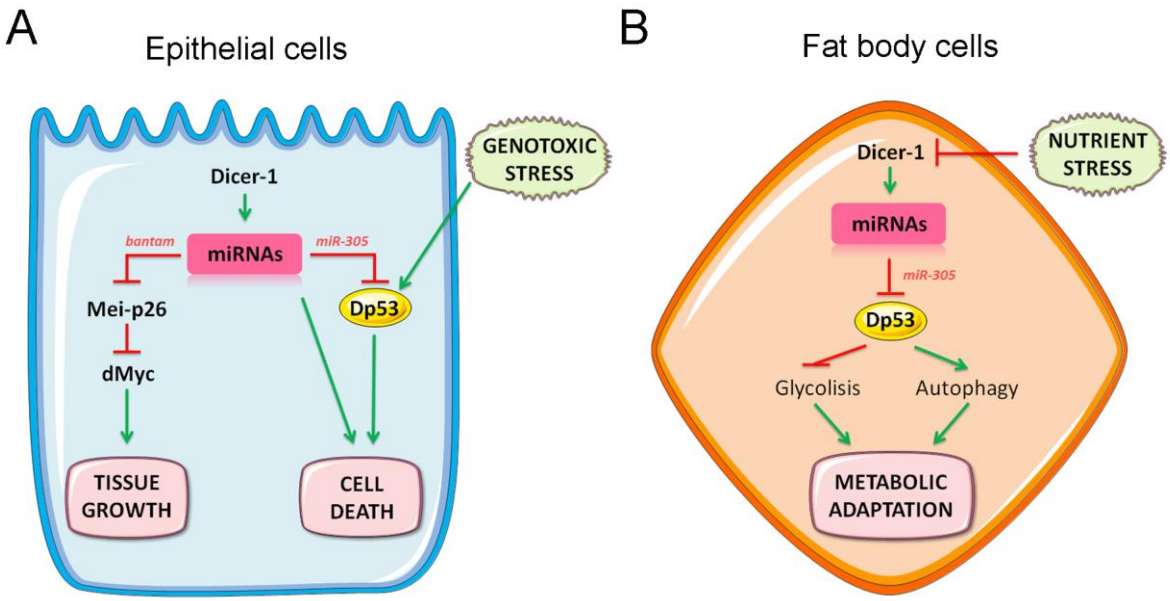

Figure 2: Context dependent roles and regulation of the miRNA-mediated regulation of Dp53

The miRNA machinery has a generalized role in targeting *dp53* in several *Drosophila* tissues. **(A)** In epithelial cells, the miRNA machinery controls tissue growth and cell death by independently targets. Whereas a double repression mechanism involving Mei-P26 and dMyc are responsible for the tissue growth promoting functions of the miRNA machinery, inhibition of Dp53 significantly contributes to the pro-survival function of the miRNA machinery in epithelial cells. (B) In fat body cells, the miRNA machinery also inhibits Dp53, which plays an important role in organismal adaptation to nutrient deprivation by modulating cellular metabolism (e.g. inhibition of glycolysis and/or activation of autophagy). Whereas activation of Dp53 upon genotoxic stress does not depend on the de-regulation of the miRNA-mediated targeting of *dp53*, the miRNA machinery plays a crucial role in the regulation of Dp53 under metabolic stress.

A possible double-negative feedback loop between p53 and miRNAs: reinforcing the signal

In the literature we found multiple examples showing that p53 activity and expression are controlled by a dense network of miRNA that, in response to stress, form diverse types of feedforward and feedback loops *(Hermeking, 2012)*. Indeed, computational studies suggested that miRNAs are overrepresented in gene regulatory networks, leading to the proposal that this class of regulators of gene expression confer stability to biological processes *(Herranz and Cohen, 2010).* MicroRNAs participate in different types of feedback and feed-forward mechanisms that mediate amplification,

robustness, fine-tuning and buffering of signals, and collectively contribute to appropriate cellular reactions *(Cohen et al., 2006; Shomron, 2010; Tsang et al., 2007)*.

As a preliminary experiment, we check the capacity of Dp53 to modulate its own 3' UTR sensor since in mammals, p53 regulates the expression not only of protein-coding genes but also of miRNA-coding genes *(Hermeking, 2007; Liao et al., 2014; Takwi and Li, 2009)*. Interestingly, overexpression of Dp53 induced an increase in the EGFP levels of the *dp53-sensor* in epithelial cells compared to the control-sensor and similar results were observed in luciferase assay performed in S2 cells (data not shown). These results suggest that Dp53 is able to inhibit the miRNA machinery and raise the possibility of the existence of a double-negative feedback loop involving Dp53 and the microRNAs. This kind of loops helps to set the threshold in determining when a target gene expression becomes sufficiently strong to signal a transition *(Mukherji et al., 2011).* When miRNAs are embedded in a double-negative feedback loop they become part of a bistable switch to enforce a new gene expression pattern (activation of Dp53), therefore committing cells to change for good and adapt to new environments (nutrient deprivation). In our model, nutrient deprivation through the TOR signaling pathway will be the primary input that leads to Dp53 activation through de-repression of the *miR-305*-mediated inhibition, and then, Dp53 by itself might contribute to its sustained activation. In a similar way, the p53-induced miRNAs *miR-605* inhibits MDM2 activity to enhance p53 activation in response to stress [Figure 3A, *(Xiao et al., 2011)]*. Since in *Drosophila* there is no MDM2 homolog, we speculate that in our hypothetical double-repression feedback loop, Dp53 could transcriptionally regulate its own miRNAs or elements of the miRNA machinery [(Figure 3B,(1)]. Remarkably, p53 has been shown to regulate the processing of precursor miRNAs through association with Drosha *(Suzuki et al., 2009)*. Another possibility would be that Dp53 affects intermediate components able to regulate the miRNA machinery. For instance, Dp53 could repress positive modulators of the miRNA machinery such as TOR [(Figure 3B,(2)], since in mammals p53 and mTORC1 signaling machineries can cross-talk to coordinately regulate cell growth, proliferation and death *(Feng et al., 2007; Levine et al., 2006)*. Alternatively, Dp53 could induce negative regulators of the miRNA machinery [(Figure 3B, (3)]. Our preliminary observations with Dp53 overexpression experiments seem to indicate a complex regulation between Dp53 and the miRNA machinery and the underlying mechanism requires further experiments.

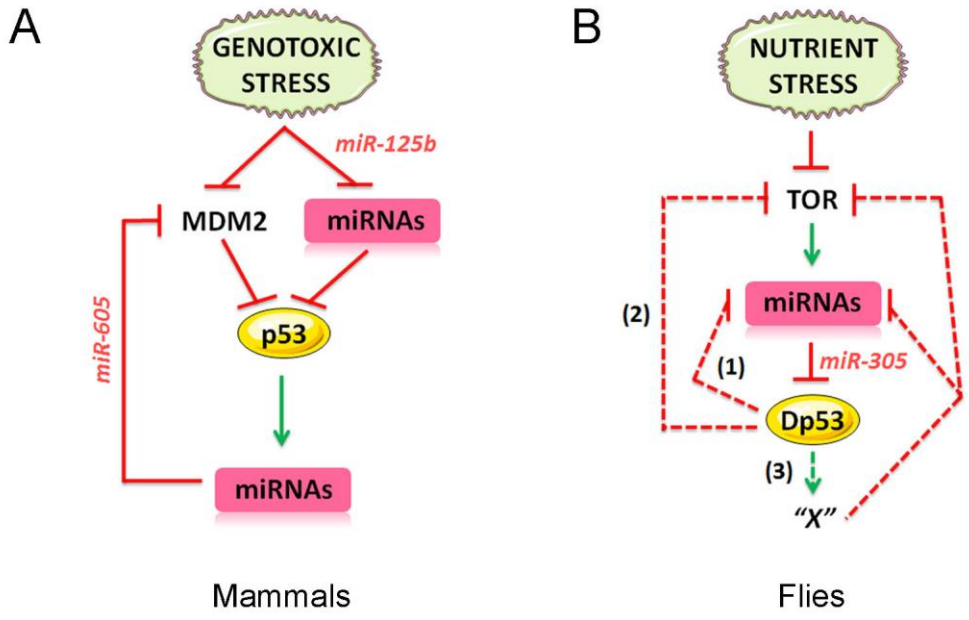

Figure 3: Feedback amplification loops between miRNAs and p53 promote adaptation to stress situations

MicroRNAs are frequently embedded in feedback amplification loop to enforce a new gene expression pattern, therefore committing cells to change for good and adapt to new environments. **(A)** In mammals, the p53-induced miRNAs *miR-605* inhibits MDM2 activity to enhance p53 activation in response to genotoxic stress (Xiao et al., 2011). (B) In *Drosophila* fat body cells nutrient deprivation through the TOR signaling pathway could be the primary input that leads to Dp53 activation through de-repression of the *miR-305*-mediated inhibition, and a possible double-negative feedback loop might contribute to its sustained activation in fasting conditions.

4. TOR signaling and the miRNA machinery

Is miRNA-mediated regulation of Dp53 by TOR tissue-specific?

The TOR signaling is the main nutrient sensor of the cell and is able to couple dietary nutrition to cell and tissue growth. TOR activity is required cell-autonomously to control growth in all larval tissues. In addition, stimulation of TOR in specific tissues, like the fat body, also plays a non-autonomous role in systemic growth and metabolic homeostasis *(Hietakangas and Cohen, 2009)*. TOR signaling can differentially regulate both tissue growth and metabolism, the relative strength of these two activities depending on the context (e.g., adipose tissue vs. imaginal disc). This dichotomy is observed also by the relative phenotypic outputs of different targets. For instance, the activity of S6K has profound effects on cellular and tissue growth *(Thomas, 2002)*, whereas 4EBP has insignificant effects on tissue growth but

profound effects on fat metabolism *(Teleman et al., 2005)*. In our model, we found that the miRNA-mediated regulation of Dp53 is controlled by nutrient availability and the TOR signaling pathway in the fat body. But, is this regulation by the TOR signaling pathway specific of this important metabolic tissue? Consistent with the important role of the TOR signaling in regulating metabolic homeostasis in the fat body, reduced activity of TOR in wing disc cells (by expressing the truncated form TOR^{TED} in the posterior compartment of the wing disc) didn't affect the levels of the *dp53-sensor* (Figure 4A) whereas it was able to modulate it in FB cells. This observation suggests that the modulation of the miRNA-mediated regulation of Dp53 by the TOR signaling pathway occurs specifically in fat body cells. Thus, the requirement of a certain co-factor or downstream effector whose expression should be FB-specific may help to explain why TOR activity can have different phenotypic outputs in what concern to miRNA regulation.

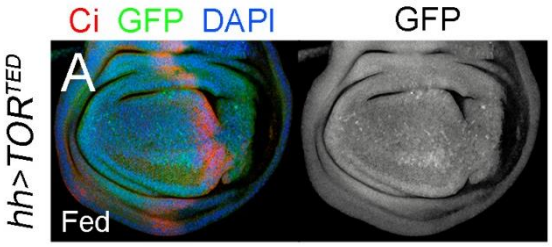

Figure 4: The miRNA-mediated regulation of *dp53* by TOR does not occur in the wing disc

Wing discs expressing TOR^{TED} (a truncated from of TOR with a dominant negative effect) under the control of the *hh-gal4* driver carrying the *dp53-sensor* and labeled to visualized GFP (green or grey), Ci (red) protein expression and DAPI (blue). *hh-gal4* drive transgene expression in the posterior compartment and Ci expression was used to labelled the anterior compartment. Note that upon expression of TOR^{TED} the EGFP expression levels of the *dp-53 sensor* is not affected.

Between TOR signaling and the miRNA machinery

The TOR signaling pathway is one of the most pleiotropic pathways able to influence multiple cellular responses that range from basic biological processes, such as translation and protein synthesis, to more complex stress responses like autophagy *(De Virgilio and Loewith, 2006; Grewal, 2009;*

Wullschleger et al., 2006). In this thesis, we provided evidence that nutrient conditions through the TOR signaling pathway were able to modulate the miRNA machinery, a very potent regulator of gene expression, thus, significantly expanding the pleiotropic capability of the TOR signaling pathway. We found that in standard feeding conditions, TOR signaling contributed to miRNA-mediated targeting of *dp53.* In contrast, nutrient deprivation reduced the expression levels of major elements of the miRNA machinery, including *dicer-1*, *Drosha* and *Ago1,* and as a consequence, the *miR-305*-mediated repression of *dp53* was alleviated. How TOR regulates several components of the miRNA machinery at the same time is an interesting missing link in our model. Elucidating which are the mechanisms downstream of TOR signaling will require further analysis. *A priori* we can think of different possibilities.

An easy explanation would be that TOR is likely to act via an intermediate transcription factor to regulate these genes. One possibility would be the proto-oncogene dMyc, since it has been shown (1) to be posttranscriptional regulated by TORC1 in a nutrition dependent manner, (2) to mediate transcriptional regulation of TORC1 target genes and (3) to play a key role in mediating the effects of TOR on growth and metabolism *(Teleman et al., 2008)*. In addition, the transcriptional modulation of certain miRNA by Myc has been extensively studied in human and mouse cancer lines, were widespread miRNA repression by Myc significantly contributes to tumourogensis *(Chang et al., 2008).* Considering these observations, it would be interesting to analyze whether in *Drosophila*, dMyc is able to modulate the miRNA machinery and whether in our model dMyc could be the missing factor downstream of TORC1 an upstream of the miRNA machinery.

Another possibility could be the process of autophagy. On one hand, in *Drosophila* fat bodies, the induction of autophagy following nutrient deprivation has been well documented to be a consequence of TORC1 downregulation *(Scott et al., 2004)*. On the other hand, recent evidences in mammalian cells and in *C.elegans* support the proposal that autophagy is able to modulate miRNA mediated gene silencing by directly degrading Dcr-1 or several components of the miRISC *(Gibbings et al., 2012; Zhang and Zhang, 2013).* Thus, it would be also very interesting to check whether activation of Dp53 under nutrient deprivation could be due to an autophagic-mediated repression of the miRNA machinery.

5. **Regulation of Dp53 upon starvation**

We have uncovered the importance of the *miR-305*-mediated release of Dp53 during conditions of nutrient deprivation. However, considering the literature, other possibilities could contribute to Dp53 activation upon a metabolic challenge.

During energetic stress, AMP-activated protein kinase (AMPK) is activated in response to an increase in the AMP:ATP ratio. AMPK is a cellular fuel sensor that acts as master regulator of cellular metabolism, directly influencing many key pathways involved in carbohydrate and lipid metabolism, and in autophagy as well *(Hardie et al., 2012)*. Moreover, AMPK activity can also be negatively regulated by glycogen levels *(McBride et al., 2009)*. Thus, AMPK has the ability to monitor the amount of immediately available energy in the form of ATP as well as reserve energy stores in the form of glycogen, ensuring sensitive monitoring of the cell's energy status. One of the key pathways that can be downregulated by AMPK is the mTORC1 pathway *(Inoki et al., 2003b)*. Interestingly, upon glucose deprivation, AMPK is also able to activate p53, directly via serine-15 phosphorylation *(Jones et al., 2005)* or indirectly through inhibition of the deacetylase Sirt1 *(Lee et al., 2012)*, which in turn establishes a p53-dependent G_1-S checkpoint that prevents S phase entry when cellular energy supplies are inadequate to support the demands of cell division. Although Jones et al. have focused on the effects of low glucose, many forms of energetic stress regulate AMPK, and its ability to activate p53 may be a common coping mechanism. In our work, we found that amino acid deprivation (by downregulation of Slimfast, the main amino acid transporter in cells) was able to activate Dp53 in a TOR-dependent manner. However, we can't rule out the contribution of a possible AMPK input in raising the levels in our severe starvation conditions where we also remove the glucose content from the diet. Organism-wide reduction of AMPK function in *Drosophila* leads to heightened starvation sensitivity, greater hyperactive responses to starvation and reduced TAG levels *(Johnson et al., 2010)*. Two of these three phenotypes are similar to our phenotypes, thus, considering the presented literature, could be interesting to analyze whether in our model AMPK could be also affecting TOR/Dp53 regulation as well.

Sir2 is a deacetylase that has been shown to physically interact with Dp53, and efficiently deacetylate Dp53-derived peptides. In a situation of calorie restriction (CR), both proteins genetically interact to mediate life span extension in a linear pathway. However, due to technical issues, there are no evidences showing the effect of endogenous Dp53 acetylation dynamics in response to CR conditions

(Bauer et al., 2009). In starvation, as it occurs in CR conditions, Sir2 expression is increased, and loss of Sir2 activity in the FB reduced the levels of TAG and the survival rates to nutrient deprivation, similar to what we observe with Dp53. Thus, we don't expect a molecular interaction between these molecules in FB cells, or at least not in the same direction (Sir2 inhibiting Dp53). It could be that Sir2 in FB cells induces acetylation of another residue that promotes Dp53 activation instead of repression, or maybe, starvation regulates these too components independently, and the role of Sir2 in regulating p53 might be tissue-specific and/or restricted to the IPCs. Another example supporting this proposal is shown by the fact that over-expression of Sir2 in the eye primordium promotes a caspase-dependent but Dp53-independent apoptosis that is mediated by the JNK and FOXO signaling pathways *(Griswold et al., 2008)*. In this case, again, Dp53 and Sir2 work in parallel pathways to induce similar phenotypes.

6. **MicroRNA-mediated regulation of p53 and metabolic disorders**

Animals sense their nutritional status and respond in a concerted manner to coordinate growth and maintain energy homeostasis. As a result, metabolic regulation and physiological feedback systems are central to many aspects of animal life. In this thesis, we analyzed the role of Dp53 in balancing energy needs with dietary input to promote survival in a situation of nutrient deprivation. Deregulation of the processes that coordinate nutrient availability and energy balance are associated with several metabolic disorders including obesity and diabetes, cardiovascular diseases and some forms of cancer. Thus, an immediate question that comes to our minds is, could be Dp53 involved in those metabolic disorders? Our work demonstrated that Dp53 is activated in the absence of nutrients, but can Dp53 work as a dual sensor and also be involved in the opposed situation? Interestingly, recent evidences in mice and human cells suggest that activation of p53 in endothelial cells in response to high-calorie diet contributes to metabolic abnormalities through regulation of glucose homeostasis in skeletal muscle *(Yokoyama et al., 2014)*. However, in this study, the mechanism that leads to p53 activation in a high-calorie state is unknown. Thus, an interesting follow-up of our study would be to address whether miRNA-mediated regulation of Dp53 could be also involved in the metabolic defects associated with high-calorie diet and obesity. In that sense, *Drosophila* has been established as a good model to study diabetes and the effect of high-sugar diets *(Musselman et al., 2011; Na et al., 2013; Pasco and Léopold, 2012)* as well as for obesity and high-fat diet effects *(Birse et al., 2010)*. If Dp53 is activated by these diets, miRNA-mediated release of Dp53 in this hypothetic scenario is unlikely to be regulated in the same way as in nutrient

deprivation, it should occur by a TOR-independent mechanism. Moreover, it would be interesting to test what would happen to *dp53* mutant or Dp53-overexpressing flies fed with high-fat or high-sugar diet. Our findings suggest the possibility that control of Dp53 or the miRNA machinery activity could provide a means to improve metabolic abnormalities related to dietary obesity or diabetes, such as glucose tolerance or fat accumulation, and thus might be of clinical use in treating this metabolic disorders.

7. Is stress-induced depletion of the miRNA machinery a general process?

Since the discovery of miRNAs in 1990, a new paradigm of gene regulation has been established. Over the past twenty years, the regulation of gene expression by these small non-coding RNAs has been linked to virtually all known biological processes and in the pathogenesis of human diseases, including cancer *(Kloosterman and Plasterk, 2006; Lujambio and Lowe, 2012)*. The important feature of miRNAs is its capacity to modulate tens to hundreds of target mRNAs (it is accepted that miRNAs are able to regulate over 30% of mRNAs in a cell), resulting in the efficient activation or repression of signaling networks at specific times and places *(Tétreault and De Guire, 2013)*. Of relevance for our work, in the last decade multiple lines of genetic evidence indicate that miRNAs play key roles in mediating stress responses and in controlling energy homeostasis *(Dumortier et al., 2013; Leung and Sharp, 2010)*. MicroRNA dysfunction therefore causes defects in the integration of signaling networks essential for the maintenance of cellular homeostasis.

Interestingly, specific miRNA expression has been demonstrated to be under the control of nutrient availability *(Carrer et al., 2012; García-Segura et al., 2013; Ouaamari et al., 2008)*. On the basis of our findings, we proposed an alternative model in which central elements of the miRNA machinery pathway *per se* are sensitive to nutrients, and we define the TOR signaling as a link between nutrition/amino acids and miRNAs expression. We showed that the expression levels drosha and dicer-1, two genes involved in the biogenesis of miRNAs, and argonaute 1, a component of the miRISC, were downregulated during starvation. Whether starvation-induced activation of vertebrate p53 does rely on reduced miRNA-mediated targeting of the p53-3'UTR remains to be elucidated. Remarkably, a similar impact on the activity of the whole miRNA machinery has been observed during the aging process in mice, C.elegans

and human preadipocytes *(Anderson, 2012)* and in culture cells under several stress conditions, including hypoxia, autophagy, UV radiation and oxidative stress *(Blandino et al., 2012; Gibbings et al., 2012; Ho et al., 2012)*. Thus, stress-induced depletion of the miRNA machinery appears to be a conserved mechanism that contributes to the de-repression of certain genes involved in the biological responses to the original stress.

The miRNA machinery was previously shown to promote cellular and tissue growth by targeting the Drosophila orthologue of the TRIM32 tumour suppressor gene Mei-P26, which triggers proteasome-dependent degradation of the proto-oncogene dMyc *(Herranz et al., 2010)*. In addition, the conserved miRNA *miR-8* and its target, USH, regulate body size in Drosophila *(Hyun et al., 2009)*. USH is a negative regulator of the PI3K signaling pathway, and overexpression of *miR-8* in FB cells activates PI3K and promotes growth cell-autonomously. Finally, our identification of Dp53 as a critical element modulating the consumption of energy resources in FB cells and its regulation by the miRNA machinery points to a central role of miRNAs in coordinating the cellular and physiological responses to nutritional starvation. In response to nutrient deprivation, down-regulation of *dicer-1, Drosha* and *Ago-1* expression levels result in a general reduction of active mature miRNAs in FB cells, which in turn might contribute to the expected decrease in the activity of growth-promoting genes (*dMyc*) or pathways (PI3K) and a concomitant increase in the activity of genes, such as Dp53, that modulate the rates of glycogen and TAG catabolism.

Because of the high abundance of miRNAs in the genomes of all metazoans and the widespread capacity of some miRNAs to downregulate large numbers of target mRNAs *(Farh et al., 2005; Lim et al., 2003a; Lim et al., 2005)*, regulation of only few target genes (components of the miRNA machinery) can induce a broad and fast reaction to promote adaptation to a particular stress situation. Although care must be taken when generalizing interpretations of miRNA functions across different contexts and tissues, we want to propose the miRNA machinery as an integral component of a regulatory circuit that functions under conditions of metabolic stress to control cell-autonomous and systemic energy homeostasis and the overall adaptive capacity of the organism. Thus, these components of the miRNA machinery shown to be regulated by nutrient availability provide potential targets for pharmacologic intervention in obesity and metabolic syndrome.

8. A model for the miRNA-mediated regulation of Dp53 in the adaptation to nutrient deprivation

In conclusion, our results regarding the regulation of Dp53 activity by the miRNA machinery in FB cells downstream of nutrient availability tend to place Dp53 as a key player in metabolic adaptation to nutrient deprivation at the organismal level. As a summary of this, we show that: **(1)** depletion of Dp53 activity levels specifically in FB cells accelerates the consumption of the main energy stores, reduces the levels of sugars in the animal, and compromises organismal survival upon fasting; **(2)** the levels of fasting hormones (Insulin and Adipokinetic hormone) and metabolic enzymes that mobilize energy resources are similarly modulated by starvation in *control* and *dp53* mutant animals and unveil a cell autonomous role of Dp53 in modulating the metabolic changes of FB cells to nutrient deprivation; **(3)** Dp53 is regulated by the microRNA machinery in a nutrition-dependent in FB cells and identify *miR-305* as a major regulatory element; **(4)** in well-fed animals, TOR signaling contributes to *miR-305*-mediated inhibition of Dp53; **(5)** nutrient deprivation reduces the levels of major elements of the miRNA machinery and leads to Dp53 de-repression (Figure 5).

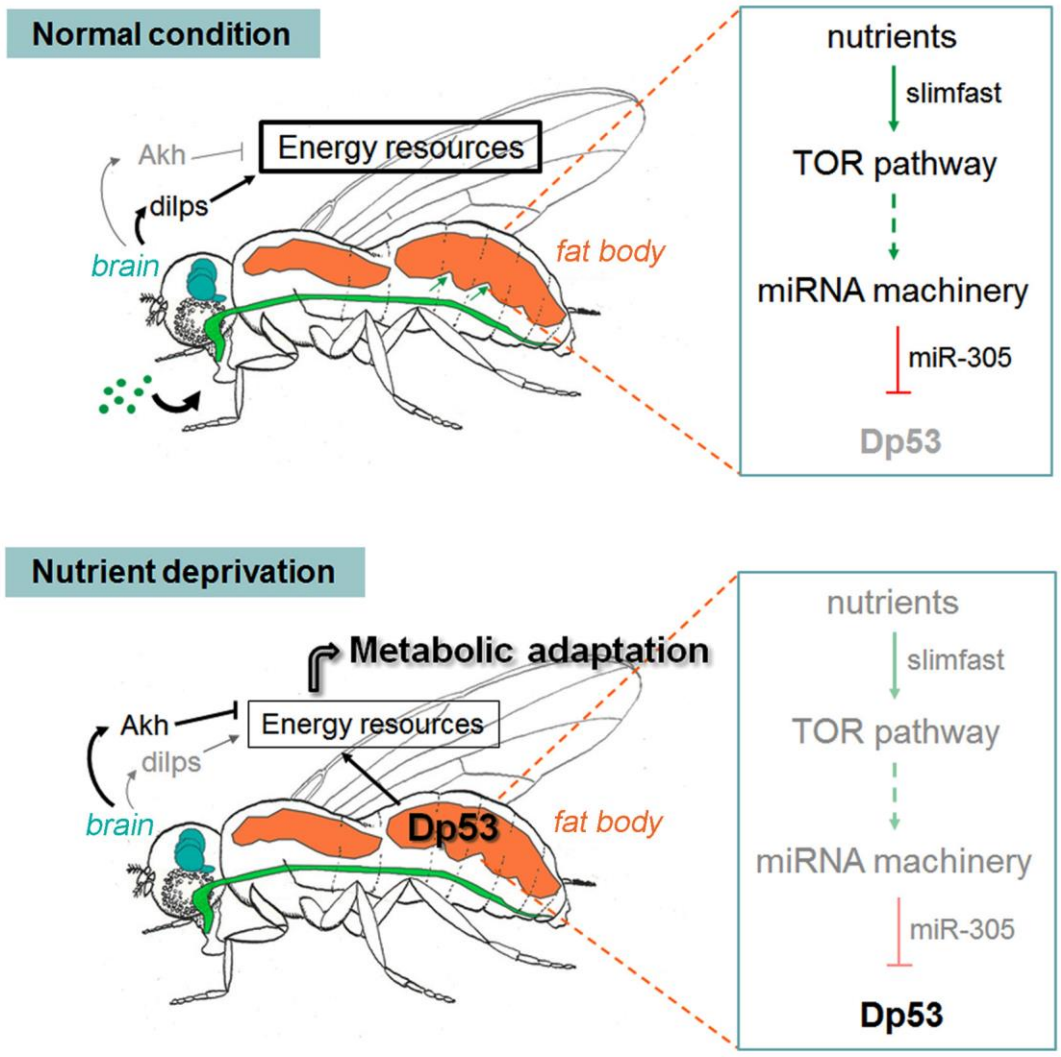

Figure 5: MicroRNA-mediated regulation of p53 in *Drosophila*: a new role in adaptation to nutrient deprivation

In well-fed animals, TOR signaling contributes to miR-305-mediated inhibition of Dp53 in fat body (FB) cells. However, nutrient deprivation reduces the levels of major elements of the miRNA machinery and leads to Dp53 de-repression. Specific depletion of Dp53 activity levels FB cells accelerates the consumption of the main energy stores and compromises organismal survival upon fasting.

CONCLUSIONS

CONCLUSIONS

1. *Drosophila* p53 (Dp53) plays a fundamental role in organismal adaptation to nutrient deprivation. Dp53 is specifically required in the *Drosophila* fat body to promote metabolic adaptation to nutrient deprivation at the level of organism.
2. Fat body-depletion of Dp53 causes accelerated depletion of the main energy storages and compromises organismal survival in fasting conditions.
3. The impact of Dp53 in energy balance upon nutrient deprivation is independent of the systemic regulation of the endocrine signaling network involved in metabolic homeostasis.
4. Dp53 plays a cell-autonomous role in fat body cells in the metabolic adaptation to nutrient deprivation.
5. Dp53 is a direct target of the miRNA machinery in *Drosophila,* and *miR-305* is a major regulator of Dp53.
6. Nutrient availability regulates the miRNA machinery through TOR and maintains low levels of Dp53 in fat body cells.
7. Nutrient deprivation induces Dp53 activation by releasing *miR305*-mediated repression of the *dp53-3'UTR*.
8. In epithelial cells, Dp53 has conserved the capacity to induce programmed cell death, stop the cell cycle and repair the DNA, the classical functions of mammalian p53 as a tumour suppressor.
9. Upon ionizing radiation (IR)-induced DNA damage, Dp53 only regulates the early apoptotic response and induces DNA repair.
10. The miRNA machinery targets Dp53 in epithelial cells, thus preventing induction of programmed cell death.

11. Dp53 activation upon DNA damage does not rely on the alleviation of *miR305*-mediated repression of the *dp53-3'UTR*.

MaTeRiaLS and MeTHoDS

MATERIALS AND METHODS

1. **Materials**

Drosophila strains

Flies were raised at 25° C (unless otherwise specified) in a 12/12 h day/night period on standard *Drosophila* medium containing 4% glucose, 55 g/L yeast, 0,65% agar, 28 g/L wheat flour, 4 ml/L propionic acid and 1,1 g/L nipagin).

Gal4 driver lines: *en-gal4*, *hh-gal4*, *ci-gal4*, *act-gal4* were from the Bloomington Stock Center and are described in Flybase; *ap-gal4* (Milán and Cohen, 1999); *spalt^{PE}-gal4* (Barrio and de Celis, 2004)*; mef2-gal4* [gift from N. Perrimon,(Demontis and Perrimon, 2010); *ppl-gal4* [kind gift from J. Colombani and P. Leopold (Colombani et al., 2003)], *cg-gal4* and *yolk-gal4* (gift from JM Reichhard) were used to drive expression in a fat body (FB)-specific manner. *ppl-gal4* and *cg-gal4* are expressed in non-FB-related tissues, but their expression domains intersect only in the FB (Géminard et al., 2009). *yolk-gal4* is expressed only in FB cells of adult females (JM Reichhard, personal communication to Flybase). In all the presented experiments, all drivers produced identical results, ensuring that the effects are due to fat-body expression. Expression levels of the three Gal4 drivers, monitored by the expression of an UAS-GFP transgene, was mildly reduced upon starvation (Figure 1), most probably as a consequence of the decrease in whole-animal metabolism. Since all experimental conditions were compared with control flies expressing GFP under the same FB-Gal4 driver, these changes might not explain the reduced survival rates or accelerated consumption of energy resources observed in FB>Dp53-DN and FB>Dp53-RNAi flies.

UAS – lines: *UAS-miR-305*, *UAS-miR-219*, *UAS-miR-279*, *UAS-miR-283* and *UAS-miR-1014* (kind gifts from Norbert Perrimon); *UAS-slif^{Anti}* [kind gift from J. Colombani and P. Leopold, (Colombani et al., 2003)]; *UAS-p35* (Hay et al., 1994); *UAS-GFP*, *UAS-RFP*, *UAS-myr-Tomato*, *UAS-TOR^{TED}*, *UAS-Rheb,* UAS–dp53$^{H159.N}$, UAS–dp53$^{2.1}$ were from the Bloomington Stock Center and are described in Flybase; *UAS-dp53^{RNAi}* (ID number 38232), *UAS-dicer^{RNAi}* (ID number 11429), *UAS-dMyc-^{RNAi}* (ID number 1418), *UAS-okra^{RNAi}* (ID number 104323) and *UAS-grapes^{RNAi}* (ID number 12680) were obtained from the Vienna *Drosophila* RNAi Center.

Other lines: *E2F-sensor* [a dE2F1-responsive reporter *ORC1-GFP*,(Asano and Wharton, 1999)]; *dcr-1*^{Q1147X} (Hatfield et al., 2005); *puckered-lacZ* (Martín-Blanco et al., 1998); *control-sensor* (Brennecke et al., 2003); *Dp53R-GFPnls* [a biosensor used to visualized dp53 activity, gift from John M. Abrams, (Lu et al., 2010)]; actin>CD2>Gal4 (Pignoni and Zipursky, 1997); *hs-FLP*, *arm-LacZ*, *FRT82B*, *FRT40*, *w*^{1118}, *ry*^{506} *dp53*^{ns} , *dp53*^{5A14}, *Df(2L)exel7031* [*Df(miR-305)* in the text, a deficiency of 130 kbp that covers the miR-305 locus] were from the Bloomington Stock Center and are described in Flybase.

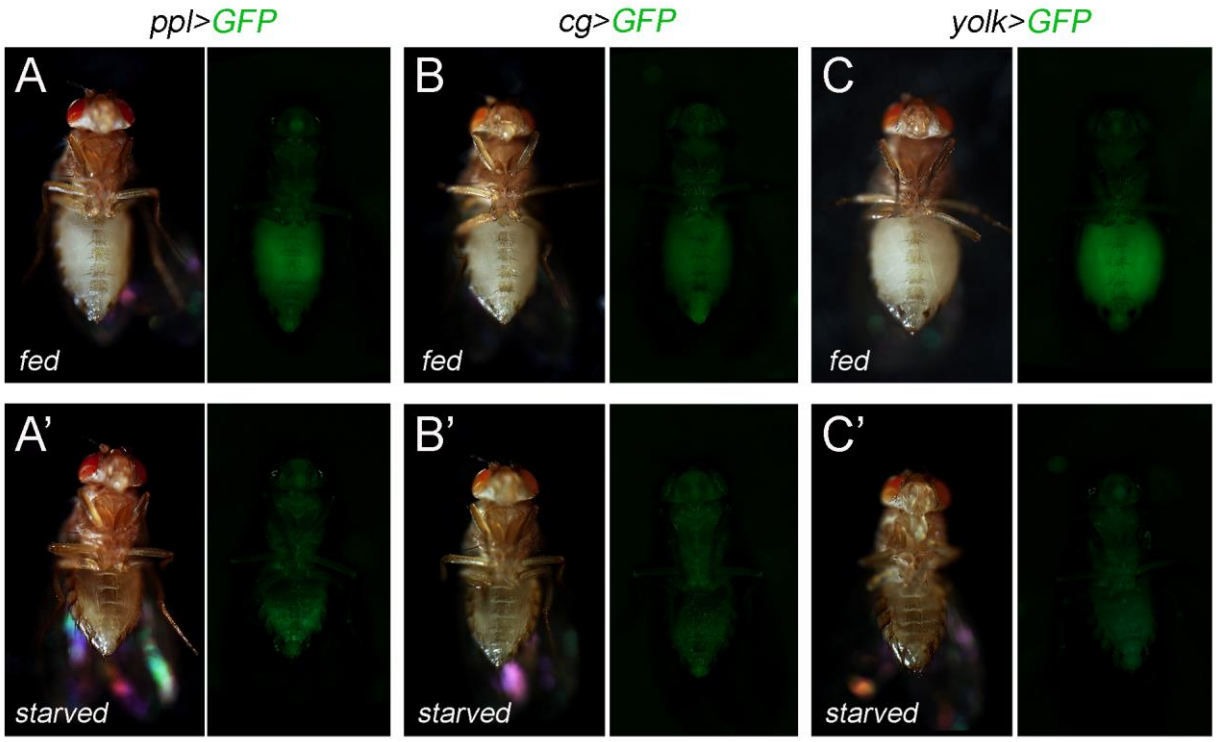

Figure 1: Expression levels of the three fat body-Gal4 drivers in adults

(A-C') Representative examples of adult flies expressing the UAS-GFP transgene used in our control experiments under the expression of the three fat body-Gal4 drivers used in this thesis, *ppl-gal4* (A, A`), *cg-gal4* (B. B') and *yolk-gal4* (C, C') in fed conditions (A, B, C) or starved in 2% agar, 1% sugar for 5 days (A', B', C'). Note that GFP expression was mildly reduced upon starvation, most probably as a consequence of the decrease in whole-animal metabolism.

Antibodies

Table 1 depicts all the primary antibodies used in this thesis, their characteristics and origin.

The fluorescent secondary antibodies that have been used are from Molecular Probes (used 1/500).

Antibody	Abreviation	Host specie	Concentration	Origin
β-galactosidase	β-gal	Rabbit	1/600	Cappel
Bromo-2-deoxiUridine	BrdU	Rat	1/100	Abcam
Caspase-3-cleaved	Caspase-3*	Rabbit	1/100	Cell Signalling Technology
CD2	CD2	Mouse	1/100	Santa Cruz Biothecnology
Cubitus interruptus	Ci	Rat	1/5	DSHB (Hybridoma Bank)
Cyclin B	CycB	Rabbit	1/100	Santa Cruz Biothecnology
Cyclin E	CycE	Rabbit	1/50	Santa Cruz Biothecnology
Dacapo	Dap	Mouse	1/50	DSHB (Hybridoma Bank)
Drosophila insulin-like peptide 2	dilp2	Rat	1/1000	*Pierre Leopold*
Fibrillarin	Fibri	Mouse	1/100	Abcam
Gal-4	Gal4	Rabbit	1/100	Santa Cruz Biothecnology
Green Fluorescence Protein	GFP	Rabbit	1/100	Invitrogen
Green Fluorescence Protein	GFP	Mouse	1/100	Roche
meiP-29	meiP-26	Rabbit	1/100	*Paul Lasko*
Drosophila Myc	dMyc	Guinea pig	1/1000	*Stephen Cohen*
Drosophila p53	dp53	Mouse	1/25	DSHB (Hybridoma Bank)
Phospho-histone 2av	pH2av	Rabbit	1/500	Rockland
Phospho-histone 3	PH3	Rabbit	1/100	Cell Signalling Technology

Table 1: List of primary antibodies used

Table compiling all primary antibodies, its chracteristics and orgin, used for immunohistochemistry assays.

Constructs

In order to generate the dp53-3'UTR GFP-sensor, the dp53-3'UTR was amplified by PCR from the GH11591 plasmid (DGRC) and cloned into the control-sensor plasmid (P-CaSper4-tub-EGFP, (Brennecke et al., 2003)) via the NotI-XhoI cloning sites. The following primers were used: forward: 5'-CTTCTGATCTGGTCGACAATC-3'; reverse: 5'-TTTGCAAAATATGACAACTCT-3'. In order to generate the dp53-3'UTR-Δ305 GFP-sensor, the seed region of miR-305 (GTACAAA) on the dp53 3'UTR was deleted by PCR. The following primers were used to generate the internal deletion: forward: 5'-AACATACTCTAAAGCCAAAAGTGAA-3'; reverse: 5'- TTGGCTTTAGAGTATGTTTGTTG-3'. Multiple transgenic lines were generated per construct.

To generate a dp53-luciferase reporter, the 3'UTR of dp53 was amplified by PCR from the GH11591 plasmid (DGRC) and cloned downstream of the pJ-Luc reporter plasmid (gift from E. Izaurralde) via the XhoI-Xba cloning sites. A plasmid expressing Renilla luciferase (RLuc, gift from E. Izaurralde) was used as a transfection control. The 10 candidate miRNAs were amplified by PCR from genomic DNA and cloned into the pAC5.1 plasmid (Invitrogen) via the NotI-Xba cloning sites.

2. **Methods**

Mosaic analysis

MARCM clones. The following *Drosophila* genotypes were used to generate loss-of-function clones in wing discs by the MARCM (mosaic analysis with a repressible cell marker) technique to simultaneously express diverse transgenes in the clones *(Lee and Luo, 2001)*:

hs-FLP tub-gal4 UAS-GFP; UAS-p35/+; FRT82 dcr-1^{Q1147X}/FRT82 tub-Gal80;

hs-FLP tub-gal4 UAS-GFP; UAS-p53$^{H159.N}$/+; FRT82 dcr-1^{Q1147X}/FRT82 tub-Gal80;

hs-FLP tub-gal4 UAS-GFP; FRT82 dcr-1^{Q1147X}/FRT82 tub-Gal80;

hs-FLP tub-gal4 UAS-GFP; FRT82 ry^{506}/FRT82 tub-Gal80

Heat-shock (45 min at 37° C) was induced 3, 4 or 5 days after egg laying (AEL) and late third instar wing discs were dissected. Mutant cells were marked by the presence of GFP.

FRT clones. The following *Drosophila* genotypes were used to generate loss-of-function clones in wing discs by the FLP/FRT system *(Xu and Rubin, 1993)*:

hs-FLP/+; GFP-dp53-sensor/+; FRT82 dcr-1^{Q1147X}/FRT82 arm-lacZ

hs-FLP/+; GFP-dp53-Δ305-sensor/+; FRT82 dcr-1^{Q1147X}/FRT82 arm-lacZ

hs-FLP/+; Df(2L)exel7031 FRT40 / arm-lacZ FRT40; GFP-dp53-sensor/+

hs-FLP/+; Df(2L)exel7031 FRT40 / arm-lacZ FRT40; GFP-dp53-Δ305-sensor/+

Heat-shock (45 min at 37° C) was induced 3 days (for *Df(miR-305)* clones) or 5 days (for *dcr-1^{Q1147X}* clones) AEL and late third instar wing discs were dissected. Mutant cells were marked by the absence of β-gal.

FlipOut 'clones'. The following genotypes were used to induce the expression of various transgenes in single FB cells:

hs-FLP/+; GFP-dp53-sensor/UAS-dcr-1^{RNAi}; actin>CD2>GAL4, UAS-RFP/+

hs-FLP/+; GFP-dp53-sensor/UAS-miR-305; actin>CD2>Gal4, UAS-RFP/+

hs-FLP/+; GFP-dp53-sensor/UAS-TOR^{TED}; actin>CD2>Gal4, UAS-RFP/+

hs-FLP/+; GFP-dp53-Δ305-sensor /UAS-TOR^{TED}; actin>CD2>Gal4, UAS-RFP/+

hs-FLP/+; GFP-dp53-sensor/UAS-slif^{Anti}; actin>CD2>Gal4, UAS-RFP/+

hs-FLP/+; GFP-dp53-sensor/UAS-Rheb; actin>CD2>Gal4, UAS-RFP/+

hs-FLP/+; actin>CD2>Gal4, UAS-GFP/UAS-dp53$^{H159.N}$

hs-FLP/+; actin>CD2>Gal4, UAS-GFP/UAS-dp53^{RNAi}

Heat-shock (3-5 min at 37° C) was induced 36 h AEL and 60-72 h later (including the starvation treatments) were dissected (except for *UAS-TOR^{TED}* and *UAS-slif^{Anti}*, which were induced 60 h AEL and dissected 24 h later). Clones were marked by the presence of RFP or GFP or by the absence of CD2.

Temperature shifts for Dp53 overexpression experiments

We used the Gal4/UAS system (Brand and Perrimon, 1993), combined with the thermosensitive version of Gal80 [Gal80^{ts}, (McGuire et al., 2004)], a repressor of Gal4 protein activity, to precisely control, in time and space, expression of a wilt-type form of Dp53 in the wing primordium. Adult flies carrying the *en-gal4* driver, the Gal80^{ts} construct and the UAS-Dp53 transgene were allowed to lay eggs over a period of 24 hours (or less) at 18 °C. The progeny was then raised at 18 °C to maintain the Gal4/UAS system switched off and transferred to 29 °C (all the incubations at 29 °C were done in a bath) at third instar stage (144-192 AEL at 18 °C) for a period of 12 hours to induce Gal4/UAS dependent gene expression. Larvae were dissected immediately after of the induction period.

Immunostaining

Larvae were dissected in PBS, fixed for 20 minutes in PBS + 4% formaldehyde, rinsed 3 times during 15 minutes with PBT (PBS + 0.1% Triton X-100), and blocked for 1 hour with BBT (PBT + BSA 0'3% + 250 mM NaCl). Incubation with primary antibodies in 50µl of BBT was performed overnight at 4° C. After incubation, samples were rinsed 4 times during 15 minutes with BBT and stained with secondary

antibodies conjugated with different Alexa-fluorophores in 100µl of BBT for 2 hours at room temperature. DAPI was added to the last 15 minutes of secondary antibody staining to detect DNA. Samples were finally rinsed with PBT and mounted in mounting medium (40ml Glycerol + 5ml PBS10X + 400µl N-propyl-gallate 50% diluted in ethanol). Images were captured using a Leica TCS SP2 confocal microscope and process and treated with FiJi (NIH, USA) and Adobe Photoshop softwares.

Other fluorescence assays

- **TUNEL assay**

  TUNEL analysis was performed as described in *(Milán et al., 1996)* and it was used to label the DNA break of death cells (kit provided by Roche Diagnostics).

- **Nile Red staining**

Nile Red is a lipophilic stain used to labeled intracellular lipid droplets. The protocol was adapted from (Grönke et al., 2005). Briefly, larvae were synchronized in the second to third larval transition and placed in tubes with 2% agar 1% sucrose (starved) or standard food (fed) 12 h later. After 24 h, FBs were dissected in PBS, fixed with formaldehyde 4% and stained with Nile red (0.2 µg/ml Nile red) for 30 min.

BrdU incorporation

BrdU incorporation was performed as described in *(Milán et al., 1996)*. It was used to measure DNA synthesis (S phase) in proliferating cells. 5-bromo2'-deoxy-uridine (BrdU) was incorporated into DNA in place of thymidine. Then, cells which have incorporated BrdU into DNA were detected using a monoclonal antibody against BrdU (Roche).

In situ hybridization

In situ hybridization was performed as described in (Milán et al., 1996). A Digoxigenin- RNA Labelling kit (Roche) was used to synthesize antisense probes of *string* (from the cDNA clone LD47579 linearizing the plasmid with EcoRI and using Sp6 polymerase) and *dp53* (from the cDNA clone GH11591 linearizing the plasmid with SalI and using Sp7 polymerase).

Quantification of tissue growth in adult wings and wing discs

dcr-1 clones expressing $dp53^{H159.N}$ or *p35 (wing discs)*: larvae of the corresponding phenotypes (see Mosaic analysis: MARCM clones section) were dissected 48, 72 and 96 h after clone induction. The clonal area was measured using the Fiji software (NIH, USA) as the ratio of GFP positive area to the total wing pouch area in the different experimental conditions. This ratio was normalized to the ratio obtained with wild type clones and presented as a percent.

$dcr\text{-}1^{RNAi}$ expression (adult wings): *en-gal4* virgins were crossed with males carrying different UAS-transgenes and allowed to lay eggs for 24h at 25° C. The resulting larvae developed at 29° C until adulthood. At least 15 adult flies per genotype were mounted in Faure medium. Size of the engrailed domain (P compartment) was measured using the Fiji software (NIH, USA). Final area values were normalized as a percent of the control *en-gal4, UAS-GFP* value.

Using Microsoft Excel, average values and the corresponding standard deviations were calculated and t-test analysis was carried out.

Fluorescence quantifications

- **Quantification of GFP intensity levels in wing discs**

Due to sample thickness, to quantify GFP intensity of wing discs carrying distinct 3'UTR-sensors, images from 7 focal planes were considered for the determination of mean intensity. The settings on the confocal microscope and all subsequent treatments of images were identical between control and experimental samples. For GFP intensity quantification, the wing pouch of each disc was selected, and mean fluorescence intensity was calculated using Fiji software (NIH, USA). Data were normalized respect to control animals. Using Microsoft Excel, average values and SEM were calculated and Student's t-test analysis was carried out for statistical significance.

- **Fluorescence quantification in IPCs and FB cells**

For fluorescence quantification the correspondence tissues from starved or well-fed larvae confocal Z series were taken as described below and identical microscope settings and all subsequent treatments of images were used between control and experimental samples to allow comparison. Mean

fluorescence intensity of average Z-projections was measured using Fiji software (NIH) and data were normalized with respect to control animals (fed state). Using Microsoft Excel, average values and SEM were calculated and Student's t-test analysis was carried out for statistical significance. To quantify GFP intensity levels of fat body cells carrying distinct 3'UTR-sensors, confocal sections covering the entire nuclei were taken from 10 FBs and a total of at least 100 nuclei per genotype and condition were analyzed. To quantify Dilp2 intensity levels in larval brains, confocal sections covering the IPCs were obtained for at least 20 brains per condition.

Sequence analysis

The search for putative miRNAs binding sites in the 3'UTR of *dp53* was done using three online progams:

- TargetScanFly: http://www.targetscan.org/fly_12/
- MicroCosm Targets: http://www.ebi.ac.uk/enright-srv/microcosm/htdocs/targets/v5/
- RNAhybrid: http://bibiserv.techfak.uni-bielefeld.de/rnahybrid/submission.html

Analysis of sequence conservation was realized thanks to the UCSC-genome browser: http://genome.ucsc.edu/cgi-bin/hgBlat.

Transfection and Luciferase assay in S2 cells

Luciferase assays were performed by co-transfecting S2 cells growing in SFM with the dp53-luciferase reporter plasmids, the RLuc (a renilla transfection control) plasmid and the corresponding pAc5.1-miRNAs overexpression plasmid, or with the empty vector (pAC5.1) as a control.

The transfection was performed in a 24 well plate, in triplicates for each condition. 10^6 cells were plated per well in 100µl of medium without serum directly on each well before transfection. For each triplicate, DNAs were mixed in 150µl of medium without serum, and 21µl of the transfection reagent Insectogene (7µl/well; Biontex Laboratories) were mixed to 150µl of medium without serum. The 150µl of medium+DNAs from each sample were added to the 150µl of medium+Insectogene and mixed well. The mixes were left standing for 30 min and 100µl of the mix were added to each well. The transfection was left to proceed for 6 hours before adding 800µl of complete medium to each well. Luciferase assays were performed 24 h after transfection following the manufacturer's instructions (Dual-Glo Luciferase

Assay System, Promega). Changes in luciferase activity were normalized to a co-transfected renilla luciferase (RLuc) control, and experimental samples were normalized to the levels of the control dp53-luciferase construct containing only the empty vector.

Protein extraction and Western Blot

Five third-instar larvae (full) or wing discs from 20 third-instar larvae (depending on the experiment) were collected/dissected in PBS on ice, homogenized in RIPA buffer (50mM Tris pH 7.5, 150 mM NaCl, 1% SDS, 0.5% Na-deoxycholate, 1% Triton X-100, 1 mM PMSF) supplemented with a protease inhibitor cocktail and centrifuged for 30 min. The samples were separated on 12% SDS PAGE and blotted on PVDF membranes. The membranes were probed with 1:2000 rabbit anti-GFP antibody and 1:5000 mouse anti-α-tubulin antibody (as a loading control), followed by fluorescence-conjugated secondary antibodies (ALEXA mouse-680, Invitrogen and ALEXA rabbit-800, Rockland) and detected by an infrared imaging system, ODYSSEY (LI-COR).

RNA extraction and quantitative Real Time PCR

- **RNA extraction**

Depending of the experiment, RNA was extracted from: the fat body of 10 mid third-instar larvae, the 'empty' abdomens of 10 adult males (only carcasses and FB adhered to it), 5 decapitated adult males or 6 adult males heads. Three samples per genotype and condition were always collected and the protocol for RNA extraction was the following:

- Homogenize samples in 500µl of Trizol, add 3,3µl of PelletPaint (Novagen). Incubate 5 min at room temperature, add 100µl chloroform. Shake vigorously for 15 sec, and incubate 5 min at room temperature.
- Centrifuge 15 min at 4° C, max speed. Carefully transfer supernatant (180-200µl) into a new tube. Do not touch the interphase.
- Add 1 volume isopropanol (180-200µl), shake vigorously, and incubate 5 min on ice.
- Centrifuge 30 min at 4° C, full speed. Do not disturb the pellet after centrifugation.
- Carefully remove supernatant. Wash with 300µl 75% EtOH by vortexing.
- Centrifuge 10 min at 4° C, max speed. Do not disturb the pellet after centrifugation.

- Carefully remove supernatant immediately and completely by pipetting.
- Add 100µl of water and incubate 10 min at room temperature. Vortex for 1 min, add 10µl of 3M NaAc (comes with PelletPaint), vortex. Add 250µl icecold EtOH and incubate 1 hour at -20° C. The re-precipitation described here is mandatory to remove remaining phenol.
- Centrifuge 30 min at 4° C, full speed. Do not disturb the pellet after centrifugation.
- Carefully remove supernatant. Wash with 300µl 75% EtOH by vortexing.
- Centrifuge 10 min at 4° C, max speed. Do not disturb the pellet after centrifugation.
- Carefully remove supernatant immediately and completely by pipetting. Let the pellet dry for 5 min at room temperature in the open tube.
- Add 20µl of commercial RNase free water (neither milliQ, nor DEPC-treated water) without pipetting. Leave 5 min at RT. Vortex 1 min, spin down briefly. Pipet up and down, spin down quickly and quantify by Nanodrop

♦ **Quantification of mRNA levels**

For quantification of mRNA levels, 1 to 5 µg of total RNA was treated with DNAse (Thermo Scientific) and used as a template for cDNA synthesis, using the Maxima Reverse Transcriptase (Thermo Scientific) and oligo-dT (Invitrogen) according to manufacturer's protocol. Quantitative Real time PCR was performed using Maxima SYBR Green/ROX qPCR Master Mix (Thermo Scientific) according to manufacturer's protocol (final reaction volume of 12,5 µl) and reactions were run in a Light Cycler® 480 Real Time qPCR machine (Roche). Transcript levels were normalized to Tubulin. Three independent samples were collected from each condition and genotype, and duplicate measurements were conducted. All the primer pairs used are tabulated in Table 2.

♦ **Quantification of mature miRNA levels**

For quantification of mature miRNA levels, 10 ng of RNA were used as a template for miRNA-specific cDNA synthesis (Applied Biosystems). miRNAs were quantified using TaqMan miRNA Assays (Applied Biosystems) and reactions were run in a Light Cycler® 480 Real Time qPCR machine (Roche) according to manufacturer's protocol. Snor442 and U27 were used for normalization. Three independent samples were collected from each condition and genotype, and duplicate measurements were conducted.

Gene/transcript	Annotation symbol	Primer pair used for qRT-PCR
AKH	CG1171	F: ATGAATCCCAAGAGCGAAGTCCTC R: CTACTCGCGGTGCTTGCAGTCCAG
INR	CG18402	F: GCTGTCAAGCAAGCAGTGAA R: TCTTTTTACCCGTCGTCTCC
4EBP	CG8846	F: AACCCTCTACTCCACCACTC R: CAATCTTCAGCGACTTGG
DP53	CG33336	F: GTCCGCTGTCAAAATCACCT R: TTTCTTTTCGCCCGATACAC
FAS	CG3523	F: CGGAGAAGAGTTACATCCTG R: CAATCACCACCTTTACGC
MDY	CG31991	F: CTCTTTAGTGCATATCTCGCTCTG R: AACAAGCCCAAGCCCTCT
BMM	CG5295	F: TCCCGAGTTTCTGTCCAAGT R: GCGTCCTTTCTGTGCTTCTT
CG5966 (lipase)	CG5966	F: CTCGCAGTGTCCTTTCCTTG R: TGCTCCTGGTAATCCTCCTG
LPIN	CG8709	F: CTCGGCGGCTATCAAAAA R: ACCTTGTCGTTGTGCTTCCA
UGP	CG4347	F: AACAACATTTGGGCCAACC R: TCCATGTTTAAGGTACGCTCAC
PYK	CG7070	F: CGAACAGATCGCCGGACGCA R: TGACAGTAAAGGTGAACTCGCGG
PGM	CG5165	F: AACTGGCTCCAATCACATCC R: AGCGCACTCCTCATAATCGT
HEX-C	CG8094	F: CACTGGCACCTTGATGTCCT R: GTCCAACTGACCACCCTCAC
TRE T1	CG30035	F: TTGAGGTCACCCAAGATGCT R: AAGGGTCCTCCGGCTATG
GLU T1	CG43946	F: TCTCGGATTCGTCGTCTTCT R: TGAACGGCAAGAACGTGTAG

Gene/transcript	Annotation symbol	Primer pair used for qRT-PCR
PDH	CG7010	F: GCAAGGGCGTCAATCACTAA R: TTCTACGGGGTTCTCATCGT
ACOT	CG4581	F: GAAGAACAGCCAGAATATCG R: CACGATGTAGTCGATGAGC
SCOX	CG8885	F: CTCCCGCAGATTCCACTAAA R: TCCTTCATTCTCGCCTCATC
GLS	CG42708	F: CGAGACGGGTTCTTCGGCGG R: CGTGCAGATGCTCAGGCCCC
DCR-1	CG4792	F: CATTGCGTTCACCTCCAAG R: TACTGCCGCTCGTTAGCATT
DROSHA	CG8730	F: TTTCACCCACTTGACCCTTG R: ATTCCCAAATCATCGCAAAC
AGO1	CG6671	F: ATGGAAACCGAACCAAACCT R: GCGGCAGATACCCTATGATG
PRI-MIR-305	CR43032	F: ATCAGGTGCTCTGGTGTGTCT R: CTTGTATCGGTCGCTTTCGT
PRI-MIR-2a	CR42899	F: ATTATGTGGCGGGAGGTATT R: TGGGCTCTCAAAGTGGTTGT
PRI-MIR-8	CR42988	F: TCTTACCGGGCAGCATTAGA R: AAGGTTAAGGACACGGACGA
PRI-MIR-79	CR43019	F: AGCTGACTTGCCATTGCTTT R: TTGTTTCTGACGATTGACCTG
PRI-MIR-184	CR42925	F: TCAGTTCTCCGTCCAGTTGTC R: AGAAAAGTGTGCAAATCAGTGG
PRI-MIR-279	CR43015	F: GGACTGGAGCTGGAATTGG R: CGAATGAAGTACACGCGAAG
PRI-MIR-306	CR42914	F: AAACCCTGGATCACAAATGG R: CAGCACAGGCACAGAGTGA
PRI-BANTAM	CR43018	F: GAAAAACGGAAAACGAACGA R: ACCATCGGAATGTGGAATGT

Table 2: List of primers used

Table compiling the list of primers used for expression analyses and the corresponding gene names and annotation symbols. All primers were synthetized by Life technologies.

Metabolic Assays

TAG, glycogen and trehalose levels were adapted from *(Palanker et al., 2009; Sieber and Thummel, 2009)*. For all measurements 5-6 days old males were used and five replicates for each genotype and condition were performed. To avoid possible interference of eye pigment in the colorimetric quantifications the head of the adult flies was pull out. Quantifications were done using a XFluor4 Safire II spectrophotometer plate reader (TECAN). Data were normalized with respect to the corresponding levels in control flies.

Colorimetric-based methods were used to measure all metabolites. Overall quantification of TAG was performed using a coupled colorimetric assay that detects free glycerol levels after cleaving TAG with lipoprotein lipase. Quantification of both glycogen and trehalose levels rely on a colorimetric-based enzymatic assay that, after treatment with amyloglucosidase and trehalase respectively, detect free

glucose levels. This method employs Glucose Oxidase (GO) activity to catalyze the oxidation of glucose to hydrogen peroxide and gluconic acid. Subsequently, the hydrogen peroxide and an added compound (o-dianisidine) react to produce and oxidized form of the compound in the presense of peroxidase.

- **TAG assay**

For TAG assays, 5 adult males were quick frozen in liquid nitrogen and homogenized in 200 μl of PBST (PBS, 0.1% Tween 20) and immediately heated for 5 min at 70° C to inactivate endogenous enzymes. Twenty μl of heat-treated homogenate was incubated with 20 μl of Triglyceride Reagent (Sigma, T2449) or PBS for 30 min at 37ºC. Samples were centrifuged, and 30 μl of supernatant was transferred to a 96-well plate. One hundred microliters of Free Glycerol Reagent (Sigma) was added and incubated for 5 min at 37° C. Absorbance was measured at 540 nm. Glycerol amounts were determined using a standard curve, and TAG was determined by subtracting from the total amount of glycerol present in the sample treated with Triglyceride Reagent the amount of free glycerol in the PBS-treated samples and normalized to protein concentration (BioRad).

- **Glycogen assay**

For glycogen assays, 5 adult males were quick frozen in liquid nitrogen, homogenized in 200 μl of PBS and immediately heated for 5 min at 70° C to inactivate endogenous enzymes. Fourty μl of heat-treated homogenate was incubated with or without 1 unit of amiloglucosidase (Sigma) for 2 h at 37° C. Samples were centrifuged and the supernatant was diluted 1:10 with PBS, then 30 μl of diluted supernatant was transferred to a 96-well plate. Glucose assay was performed by adding 100 μl of Glucose Reagent (Sigma) and the plate was incubated 30 min at 37° C. The reaction was stopped by adding 100 μl of 12 N H_2SO_4 (the samples should visibly change color from yellow/orange to pink). Absorbance was assessed at 540 nm. Glucose amounts were determined using a standard curve, and glycogen amounts were determined by subtracting from the total amount of glucose present in the sample treated with amiloglucosidase the amount of free glucose of untreated samples and normalized to protein concentration (BioRad).

- **Trehalose assay and hemolymph extraction**

For trehalose assay in total bodies, 5 adult males were quick frozen in liquid nitrogen, homogenized in 200 μl of trehalase buffer [TB: 5mM Tris pH 6.6, 137 mM NaCl, 2.7 mM KCl, (Teleman et al., 2005)] and

immediately heated for 5 min at 70 °C to inactivate endogenous enzymes. For quantification of sugars in circulation, hemolymph was pooled from 40–45 adult flies (see the protocol below), diluted 1:100 and incubated at 70 °C for 5 min. Trehalose was converted into glucose by incubating 40 μl of heat-treated homogenate with 0.05 units.ml^{-1} of porcine trehalase (Sigma) at 37 °C overnight. Samples were centrifuged for 5 minutes and 30 μl of supernatant was transferred to a 96-well plate. Glucose assay was performed by adding 100 μl of Glucose Reagent (Sigma) and the plate was incubated 30 min at 37 °C. The reaction was stopped by adding 100 μl of 12 N H_2SO_4 (the samples should visibly change color from yellow/orange to pink). Absorbance was assessed at 540 nm. Glucose amounts were determined using a standard curve and normalized to protein concentration (BioRad).

- **Hemolymph extraction**

While analysis of whole animal homogenates provides a more general approach for quantifying glucose and trehalose, this method does not distinguish between circulating and stored sugars in the animal. Therefore, hemolymph samples are used to directly assay circulating sugars. We used a protocol based on filtration by centrifugation to collect the hemolymph. Approximately 40-50 adult males carefully punctured in the thorax using a tungsten needle were used. Punctured flies were placed in a 0.5 ml microfuge tube that contains a hole at the bottom of the tube. This tube was placed within a 1.5 ml collection tube and centrifuged at 9000xg for 5 min at 4 °C to collect approximately 1 to 1.5 μl of hemolymph. Finally, 1 μl of the collected hemolymph was diluted 1:100 in trehalase buffer and immediately incubated at 70ºC for 5 min to inactivate endogenous trehalase before the assay.

3. **Treatments**

Irradiation treatments

Irradiations (IR) were carried out in an YXLON MaxiShot X-ray system at the standard dose of 40 Gy. Larvae were grown in non-over-crowding conditions and early third-instar larvae (72 h AEL) were irradiated for collections 48-96 h after IR treatment or late third-instar larvae (120 h AEL) were irradiated for collections 5-24 h after IR treatment.

Starvation treatments

Our standard food composition is: 4% glucose, 55 g/L yeast, 0,65% agar, 28 g/L wheat flour, 4 ml/L propionic acid and 1,1 g/L nipagin). All starvation procedures were adapted *from (Géminard et al., 2009; Palanker et al., 2009; Rajan and Perrimon, 2012)*. Starvation provides an important dietary stress that tests the animal's ability to mobilize stored nutrients for survival.

- **Starvation sensitivity assays**

For starvation sensitivity assays in adults, 1- to 2-days old flies (males or females, depending on the experiment) were commonly used. To discard possible effects of fat-body remodeling during metamorphosis and young adult flies, in Figure 6A and B starvation sensitivity was done using 5- to 7-days old flies and the results obtained were the same. Starvation sensitivity assays were conducted in animals developed in non-over-crowding conditions by transferring 15-20 flies of each genotype into vials containing 2% agar and 0%, 1% or 10% sucrose, depending on the experiment. Flies were transferred to new tubes every day and dead flies were counted every six hours (in experiments of complete starvation with 2% agar and 0%) or daily (in experiments with 1% or 10% sucrose).

For starvation sensitivity studies in larvae, eggs were collected for 3 h intervals, and larvae were raised at 25° C for 48-51 h prior to the starvation assay. Early second instar larvae were washed with water and placed in an inverted 55mm petri dish with two pieces of Whatman filter and soaked with 1 ml PBS 1X. Each plate was sealed with parafilm and incubated at 25° C for the duration of the experiment. Animals were scored for viability every 6 h and dead larvae were removed.

At least 100 individuals per genotype were scored. Control animals were always analyzed in parallel in each experimental condition. Statistics were performed using Graphpad Prism 4.0 software which uses the Kaplan–Meier estimator to calculate survival fractions as well as median and maximum survival values. The Log-rank (Mantel–Cox) test was used to compare the survival distributions of control and experimental conditions at each observed event time. Accordingly, the two-tailed p-value indicates the value of the difference between the two entire survival distributions at comparison.

For the long-term effect of chronic starvation sensitivity, eggs were collected for 3h interval and larvae were raised on either standard food (Std food) or diluted food (0,2X food) immediately after eclosion. Survival rates were measured as the percent of individuals entering pupariation or giving rise to

adult flies. At least 120 larvae per each genotype were scored. Data were normalized with respect to the standard food values and Student's t-test analysis was carried out for statistical significance.

- **Starvation treatments**

For starvation treatments in adults, 5- to 7-days old flies were used and subjected to 24 h (for glycogen and trehalose measurements, as well as for expression analysis) or 72 h (for TAG measurements) of starvation in 2% agar 1% sucrose.

For starvation treatments in larvae, animals were synchronized in the second to third larval transition and 6 h later were shifted on agar plates containing PBS/1% sucrose (starvation) or standard food (fed). After 24-48 h, FBs were dissected in PBS and used for immunohistochemistry or RNA extraction.

BiBLioGRaPhy

BIBLIOGRAPHY

Adams, M. D. (2000). The Genome Sequence of Drosophila melanogaster. *Science (80-.).* **287**, 2185–2195.

Akdemir, F., Christich, a, Sogame, N., Chapo, J. and Abrams, J. M. (2007). p53 directs focused genomic responses in Drosophila. *Oncogene* **26**, 5184–93.

Allton, K., Jain, A. K., Herz, H.-M., Tsai, W.-W., Jung, S. Y., Qin, J., Bergmann, A., Johnson, R. L. and Barton, M. C. (2009). Trim24 targets endogenous p53 for degradation. *Proc. Natl. Acad. Sci. U. S. A.* **106**, 11612–6.

Aloni-Grinstein, R., Shetzer, Y., Kaufman, T. and Rotter, V. (2014). p53: The barrier to cancer stem cell formation. *FEBS Lett.*

Ambros, V. (2003). MicroRNA pathways in flies and worms: growth, death, fat, stress, and timing. *Cell* **113**, 673–6.

Amoyel, M. and Bach, E. a (2014). Cell competition: how to eliminate your neighbours. *Development* **141**, 988–1000.

Anderson, R. M. (2012). A role for dicer in aging and stress survival. *Cell Metab.* **16**, 285–6.

Arrese, E. and Soulages, J. (2010). Insect fat body: energy, metabolism, and regulation. *Annu. Rev. Entomol.* 207–225.

Asano, M. and Wharton, R. P. (1999). E2F mediates developmental and cell cycle regulation of ORC1 in Drosophila. *EMBO J.* **18**, 2435–48.

Assaily, W., Rubinger, D. a, Wheaton, K., Lin, Y., Ma, W., Xuan, W., Brown-Endres, L., Tsuchihara, K., Mak, T. W. and Benchimol, S. (2011). ROS-mediated p53 induction of Lpin1 regulates fatty acid oxidation in response to nutritional stress. *Mol. Cell* **44**, 491–501.

Bai, H., Kang, P. and Tatar, M. (2012). Drosophila insulin-like peptide-6 (dilp6) expression from fat body extends lifespan and represses secretion of Drosophila insulin-like peptide-2 from the brain. *Aging Cell* **11**, 978–85.

Balaburski, G. M., Hontz, R. D. and Murphy, M. E. (2010). p53 and ARF: unexpected players in autophagy. *Trends Cell Biol.* **20**, 363–9.

Banerjee, K. K., Ayyub, C., Sengupta, S. and Kolthur-Seetharam, U. (2012). dSir2 deficiency in the fatbody, but not muscles, affects systemic insulin signaling, fat mobilization and starvation survival in flies. *Aging (Albany. NY).* **4**, 206–23.

Barrio, R. and de Celis, J. F. (2004). Regulation of spalt expression in the Drosophila wing blade in response to the Decapentaplegic signaling pathway. *Proc Natl Acad Sci U S A* **101**, 6021–6026.

Bauer, J. H., Poon, P. C., Glatt-Deeley, H., Abrams, J. M. and Helfand, S. L. (2005). Neuronal expression of p53 dominant-negative proteins in adult Drosophila melanogaster extends life span. *Curr. Biol.* **15**, 2063–8.

Bauer, J. H., Chang, C., Morris, S. N. S., Hozier, S., Andersen, S., Waitzman, J. S. and Helfand, S. L. (2007). Expression of dominant-negative Dmp53 in the adult fly brain inhibits insulin signaling. *Proc. Natl. Acad. Sci. U. S. A.* **104**, 13355–60.

Bauer, H., Nur, S., Morris, S., Chang, C., Flatt, T., Wood, J. G. and Helfand, L. (2009). dSir2 and Dmp53 interact to mediate aspects of CR-dependent lifespan extension in D. melanogaster. **1**, 1–11.

Bauer, J., Chang, C. and Bae, G. (2010). Dominant-negative Dmp53 extends life span through the dTOR pathway in D. melanogaster. *Mech. ageing …* **131**, 193–201.

Becam, I., Rafel, N., Hong, X., Cohen, S. M. and Milán, M. (2011). Notch-mediated repression of bantam miRNA contributes to boundary formation in the Drosophila wing. *Development* **138**, 3781–9.

Bejarano, F., Smibert, P. and Lai, E. C. (2010). miR-9a prevents apoptosis during wing development by repressing Drosophila LIM-only. *Dev. Biol.* **338**, 63–73.

Beller, M., Bulankina, A. V, Hsiao, H.-H., Urlaub, H., Jäckle, H. and Kühnlein, R. P. (2010). PERILIPIN-dependent control of lipid droplet structure and fat storage in Drosophila. *Cell Metab.* **12**, 521–32.

Belyi, V. a, Ak, P., Markert, E., Wang, H., Hu, W., Puzio-Kuter, A. and Levine, A. J. (2010). The origins and evolution of the p53 family of genes. *Cold Spring Harb. Perspect. Biol.* **2**, a001198.

Bensaad, K. and Vousden, K. H. (2007). P53: New Roles in Metabolism. *Trends Cell Biol.* **17**, 286–91.

Berezikov, E., Chung, W.-J., Willis, J., Cuppen, E. and Lai, E. C. (2007). Mammalian mirtron genes. *Mol. Cell* **28**, 328–36.

Berkers, C. R., Maddocks, O. D. K., Cheung, E. C., Mor, I. and Vousden, K. H. (2013). Metabolic regulation by p53 family members. *Cell Metab.* **18**, 617–33.

Bharucha, K. N., Tarr, P. and Zipursky, S. L. (2008). A glucagon-like endocrine pathway in Drosophila modulates both lipid and carbohydrate homeostasis. *J. Exp. Biol.* **211**, 3103–10.

Bhattacharyya, S. N., Habermacher, R., Martine, U., Closs, E. I. and Filipowicz, W. (2006). Stress-induced reversal of microRNA repression and mRNA P-body localization in human cells. *Cold Spring Harb. Symp. Quant. Biol.* **71**, 513–21.

Birse, R., Choi, J., Reardon, K. and Rodriguez, J. (2010). High-Fat-Diet-Induced Obesity and Heart Dysfunction Are Regulated by the TOR Pathway in Drosophila. *Cell Metab.* **12**, 533–544.

Biteau, B. and Jasper, H. (2009). It's all about balance: p53 and aging. *Aging (Albany. NY).* **1**, 884–886.

Blandino, G., Valerio, M., Cioce, M., Mori, F., Casadei, L., Pulito, C., Sacconi, A., Biagioni, F., Cortese, G., Galanti, S., et al. (2012). Metformin elicits anticancer effects through the sequential modulation of DICER and c-MYC. *Nat. Commun.* **3**, 865.

Bodai, L., Pardi, N., Ujfaludi, Z., Bereczki, O., Komonyi, O., Balint, E. and Boros, I. M. (2007). Daxx-like protein of Drosophila interacts with Dmp53 and affects longevity and Ark mRNA level. *J. Biol. Chem.* **282**, 36386–93.

Bondar, T. and Medzhitov, R. (2010). P53-Mediated Hematopoietic Stem and Progenitor Cell Competition. *Cell Stem Cell* **6**, 309–22.

Borchert, G. M., Lanier, W. and Davidson, B. L. (2006). RNA polymerase III transcribes human microRNAs. *Nat. Struct. Mol. Biol.* **13**, 1097–101.

Boulan, L., Martín, D. and Milán, M. (2013). bantam miRNA promotes systemic growth by connecting insulin signaling and ecdysone production. *Curr. Biol.* **23**, 473–8.

Braco, J. T., Gillespie, E. L., Alberto, G. E., Brenman, J. E. and Johnson, E. C. (2012). Energy-dependent modulation of glucagon-like signaling in Drosophila via the AMP-activated protein kinase. *Genetics* **192**, 457–66.

Brand, a H. and Perrimon, N. (1993). Targeted gene expression as a means of altering cell fates and generating dominant phenotypes. *Development* **118**, 401–15.

Brennecke, J., Hipfner, D. R., Stark, A., Russell, R. B. and Cohen, S. M. (2003). bantam encodes a developmentally regulated microRNA that controls cell proliferation and regulates the proapoptotic gene hid in Drosophila. *Cell* **113**, 25–36.

Brodsky, M. H., Nordstrom, W., Tsang, G., Kwan, E., Rubin, G. M. and Abrams, J. M. (2000). Drosophila p53 binds a damage response element at the reaper locus. *Cell* **101**, 103–13.

Brodsky, M. H., Weinert, B. T., Tsang, G., Rong, Y. S., Mcginnis, N. M., Golic, K. G., Rio, D. C. and Rubin, G. M. (2004). Drosophila melanogaster MNK / Chk2 and p53 Regulate Multiple DNA Repair and Apoptotic Pathways following DNA Damage. *Society* **24**, 1219–1231.

Bryk, B., Hahn, K., Cohen, S. M. and Teleman, A. A. (2010). MAP4K3 regulates body size and metabolism in Drosophila. *Dev. Biol.* **344**, 150–157.

Buch, S., Melcher, C., Bauer, M., Katzenberger, J. and Pankratz, M. J. (2008). Opposing effects of dietary protein and sugar regulate a transcriptional target of Drosophila insulin-like peptide signaling. *Cell Metab.* **7**, 321–32.

Budanov, A. V and Karin, M. (2008). p53 target genes sestrin1 and sestrin2 connect genotoxic stress and mTOR signaling. *Cell* **134**, 451–60.

Bülow, M. H., Aebersold, R., Pankratz, M. J. and Jünger, M. a (2010). The Drosophila FoxA ortholog Fork head regulates growth and gene expression downstream of Target of rapamycin. *PLoS One* **5**, e15171.

Cairns, R. a, Harris, I., McCracken, S. and Mak, T. W. (2011). Cancer cell metabolism. *Cold Spring Harb. Symp. Quant. Biol.* **76**, 299–311.

Canavoso, L. E., Jouni, Z. E., Karnas, K. J., Pennington, J. E. and Wells, M. A. (2001). Fat metabolism in insects. *Annu. Rev. Nutr.* **21**, 23–46.

Carrer, M., Liu, N., Grueter, C. E., Williams, A. H., Frisard, M. I. and Hulver, M. W. (2012). Control of mitochondrial metabolism and systemic energy homeostasis by microRNAs 378 and 378 *.

Carthew, R. W. and Sontheimer, E. J. (2009). Origins and Mechanisms of miRNAs and siRNAs. *Cell* **136**, 642–55.

Caygill, E. E. and Johnston, L. a (2008). Temporal regulation of metamorphic processes in Drosophila by the let-7 and miR-125 heterochronic microRNAs. *Curr. Biol.* **18**, 943–50.

Cayirlioglu, P., Kadow, I. G., Zhan, X., Okamura, K., Suh, G. S. B., Gunning, D., Lai, E. C. and Zipursky, S. L. (2008). Hybrid neurons in a microRNA mutant are putative evolutionary intermediates in insect CO2 sensory systems. *Science* **319**, 1256–60.

Ceddia, R. B., Bikopoulos, G. J., Hilliker, A. J. and Sweeney, G. (2003). Insulin stimulates glucose metabolism via the pentose phosphate pathway in Drosophila Kc cells. *FEBS Lett.* **555**, 307–310.

Chang, T.-C., Yu, D., Lee, Y.-S., Wentzel, E. a, Arking, D. E., West, K. M., Dang, C. V, Thomas-Tikhonenko, A. and Mendell, J. T. (2008). Widespread microRNA repression by Myc contributes to tumorigenesis. *Nat. Genet.* **40**, 43–50.

Chen, S., Wei, H.-M., Lv, W.-W., Wang, D.-L. and Sun, F.-L. (2011). E2 ligase dRad6 regulates DMP53 turnover in Drosophila. *J. Biol. Chem.* **286**, 9020–30.

Chivukula, R. R. and Mendell, J. T. (2008). Circular reasoning: microRNAs and cell-cycle control. *Trends Biochem. Sci.* **33**, 474–81.

Clancy, D. J., Gems, D., Harshman, L., Oldham, S., Stocker, H., Hafen, E., Leevers, S. J. and Partridge, L. (2001). Extension of life-span by loss of CHICO, a Drosophila insulin receptor substrate protein. *Science (80-.).* **292**, 104–6.

Cohen, S. M., Brennecke, J. and Stark, A. (2006). Denoising feedback loops by thresholding--a new role for microRNAs. *Genes Dev.* **20**, 2769–72.

Colombani, J., Raisin, S., Pantalacci, S., Radimerski, T., Montagne, J. and Leopold, P. (2003). A Nutrient Sensor Mechanism Controls Drosophila Growth. *Cell* **114**, 739–749.

Colombani, J., Polesello, C., Josué, F. and Tapon, N. (2006). Dmp53 activates the Hippo pathway to promote cell death in response to DNA damage. *Curr. Biol.* **16**, 1453–8.

Cova, C. de la, Abril, M., Bellosta, P., Gallant, P. and Johnston, L. A. (2004). Drosophila Myc Regulates Organ Size by Inducing Cell Competition. *Cell* **117**, 107–116.

Crighton, D., Wilkinson, S., O'Prey, J., Syed, N., Smith, P., Harrison, P. R., Gasco, M., Garrone, O., Crook, T. and Ryan, K. M. (2006). DRAM, a p53-induced modulator of autophagy, is critical for apoptosis. *Cell* **126**, 121–34.

Dai, C. and Gu, W. (2010). P53 Post-Translational Modification: Deregulated in Tumorigenesis. *Trends Mol. Med.* **16**, 528–36.

De Beco, S., Ziosi, M. and Johnston, L. a (2012). New frontiers in cell competition. *Dev. Dyn.* **241**, 831–41.

De la Cova, C., Senoo-Matsuda, N., Ziosi, M., Wu, D. C., Bellosta, P., Quinzii, C. M. and Johnston, L. a (2014). Supercompetitor status of Drosophila Myc cells requires p53 as a fitness sensor to reprogram metabolism and promote viability. *Cell Metab.* **19**, 470–83.

De Lella Ezcurra, A. L., Bertolin, A. P., Melani, M. and Wappner, P. (2012). Robustness of the hypoxic response: another job for miRNAs? *Dev. Dyn.* **241**, 1842–8.

De Virgilio, C. and Loewith, R. (2006). The TOR signalling network from yeast to man. *Int. J. Biochem. cell Biol.* **38**, 1476–1481.

DeBerardinis, R. J., Lum, J. J., Hatzivassiliou, G. and Thompson, C. B. (2008). The biology of cancer: metabolic reprogramming fuels cell growth and proliferation. *Cell Metab.* **7**, 11–20.

Dekanty, A., Barrio, L., Muzzopappa, M., Auer, H. and Milán, M. (2012). Aneuploidy-induced delaminating cells drive tumorigenesis in Drosophila epithelia. *Proc. Natl. Acad. Sci. U. S. A.* **109**, 20549–54.

Demontis, F. and Perrimon, N. (2010). FOXO/4E-BP signaling in Drosophila muscles regulates organism-wide proteostasis during aging. *Cell* **143**, 813–25.

Deng, C., Zhang, P., Harper, J. W., Elledge, S. J. and Leder, P. (1995). Mice Lacking p21 c ~ P7 / wAF7 Undergo Normal Development , in Gl Checkpoint Control but Are Defective. **82**, 875–884.

Di Leva, G., Garofalo, M. and Croce, C. M. (2014). MicroRNAs in cancer. *Annu. Rev. Pathol.* **9**, 287–314.

Dichtel-Danjoy, M.-L., Ma, D., Dourlen, P., Chatelain, G., Napoletano, F., Robin, M., Corbet, M., Levet, C., Hafsi, H., Hainaut, P., et al. (2013). Drosophila p53 isoforms differentially regulate apoptosis and apoptosis-induced proliferation. *Cell Death Differ.* **20**, 108–16.

Donehower, L. a (2009). Longevity regulation in flies: a role for p53. *Aging (Albany. NY).* **1**, 6–8.

Dong, J. and Pan, D. (2004). Tsc2 is not a critical target of Akt during normal Drosophila development. *Genes Dev.* **18**, 2479–84.

Dumortier, O., Hinault, C. and Van Obberghen, E. (2013). MicroRNAs and metabolism crosstalk in energy homeostasis. *Cell Metab.* **18**, 312–24.

Dynlacht, B. D., Brook, a, Dembski, M., Yenush, L. and Dyson, N. (1994). DNA-binding and trans-activation properties of Drosophila E2F and DP proteins. *Proc. Natl. Acad. Sci. U. S. A.* **91**, 6359–63.

Eulalio, A., Rehwinkel, J., Stricker, M., Huntzinger, E., Yang, S., Doerks, T., Dorner, S., Bork, P., Boutros, M. and Izaurralde, E. (2007a). Target-specific requirements for enhancers of decapping in miRNA-mediated gene silencing. **54**, 2558–2570.

Eulalio, A., Behm-Ansmant, I. and Izaurralde, E. (2007b). P bodies: at the crossroads of post-transcriptional pathways. *Nat. Rev. Mol. Cell Biol.* **8**, 9–22.

Eulalio, A., Huntzinger, E. and Izaurralde, E. (2008). Getting to the root of miRNA-mediated gene silencing. *Cell* **132**, 9–14.

Fan, Y., Lee, T. V, Xu, D., Chen, Z., Lamblin, a-F., Steller, H. and Bergmann, a (2010). Dual roles of Drosophila p53 in cell death and cell differentiation. *Cell Death Differ.* **17**, 912–21.

Fan, Y., Yin, S., Hao, Y., Yang, J., Zhang, H., Sun, C., Ma, M., Chang, Q. and Xi, J. (2014). miR-19b promotes tumor growth and metastasis via targeting TP53. *RNA* **20**, 765–72.

Farh, K. K.-H., Grimson, A., Jan, C., Lewis, B. P., Johnston, W. K., Lim, L. P., Burge, C. B. and Bartel, D. P. (2005). The widespread impact of mammalian MicroRNAs on mRNA repression and evolution. *Science* **310**, 1817–21.

Feng, Z., Hu, W., de Stanchina, E., Teresky, A. K., Jin, S., Lowe, S. and Levine, A. J. (2007). The regulation of AMPK beta1, TSC2, and PTEN expression by p53: stress, cell and tissue specificity, and the role of these gene products in modulating the IGF-1-AKT-mTOR pathways. *Cancer Res.* **67**, 3043–53.

Feng, Z., Zhang, C., Wu, R. and Hu, W. (2011). Tumor suppressor p53 meets microRNAs. *J. Mol. Cell Biol.* **3**, 44–50.

Filipowicz, W., Bhattacharyya, S. N. and Sonenberg, N. (2008). Mechanisms of post-transcriptional regulation by microRNAs: are the answers in sight? *Nat. Rev. Genet.* **9**, 102–14.

Forman, J. J. and Coller, H. A. (2010). MicroRNAs target coding regions. 1533–1541.

Foulkes, W. D. (2007). P53--Master and Commander. *N. Engl. J. Med.* **357**, 2539–41.

Friedman, R. C., Farh, K. K.-H., Burge, C. B. and Bartel, D. P. (2009). Most mammalian mRNAs are conserved targets of microRNAs. *Genome Res.* **19**, 92–105.

Fullaondo, A. and Lee, S. Y. (2012). Identification of putative miRNA involved in Drosophila melanogaster immune response. *Dev. Comp. Immunol.* **36**, 267–73.

Garcia-Bellido, A. (1975). Genetic control of wing disc development in Drosophila. *Ciba Found Symp* **0**, 161–82.

Garcia-Bellido, A. and Merriam, J. (1971). Parameters of the wing imaginal disc development of Drosophila melanogaster. *Dev. Biol.*

Garcia-Bellido, A., Ripoll, P. and Morata, G. (1973). Developmental compartimentalisation of the wing disk of Drosophila. *Nat New Biol* **245**, 251–3.

García-Segura, L., Pérez-Andrade, M. and Miranda-Ríos, J. (2013). The emerging role of MicroRNAs in the regulation of gene expression by nutrients. *J. Nutrigenet. Nutrigenomics* **6**, 16–31.

Garg, D. and Cohen, S. M. (2014). miRNAs and aging: A genetic perspective. *Ageing Res. Rev.* 2010–2015.

Garofalo, R. S. (2002). Genetic analysis of insulin signaling in Drosophila. *Trends Endocrinol. Metab.* **13**, 156–62.

Ge, W., Chen, Y.-W., Weng, R., Lim, S. F., Buescher, M., Zhang, R. and Cohen, S. M. (2012). Overlapping functions of microRNAs in control of apoptosis during Drosophila embryogenesis. *Cell Death Differ.* **19**, 839–46.

Géminard, C., Rulifson, E. J. and Léopold, P. (2009). Remote control of insulin secretion by fat cells in Drosophila. *Cell Metab.* **10**, 199–207.

Gershman, B., Puig, O., Hang, L., Peitzsch, R. M., Tatar, M. and Garofalo, R. S. (2007). High-resolution dynamics of the transcriptional response to nutrition in Drosophila: a key role for dFOXO. *Physiol. Genomics* **29**, 24–34.

Gibbings, D., Mostowy, S., Jay, F., Schwab, Y., Cossart, P. and Voinnet, O. (2012). Selective autophagy degrades DICER and AGO2 and regulates miRNA activity. *Nat. Cell Biol.* **14**, 1314–1321.

Gomes, A. Q., Nolasco, S. and Soares, H. (2013). Non-coding RNAs: multi-tasking molecules in the cell. *Int. J. Mol. Sci.* **14**, 16010–39.

Gostissa, M., Morelli, M., Mantovani, F., Guida, E., Piazza, S., Collavin, L., Brancolini, C., Schneider, C. and Del Sal, G. (2004). The transcriptional repressor hDaxx potentiates p53-dependent apoptosis. *J. Biol. Chem.* **279**, 48013–23.

Gottlieb, E. and Vousden, K. H. (2010). P53 Regulation of Metabolic Pathways. *Cold Spring Harb. Perspect. Biol.* **2**, a001040.

Gowda, P. S., Zhou, F., Chadwell, L. V and McEwen, D. G. (2012). p53 binding prevents phosphatase-mediated inactivation of diphosphorylated c-Jun N-terminal kinase. *J. Biol. Chem.* **287**, 17554–67.

Gregory, R. I., Yan, K.-P., Amuthan, G., Chendrimada, T., Doratotaj, B., Cooch, N. and Shiekhattar, R. (2004). The Microprocessor complex mediates the genesis of microRNAs. *Nature* **432**, 235–40.

Grewal, S. S. (2009). Insulin/TOR signaling in growth and homeostasis: a view from the fly world. *Int. J. Biochem. Cell Biol.* **41**, 1006–10.

Grewal, S. S., Li, L., Orian, A., Eisenman, R. N. and Edgar, B. a (2005). Myc-dependent regulation of ribosomal RNA synthesis during Drosophila development. *Nat. Cell Biol.* **7**, 295–302.

Grewal, S. S., Evans, J. R. and Edgar, B. a (2007). Drosophila TIF-IA is required for ribosome synthesis and cell growth and is regulated by the TOR pathway. *J. Cell Biol.* **179**, 1105–13.

Griffiths-Jones, S., Saini, H. K., van Dongen, S. and Enright, A. J. (2008). miRBase: tools for microRNA genomics. *Nucleic Acids Res.* **36**, D154–8.

Grimson, A., Farh, K. K.-H., Johnston, W. K., Garrett-Engele, P., Lim, L. P. and Bartel, D. P. (2007). MicroRNA targeting specificity in mammals: determinants beyond seed pairing. *Mol. Cell* **27**, 91–105.

Griswold, A. J., Chang, K. T., Runko, A. P., Knight, M. a and Min, K.-T. (2008). Sir2 mediates apoptosis through JNK-dependent pathways in Drosophila. *Proc. Natl. Acad. Sci. U. S. A.* **105**, 8673–8.

Grönke, S., Beller, M. and Fellert, S. (2003). Control of Fat Storage by a Drosophila PAT Domain Protein. *Curr. Biol.* **13**, 603–606.

Grönke, S., Mildner, A., Fellert, S., Tennagels, N., Petry, S., Müller, G., Jäckle, H. and Kühnlein, R. P. (2005). Brummer lipase is an evolutionary conserved fat storage regulator in Drosophila. *Cell Metab.* **1**, 323–30.

Gu, B. and Zhu, W.-G. (2012). Surf the post-translational modification network of p53 regulation. *Int. J. Biol. Sci.* **8**, 672–84.

Gutierrez, E., Wiggins, D., Fielding, B. and Gould, A. P. (2007). Specialized hepatocyte-like cells regulate Drosophila lipid metabolism. **445**, 275–280.

Han, B. W., Hung, J.-H., Weng, Z., Zamore, P. D. and Ameres, S. L. (2011). The 3’-to-5' exoribonuclease Nibbler shapes the 3' ends of microRNAs bound to Drosophila Argonaute1. *Curr. Biol.* **21**, 1878–87.

Hardie, D. G. (2007). AMP-activated/SNF1 protein kinases: conserved guardians of cellular energy. *Nat. Rev. Mol. Cell Biol.* **8**, 774–785.

Hardie, D. G., Ross, F. a and Hawley, S. a (2012). AMPK: a nutrient and energy sensor that maintains energy homeostasis. *Nat. Rev. Mol. Cell Biol.* **13**, 251–62.

Hatfield, S. D., Shcherbata, H. R., Fischer, K. a, Nakahara, K., Carthew, R. W. and Ruohola-Baker, H. (2005). Stem cell division is regulated by the microRNA pathway. *Nature* **435**, 974–8.

Hay, B. a, Wolff, T. and Rubin, G. M. (1994). Expression of baculovirus P35 prevents cell death in Drosophila. *Development* **120**, 2121–9.

Haynie, J. and Bryant, P. (1976). Intercalary regenration in imaginal wing disk of Drosophila melanogaster. *Nature* **259**, 659–62.

Hennig, K. M. and Neufeld, T. P. (2002). Inhibition of cellular growth and proliferation by dTOR overexpression in Drosophila. *Genesis* **34**, 107–10.

Hennig, K., Colombani, J. and Neufeld, T. (2006). TOR coordinates bulk and targeted endocytosis in the Drosophila melanogaster fat body to regulate cell growth. *J. Cell Biol.* **173**, 963–974.

Hermeking, H. (2007). p53 enters the microRNA world. *Cancer Cell* **12**, 414–8.

Hermeking, H. (2012). MicroRNAs in the p53 network: micromanagement of tumour suppression. *Nat. Rev. Cancer* **12**, 613–26.

Herranz, H. and Cohen, S. M. (2010). MicroRNAs and gene regulatory networks: managing the impact of noise in biological systems. *Genes Dev.* **24**, 1339–44.

Herranz, H., Hong, X., Pérez, L., Ferreira, A., Olivieri, D., Cohen, S. M. and Milán, M. (2010). The miRNA machinery targets Mei-P26 and regulates Myc protein levels in the Drosophila wing. *EMBO J.* **29**, 1688–98.

Herranz, H., Hong, X. and Cohen, S. M. (2012a). Mutual repression by bantam miRNA and Capicua links the EGFR/MAPK and Hippo pathways in growth control. *Curr. Biol.* **22**, 651–7.

Herranz, H., Hong, X., Hung, N. T., Voorhoeve, P. M. and Cohen, S. M. (2012b). Oncogenic cooperation between SOCS family proteins and EGFR identified using a Drosophila epithelial transformation model. *Genes Dev.* **26**, 1602–11.

Herrera, S. C. and Morata, G. (2014). Transgressions of compartment boundaries and cell reprogramming during regeneration in Drosophila. 1–15.

Herzog, G., Joerger, A. C., Shmueli, M. D., Fersht, A. R., Gazit, E. and Segal, D. (2012). Evaluating Drosophila p53 as a model system for studying cancer mutations. *J. Biol. Chem.* **287**, 44330–7.

Hietakangas, V. and Cohen, S. M. (2009). Regulation of tissue growth through nutrient sensing. *Annu. Rev. Genet.* **43**, 389–410.

Ho, J. J. D., Metcalf, J. L., Yan, M. S., Turgeon, P. J., Wang, J. J., Chalsev, M., Petruzziello-Pellegrini, T. N., Tsui, A. K. Y., He, J. Z., Dhamko, H., et al. (2012). Functional importance of Dicer protein in the adaptive cellular response to hypoxia. *J. Biol. Chem.* **287**, 29003–20.

Hock, A. and Vousden, K. H. (2010). Regulation of the p53 pathway by ubiquitin and related proteins. *Int. J. Biochem. Cell Biol.* **42**, 1618–21.

Hock, A. K. and Vousden, K. H. (2014). The role of ubiquitin modification in the regulation of p53. *Biochim. Biophys. Acta* **1843**, 137–49.

Hoffmann, J., Romey, R., Fink, C. and Roeder, T. (2013). Drosophila as a Model to Study Metabolic Disorders.

Holz, M. K., Ballif, B. A., Gygi, S. P. and Blenis, J. (2005). mTOR and S6K1 mediate assembly of the translation preinitiation complex through dynamic protein interchange and ordered phosphorylation events. *Cell* **123**, 569–580.

Horn, H. F. and Vousden, K. H. (2007). Coping with stress: multiple ways to activate p53. *Oncogene* **26**, 1306–16.

Hornstein, E. and Shomron, N. (2006). Canalization of development by microRNAs. *Nat. Genet.* **38 Suppl**, S20–4.

Hsu, P. P. and Sabatini, D. M. (2008). Cancer cell metabolism: Warburg and beyond. *Cell* **134**, 703–7.

Hu, W., Chan, C. S., Wu, R., Zhang, C., Sun, Y., Song, J. S., Tang, L. H., Levine, A. J. and Feng, Z. (2010). Negative regulation of tumor suppressor p53 by microRNA miR-504. *Mol. Cell* **38**, 689–99.

Huh, J., Guo, M. and Hay, B. (2004). Proliferation Induced by Cell Death in the Drosophila Wing Disc Requires Activity of the Apical Cell Death Caspase Dronc in a Nonapoptotic Role. *Curr. Biol.* **14**, 1262–1266.

Huntzinger, E. and Izaurralde, E. (2011). Gene silencing by microRNAs: contributions of translational repression and mRNA decay. *Nat. Rev. Genet.*

Hyun, S., Lee, J. H., Jin, H., Nam, J., Namkoong, B., Lee, G., Chung, J. and Kim, V. N. (2009). Conserved MicroRNA miR-8/miR-200 and its target USH/FOG2 control growth by regulating PI3K. *Cell* **139**, 1096–108.

Ikeya, T., Galic, M., Belawat, P., Nairz, K. and Hafen, E. (2002). Nutrient-dependent expression of insulin-like peptides from neuroendocrine cells in the CNS contributes to growth regulation in Drosophila. *Curr. Biol.* **12**, 1293–300.

Inoki, K., Li, Y., Zhu, T., Wu, J. and Guan, K.-L. (2002). TSC2 is phosphorylated and inhibited by Akt and suppresses mTOR signalling. *Nat. Cell Biol.* **4**, 648–57.

Inoki, K., Li, Y., Xu, T. and Guan, K.-L. (2003a). Rheb GTPase is a direct target of TSC2 GAP activity and regulates mTOR signaling. *Genes Dev.* **17**, 1829–1834.

Inoki, K., Zhu, T. and Guan, K.-L. (2003b). TSC2 mediates cellular energy response to control cell growth and survival. *Cell* **115**, 577–90.

Iovino, N., Pane, A. and Gaul, U. (2009). miR-184 has multiple roles in Drosophila female germline development. *Dev. Cell* **17**, 123–33.

Isabel, G., Martin, J.-R., Chidami, S., Veenstra, J. a and Rosay, P. (2005). AKH-producing neuroendocrine cell ablation decreases trehalose and induces behavioral changes in Drosophila. *Am. J. Physiol. Regul. Integr. Comp. Physiol.* **288**, R531–8.

Ishizu, H., Siomi, H. and Siomi, M. C. (2012). Biology of PIWI-interacting RNAs: new insights into biogenesis and function inside and outside of germlines. *Genes Dev.* **26**, 2361–73.

Jackson, S. P. and Bartek, J. (2009). The DNA-damage response in human biology and disease. *Nature* **461**, 1071–8.

Jaklevic, B. R. and Su, T. T. (2004). Relative Contribution of DNA Repair, Cell Cycle Checkpoints, and Cell Death to Survival after DNA Damage in Drosophila Larvae. *Curr. Biol.* **14**, 23–32.

Jaklevic, B., Uyetake, L., Lemstra, W., Chang, J., Leary, W., Edwards, A., Vidwans, S., Sibon, O. and Tin Su, T. (2006). Contribution of growth and cell cycle checkpoints to radiation survival in Drosophila. *Genetics* **174**, 1963–72.

Jassim, O. W., Fink, J. L. and Cagan, R. L. (2003). Dmp53 protects the Drosophila retina during a developmentally regulated DNA damage response. *EMBO J.* **22**, 5622–32.

Jaubert, S., Mereau, A., Antoniewski, C. and Tagu, D. (2007). MicroRNAs in Drosophila: the magic wand to enter the Chamber of Secrets? *Biochimie* **89**, 1211–20.

Jiang, P., Du, W. and Yang, X. (2013). p53 and regulation of tumor metabolism. *J. Carcinog.*

Jin, Z. and Xie, T. (2007). Dcr-1 maintains Drosophila ovarian stem cells. *Curr. Biol.* **17**, 539–44.

Jin, S., Martinek, S., Joo, W. S., Wortman, J. R., Mirkovic, N., Sali, a, Yandell, M. D., Pavletich, N. P., Young, M. W. and Levine, a J. (2000). Identification and characterization of a p53 homologue in Drosophila melanogaster. *Proc. Natl. Acad. Sci. U. S. A.* **97**, 7301–6.

Jin, H., Kim, V. N. and Hyun, S. (2012). Conserved microRNA miR-8 controls body size in response to steroid signaling in Drosophila. *Genes Dev.* **26**, 1427–32.

Johnson, E. C., Kazgan, N., Bretz, C. a, Forsberg, L. J., Hector, C. E., Worthen, R. J., Onyenwoke, R. and Brenman, J. E. (2010). Altered metabolism and persistent starvation behaviors caused by reduced AMPK function in Drosophila. *PLoS One* **5**,.

Johnston, L. a (2009). Competitive interactions between cells: death, growth, and geography. *Science* **324**, 1679–82.

Jones, C. I. and Newbury, S. F. (2010). Functions of microRNAs in Drosophila development. *Biochem. Soc. Trans.* **38**, 1137–43.

Jones, R. G., Plas, D. R., Kubek, S., Buzzai, M., Mu, J., Xu, Y., Birnbaum, M. J. and Thompson, C. B. (2005). AMP-activated protein kinase induces a p53-dependent metabolic checkpoint. *Mol. Cell* **18**, 283–93.

Junger, M. A., Rintelen, F., Stocker, H., Wasserman, J. D., Vegh, M., Radimerski, T., Greenberg, M. E. and Hafen, E. (2003). The Drosophila forkhead transcription factor FOXO mediates the reduction in cell number associated with reduced insulin signaling. *J Biol* **2**, 20.

Kadener, S., Menet, J. S., Sugino, K., Horwich, M. D., Weissbein, U., Nawathean, P., Vagin, V. V, Zamore, P. D., Nelson, S. B. and Rosbash, M. (2009). A role for microRNAs in the Drosophila circadian clock A role for microRNAs in the Drosophila circadian clock. 2179–2191.

Kannan, K. and Fridell, Y.-W. C. (2013). Functional implications of Drosophila insulin-like peptides in metabolism, aging, and dietary restriction. *Front. Physiol.* **4**, 288.

Kaplan, D. D., Zimmermann, G., Suyama, K., Meyer, T. and Scott, M. P. (2008). A nucleostemin family GTPase, NS3, acts in serotonergic neurons to regulate insulin signaling and control body size. *Genes Dev.* **22**, 1877–93.

Karres, J. S., Hilgers, V., Carrera, I., Treisman, J. and Cohen, S. M. (2007). The conserved microRNA miR-8 tunes atrophin levels to prevent neurodegeneration in Drosophila. *Cell* **131**, 136–45.

Kennell, J. a, Gerin, I., MacDougald, O. a and Cadigan, K. M. (2008). The microRNA miR-8 is a conserved negative regulator of Wnt signaling. *Proc. Natl. Acad. Sci. U. S. A.* **105**, 15417–22.

Kheradpour, P., Stark, A., Roy, S. and Kellis, M. (2007). Reliable prediction of regulator targets using 12 Drosophila genomes. *Genome Res.* **17**, 1919–31.

Khoury, M. P. and Bourdon, J.-C. (2010). The Isoforms of the p53 Protein. *Cold Spring Harb. Perspect. Biol.* **2**, a000927.

Kim, S. K. and Rulifson, E. J. (2004). Conserved mechanisms of glucose sensing and regulation by Drosophila corpora cardiaca cells. **431**, 316–320.

Kim, E., Goraksha-Hicks, P., Li, L., Neufeld, T. P. and Guan, K.-L. (2008). Regulation of TORC1 by Rag GTPases in nutrient response. *Nat. Cell Biol.* **10**, 935–945.

Kim, V. N., Han, J. and Siomi, M. C. (2009). Biogenesis of small RNAs in animals. *Nat. Rev. Mol. Cell Biol.* **10**, 126–39.

Kloosterman, W. P. and Plasterk, R. H. a (2006). The diverse functions of microRNAs in animal development and disease. *Dev. Cell* **11**, 441–50.

Kooistra, R., Vreeken, K., Zonneveld, J. B. M., Jong, A., Eeken, J. C. J., Osgood, C. J., Buerstedde, J.-M., Lohman, P. H. M. and Pastink, A. (1997). The Drosophila melanogaster RAD54 homolog, DmRAD54, is involved in the repair of radiation damage and recombination. *Mol. Cell. Biol.* **17**, 6097–6104.

Kraemer, A., Anastasov, N., Angermeier, M., Winkler, K., Michael, J., Moertl, S. and Atkinson, J. (2011). MicroRNA-Mediated Processes are Essential for the Cellular Radiation Response MicroRNA-Mediated Processes are Essential for the Cellular Radiation Response. **176**, 575–586.

Kramer, J. and Davidge, J. (2003). Expression of Drosophila FOXO regulates growth and can phenocopy starvation. *BMC Dev. Biol.* **3**, 5.

Kruse, J.-P. and Gu, W. (2009). Modes of p53 regulation. *Cell* **137**, 609–22.

Krützfeldt, J. and Stoffel, M. (2006). MicroRNAs: a new class of regulatory genes affecting metabolism. *Cell Metab.* **4**, 9–12.

Kühnlein, R. P. (2011). The contribution of the Drosophila model to lipid droplet research. *Prog. Lipid Res.* **50**, 348–56.

Kühnlein, R. P. (2012). Thematic review series: Lipid droplet synthesis and metabolism: from yeast to man. Lipid droplet-based storage fat metabolism in Drosophila. *J. Lipid Res.* **53**, 1430–6.

Kuma, A. and Mizushima, N. (2010). Physiological role of autophagy as an intracellular recycling system: with an emphasis on nutrient metabolism. *Semin. Cell Dev. Biol.* **21**, 683–90.

Kumar, M., Lu, Z., Takwi, a a L., Chen, W., Callander, N. S., Ramos, K. S., Young, K. H. and Li, Y. (2010). Negative regulation of the tumor suppressor p53 gene by microRNAs. *Oncogene* 1–11.

Kwon, C., Han, Z., Olson, E. N. and Srivastava, D. (2005). MicroRNA1 influences cardiac differentiation in Drosophila and regulates Notch signaling. 1–6.

Lai, E. C., Tomancak, P., Williams, R. W. and Rubin, G. M. (2003). Computational identification of Drosophila microRNA genes. *Genome Biol.* **4**, R42.

Lakin, N. D. and Jackson, S. P. (1999). Regulation of p53 in response to DNA damage. *Oncogene* **18**, 7644–55.

Landthaler, M., Yalcin, A. and Tuschl, T. (2004). The Human DiGeorge Syndrome Critical Region Gene 8 and Its D . melanogaster Homolog Are Required for miRNA Biogenesis. **14**, 2162–2167.

Lane, D. and Levine, A. (2010). p53 Research: the past thirty years and the next thirty years. *Cold Spring Harb. Perspect. Biol.* **2**, a000893.

Lane, D. P. and Verma, C. (2012). Mdm2 in Evolution. *Genes Cancer* **3**, 320–324.

Lane, M. E., Sauer, K., Wallace, K., Jan, Y. N., Lehner, C. F. and Vaessin, H. (1996). Stops Cell Proliferation during Drosophila Development. *Cell* **87**, 1225–1235.

LaRocque, J. R., Dougherty, D. L., Hussain, S. K. and Sekelsky, J. (2007). Reducing DNA polymerase alpha in the absence of Drosophila ATR leads to P53-dependent apoptosis and developmental defects. *Genetics* **176**, 1441–51.

Lawrence, P. and Struhl, G. (1996). Morphogens, compartments, and pattern: lessons from drosophila? *Cell* **85**, 951–961.

Le, M. T. N., Teh, C., Shyh-chang, N., Xie, H., Zhou, B., Korzh, V., Lodish, H. F. and Lim, B. (2009). MicroRNA-125b is a novel negative regulator of p53. *Genes Dev.* 862–876.

Lee, G. J. and Hyun, S. (2014). Multiple targets of the microRNA miR-8 contribute to immune homeostasis in Drosophila. *Dev. Comp. Immunol.* **45**, 245–251.

Lee, T. and Luo, L. (2001). Mosaic analysis with a repressible cell marker (MARCM) for Drosophila neural development. *Trends Neurosci.* **24**, 251–4.

Lee, G. and Park, J. H. (2004). Hemolymph sugar homeostasis and starvation-induced hyperactivity affected by genetic manipulations of the adipokinetic hormone-encoding gene in Drosophila melanogaster. *Genetics* **167**, 311–23.

Lee, R. C., Feinbaum, R. L. and Ambros, V. (1993). The C. elegans heterochronic gene lin-4 encodes small RNAs with antisense complementarity to lin-14. *Cell* **75**, 843–54.

Lee, Y., Jeon, K., Lee, J.-T., Kim, S. and Kim, V. N. (2002). MicroRNA maturation: stepwise processing and subcellular localization. *EMBO J.* **21**, 4663–70.

Lee, J. H., Lee, E., Park, J., Kim, E., Kim, J. and Chung, J. (2003a). In vivo p53 function is indispensable for DNA damage-induced apoptotic signaling in Drosophila. *FEBS Lett.* **550**, 5–10.

Lee, Y., Ahn, C., Han, J., Choi, H., Kim, J., Yim, J., Lee, J., Provost, P., Rådmark, O., Kim, S., et al. (2003b). The nuclear RNase III Drosha initiates microRNA processing. *Nature* **425**, 415–9.

Lee, Y. S., Nakahara, K., Pham, J. W., Kim, K., He, Z., Sontheimer, E. J. and Carthew, R. W. (2004a). Distinct roles for Drosophila Dicer-1 and Dicer-2 in the siRNA/miRNA silencing pathways. *Cell* **117**, 69–81.

Lee, Y., Kim, M., Han, J., Yeom, K.-H., Lee, S., Baek, S. H. and Kim, V. N. (2004b). MicroRNA genes are transcribed by RNA polymerase II. *EMBO J.* **23**, 4051–60.

Lee, Y. L., Peng, Q., Fong, S. W., Chen, A. C. H., Lee, K. F., Ng, E. H. Y., Nagy, A. and Yeung, W. S. B. (2012). Sirtuin 1 facilitates generation of induced pluripotent stem cells from mouse embryonic fibroblasts through the miR-34a and p53 pathways. *PLoS One* **7**, e45633.

Leopold, P. and Perrimon, N. (2007). Drosophila and the genetics of the internal milieu. *Nature* **450**, 186–8.

Leung, A. K. L. and Sharp, P. a (2007). microRNAs: a safeguard against turmoil? *Cell* **130**, 581–5.

Leung, A. K. L. and Sharp, P. a (2010). MicroRNA functions in stress responses. *Mol. Cell* **40**, 205–15.

Levayer, R. and Moreno, E. (2013). Mechanisms of cell competition: themes and variations. *J. Cell Biol.* **200**, 689–98.

Levine, B. and Abrams, J. (2008). p53: The Janus of autophagy? *Nat. Cell Biol.* **10**, 637–9.

Levine, B., Klionsky, D. J. and Arbor, A. (2004). Development by Self-Digestion : Molecular Mechanisms and Biological Functions of Autophagy Review. **6**, 463–477.

Levine, A. J., Feng, Z., Mak, T. W., You, H. and Jin, S. (2006). Coordination and communication between the p53 and IGF-1-AKT-TOR signal transduction pathways. *Genes Dev.* **20**, 267–75.

Lewis, B. P., Burge, C. B. and Bartel, D. P. (2005). Conserved seed pairing, often flanked by adenosines, indicates that thousands of human genes are microRNA targets. *Cell* **120**, 15–20.

Li, X. and Carthew, R. W. (2005). A microRNA mediates EGF receptor signaling and promotes photoreceptor differentiation in the Drosophila eye. *Cell* **123**, 1267–77.

Li, Y. and Padgett, R. W. (2012). Bantam Is Required for Optic Lobe Development and Glial Cell Proliferation. *PLoS One* **7**, e32910.

Li, Y., Wang, F., Lee, J.-A. and Gao, F.-B. (2006). MicroRNA-9a ensures the precise specification of sensory organ precursors in Drosophila. *Genes Dev.* **20**, 2793–805.

Liang, Y., Liu, J. and Feng, Z. (2013). The regulation of cellular metabolism by tumor suppressor p53. *Cell Biosci.* **3**, 9.

Liao, J.-M., Cao, B., Zhou, X. and Lu, H. (2014). New insights into p53 functions through its target microRNAs. *J. Mol. Cell Biol.* **6**, 206–213.

Lim, L. P., Glasner, M. E., Yekta, S., Burge, C. B. and Bartel, D. P. (2003a). Vertebrate microRNA genes. *Science* **299**, 1540.

Lim, L. P., Lau, N. C., Weinstein, E. G., Abdelhakim, A., Yekta, S., Rhoades, M. W., Burge, C. B. and Bartel, D. P. (2003b). The microRNAs of Caenorhabditis elegans. *Genes Dev.* **17**, 991–1008.

Lim, L. P., Lau, N. C., Garrett-Engele, P., Grimson, A., Schelter, J. M., Castle, J., Bartel, D. P., Linsley, P. S. and Johnson, J. M. (2005). Microarray analysis shows that some microRNAs downregulate large numbers of target mRNAs. *Nature* **433**, 769–73.

Liu, Z. and Huang, X. (2013). Lipid metabolism in Drosophila : development and disease Using Drosophila System to Study Lipid Metabolism Lipids Function in Drosophila Early Development. **45**, 44–50.

Loewith, R., Jacinto, E., Wullschleger, S., Lorberg, A., Crespo, J. L., Bonenfant, D., Oppliger, W., Jenoe, P. and Hall, M. N. (2002). Two TOR complexes, only one of which is rapamycin sensitive, have distinct roles in cell growth control. *Mol. Cell* **10**, 457–468.

Loya, C. M., McNeill, E. M., Bao, H., Zhang, B. and Van Vactor, D. (2014). miR-8 controls synapse structure by repression of the actin regulator Enabled. *Development* **141**, 1864–74.

Lu, W.-J., Chapo, J., Roig, I. and Abrams, J. M. (2010). Meiotic recombination provokes functional activation of the p53 regulatory network. *Science* **328**, 1278–81.

Lucas, K. and Raikhel, A. S. (2013). Insect microRNAs: biogenesis, expression profiling and biological functions. *Insect Biochem. Mol. Biol.* **43**, 24–38.

Lujambio, A. and Lowe, S. W. (2012). The microcosmos of cancer. *Nature* **482**, 347–55.

Lund, E., Güttinger, S., Calado, A., Dahlberg, J. E. and Kutay, U. (2004). Nuclear export of microRNA precursors. *Science* **303**, 95–8.

Lytle, J. R., Yario, T. a and Steitz, J. a (2007). Target mRNAs are repressed as efficiently by microRNA-binding sites in the 5’ UTR as in the 3' UTR. *Proc. Natl. Acad. Sci. U. S. A.* **104**, 9667–72.

Maddocks, O. D. K. and Vousden, K. H. (2011). Metabolic regulation by p53. *J. Mol. Med. (Berl).* **89**, 237–45.

Maddocks, O. D. K., Berkers, C. R., Mason, S. M., Zheng, L., Blyth, K., Gottlieb, E. and Vousden, K. H. (2013). Serine starvation induces stress and p53-dependent metabolic remodelling in cancer cells. *Nature* **493**, 542–6.

Madigan, J. P., Chotkowski, H. L. and Glaser, R. L. (2002). DNA double-strand break-induced phosphorylation of Drosophila histone variant H2Av helps prevent radiation-induced apoptosis. *Nucleic Acids Res.* **30**, 3698–705.

Maes, O. C., An, J., Sarojini, H., Wu, H. and Wang, E. (2008). Changes in MicroRNA expression patterns in human fibroblasts after low-LET radiation. *J. Cell. Biochem.* **105**, 824–34.

Maier, B., Gluba, W., Bernier, B., Turner, T., Mohammad, K., Guise, T., Sutherland, A., Thorner, M. and Scrable, H. (2004). Modulation of mammalian life span by the short isoform of p53. *Genes Dev.* **18**, 306–19.

Malone, C. D. and Hannon, G. J. (2009). Molecular evolution of piRNA and transposon control pathways in Drosophila. *Cold Spring Harb. Symp. Quant. Biol.* **74**, 225–34.

Mandal, S., Guptan, P., Owusu-Ansah, E. and Banerjee, U. (2005). Mitochondrial regulation of cell cycle progression during development as revealed by the tenured mutation in Drosophila. *Dev. Cell* **9**, 843–54.

Mandal, S., Freije, W. a, Guptan, P. and Banerjee, U. (2010). Metabolic control of G1-S transition: cyclin E degradation by p53-induced activation of the ubiquitin-proteasome system. *J. Cell Biol.* **188**, 473–9.

Marcel, V., Dichtel-Danjoy, M.-L., Sagne, C., Hafsi, H., Ma, D., Ortiz-Cuaran, S., Olivier, M., Hall, J., Mollereau, B., Hainaut, P., et al. (2011). Biological functions of p53 isoforms through evolution: lessons from animal and cellular models. *Cell Death Differ.* **18**, 1815–24.

Marshall, L., Rideout, E. J. and Grewal, S. S. (2012). Nutrient/TOR-dependent regulation of RNA polymerase III controls tissue and organismal growth in Drosophila. *EMBO J.* **31**, 1916–30.

Martín-Blanco, E., Gampel, A., Ring, J., Virdee, K., Kirov, N., Tolkovsky, A. M. and Martinez-Arias, A. (1998). puckered encodes a phosphatase that mediates a feedback loop regulating JNK activity during dorsal closure in Drosophila. *Genes Dev.* **12**, 557–570.

Matheu, A., Maraver, A., Klatt, P., Flores, I., Garcia-Cao, I., Borras, C., Flores, J. M., Viña, J., Blasco, M. a and Serrano, M. (2007). Delayed ageing through damage protection by the Arf/p53 pathway. *Nature* **448**, 375–9.

Mauri, F., McNamee, L. M., Lunardi, A., Chiacchiera, F., Del Sal, G., Brodsky, M. H. and Collavin, L. (2008). Modification of Drosophila p53 by SUMO modulates its transactivation and pro-apoptotic functions. *J. Biol. Chem.* **283**, 20848–56.

Mayo, L. and Donner, D. (2002). The PTEN, Mdm2, p53 tumor suppressor–oncoprotein network. *Trends Biochem. Sci.* **27**, 462–467.

McBride, A., Ghilagaber, S., Nikolaev, A. and Hardie, D. G. (2009). The glycogen-binding domain on the AMPK beta subunit allows the kinase to act as a glycogen sensor. *Cell Metab.* **9**, 23–34.

McEwen, D. G. and Peifer, M. (2005). Puckered, a Drosophila MAPK phosphatase, ensures cell viability by antagonizing JNK-induced apoptosis. *Development* **132**, 3935–46.

McGuire, S. E., Mao, Z. and Davis, R. L. (2004). Spatiotemporal gene expression targeting with the TARGET and gene-switch systems in Drosophila. *Sci. STKE* **2004**, pl6.

McNamee, L. M. and Brodsky, M. H. (2009). p53-independent apoptosis limits DNA damage-induced aneuploidy. *Genetics* **182**, 423–35.

Mesquita, D., Dekanty, A. and Milán, M. (2010). A dp53-dependent mechanism involved in coordinating tissue growth in Drosophila. *PLoS Biol.* **8**, e1000566.

Milán, M. and Cohen, S. M. (1999). Regulation of LIM homeodomain activity in vivo: a tetramer of dLDB and apterous confers activity and capacity for regulation by dLMO. *Mol. Cell* **4**, 267–73.

Milán, M., Campuzano, S. and García-Bellido, a (1996). Cell cycling and patterned cell proliferation in the wing primordium of Drosophila. *Proc. Natl. Acad. Sci. U. S. A.* **93**, 640–5.

Milán, M., Campuzano, S. and García-Bellido, a (1997). Developmental parameters of cell death in the wing disc of Drosophila. *Proc. Natl. Acad. Sci. U. S. A.* **94**, 5691–6.

Mizushima, N. and Komatsu, M. (2011). Autophagy: renovation of cells and tissues. *Cell* **147**, 728–41.

Moll, U. M., Wolff, S., Speidel, D. and Deppert, W. (2005). Transcription-independent pro-apoptotic functions of p53. *Curr. Opin. Cell Biol.* **17**, 631–6.

Morata, G. and Ripoll, P. (1975). Minutes: mutants of Drosophila autonomously affecting cell division rate. *Dev. Biol.* **42**, 211–221.

Moreno, E. and Basler, K. (2004). dMyc Transforms Cells into Super-Competitors. *Cell* **117**, 117–129.

Mukherji, S., Ebert, M. S., Zheng, G. X. Y., Tsang, J. S., Sharp, P. a and van Oudenaarden, A. (2011). MicroRNAs can generate thresholds in target gene expression. *Nat. Genet.* **43**, 854–9.

Murray-Zmijewski, F., Lane, D. P. and Bourdon, J.-C. (2006). P53/P63/P73 Isoforms: an Orchestra of Isoforms To Harmonise Cell Differentiation and Response To Stress. *Cell Death Differ.* **13**, 962–72.

Musselman, L. P., Fink, J. L., Narzinski, K., Ramachandran, P. V., Hathiramani, S. S., Cagan, R. L. and Baranski, T. J. (2011). A high-sugar diet produces obesity and insulin resistance in wild-type Drosophila. *Dis. Model. Mech.* **4**, 842–9.

Na, J., Musselman, L. P., Pendse, J., Baranski, T. J., Bodmer, R., Ocorr, K. and Cagan, R. (2013). A Drosophila model of high sugar diet-induced cardiomyopathy. *PLoS Genet.* **9**, e1003175.

Nolo, R., Morrison, C. M., Tao, C., Zhang, X. and Halder, G. (2006). The bantam microRNA is a target of the hippo tumor-suppressor pathway. *Curr. Biol.* **16**, 1895–904.

Okamura, K., Ishizuka, A., Siomi, H. and Siomi, M. C. (2004). Distinct roles for Argonaute proteins in small RNA-directed RNA cleavage pathways. *Genes Dev.* **18**, 1655–66.

Okamura, K., Liu, N. and Lai, E. C. (2009). Distinct mechanisms for microRNA strand selection by Drosophila Argonautes. *Mol. Cell* **36**, 431–44.

Olivares-Illana, V. and Fåhraeus, R. (2010). P53 Isoforms Gain Functions. *Oncogene* **29**, 5113–9.

Ollmann, M., Young, L. M., Di Como, C. J., Karim, F., Belvin, M., Robertson, S., Whittaker, K., Demsky, M., Fisher, W. W., Buchman, a, et al. (2000). Drosophila p53 is a structural and functional homolog of the tumor suppressor p53. *Cell* **101**, 91–101.

Ouaamari, A. El, Baroukh, N., Martens, G. A., Lebrun, P., Pipeleers, D. and Obberghen, E. Van (2008). miR-375 Targets 3-Phosphoinositide–Dependent Protein Kinase-1 and Regulates Glucose-Induced Biological Responses in Pancreatic -Cells. *Diabetes* **57**, 2708–17.

Ouyang, Y., Song, Y. and Lu, B. (2011). dp53 Restrains ectopic neural stem cell formation in the Drosophila brain in a non-apoptotic mechanism involving Archipelago and cyclin E. *PLoS One* **6**, e28098.

Owusu-ansah, E. and Perrimon, N. (2014). Modeling metabolic homeostasis and nutrient sensing in Drosophila : implications for aging and metabolic diseases. 343–350.

Page, S. L., McKim, K. S., Deneen, B., Van Hook, T. L. and Hawley, R. S. (2000). Genetic studies of mei-P26 reveal a link between the processes that control germ cell proliferation in both sexes and those that control meiotic exchange in Drosophila. *Genetics* **155**, 1757–72.

Palanker, L., Tennessen, J. M., Lam, G. and Thummel, C. S. (2009). Drosophila HNF4 regulates lipid mobilization and beta-oxidation. *Cell Metab.* **9**, 228–39.

Pallares-Cartes, C., Cakan-Akdogan, G. and Teleman, A. a (2012). Tissue-specific coupling between insulin/IGF and TORC1 signaling via PRAS40 in Drosophila. *Dev. Cell* **22**, 172–82.

Papadopoulou, D., Bianchi, M. W. and Bourouis, M. (2004). Functional Studies of Shaggy / Glycogen Synthase Kinase 3 Phosphorylation Sites in Drosophila melanogaster. **24**, 4909–4919.

Pasco, M. Y. and Léopold, P. (2012). High sugar-induced insulin resistance in Drosophila relies on the lipocalin Neural Lazarillo. *PLoS One* **7**, e36583.

Pek, J. W., Lim, A. K. and Kai, T. (2009). Drosophila maelstrom ensures proper germline stem cell lineage differentiation by repressing microRNA-7. *Dev. Cell* **17**, 417–24.

Pérez-garijo, A., Martín, F. A. and Morata, G. (2004). Caspase inhibition during apoptosis causes abnormal signalling and developmental aberrations in Drosophila. *Development* 5591–5598.

Peters, M., DeLuca, C., Hirao, A., Stambolic, V., Potter, J., Zhou, L., Liepa, J., Snow, B., Arya, S., Wong, J., et al. (2002). Chk2 regulates irradiation-induced, p53-mediated apoptosis in Drosophila. *Proc. …* **99**, 1–6.

Pillai, R. S., Bhattacharyya, S. N. and Filipowicz, W. (2007). Repression of protein synthesis by miRNAs: how many mechanisms? *Trends Cell Biol.* **17**, 118–26.

Potter, C. J., Pedraza, L. G. and Xu, T. (2002). Akt regulates growth by directly phosphorylating Tsc2. *Nat. Cell Biol.* **4**, 658–65.

Puig, O., Marr, M. T., Ruhf, M. L. and Tjian, R. (2003). Control of cell number by Drosophila FOXO: downstream and feedback regulation of the insulin receptor pathway. *Genes Dev.* **17**, 2006–20.

Rajan, A. and Perrimon, N. (2012). Drosophila cytokine unpaired 2 regulates physiological homeostasis by remotely controlling insulin secretion. *Cell* **151**, 123–37.

Ranganayakulu, G., Zhao, B., Dokidis, A., Molkentin, J. D., Olson, E. N. and Schulz, R. A. (1995). A series of mutations in the D-MEF2 transcription factor reveal multiple functions in larval and adult myogenesis in Drosophila. *Dev. Biol.* **171**, 169–81.

Rebollar, E., Valadez-Graham, V., Vázquez, M., Reynaud, E. and Zurita, M. (2006). Role of the p53 homologue from Drosophila melanogaster in the maintenance of histone H3 acetylation and response to UV-light irradiation. *FEBS Lett.* **580**, 642–8.

Rehwinkel, J., Behm-Ansmant, I., Gatfield, D. and Izaurralde, E. (2005). A crucial role for GW182 and the DCP1:DCP2 decapping complex in miRNA-mediated gene silencing. *RNA* **11**, 1640–7.

Reinhart, B. J., Slack, F. J., Basson, M., Pasquinelli, a E., Bettinger, J. C., Rougvie, a E., Horvitz, H. R. and Ruvkun, G. (2000). The 21-nucleotide let-7 RNA regulates developmental timing in Caenorhabditis elegans. *Nature* **403**, 901–6.

Reiter, L. T. and Bier, E. (2002). Using Drosophila melanogaster to uncover human disease gene function and potential drug target proteins. *Expert Opin. Ther. Targets* **6**, 387–99.

Reyes-delatorre, A., Peña-rangel, M. T. and Riesgo-escovar, J. R. (2012). Carbohydrate Metabolism in Drosophila : Reliance on the Disaccharide Trehalose.

Rong, Y. S., Titen, S. W., Xie, H. B., Golic, M. M., Bastiani, M., Bandyopadhyay, P., Olivera, B. M., Brodsky, M., Rubin, G. M. and Golic, K. G. (2002). Targeted mutagenesis by homologous recombination in D. melanogaster. *Genes Dev.* **16**, 1568–81.

Ronshaugen, M., Biemar, F., Piel, J., Levine, M. and Lai, E. C. (2005). The Drosophila microRNA iab-4 causes a dominant homeotic transformation of halteres to wings. *Genes Dev.* **19**, 2947–52.

Rubinsztein, D. C., Mariño, G. and Kroemer, G. (2011). Autophagy and aging. *Cell* **146**, 682–95.

Ruby, J. G., Stark, A., Johnston, W. K., Kellis, M., Bartel, D. P. and Lai, E. C. (2007). Evolution, biogenesis, expression, and target predictions of a substantially expanded set of Drosophila microRNAs. *Genome Res.* **17**, 1850–64.

Rufini, a, Tucci, P., Celardo, I. and Melino, G. (2013). Senescence and aging: the critical roles of p53. *Oncogene* 1–15.

Rulifson, E. J., Kim, S. K. and Nusse, R. (2002). Ablation of insulin-producing neurons in flies: growth and diabetic phenotypes. *Science* **296**, 1118–20.

Rutkowski, R., Hofmann, K. and Gartner, A. (2010). Phylogeny and function of the invertebrate p53 superfamily. *Cold Spring Harb. Perspect. Biol.* **2**, a001131.

Ryoo, H. D., Gorenc, T. and Steller, H. (2004). Apoptotic cells can induce compensatory cell proliferation through the JNK and the Wingless signaling pathways. *Dev. Cell* **7**, 491–501.

Saito, K., Ishizuka, A., Siomi, H. and Siomi, M. C. (2005). Processing of pre-microRNAs by the Dicer-1-Loquacious complex in Drosophila cells. *PLoS Biol.* **3**, e235.

Sancak, Y., Thoreen, C. C., Peterson, T. R., Lindquist, R. a, Kang, S. a, Spooner, E., Carr, S. a and Sabatini, D. M. (2007). PRAS40 is an insulin-regulated inhibitor of the mTORC1 protein kinase. *Mol. Cell* **25**, 903–15.

Sancak, Y., Peterson, T. R., Shaul, Y. D., Lindquist, R. A., Thoreen, C. C., Bar-Peled, L. and Sabatini, D. M. (2008). The Rag GTPases bind raptor and mediate amino acid signaling to mTORC1. *Science (80-.).* **320**, 1496–1501.

Sancak, Y., Bar-Peled, L., Zoncu, R., Markhard, A. L., Nada, S. and Sabatini, D. M. (2010). Ragulator-Rag complex targets mTORC1 to the lysosomal surface and is necessary for its activation by amino acids. *Cell* **141**, 290–303.

Saucedo, L. J., Gao, X., Chiarelli, D. A., Li, L., Pan, D. and Edgar, B. A. (2003). Rheb promotes cell growth as a component of the insulin/TOR signalling network. *Nat Cell Biol* **5**, 566–571.

Scherz-Shouval, R., Weidberg, H., Gonen, C., Wilder, S., Elazar, Z. and Oren, M. (2010). p53-dependent regulation of autophagy protein LC3 supports cancer cell survival under prolonged starvation. *Proc. Natl. Acad. Sci. U. S. A.* **107**, 18511–18516.

Schleich, S. and Teleman, A. a (2009). Akt phosphorylates both Tsc1 and Tsc2 in Drosophila, but neither phosphorylation is required for normal animal growth. *PLoS One* **4**, e6305.

Schoppy, D. W., Ruzankina, Y. and Brown, E. J. (2010). Removing all obstacles: A critical role for p53 in promoting tissue renewal. *Cell Cycle* **9**, 1–7.

Schwamborn, J. C., Berezikov, E. and Knoblich, J. a (2009). The TRIM-NHL protein TRIM32 activates microRNAs and prevents self-renewal in mouse neural progenitors. *Cell* **136**, 913–25.

Scott, R. C., Schuldiner, O. and Neufeld, T. P. (2004). Role and regulation of starvation-induced autophagy in the Drosophila fat body. *Dev. Cell* **7**, 167–78.

Scott, R. C., Juhász, G. and Neufeld, T. P. (2007). Direct induction of autophagy by Atg1 inhibits cell growth and induces apoptotic cell death. *Curr. Biol.* **17**, 1–11.

Shen, J. and Tower, J. (2010). Drosophila foxo acts in males to cause sexual-dimorphism in tissue-specific p53 life span effects. *Exp. Gerontol.* **45**, 97–105.

Shen, J., Curtis, C., Tavaré, S. and Tower, J. (2009). A screen of apoptosis and senescence regulatory genes for life span effects when over-expressed in Drosophila. *Aging (Albany. NY).* **1**, 191–211.

Shi, D. and Gu, W. (2012). Dual Roles of MDM2 in the Regulation of p53: Ubiquitination Dependent and Ubiquitination Independent Mechanisms of MDM2 Repression of p53 Activity. *Genes Cancer* **3**, 240–8.

Shlevkov, E. and Morata, G. (2012). A dp53/JNK-dependant feedback amplification loop is essential for the apoptotic response to stress in Drosophila. *Cell Death Differ.* **19**, 451–60.

Shomron, N. (2010). MicroRNAs and developmental robustness: a new layer is revealed. *PLoS Biol.* **8**, e1000397.

Sieber, M. H. and Thummel, C. S. (2009). The DHR96 nuclear receptor controls triacylglycerol homeostasis in Drosophila. *Cell Metab.* **10**, 481–90.

Simón, R., Aparicio, R., Housden, B. E., Bray, S. and Busturia, A. (2014). Drosophila p53 controls Notch expression and balances apoptosis and proliferation. *Apoptosis*.

Simone, N. L., Soule, B. P., Ly, D., Saleh, A. D., Savage, J. E., Degraff, W., Cook, J., Harris, C. C., Gius, D. and Mitchell, J. B. (2009). Ionizing radiation-induced oxidative stress alters miRNA expression. *PLoS One* **4**, e6377.

Singh, R. and Cuervo, A. M. (2011). Autophagy in the cellular energetic balance. *Cell Metab.* **13**, 495–504.

Singh, R., Kaushik, S., Wang, Y., Xiang, Y., Novak, I., Komatsu, M., Tanaka, K., Cuervo, A. M. and Czaja, M. J. (2009). Autophagy regulates lipid metabolism. *Nature* **458**, 1131–5.

Smibert, P., Bejarano, F., Wang, D., Garaulet, D. L., Yang, J.-S., Martin, R., Bortolamiol-Becet, D., Robine, N., Hiesinger, P. R. and Lai, E. C. (2011). A Drosophila genetic screen yields allelic series of core microRNA biogenesis factors and reveals post-developmental roles for microRNAs. *RNA* **17**, 1997–2010.

Smith-Vikos, T. and Slack, F. J. (2012). MicroRNAs and their roles in aging. *J. Cell Sci.* **125**, 7–17.

Sogame, N., Kim, M. and Abrams, J. M. (2003). Drosophila p53 preserves genomic stability by regulating cell death. *Proc. Natl. Acad. Sci. U. S. A.* **100**, 4696–701.

Stehmeier, P. and Muller, S. (2009). Regulation of p53 family members by the ubiquitin-like SUMO system. *DNA Repair (Amst).* **8**, 491–8.

Stocker, H., Radimerski, T., Schindelholz, B., Wittwer, F., Belawat, P., Daram, P., Breuer, S., Thomas, G. and Hafen, E. (2003). Rheb is an essential regulator of S6K in controlling cell growth in Drosophila. *Nat Cell Biol* **5**, 559–565.

Suzuki, H. I., Yamagata, K., Sugimoto, K., Iwamoto, T., Kato, S. and Miyazono, K. (2009). Modulation of microRNA processing by p53. *Nature* **460**, 529–33.

Takwi, A. and Li, Y. (2009). The p53 Pathway Encounters the MicroRNA World. *Curr. Genomics* **10**, 194–7.

Taniguchi, C. M., Emanuelli, B. and Kahn, C. R. (2006). Critical nodes in signalling pathways: insights into insulin action. *Nat. Rev. Mol. Cell Biol.* **7**, 85–96.

Tapon, N., Ito, N., Dickson, B. J., Treisman, J. E. and Hariharan, I. K. (2001). The Drosophila tuberous sclerosis complex gene homologs restrict cell growth and cell proliferation. *Cell* **105**, 345–355.

Tasdemir, E., Maiuri, M. C., Galluzzi, L., Vitale, I., Djavaheri-Mergny, M., D'Amelio, M., Criollo, A., Morselli, E., Zhu, C., Harper, F., et al. (2008). Regulation of autophagy by cytoplasmic p53. *Nat. Cell Biol.* **10**, 676–87.

Tee, A. R., Manning, B. D., Roux, P. P., Cantley, L. C. and Blenis, J. (2003). Tuberous sclerosis complex gene products, Tuberin and Hamartin, control mTOR signaling by acting as a GTPase-activating protein complex toward Rheb. *Curr. Biol.* **13**, 1259–1268.

Teleman, A. a (2010). Molecular mechanisms of metabolic regulation by insulin in Drosophila. *Biochem. J.* **425**, 13–26.

Teleman, A. A. and Cohen, S. M. (2006). Drosophila lacking microRNA miR-278 are defective in energy homeostasis. *Genes Dev.* 417–422.

Teleman, A. A., Chen, Y. and Cohen, S. M. (2005). 4E-BP functions as a metabolic brake used under stress conditions but not during normal growth. *Genes Dev.* **19**, 1844–1848.

Teleman, A. a, Maitra, S. and Cohen, S. M. (2006). Drosophila lacking microRNA miR-278 are defective in energy homeostasis. *Genes Dev.* **20**, 417–22.

Teleman, A. a, Hietakangas, V., Sayadian, A. C. and Cohen, S. M. (2008). Nutritional control of protein biosynthetic capacity by insulin via Myc in Drosophila. *Cell Metab.* **7**, 21–32.

Tétreault, N. and De Guire, V. (2013). miRNAs: their discovery, biogenesis and mechanism of action. *Clin. Biochem.* **46**, 842–5.

Thomas, G. (2002). The S6 kinase signaling pathway in the control of development and growth. *Biol. Res.* **35**, 305–13.

Tick, G., Cserpán, I., Dombrádi, V., Mechler, B. M., Török, I. and Kiss, I. (1999). Structural and functional characterization of the Drosophila glycogen phosphorylase gene. *Biochem. Biophys. Res. Commun.* **257**, 34–43.

Titen, S. W. a and Golic, K. G. (2008). Telomere loss provokes multiple pathways to apoptosis and produces genomic instability in Drosophila melanogaster. *Genetics* **180**, 1821–32.

Titen, S. W. a, Lin, H.-C., Bhandari, J. and Golic, K. G. (2014). Chk2 and p53 regulate the transmission of healed chromosomes in the Drosophila male germline. *PLoS Genet.* **10**, e1004130.

Toledano, H., D'Alterio, C., Czech, B., Levine, E. and Jones, D. L. (2012). The let-7-Imp axis regulates ageing of the Drosophila testis stem-cell niche. *Nature* **485**, 605–10.

Tomari, Y. and Zamore, P. D. (2005). Perspective: machines for RNAi. *Genes Dev.* **19**, 517–29.

Tsang, J., Zhu, J. and van Oudenaarden, A. (2007). MicroRNA-mediated feedback and feedforward loops are recurrent network motifs in mammals. *Mol. Cell* **26**, 753–67.

Ugrankar, R., Liu, Y., Provaznik, J., Schmitt, S. and Lehmann, M. (2011). Lipin is a central regulator of adipose tissue development and function in Drosophila melanogaster. *Mol. Cell. Biol.* **31**, 1646–56.

Valentin-Vega, Y., Okano, H. and Lozano, G. (2008). The intestinal epithelium compensates for p53-mediated cell death and guarantees organismal survival. *Cell Death Differ.* **15**, 1772–1781.

Vallejo, D. M., Caparros, E. and Dominguez, M. (2011). Targeting Notch signalling by the conserved miR-8/200 microRNA family in development and cancer cells. *EMBO J.* **30**, 756–69.

Van Kouwenhove, M., Kedde, M. and Agami, R. (2011). MicroRNA regulation by RNA-binding proteins and its implications for cancer. *Nat. Rev. Cancer* **11**, 644–56.

Vander Haar, E., Lee, S.-I., Bandhakavi, S., Griffin, T. J. and Kim, D.-H. (2007). Insulin signalling to mTOR mediated by the Akt/PKB substrate PRAS40. *Nat. Cell Biol.* **9**, 316–23.

Varghese, J. and Cohen, S. M. (2007). microRNA miR-14 acts to modulate a positive autoregulatory loop controlling steroid hormone signaling in Drosophila. *Genes Dev.* **21**, 2277–82.

Varghese, J., Lim, S. F. and Cohen, S. M. (2010). Drosophila miR-14 regulates insulin production and metabolism through its target, sugarbabe. *Genes Dev.* **24**, 2748–53.

Vasudevan, S., Tong, Y. and Steitz, J. a (2007). Switching from repression to activation: microRNAs can up-regulate translation. *Science* **318**, 1931–4.

Vihervaara, T. and Puig, O. (2008). dFOXO regulates transcription of a Drosophila acid lipase. *J. Mol. Biol.* **376**, 1215–23.

Vincent, J. P. (1998). Compartment boundaries: where, why and how? *Int. J. Dev. Biol.* **42**, 311–5.

Vousden, K. H. and Prives, C. (2009). Blinded by the Light: The Growing Complexity of p53. *Cell* **137**, 413–31.

Wahl, G. M. and Carr, a M. (2001). The evolution of diverse biological responses to DNA damage: insights from yeast and p53. *Nat. Cell Biol.* **3**, E277–86.

Wang, Y. and Taniguchi, T. (2013). MicroRNAs and DNA damage response: implications for cancer therapy. *Cell Cycle* **12**, 32–42.

Wang, X., Li, W., Williams, M., Terada, N., Alessi, D. R. and Proud, C. G. (2001). Regulation of elongation factor 2 kinase by p90(RSK1) and p70 S6 kinase. *Eur. Mol. Biol. Organ. J.* **20**, 4370–4379.

Wang, B., Moya, N., Niessen, S., Hoover, H., Mihaylova, M. M., Shaw, R. J., Yates, J. R., Fischer, W. H., Thomas, J. B. and Montminy, M. (2011). A hormone-dependent module regulating energy balance. *Cell* **145**, 596–606.

Wang, Y., Wang, Z., Joshi, B. H., Puri, R. K., Stultz, B., Yuan, Q., Bai, Y., Zhou, P., Yuan, Z., Hursh, D. a, et al. (2013). The tumor suppressor Caliban regulates DNA damage-induced apoptosis through p53-dependent and -independent activity. *Oncogene* **32**, 3857–66.

Waskar, M., Landis, G. N., Shen, J., Curtis, C., Tozer, K., Abdueva, D., Skvortsov, D., Tavaré, S. and Tower, J. (2009). Drosophila melanogaster p53 has developmental stage-specific and sex-specific effects on adult life span indicative of sexual antagonistic pleiotropy. *Aging (Albany. NY).* **1**, 903–36.

Weidberg, H., Shvets, E. and Elazar, Z. (2009). Lipophagy: selective catabolism designed for lipids. *Dev. Cell* **16**, 628–30.

Wells, B. S. and Johnston, L. a (2012). Maintenance of imaginal disc plasticity and regenerative potential in Drosophila by p53. *Dev. Biol.* **361**, 263–76.

Wells, B. S., Yoshida, E. and Johnston, L. a (2006). Compensatory proliferation in Drosophila imaginal discs requires Dronc-dependent p53 activity. *Curr. Biol.* **16**, 1606–15.

Weng, R. and Cohen, S. M. (2012). Drosophila miR-124 regulates neuroblast proliferation through its target anachronism. *Development* **139**, 1427–34.

Wichmann, A., Jaklevic, B. and Su, T. T. (2006). Ionizing radiation induces caspase-dependent but Chk2- and p53-independent cell death in Drosophila melanogaster. *Proc. Natl. Acad. Sci. U. S. A.* **103**, 9952–7.

Wu, Q. and Brown, M. R. (2006). Signaling and function of insulin-like peptides in insects. *Annu. Rev. Entomol.* **51**, 1–24.

Wu, Q., Zhang, Y., Xu, J. and Shen, P. (2005). Regulation of hunger-driven behaviors by neural ribosomal S6 kinase in Drosophila. *Proc. Natl. Acad. Sci. U. S. A.* **102**, 13289–94.

Wullschleger, S., Loewith, R. and Hall, M. N. (2006). TOR signaling in growth and metabolism. *Cell* **124**, 471–84.

Wylie, A., Lu, W., Brot, A. D., Buszczak, M. and Abrams, J. M. (2014). p53 activity is selectively licensed in the Drosophila stem cell compartment. 1–16.

Xiao, J., Lin, X., Luo, X. and Wang, Z. (2011). miR-605 joins p53 network to form a p53:miR-605:Mdm2 positive feedback loop in response to stress. *EMBO J.* **30**, 524–35.

Xie, Z. and Klionsky, D. J. (2007). Autophagosome formation: core machinery and adaptations. *Nat. Cell Biol.* **9**, 1102–9.

Xu, T. and Rubin, G. M. (1993). Analysis of genetic mosaics in developing and adult Drosophila tissues. *Development* **117**, 1223–37.

Xu, P., Vernooy, S. Y., Guo, M. and Hay, B. A. (2003). The Drosophila MicroRNA Mir-14 Suppresses Cell Death and Is Required for Normal Fat Metabolism. *Current* **13**, 790–795.

Xu, D., Woodfield, S. E., Lee, T. V, Fan, Y., Antonio, C. and Bergmann, A. (2009). Genetic control of programmed cell death (apoptosis) in Drosophila. *Fly (Austin).* **3**, 78–90.

Yamada, Y., Davis, K. D. and Coffman, C. R. (2008). Programmed cell death of primordial germ cells in Drosophila is regulated by p53 and the Outsiders monocarboxylate transporter. *Development* **135**, 207–16.

Yamasaki, S., Yagishita, N., Sasaki, T., Nakazawa, M., Kato, Y., Yamadera, T., Bae, E., Toriyama, S., Ikeda, R., Zhang, L., et al. (2007). Cytoplasmic destruction of p53 by the endoplasmic reticulum-resident ubiquitin ligase “Synoviolin”. *EMBO J.* **26**, 113–22.

Yang, J.-S. and Lai, E. C. (2011). Alternative miRNA biogenesis pathways and the interpretation of core miRNA pathway mutants. *Mol. Cell* **43**, 892–903.

Yokoyama, M., Okada, S., Nakagomi, A., Moriya, J., Shimizu, I., Nojima, A., Yoshida, Y., Ichimiya, H., Kamimura, N., Kobayashi, Y., et al. (2014). Inhibition of Endothelial p53 Improves Metabolic Abnormalities Related to Dietary Obesity. *Cell Rep.* **7**, 1691–1703.

Zhang, Y. and Lu, H. (2009). Signaling to p53: ribosomal proteins find their way. *Cancer Cell* **16**, 369–77.

Zhang, P. and Zhang, H. (2013). Autophagy modulates miRNA-mediated gene silencing and selectively degrades AIN-1/GW182 in C. elegans. *EMBO Rep.* **14**, 568–76.

Zhang, Y., Gao, X., Saucedo, L. J., Ru, B., Edgar, B. A. and Pan, D. (2003). Rheb is a direct target of the tuberous sclerosis tumour suppressor proteins. *Nat Cell Biol* **5**, 578–581.

Zhang, C., Hong, Z., Ma, W., Ma, D., Qian, Y., Xie, W., Tie, F. and Fang, M. (2013). Drosophila UTX coordinates with p53 to regulate ku80 expression in response to DNA damage. *PLoS One* **8**, e78652.

Zilfou, J. T. and Lowe, S. W. (2009). Tumor suppressive functions of p53. *Cold Spring Harb. Perspect. Biol.* **1**, a001883.

INDEX OF FIGURES

INTRODUCTION

RESULTS

DISCUSSION

MATERIALS AND METHODS

INDEX OF TABLES

INTRODUCTION

RESULTS

MATERIALS AND METHODS

Abbreviations

4EBP	eukaryotic initiation factor 4E binding protein
3' UTR	3' Untranslated region
A	Anterior
AA	Amino acid
AEL	After egg laying
Ago-1	Argonaute-1
Akh	Adipokinetic hormone
AMPK	AMP-activated protein kinase
ATGL	Adipose triglyceride lipase
ATM	Ataxia telangiectasia mutated
ATR	Ataxia telangiectasia related
BrdU	Bromodeoxyuridine
Chk	Checkpoint kinase
Ci	Cubitus interruptus
Cyc	Cyclin
D	Dorsal
Dap	Dacapo
Dcp-1	Death caspase-1
Dcr-1	Dicer-1
Diap-1	*Drosophila* inhibitor of apoptosis protein-1
Dilp	*Drosophila* insulin-like peptide
DNA	Deoxyribonucleic Acid
Dp53	*Drosophila* p53
DrICE	*Drosophila* interleukin-1 converting enzyme
Dronc	*Drosophila* Nedd2-like caspase
dsRNA	Double strand ribonucleic cid
eGFP	enhanced Green Fluorescent Protein
En	Engrailed
FB	Fat body
FOXO	Forkhead Box O
Hid	Head involution defective
Hh	Hedgehog
Hpo	Hippo
IIS	Insulin/Insulin-growth factor (IGF) Signaling
IPCs	Insulin-producing cells
IR	Ionizing radiation
JNK	Jun N-terminal Kinase

Mdm2	Murine double minute 2
mRNA	Messenger Ribonucleic Acid
miRNA/miR	Micro Ribonucleic Acid
miRISC	microRNA-induced silencing complex
NLS	Nuclear Localization Signal
nt	Nucleotide
P	Posterior
PCD	Programmed cell death
PH3	Phospho histone 3
pH2Av	Phosphorylated histone 2 Av
PI3K	Phosphoinositide 3-kinase
pri-miRNA	Primary miRNA
Ptc	Patched
Puc	Puckered
qRT-PCR	Quantitative Real Time Polymerase Chain Reaction
RNAi	RNA interference
Rpr	Reaper
S6K	ribosomal protein S6 kinase
Sir2	Silent information regulator 2
Slif	Slimfast
Stg	String
Stv	Starved
TAD	Transactivation domain
TSC	Tuberous Sclerosis Complex
TOR	Target of rapamycin
TORC1	TOR complex 1
UAS	Upstream Activation Sequence
V	Ventral

RESUMEN EN CASTELLANO

El factor de transcripción p53 es un regulador central de la respuesta celular a estrés y un importante gen supresor de tumores. Se estima que más del 50% de los tumores en humanos contienen mutaciones en el gen p53. Inducción de apoptosis, parada del ciclo celular y reparación del ADN son funciones bien conocidas de p53 y tradicionalmente aceptadas como los principales mecanismos por los que esta proteína promueve la estabilidad genómica y previene la formación de tumores. Descubrimientos recientes indican que la actividad supresora de tumores de p53 también se basa en su capacidad para regular el metabolismo celular. En los últimos años, p53 ha surgido como un importante regulador de varias rutas metabólicas tales como la glucólisis y la fosforilación oxidativa, capaz de desencadenar una respuesta celular adaptativa a fluctuaciones en la disponibilidad de nutrientes, una función que puede contribuir no sólo a la capacidad supresora de tumores de p53, sino también a otras funciones más fisiológicas no asociadas con el cáncer. Una mejor comprensión de los mecanismos moleculares que regulan p53 en situaciones de estrés nutricional y el posible papel fisiológico de p53 en la homeostasis energética a nivel del organismo es importante para mejorar el conocimiento actual de esta proteína y su papel en enfermedades humanas. En este sentido, *Drosophila* es un sistema modelo muy atractivo ya que existen paralelismos significativos entre los principales procesos que regulan el control metabólico, tanto a nivel fisiológico como a nivel molecular, en las moscas y en los seres humanos.

Los organismos han desarrollado a lo largo de la evolución una amplia gama de estrategias para mantener un estado homeostático interno a pesar de ciertas fluctuaciones ambientales, tales como la disponibilidad de nutrientes. En *Drosophila,* el 'cuerpo graso', un análogo funcional del hígado y el tejido adiposo de los vertebrados, funciona como un sensor nutricional encargado de ajustar el gasto energético en función del estado nutricional del organismo. En condiciones de carencia de nutrientes, el 'cuerpo graso' suministra energía al resto del cuerpo mediante la movilización de glucógeno y triacilglicéridos (TAGs) almacenados. El homólogo de *Drosophila* de p53 (Dp53) comparte una identidad significativa en la secuencia de aminoácidos con la proteína p53 de mamíferos, incluyendo aquellos residuos frecuentemente asociados con el cáncer humano. Asimismo, Dp53 promueve la muerte celular por apoptosis y la parada del ciclo celular en respuesta a varias situaciones de estrés.

Los resultados presentados en esta tesis revelan un papel fundamental de Dp53 en la adaptación del organismo a la falta de nutrientes. Dp53 se requiere específicamente en el 'cuerpo graso' de *Drosophila* para reprogramar el metabolismo energético de la mosca y así permitir la supervivencia frente a un estrés nutricional. La reducción de los niveles de actividad de Dp53 específicamente en las células del 'cuerpo graso' acelera el consumo de las principales reservas de energía (glucógeno y TAGs), reduce los niveles de azúcares en el animal, y compromete la supervivencia del organismo en ayuno. En *Drosophila*, la homeostasis energética se mantiene por la acción combinada de dos hormonas similares a la insulina (Dilp, *Drosophila* insulin-like peptide) y al glucagón (Akh, adipokinetic hormone). En situaciones de abundancia alimenticia, los Dilps promueven el almacenamiento de energía, mientras que Akh y niveles reducidos de Dilps circulantes contribuyen a la movilización de los recursos energéticos en situaciones de escasez nutricional. Sin embargo, presentamos evidencias de que Dp53 tiene un impacto en el balance de energía de forma independiente a la regulación de estas importantes hormonas involucradas en el mantenimiento de la homeostasis metabólica. Asimismo, las principales enzimas metabólicas implicadas en la movilización de los recursos energéticos no se afectan en ausencia de Dp53. Curiosamente, desvelamos un papel autónomo-celular de Dp53 en la modulación de los cambios metabólicos que padecen las células del 'cuerpo graso' ante la ausencia de nutrientes. También identificamos el mecanismo molecular por el cual Dp53 se activa en condiciones de escasez nutricional en las células del 'cuerpo graso'. Demostramos que los microRNAs (miRNAs), una clase abundante de RNAs no codificantes endógenos de aproximadamente 22 nucleótidos de longitud, son capaces de regular la expresión de *dp53* a través de interacciones en el extremo 3 'UTR de su ARN mensajero, e identificamos *miR-305* como uno de los elementos cruciales en este sistema de regulación. La disponibilidad de nutrientes regula la maquinaria de los miRNAs a través de TOR y mantiene bajos los niveles de Dp53 en las células del 'cuerpo graso'. En una situación de carencia de nutrientes, los niveles de expresión de dos elementos implicados en la biogénesis de los miRNAs (Drosha y Dicer) y un componente catalítico del complejo represor mRISC (Argonaute-1) se ven altamente reducidos, conllevando a una reducción generalizada de los niveles de miRNAs maduros. De este modo, se pierde el efecto inhibidor mediado por *miR-305* sobre Dp53, y se induce la activación de Dp53 en las células del 'cuerpo graso'. Esta activación contribuye a la resistencia del organismo frente a una situación de carencia nutricional. Estos resultados abren nuevas vías para la comprensión del mecanismo molecular

por el cual se activa p53 bajo estrés metabólico y ponen de manifiesto la participación de p53 en la detección de nutrientes y la adaptación metabólica a nivel del organismo.

En esta tesis también hemos analizado las funciones clásicas de p53 como supresor tumoral. En las células epiteliales, Dp53 ha conservado la capacidad de inducir muerte celular programada, parar el ciclo celular y reparar el ADN. Sin embargo, al exponer a los organismos a radiaciones capaces de inducir daño al DNA, comprobamos que Dp53 sólo es capaz de regular la respuesta temprana del tejido en cuanto a inducción de apoptosis y reparación del ADN se refiere. Presentamos evidencias que confirman que la maquinaria de los miRNAs también regula Dp53 en las células epiteliales, evitando de este modo la inducción de muerte celular programada en situaciones normales. Aun así, a diferencia de lo que sucede bajo un estrés nutricional, la activación Dp53 en respuesta al daño en el ADN no se basa en el alivio de la represión mediada por *miR-305* en las células epiteliales.

Como p53 se encuentra conservado en los genomas de organismos primitivos, su función supresora de tumores probablemente no haya influenciado la evolución de este gen y no es seguramente la función original de *p53*. En los últimos años, la identificación de p53 como un importante regulador del metabolismo celular, junto a nuestros resultados, nos permiten especular que la regulación de la homeostasis metabólica pudiera ser una de las funciones ancestrales de p53.

aNNeXeS

ANNEXES

In addition to the project addressed in this PhD thesis and that has been successfully published in Cell Reports in 2014 ***(Publication 1)***, I have also contributed to other research projects that resulted in other publications from the lab.

In collaboration with Andrés Dekanty, I have been involved in two projects related with the molecular and cellular mechanisms underlying tumorigenic behaviour in Drosophila epithelial cells in response to aneuploidy and DNA damage that lead to the publication of two original research papers ***(Publication 2 and 3).*** For both of these papers, I contributed to conduct all of the experimental work. In particular, in publication 2 (Dekanty, Barrio and Milán, 2014) I helped to analyse the specific contribution of cell cycle arrest and double-strand breaks repair by error-free G2-specific homologous recombination during G2 in suppressing the tumorigenic potential of DNA damage. In publication 3 (Dekanty, Barrio, et al., 2012), I analyzed the extent of chromosomal instability genetically induced and the subsequent Dp53-independent apoptotic induction, as well as I helped to the characterization of the delaminated cell population (a group of cells that lose their apical-basal polarity, mis-localize DE-Cadherin and activate a JNK transcriptional program required for tissue overgrowth).

In the project of control of gene expression by the cross-talk between genetic and epigenetic mechanisms ***(Publication 4),*** I contributed in the experimental genetic assays performed in wing discs with the different *hh* reporter transgenes constructed by the first author that lead us to the demonstration that the communication between enhancers (genetic regulatory elements responding to transcription factors) and PRE/TRE (epigenetic regulatory elements responding to Polycomb/Trithorax-group proteins) is a general mechanism involved in the regulation of gene expression.

Main publication (1)

"MicroRNA-mediated regulation of Dp53 in the *Drosophila* fat body contributes to metabolic adaptation to nutrient deprivation"

OPEN ACCESS
CellPress

Cell Reports
Article

MicroRNA-Mediated Regulation of Dp53 in the *Drosophila* Fat Body Contributes to Metabolic Adaptation to Nutrient Deprivation

Lara Barrio,[1,3] Andrés Dekanty,[1,3,4] and Marco Milán[1,2,*]
[1]Institute for Research in Biomedicine (IRB Barcelona), Baldiri i Reixac, 10, 08028 Barcelona, Spain
[2]Institucio Catalana de Recerca i Estudis Avançats (ICREA), 08028 Barcelona, Spain
[3]Co-first author
[4]Present address: Instituto de Agrobiotecnología del Litoral (CONICET-UNL), 3000 Santa Fe, Argentina
*Correspondence: marco.milan@irbbarcelona.org
http://dx.doi.org/10.1016/j.celrep.2014.06.020

SUMMARY

Multiple conserved mechanisms sense nutritional conditions and coordinate metabolic changes in the whole organism. We unravel a role for the *Drosophila* homolog of p53 (Dp53) in the fat body (FB; a functional analog of vertebrate adipose and hepatic tissues) in starvation adaptation. Under nutrient deprivation, FB-specific depletion of Dp53 accelerates consumption of major energy stores and reduces survival rates of adult flies. We show that Dp53 is regulated by the microRNA (miRNA) machinery and *miR-305* in a nutrition-dependent manner. In well-fed animals, TOR signaling contributes to *miR-305*-mediated inhibition of Dp53. Nutrient deprivation reduces the levels of miRNA machinery components and leads to Dp53 derepression. Our results uncover an organism-wide role for Dp53 in nutrient sensing and metabolic adaptation and open up avenues toward understanding the molecular mechanisms underlying p53 activation under nutrient deprivation.

INTRODUCTION

The integration of nutrient status to metabolic homeostasis at the cellular and organismal level is a complex process performed in multicellular organisms, and the ability of an organism to respond to nutritional stress is critical for its survival. In the last few years, the tumor suppressor protein p53 has emerged as a key regulator of metabolic homeostasis that triggers a cellular adaptive response to fluctuations in nutrient availability (Berkers et al., 2013; Vousden and Ryan, 2009), a function that may contribute not only to tumor suppression activities of this molecule but also to its non-cancer-associated functions. Whereas p53 plays a major tumor suppressor role by inhibiting glycolysis and glutaminolsysis at different levels, thus suppressing glucose and glutamine flux into subsidiary pathways for biosynthesis in highly proliferative and growing tumor cells (Jiang et al., 2013), p53 induces metabolic remodelling and promotes cell survival upon transient metabolic stresses (Berkers et al., 2013). In cultured cells, p53 induces cell-cycle arrest and promotes cell survival in response to transient glucose deprivation (Jones et al., 2005), regulates autophagic flux and increases cell fitness upon starvation (Scherz-Shouval et al., 2010), and preserves the antioxidant capacity of the cell and increases survival rates upon serine deprivation (Maddocks et al., 2013).

Studies on the potential role of p53 in nutrient sensing and metabolic adaptation at the organismal level can benefit from genetically tractable model systems. In this regard, *Drosophila* is a highly attractive model system, where the fat body (FB), a functional analog of vertebrate adipose and hepatic tissues, functions as a key sensor that couples nutrient status and energy expenditure (Arrese and Soulages, 2010; Canavoso et al., 2001). In conditions of nutrient deprivation, the FB supplies energy to the rest of the body by mobilizing stored glycogen and triacylglycerides (TAGs) to circulation in the form of trehalose and diacylglycerides (DAGs), respectively (Arrese and Soulages, 2010). The *Drosophila* homolog of p53 (Dp53) shares significant amino acid identity with mammalian p53, including specific residues frequently associated with human cancer (Brodsky et al., 2000; Jin et al., 2000; Mandal et al., 2005, 2010; Ollmann et al., 2000). Like its mammalian counterparts, Dp53 promotes apoptotic cell death and cell-cycle arrest in response to several stresses, including DNA damage and mitochondrial dysfunction (Brodsky et al., 2000; Jin et al., 2000; Mandal et al., 2005, 2010; Ollmann et al., 2000).

Here, we have identified that Dp53 participates in organismal adaptation to nutrient deprivation. The depletion of Dp53 activity levels specifically in FB cells accelerates the consumption of the main energy stores, reduces the levels of sugars in the animal, and compromises organismal survival upon fasting. We present evidence that the levels of fasting hormones and metabolic enzymes that mobilize these energy resources are similarly modulated by starvation in control and *dp53* mutant animals and unveil a cell-autonomous role of Dp53 in modulating the metabolic changes of FB cells to nutrient deprivation. We also identified the molecular mechanism by which Dp53 is activated by nutrient conditions in FB cells. We present evidence that microRNAs (miRNAs), an abundant class of endogenous noncoding RNAs measuring 22–23 nt in length (Huntzinger and Izaurralde, 2011),

regulate *dp53* expression by targeting its 3′ UTR, and we identify *miR-305* as a major regulatory element. Interestingly, two elements involved in the biogenesis of miRNAs, Drosha and Dicer, and one catalytic component of the RNA-induced silencing complex (RISC), Argonaute-1, are downregulated during starvation, thus alleviating *miR-305*-dependent targeting of the *dp53-3′UTR* and contributing to organismal resistance to starvation. These results open up avenues toward the molecular understanding of p53 activation under metabolic stress and reveal the participation of p53 in nutrient sensing and metabolic adaptation at the organismal level.

RESULTS

Dp53 Plays an FB-Specific Role in Regulating Energy Metabolism under Nutrient Deprivation

To study whether Dp53 is involved in nutrient sensing and metabolic adaptation at the organismal level, we exposed young adult flies (1 to 2 days old) to acute starvation (2% agar, 1% sucrose; Géminard et al., 2009) and compared the survival rates of *dp53* mutant and control animals. Two null alleles of *dp53* (*dp53^{ns}* and *dp53^{5A14}*), backcrossed six times into the *w^{1118}* genetic background, were used. Loss of Dp53 activity produces phenotypically wild-type adult flies and induces a lifespan extension under normal food conditions (Bauer and Helfand, 2009; Waskar et al., 2009). Under nutrient deprivation, however, a clear reduction in the survival rates of *dp53* mutant adult flies was observed when compared to controls (Figures 1A–1D; Table S1). Reduced survival rates were observed in both males and females and also in 5- to 7-day-old adult flies subjected to starvation (Figure S1; Table S1). Similar effects on survival rates were obtained in young adult flies or larvae exposed to complete nutrient deprivation (2% agar, 0% sucrose in the case of adults, and PBS-soaked paper in the case of larvae), as well as in larvae exposed to diluted (0,2X) food (Figure S1; Table S1). In the latter case, survival rates were measured as the percent of individuals entering pupariation or giving rise to adult flies (Figure S1). Flies store energy mainly as TAGs and glycogen (Arrese and Soulages, 2010), and these reserves are used under nutrient deprivation. While TAG and glycogen levels were not significantly different in *dp53* mutant and control animals at the beginning of the starvation procedure (Figure S1), they were used at higher rates in fasted *dp53*-depleted animals (Figures 1E and 1F). These results indicate that *dp53* mutant flies deplete their energetic reserves faster, which might contribute to their poor survival rates in fasting conditions.

The molecular mechanisms by which vertebrates and flies regulate the storage and release of fuel molecules at the systemic level display significant parallels. The adipokinetic hormone (AKH), the functional analog of the vertebrate glucagon, plays a key role in mobilizing energy resources during fasting, whereas *Drosophila* insulin-like peptides (dILPs) promote energy storage in normal feeding conditions, recapitulating the role of the vertebrate insulin pathway (Bharucha et al., 2008; Kim and Rulifson, 2004; Rulifson et al., 2002). Brain insulin-producing cells (IPCs) secrete dILPs in response to nutrition and accumulate dILPs under nutrient deprivation (Géminard et al., 2009). Despite the accelerated consumption of energy resources observed in starved *dp53* mutant animals when compared to control individuals, AKH production was increased, in a similar manner, in both genotypes upon fasting (Figure 1G; see also Figure S1). Insulin signaling (measured as an increase in the levels of the *Drosophila* insulin receptor, *dInR*, and *4EBP*) was also similarly reduced in both genotypes upon fasting (Figures 1H and 1I). *4EBP* and *dInR* are two targets of dFOXO transcription factor (Puig et al., 2003; Teleman et al., 2005), which is negatively regulated by the insulin pathway. Thus, an increase in the levels of these two genes reflects a reduction in insulin signaling. Consistent with this, dILP2 protein was similarly accumulated in IPCs of both control and *dp53* mutant animals upon fasting (Figures 1J and 1K). Altogether, these results indicate that Dp53 has an impact on energy balance upon fasting that cannot be explained merely by a failure in the regulation of dILPs and AKH production, thus suggesting a tissue-specific role of Dp53.

The FB of insects functions as a key sensor to couple nutrient status and energy expenditure and serves as a repository for both TAGs and glycogen, combining the energy storage functions of vertebrate adipose and hepatic tissues, respectively (Arrese and Soulages, 2010; Canavoso et al., 2001). We then analyzed whether Dp53 plays a role in this key organ during starvation. We specifically reduced Dp53 activity in the FB using the Gal4/upstream activating sequence (UAS) system (Brand and Perrimon, 1993) and determined survival rates as well as the consumption of energy reserves upon fasting. We used two transgenes (*UAS-dp53$^{H159.N}$*, a dominant-negative version of Dp53 carrying a point mutation in the DNA binding domain [Ollmann et al., 2000], and *UAS-dp53^{RNAi}*, a double-stranded RNA [dsRNA] form of *dp53*) and three GAL4 drivers expressed in the adult FB (*ppl-GAL4*, *cg-GAL4*, and *yolk-GAL4*) to deplete Dp53 activity in this key organ. In all cases, depletion of Dp53 activity in the FB reduced survival rates upon fasting (Figures 2A–2D and 2F; Table S1) when compared to control flies expressing GFP under the same drivers in the FB. Similar effects on survival rates were obtained in flies exposed to complete nutrient deprivation (2% agar, 0% sucrose; Figure S2; Table S1). Parental UAS lines alone (*UAS-dp53$^{H159.N}$* and *UAS-dp53^{RNAi}*) showed similar survival rates upon fasting than control UAS-GFP flies (Figure S2; Table S1). Interestingly, muscle-specific depletion of Dp53 activity (using the *mef2-gal4* driver; Demontis and Perrimon, 2010; Ranganayakulu et al., 1995) did not have any impact on the survival rates upon fasting (Figure 2E; Table S1). In accordance with the reduced viability upon fasting caused by targeted reduction of Dp53 in FB cells, TAGs and glycogen were consumed at accelerated rates in these animals (Figures 2I and 2J) and the levels of sugars in the animal were further reduced when compared to control individuals (Figure 2K). Remarkably, and consistent with the fact that the starvation-induced reduction in dILP secretion and the increase in Akh transcription, hormones involved in the tight regulation of sugars in circulation, were unaffected by Dp53 depletion (Figures 1G–1K), the levels of circulating sugars were similarly reduced upon fasting in wild-type and Dp53-depleted animals (Figure 2L). Thus, FB-specific depletion of Dp53 causes an accelerated consumption of energy resources. The levels of TAGs, glycogen, and sugars were largely similar in *dp53*-depleted and control animals at the beginning of the starvation procedure (Figure S2).

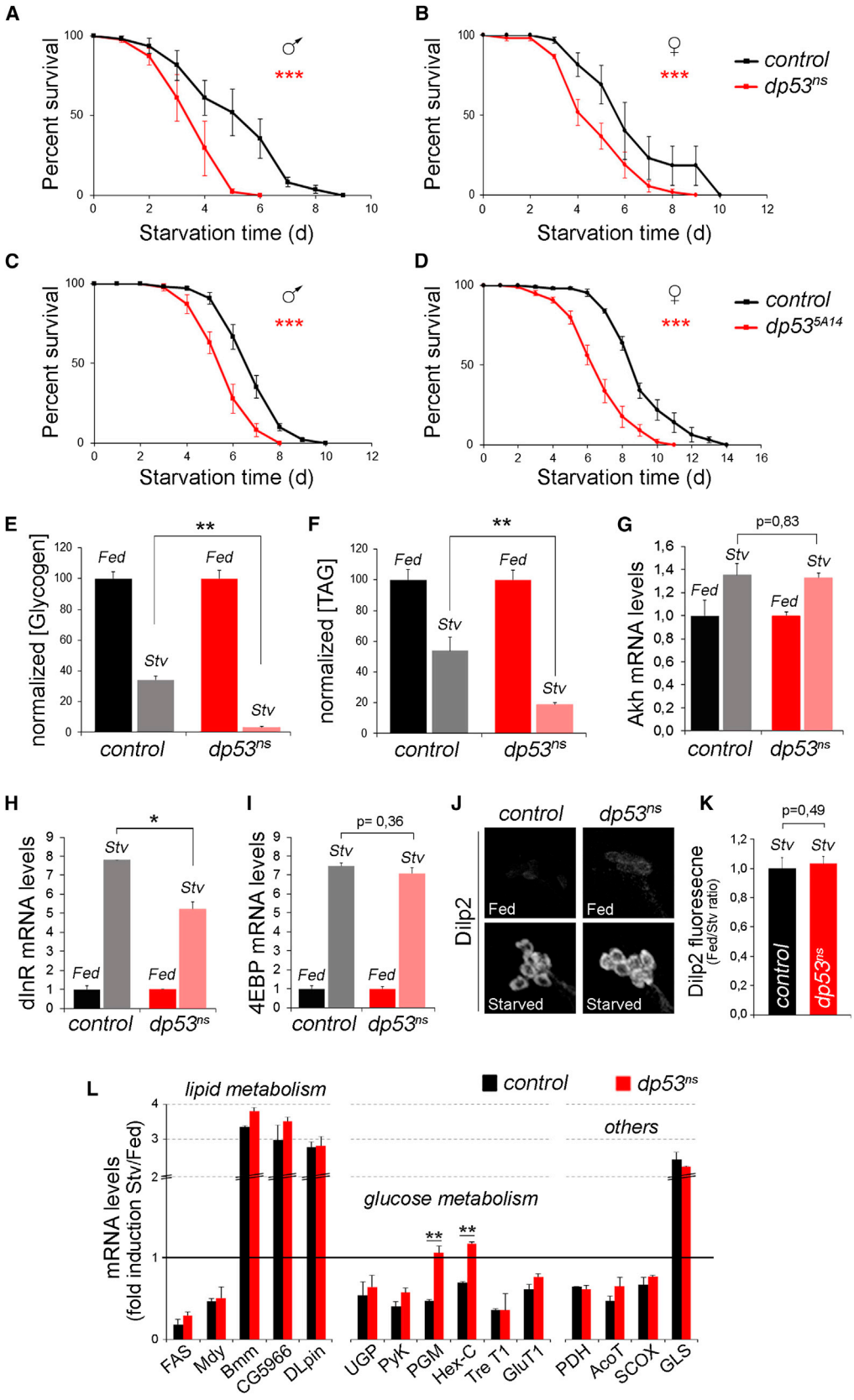

(legend on next page)

Intracellular TAG storage occurs in specialized cytoplasmic compartments called lipid droplets. In line with the accelerated TAG consumption observed in starved *dp53* mutant flies, specific depletion of Dp53 in single FB cells caused smaller lipid droplets (labeled by Nile red staining) than in wild-type cells upon fasting (Figure 2N). No significant change in lipid droplet size was observed in well-fed FB cells depleted for Dp53 activity (Figure 2M). Altogether, these results indicate that Dp53 plays a cell-autonomous and FB-specific role in metabolic adaptation to starvation, as energy store breakdown is accelerated in Dp53-depleted animals and survival rates are compromised. Consistent with this proposal, overexpression of Dp53 in FB cells increased the starvation resistance of adult flies (Figure 2G), and FB-specific expression of Dp53 rescued the reduced survival rates of starved *dp53* mutant animals (Figure 2H).

Since Dp53 activity modulates the levels of energy store breakdown and the amount of stored fat in individual cells, it is likely to operate via the regulation of cellular metabolism. We thus measured RNA levels, by quantitative RT-PCR, of a panel of 15 key metabolic enzymes in fed and starved individuals (Figure 1L). In conditions of nutrient deprivation, the FB supplies energy to the rest of the body by mobilizing stored resources to circulation (Arrese and Soulages, 2010). Consistently, a pronounced increase in the expression levels of the Brummer lipase (the homolog of the mammalian adipose triglyceride lipase; Grönke et al., 2005) and the CG5966 lipase, both used to mobilize stored TAGs in the FB (Kühnlein, 2012), and a clear reduction in the expression levels of lipogenic enzymes, such as fatty acid synthase and Midway, were observed in control animals upon fasting (Figure 1L). We also observed in these animals a drastic reduction in the expression levels of metabolic enzymes involved in glycolysis (pyruvate kinase, phosphoglucose mutase, and hexokinase C), cellular respiration (pyruvate dehydrogenase), and fatty acid oxidation (acetyl-coenzyme A thiolase and cytochrome *c* oxidase). These changes might reflect reduced rates of glucose and fatty acid catabolism in starved FB cells and a preferential use of these metabolites for the production of circulating sugars and lipids to be used by peripheral tissues during fasting periods.

Dp53 activity does not appear to directly modulate the levels of those enzymes involved in mobilizing energy resources during starvation (Figure 1L). *Drosophila* Lipin (dLpin), a central regulator of adipose tissue development that promotes survival to starvation (Ugrankar et al., 2011), was also similarly upregulated in control and *dp53* mutant flies. Interestingly, we noticed that the levels of the glycolytic enzymes phosphoglucose mutase (PGM) and hexokinase-C (HexC) remained unchanged in *dp53* mutant flies (Figure 1L). These differences suggest an active glycolytic pathway in starved *dp53* mutant flies, which is consistent with the reduced amount of sugars under nutrient deprivation (Figure 2K). This reduction might contribute to their poor survival rates, as an increase in the concentration of sugar in the medium (2% agar, 10% sucrose) rescued the survival rates of starved *dp53* mutant animals (Figure S1). These results point to a role of Dp53 in metabolic adaptation to nutrient deprivation of FB cells and suggest that reduced survival rates of fasted *dp53* mutant animals are most probably a consequence of deregulated consumption of sugar and faster depletion of energy resources.

Dp53 Is a Target of the miRNA Machinery

p53 is tightly regulated and maintained at low physiological levels in unstressed cells to prevent its deleterious effects on living organisms. We then examined whether Dp53 is specifically activated upon starvation in FB cells. For this purpose, we used a reporter of Dp53 activity that places a nuclear GFP (GFPnls) under the control of an enhancer of the *reaper* (rpr) locus that includes a p53 consensus binding site (*dp53R-GFPnls*; Lu et al., 2010). This reporter has been used in different cellular contexts to monitor induction of Dp53 activity upon several stresses. As shown in Figures 2O and 2P, Dp53 activity levels were increased in FB cells subjected to starvation as monitored by the rise in nuclear GFP expression levels of starved *dp53R-GFPnls* animals.

In mammals, a complex array of posttranslational modifications negatively regulates the stability, localization, conformation, and transcriptional activity of p53 in healthy cells (Gu and Zhu, 2012). Although the most critical step is the regulation of p53 by ubiquitin ligases such as Mdm2 (Toledo and Wahl, 2006), recent studies confirmed the old hypothesis that *Drosophila* lacks Mdm2 (Lane and Verma, 2012). In the last few years, the expression and activity of vertebrate p53 has been shown to be under the control of miRNAs (Hermeking, 2012). In order to address the contribution of the miRNA machinery to regulating Dp53 levels, we constructed a transgene consisting of the 3′ UTR of *dp53*, which is shared by the three alternative spliced forms, cloned into a tubulin-promoter-EGFP reporter plasmid (*dp53-sensor*; Figure 3A). The contribution of the miRNA machinery to regulating Dp53 levels was tested by depleting Dcr-1 activity, a critical element for miRNA biogenesis (Lee

Figure 1. Dp53 Modulates the Consumption of the Main Energy Storages upon Fasting and Contributes to Animal Resistance to Starvation

(A–D) Survival rates to nutrient deprivation of *dp53* mutant ($dp53^{ns}$ in A and B and $dp53^{5A14}$ in C and D) and control (w^{1118}) flies. Both males (A and C) and females (B and D) are shown. See Table S1 for n, p, median, and maximum survival values. The p value tests the null hypothesis that the survival curves are identical.

(E and F) Histograms plotting glycogen (E) and TAG (F) levels from adult male *dp53* mutant ($dp53^{ns}$) and control (w^{1118}) flies under fed or starved (Stv) conditions. Data were normalized to protein concentration and presented as a percentage of the fed values for each genotype.

(G–I) Histograms plotting Akh (G), dInR (H), and 4EBP (I) mRNA levels from adult male *dp53* mutant ($dp53^{ns}$) and control (w^{1118}) flies subjected to fed or starved (Stv) conditions. Results are expressed as fold induction with respect to fed conditions for each genotype. Heads were used in (G) and full bodies in (H) and (I).

(J) Brain IPCs stained to visualize dILP2 (white) protein levels in *dp53* mutant ($dp53^{ns}$) and control (w^{1118}) animals under fed or starved conditions.

(K) Histogram plotting mean dILP2 fluorescence intensity as a Fed/Stv ratio of IPCs shown in (I). Results were normalized to control flies.

(L) Histograms plotting mRNA levels of a collection of 15 key metabolic enzymes from adult males of *dp53* mutant ($dp53^{ns}$) and control (w^{1118}) flies subjected to fed or starved (Stv) conditions. Results are expressed as fold induction with respect to fed conditions for each genotype.

Animals were starved on 2% agar, 1% sucrose chronically (A–D), for 24 hr (E and G–L), or for 72 hr (F).

Error bars represent SEM. ***$p < 0.001$, **$p < 0.01$, and *$p < 0.05$.

See also Figure S1 and Tables S1 and S2.

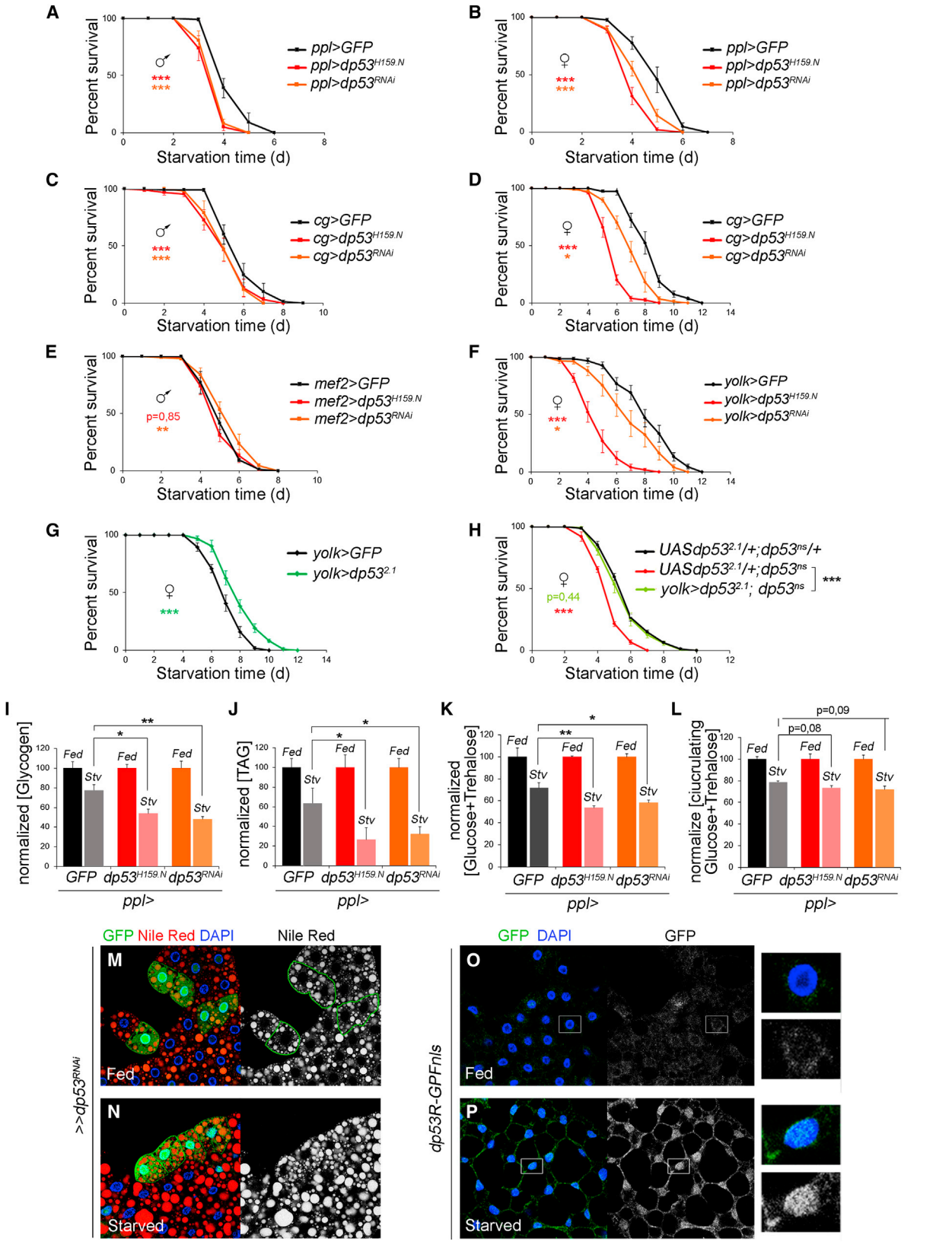

(legend on next page)

et al., 2003). miRNA-mediated targeting of the *dp53 3′UTR* is expected to maintain enhanced GFP (EGFP) expression levels of the *dp53 sensor* low under normal physiological conditions (Figures 3B and 3G). We first used the larval wing primordium, a simple epithelium, to address the contribution of the miRNA machinery to targeting the *dp53-sensor*. Expression of a dsRNA form of *dcr-1* (*dcr-1*^{RNAi}) either with ubiquitous (*actin*-Gal4; Figure S3) or region-specific (*hh*-Gal4 and *ptc*-Gal4; Figures 3C and S3) Gal4 drivers induced an increase in EGFP levels of the *dp53-sensor* in wing cells. Clones of cells mutant for a null allele of *dcr-1* (*dcr-1*^{Q1147X}; marked by the absence of β-galactosidase [β-gal]) also showed increased EGFP expression levels of the *dp53-sensor* when compared to the surrounding heterozygous tissue (Figure 3D, red arrows).

To further characterize the regulation of *dp53* by the miRNA machinery, we searched for potential miRNA binding sites in its 3′ UTR. Ten putative miRNAs were predicted to target the 3′ UTR of *dp53* (Figure S3). We assessed the capacity of these miRNAs to reduce the activity of a *dp53* 3′ UTR luciferase reporter in S2 cells and the EGFP expression levels of the *dp53-sensor* in wing disc cells. Five miRNAs reduced the activity of the *dp53* 3′ UTR luciferase reporter when overexpressed in S2 cells (Figure S3), and only three of these five (*miR-219*, *miR-283*, and *miR-305*) reduced the *dp53-sensor* in wing disc cells (Figures 3H and S3). Interestingly, the predicted binding site for *miR-305* targeted *dp53* in a region that is conserved among *Drosophila* species (Figure S3). In addition, *miR-305* showed high expression values in a large-scale sequencing of small RNAs in *Drosophila*, while miR-219 and miR-283 were underrepresented (Ruby et al., 2007). Using quantitative RT-PCR, we confirmed that *miR-305* was indeed highly enriched in FB cells (data not shown). These results support the proposal that *miR-305* is a biologically relevant candidate miRNA involved in regulating Dp53 levels in *Drosophila* tissues. To further characterize the role of *miR-305* in regulating *dp53*, we generated an EGFP sensor carrying the *dp53 3′UTR* lacking the predicted *miR-305* binding site (*dp53Δ305-sensor*; Figures 3E and 3F). *miR-305* overexpression did not reduce the EGFP levels of the *dp53Δ305-sensor* (compare Figures 3H and 3J), thereby indicating that regulation of the *dp53 3′UTR* by this miRNA depends on the presence of the predicted *miR-305* binding site. We observed that the EGFP expression levels of the *dp53Δ305-sensor* were consistently higher than those in the *dp53-sensor* carrying the whole 3′ UTR (compare Figures 3G and 3I). This finding thus suggests that *miR-305* has an active role in targeting *dp53 3′UTR* under normal physiological conditions. Consistent with this proposal, clones of cells (marked by the absence of β-gal) homozygous for a small deficiency covering the *miR-305* locus (*Df-miR-305*, for details see the Experimental Procedures) showed increased EGFP levels of the *dp53-sensor* (Figure 3K, red arrows). The resulting *wild-type* twin clones (marked by two copies of β-gal) showed reduced levels of the *dp53-sensor* (Figure 3K, yellow arrows) when compared to the surrounding heterozygous tissue. Thus, regulation of the *dp53-3′UTR* appears to be highly sensitive to the doses of *miR-305*. Interestingly, no apparent differences in the *dp53Δ305-sensor* were observed in clones of cells lacking *miR-305* (Figure 3L, red arrows). These results indicate that *miR-305* contributes to the regulation of *dp53* and that this regulation depends on the presence of the predicted *miR-305* binding site. We found that the increase in EGFP expression levels caused by *miR-305* depletion was milder than that observed in clones of cells mutant for *dcr-1* (compare Figures 3D and 3K). Thus, other miRNAs might contribute to regulating Dp53 levels in the wing disc. Consistently, clones of cells mutant for a null allele of *dcr-1* showed increased EGFP expression levels of the *dp53Δ305-sensor* (Figure S3).

Regulation of Dp53 by *miR-305* Is Modulated by Nutritional Conditions

We next addressed whether the regulation of *dp53* by the miRNA machinery also takes place in FB cells and whether this regulation is modulated by the nutritional status of the animal. Dp53 is indeed a target of the miRNA machinery in FB cells, as FB cells expressing *dcr-1*^{RNAi} showed increased EGFP levels of the *dp53-sensor* (Figure 4A; cells were marked by the absence of CD2) and FB cells expressing *miR-305* showed a reduction in the *dp53-sensor* EGFP levels (Figure 4B; cells were marked by the expression of red fluorescent protein). In order to address the potential modulation of this regulation by nutritional status, the EGFP levels of the *dp53-sensor* were analyzed in FB cells of starved and nonstarved animals. Although the EGFP

Figure 2. A FB-Specific Role of Dp53 in the Metabolic Adaptation to Nutrient Deprivation

(A–F) Survival rates to nutrient deprivation of adult flies expressing *GFP*, *Dp53*$^{H159.N}$, or *dp53*^{RNAi} in FB cells (A–D and F) or muscle cells (E) under the control of the *ppl-gal4* (A and B), *cg-gal4* (C and D), *mef2-gal4* (E), and *yolk-gal4* (F) drivers. Both males (A, C, and E) and females (B, D, and F) are shown. *yolk-GAL4* is expressed only in females.

(G) Survival rates to nutrient deprivation of adult females expressing *GFP* or a wild-type form of Dp53 (Dp53$^{2.1}$) under the control of the *yolk-gal4* driver.

(H) Survival rates to nutrient deprivation of adult females of the indicated genotypes. Note rescue in the survival rates to starvation of *dp53*^{ns} mutant flies upon expression of Dp53$^{2.1}$ in the FB.

See Table S1 for n, p, median, and maximum survival values. The p value tests the null hypothesis that the survival curves are identical.

(I–L) Histograms plotting whole-body glycogen (I), TAG (J), total glucose plus trehalose (K), or hemolymph glucose plus trehalose (L) levels from adult flies expressing *GFP*, *Dp53*$^{H159.N}$, or *dp53*^{RNAi} in FB cells under fed or starved (Stv) conditions. Data were normalized to protein concentration and presented as a percent of the fed values for each genotype.

Animals were starved on 2% agar, 1% sucrose chronically (A–H), for 24 hr (I, K, and L), or for 72 hr (J). Error bars represent SEM. ***$p < 0.001$; **$p < 0.01$, and *$p < 0.05$.

(M and N) Lipid droplets, visualized by Nile red staining (in red or white), in FB cells of fed (M) and starved (N) animals. Starved FB cells expressing *dp53*^{RNAi} (marked by the expression of GFP, in green) showed smaller lipid droplets that the neighboring wild-type cells. DAPI (in blue) labels FB nuclei.

(O and P) FB cells labeled to visualize the GFP levels (in green or white) of a Dp53 activity reporter construct (*dp53R-GFPnls*) in fed (O) or starved for 48 hr (P) animals.

See also Figure S2 and Table S1.

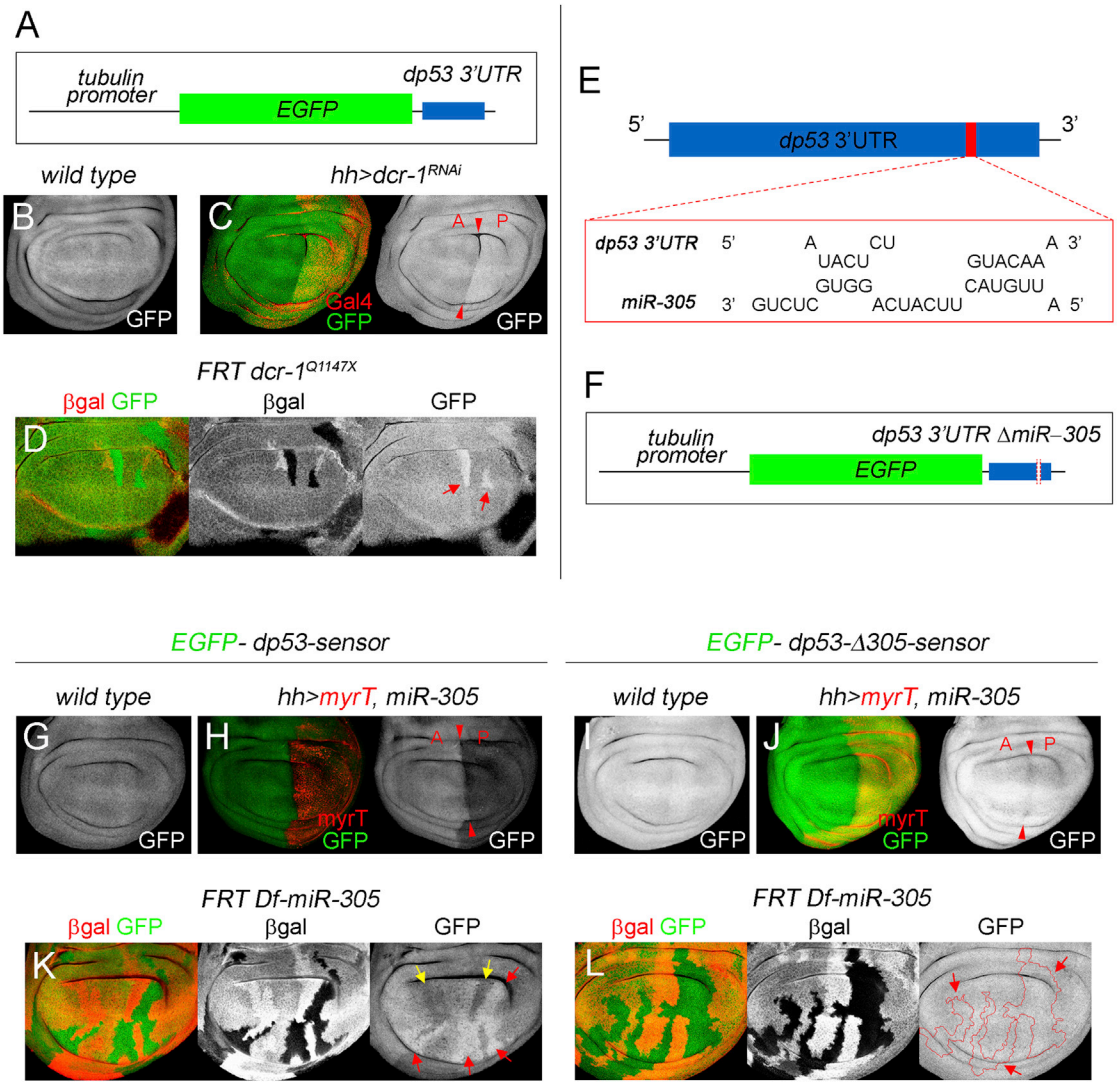

Figure 3. Dp53 Is a Target of *miR-305*

(A) Cartoon depicting the tubulin-EGFP transgene carrying the 3′ UTR of dp53 (*dp53-sensor*).

(B and C) Wing discs carrying the *dp53-sensor* and stained to visualize EGFP (green) and Gal4 (red) protein expression. The wing disc in (C) expressed *dcr-1*^{RNAi} under the control of the *hh-Gal4* driver. Red arrowheads depict the anterior-posterior (A-P) boundary.

(D) *dcr-1*^{Q1147X} homozygous clones (marked by the absence of *β-gal*, in red) showing expression of the *dp53-sensor* (green). Note increased levels of EGFP in *dcr-1*-depleted cells (red arrows).

(E) Representation of the putative binding site of *miR-305* in the *3′UTR* of *dp53*.

(F) Cartoon depicting the tubulin-EGFP transgene carrying the *3′UTR* of *dp53* with a deletion covering the *miR-305* seed region (*dp53Δ305-sensor*).

(G–J) Wing discs carrying the *dp53-sensor* (G and H) or the *dp53Δ305-sensor* (I and J) and stained to visualize EGFP (green) protein expression. Wing discs in (H) and (J) overexpressed *miR-305* and myrTomato (myrT) under the control of the *hh-Gal4* driver. Note reduced levels of the *dp53-sensor*, but not the *dp53Δ305-sensor*, in *miR-305*-overexpressing cells. Red arrowheads depict the A-P boundary.

(K and L) *Df(miR-305)* homozygous clones (marked by the absence of *β-gal* in red) showing expression of the *dp53-sensor* (K) or *dp53Δ305-sensor* (L). Note increased levels of the *dp53-sensor*, but not the *dp53Δ305-sensor*, in *Df(miR-305)* cells (red arrows). Also note in (K) decreased EGFP levels in twin clones with two wild-type copies of *miR-305* (yellow arrows).

See also Figure S3.

levels of a control sensor (Brennecke et al., 2003) were mildly reduced upon starvation, most probably as a consequence of the decrease in whole-animal metabolism (Figures 4C and 4C′; quantification in Figure 4F), the *dp53-sensor* was expressed at higher levels in starved than in normally fed individuals (Figures 4D and 4D′; quantification in Figure 4F). Remarkably, the impact of nutritional conditions on the *dp53-sensor* depended on the presence of the *miR-305* binding site, as no significant changes in the EGFP levels were observed in FB cells carrying the *dp53Δ305-sensor* and subjected to starvation (Figures 4E and

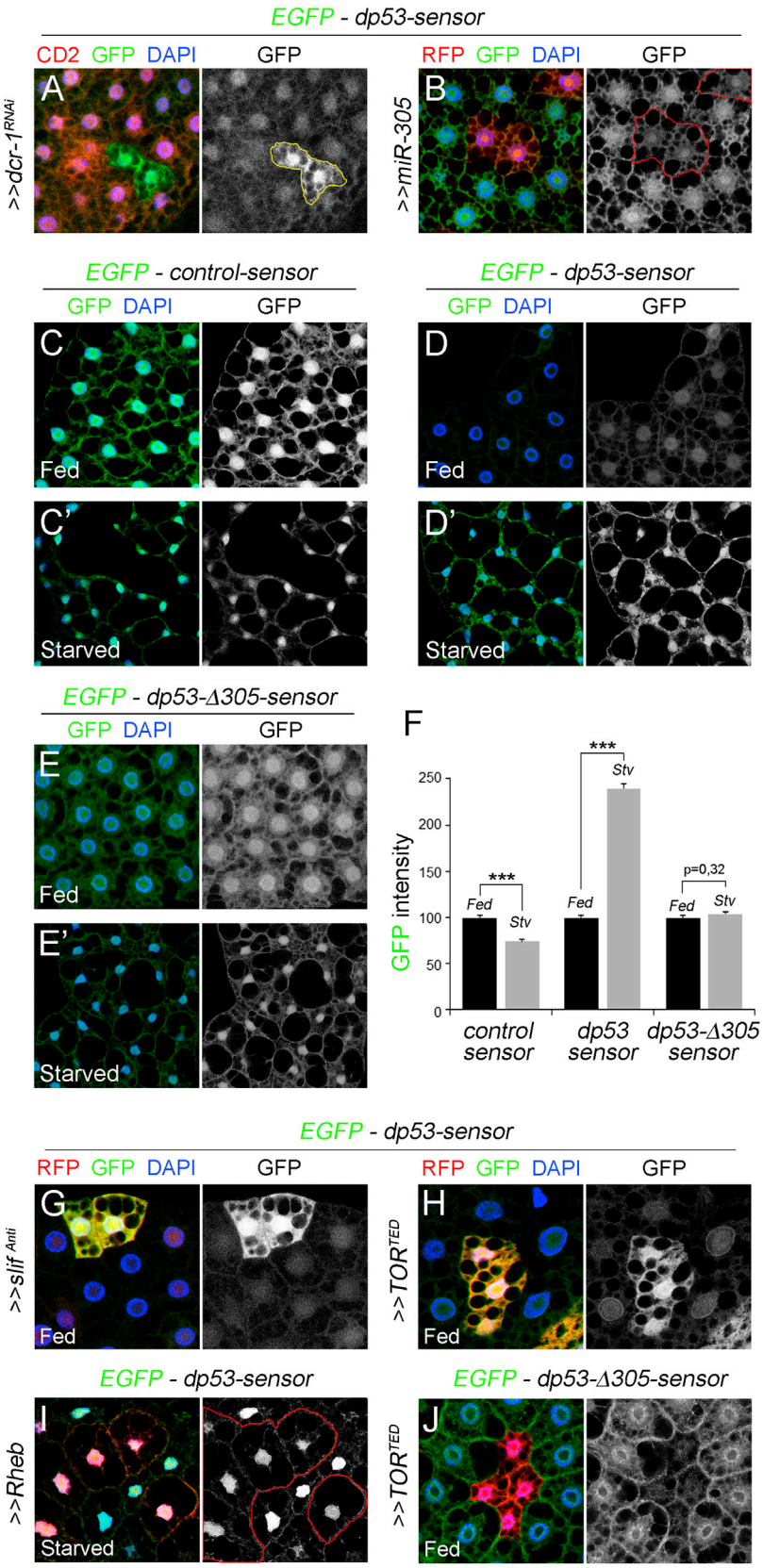

Figure 4. *miR-305*-Dependent Regulation of Dp53 Is Modulated by Nutrition

(A and B) FB cells of well-fed animals expressing *dcr-1*^{RNAi} (marked by the absence of CD2) or overexpressing *miR-305* and red fluorescent protein (RFP) (red), carrying the *dp53-sensor*, and stained to visualize EGFP (green) and CD2 (red) protein expression. Note increased EGFP levels in *dcr-1*^{RNAi} expressing cells and reduced EGFP levels upon *miR-305* overexpression.

(C–E) EGFP levels of the control sensor (C and C′), *dp53-sensor* (D and D′), or *dp53Δ305-sensor* (E and E′) in the FB of animals fed (C, D, and E) or starved for 48 hr (C′, D′, and E′).

(F) Histogram plotting EGFP expression levels of FB cells shown in (C)–(E). Results are normalized to the fed condition for each genotype. Note increased levels of *the dp53-sensor*, but not of the *dp53Δ305-sensor* and control sensor, under starvation. Error bars represent SEM. ***$p < 0.001$.

(G, H, and J) FB cells expressing RFP (red) and slif^{Anti} (G) or TOR^{TED} (H and J) in well-fed animals carrying the *dp53-sensor* (G and H) or the *dp53Δ305-sensor* (J) and stained to visualize EGFP (green) protein expression.

(I) FB cells expressing RFP and Rheb in starved animals carrying the *dp53-sensor* and stained to visualize EGFP (green) protein expression. Note increased EGFP levels in starved FB cells and reduced levels upon Rheb overexpression (enlarged cells delimited by red lines).

4E′; quantification in Figure 4F). These results support a major contribution of *miR-305* in targeting Dp53 in FB cells and imply that the regulation of the *dp53 3′UTR* is modulated by the nutritional status of the animal.

The major nutritional signal sensed by FB cells is amino acid availability, and downregulation of the amino acid transporter Slimfast (Slif) in the FB phenocopies amino acid deprivation (Colombani et al., 2003). TOR, an essential regulator of cell and tissue growth, is regulated in response to amino acid availability (Grewal, 2009; Hietakangas and Cohen, 2009). Once activated, TOR signaling modulates a variety of cellular processes such as protein synthesis, ribosome biogenesis, and autophagy. Thus, TOR signaling functions as the main nutritional sensor of a cell by coupling nutrient status to metabolic activity. We then examined whether genetic modulation of Slif or TOR activities in FB cells modulates the EGFP levels of the *dp53-sensor*. Well-fed animals showed a clear increase in the EGFP expression levels of the *dp53-sensor* in FB cells expressing an RNA antisense form of slif ($slif^{Anti}$; Figure 4G) or a dominant-negative version of TOR (TOR^{TED}; Figure 4H; Hennig and Neufeld, 2002). In contrast, activation of TOR (by expressing the GTPase Rheb, a positive regulator of TOR complex 1) in otherwise starved animals is expected to genetically mimic feeding conditions. Consistently, Rheb overexpression in FB cells strongly reduced the capacity of nutrient deprivation to upregulate the EGFP expression levels of the *dp53-sensor* (Figure 4I). Taken together, these results indicate that modulation of the *dp53-sensor* in FB cells is a cell-autonomous process that depends on TOR activity and support the notion that Dp53 is activated in FB cells by nutrient deprivation. Interestingly, the impact of TOR on the *dp53-sensor* depended on the presence of the *miR-305* binding site, as no increase in the EGFP levels was observed in FB cells carrying the *dp53Δ305-sensor* and expressing TOR^{TED} (Figure 4J; compare with Figure 4H). On the contrary, GFP expression levels were mildly reduced, most probably due to the reduction in translation caused by the strong depletion of TOR activity in these cells. These results reinforce the proposal that TOR signaling affects Dp53 activity levels through *miR-305*.

Nutrition-Dependent Regulation of the miRNA Machinery Contributes to Starvation Resistance

Nutrient conditions modulate, through Slif and TOR signaling, the capacity of *miR-305* to target *dp53* via its 3′ UTR, thus raising the possibility that *miR-305* levels are directly regulated by nutritional status. In order to address this possibility, we subjected adult flies to starvation and determined the levels of *miR-305* and seven other miRNAs by quantitative RT-PCR. Remarkably, the levels of six miRNAs, including *miR-305*, were reduced upon starvation (Figure 5A), suggesting a general rather than specific downregulation of miRNAs upon starvation. Emerging data have provided evidence that the whole miRNA machinery can be targeted under several stress conditions (Blandino et al., 2012; Gibbings et al., 2012; Ho et al., 2012), thus opening up the possibility that the miRNA-processing machinery itself is targeted under nutrient deprivation in FB cells. Consistent with this proposal, the expression levels of Dicer-1 and Drosha, enzymes involved in miRNA processing, and Argonaute-1, a catalytic component of RISC (Huntzinger and Izaurralde, 2011), were reduced both in starved adult flies and starved larval FBs (Figures 5B and 5C). These results indicate that starvation reduces the expression levels of central elements of the miRNA machinery and, consequently, alleviates *miR305*-mediated targeting of the *dp53-sensor* in FB cells. Consistent with this proposal, overexpression of *miR-305* in FB cells of starved animals was unable to reduce the EGFP levels of the *dp53-sensor* (Figure 5D, red arrowheads), whereas it was able to do so in well-fed animals (Figure 4B), and the levels of mature *miR-305* were reduced in starved animals that overexpressed *miR-305* in FB cells when compared to normally fed animals of the same genotype (Figure 5E). These results indicate that processing of *miR-305* is compromised in starvation.

We then determined whether systemic or FB-specific depletion of the miRNA processing machinery increased the survival rates of adult flies subjected to starvation and whether this extension relied on the activity of Dp53. Halving the doses of the *dcr-1* gene ($dcr\text{-}1^{Q1147X}$/+ flies show reduced levels of mature miRNAs including *miR-305*; Figure S4), or having the doses of the *miR-305* locus (in *Df-miR-305*/+ flies) increased the survival rates of both males and female adult flies subjected to nutrient starvation when compared to *control* flies (Figures 6A–6D and 6I; Table S1). The levels of TAGs and glycogen were increased in both genotypes at the beginning of the starvation procedure, and the consumption of energy resources was delayed with time (Figure S4). This is most likely a consequence of increased levels of Dp53 activity and the proposed role of Dp53 in reducing glycolysis in FB cells, as halving the doses of the *dp53* gene reverted the survival rates of *dcr-1* heterozygous flies (in $dcr\text{-}1^{Q1147X}/dp53^{ns}$ flies; Figure 6I). Targeted expression of a dsRNA form of *dcr-1* in FB cells (in $ppl > dcr\text{-}1^{RNAi}$ flies) also increased starvation resistance (Figures 6E and 6F; Table S1), and the extended survival rates were reverted upon coexpression of a dominant-negative version of Dp53 (in $ppl > dcr\text{-}1^{RNAi}$, $dp53^{H159.N}$ flies; Figures 6G and 6H). Parental UAS lines (*UAS-dcr-1*^{RNAi}, and *UAS-dcr-1*^{RNAi} *UAS-dp53*$^{H159.N}$) showed similar survival rates upon fasting than control UAS-GFP flies (Figure S4; Table S1). Altogether, these results indicate that depletion of nutrients reduces the activity of the miRNA machinery in FB cells and as a consequence alleviates *miR-305*-mediated targeting of *dp53,* which eventually contributes to organismal resistance to nutrient deprivation.

DISCUSSION

The tumor suppressor gene p53 has been reported to mediate metabolic changes in cells through the regulation of several metabolic pathways and can promote cell survival upon nutrient deprivation (Maddocks et al., 2013; Vousden and Ryan, 2009). Here, we provide evidence that *Drosophila* p53 participates in organismal adaptation to nutrient deprivation and exerts its function by modulating the breakdown of energy resources in FB cells. The response of an organism to metabolic stress, such as starvation, is largely dependent on its capacity to derive energy from stored reserves like TAGs and glycogen (Arrese and Soulages, 2010). Energy storage in FB cells is known to be modulated by the combined action of dILPs and AKH. In

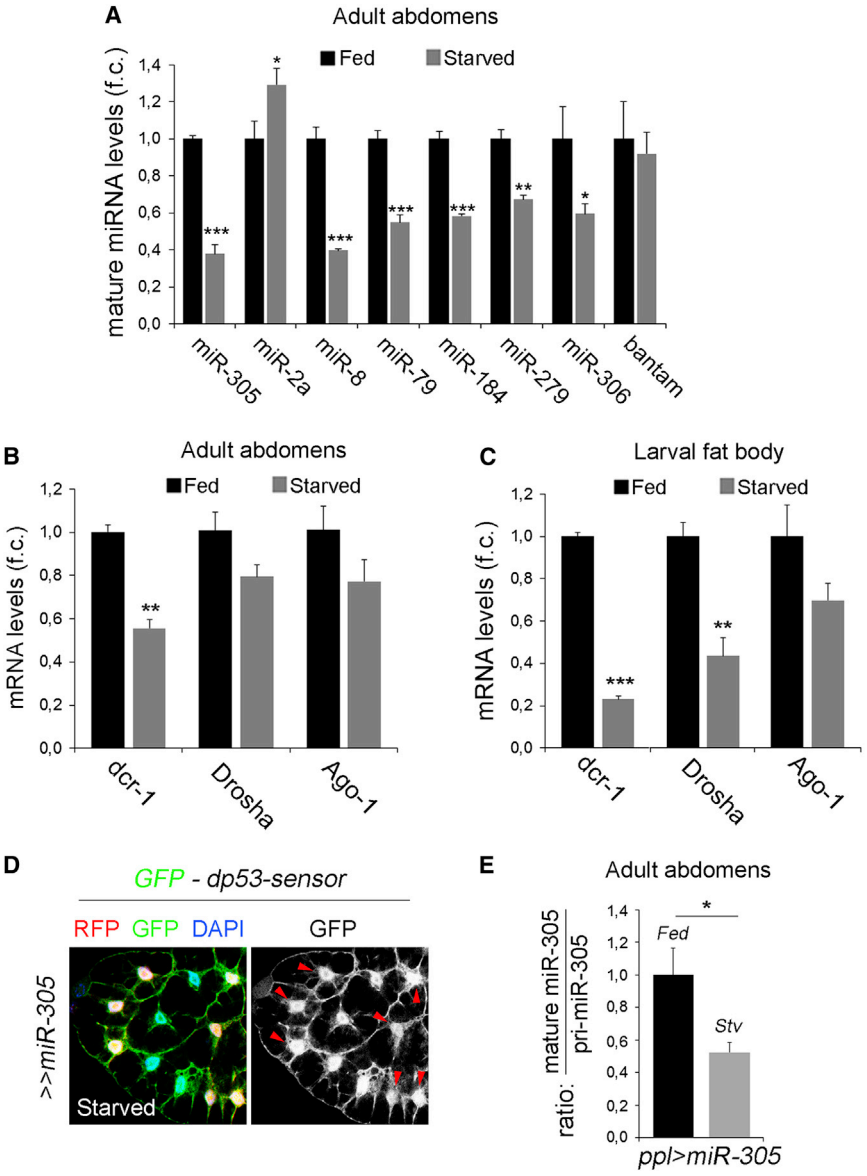

Figure 5. Reduced Activity of the miRNA Pathway Caused by Nutrient Deprivation

(A–C) Histograms plotting mature miRNAs levels (A) or Drosha, Dicer-1, and Argonaute-1 expression levels (B and C) measured by quantitative RT-PCR of adult abdomens (A and B) or larval FBs (C) of fed (black bars) or starved (gray bars) control animals. Results are expressed as fold induction with respect to fed conditions.

(D) FB cells of starved animals overexpressing RFP and *miR-305*, carrying the *dp53-sensor*, and stained to visualize EGFP (green) protein expression. Note that *miR-305* overexpression did not reduce EGFP levels under these circumstances (compare with well-fed animals shown in Figure 4B).

(E) Histograms plotting the ratio between mature and primary *miR-305* levels measured by quantitative RT-PCR of adult abdomens of fed (black bar) or starved (gray bar) animals overexpressing *miR-305* in the FB (*ppl>miR-305*). Results are expressed as fold induction with respect to fed conditions.

Error bars represent SEM. ***$p < 0.001$, **$p < 0.01$ and *$p < 0.05$. See also Table S2.

well-fed animals, insulin signaling promotes energy storage, whereas during fasting periods, AKH and reduced levels of circulating dILPs contribute to the mobilization of energy resources (Bharucha et al., 2008; Kim and Rulifson, 2004; Rulifson et al., 2002). The changes in insulin signaling and AKH expression produced by nutrient deprivation were very similar in *Dp53*-depleted and control animals. Moreover, and consistent with the accelerated TAG consumption observed in starved *dp53* mutant flies, specific depletion of Dp53 activity in single FB cells caused smaller lipid droplets. Altogether, these observations support the notion that Dp53 has a cell-autonomous activity in FB cells, which impacts the rates of energy resources breakdown upon nutrient deprivation. The activity of Dp53 in FB cells also promotes organismal survival upon nutrient deprivation. Reduced survival rates of fasting *dp53* mutant animals are most probably a consequence of reduced amount of sugar in the animal, as increasing the concentration of sugar in the food rescued the survival rates of fasting *dp53* mutant animals.

The accelerated consumption of energy resources observed in starved *Dp53*-depleted animals does not appear to be a consequence of altered changes in metabolic enzymes involved in mobilizing these resources. Fasting also induces a decrease in the levels of enzymes involved in glycolysis, cellular respiration, and fatty acid β-oxidation. Reduced rates of glucose and fatty acid catabolism in starved FB cells might reflect a preferential use of these metabolites for the production of circulating sugars and lipids to be used by peripheral tissues upon starvation. Interestingly, the levels of the glycolytic enzymes PGM and Hex-C are reduced in control animals upon fasting but remain unchanged in *dp53* mutant flies. These results most probably reflect a defective functional specialization of *dp53* mutant FB cells toward the production of sugars in fasting conditions and support a role of Dp53 in metabolic adaptation to nutrient deprivation. Of note, PGM is negatively regulated by p53 in cultured mammalian cells (Kondoh et al., 2005), suggesting a conserved role of p53 in regulating glycolysis in vertebrate and invertebrate tissues.

In the last few years, the expression of p53 has been shown to be under the control of miRNAs (Hermeking, 2012). We have analyzed the involvement of the miRNA machinery in targeting *dp53* in normal physiological conditions and upon nutritional starvation. We present evidence that, in normal physiological conditions, the miRNA machinery targets the *dp53 3′UTR* and have identified *miR-305* as a major regulatory element. Nutrient

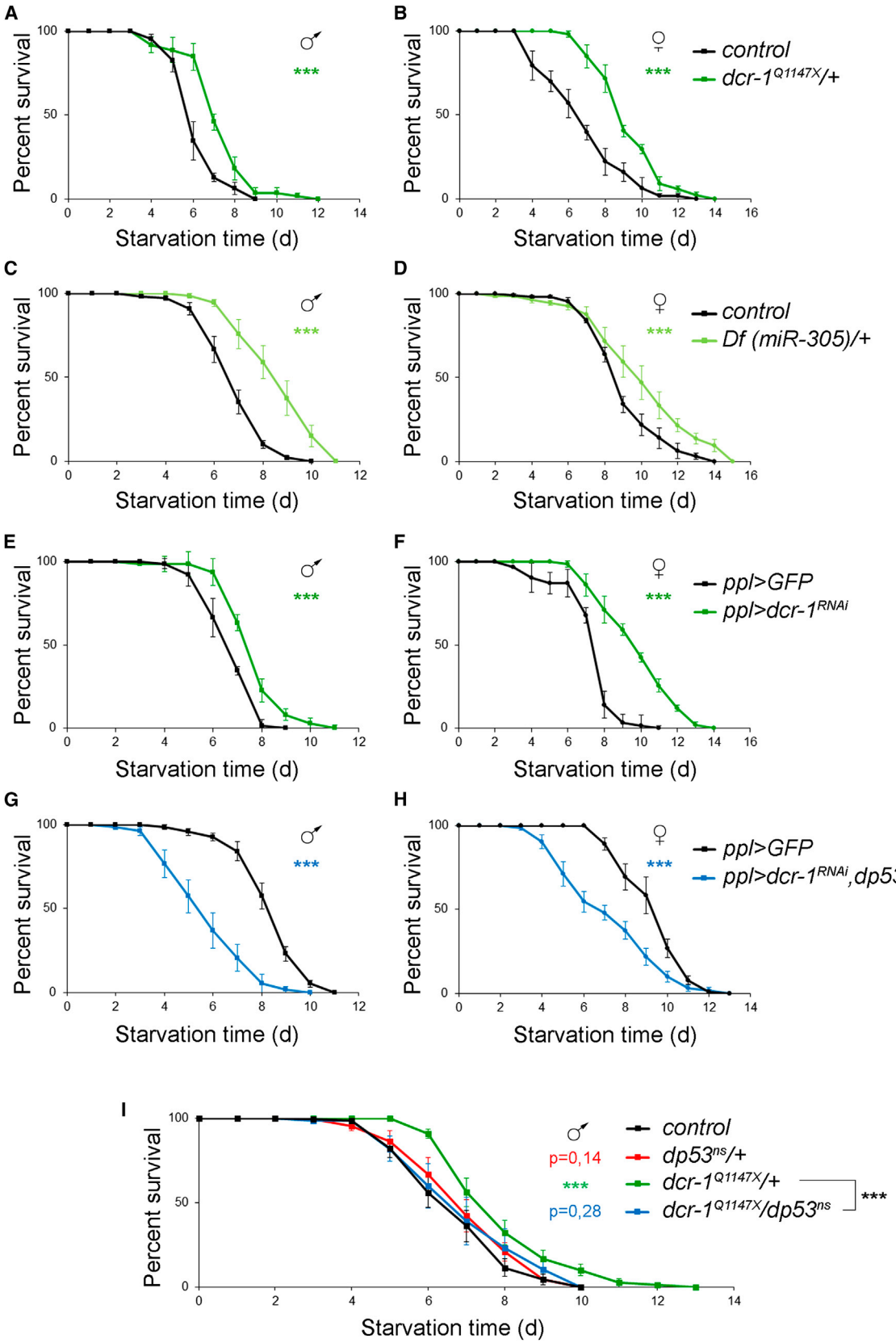

(legend on next page)

conditions modulate the capacity of the miRNA machinery to target Dp53, as nutrient deprivation, depletion of the Slimfast amino acid transporter, or reduced activity of TOR signaling diminishes the ability of *miR-305* to target the *dp53 3′UTR.* Although these results open up the possibility of a specific modulation of *miR-305* levels by nutrition, our findings unravel a general downregulation of miRNA levels in fasted FB cells. Thus, the expression levels of Drosha and Dicer, involved in miRNA processing, and Ago1, a component of RISC, were downregulated upon nutrient deprivation. A similar impact on the activity of the whole miRNA machinery has been observed under several stress conditions, including hypoxia, autophagy, UV radiation, and oxidative stress (Blandino et al., 2012; Gibbings et al., 2012; Ho et al., 2012). Thus, stress-induced depletion of the miRNA machinery appears to be a conserved mechanism that contributes to the derepression of certain genes involved in the biological responses to the original stress, in this particular case to nutrient deprivation.

The miRNA machinery was previously shown to promote tissue growth by targeting the *Drosophila* ortholog of the TRIM32 tumor suppressor gene Mei-P26, which triggers proteasome-dependent degradation of the proto-oncogene dMyc (Herranz et al., 2010). Increased levels of Mei-P26 target dMyc protein for degradation, thus reducing the capacity of the tissue to increase cellular mass. In addition, the conserved miRNA *miR-8* and its target, *USH*, regulate body size in *Drosophila* (Hyun et al., 2009). USH is a negative regulator of the PI3K signaling pathway, and overexpression of *miR-8* in FB cells activates PI3K and promotes growth cell autonomously. The identification of Dp53 as a critical element modulating the consumption of energy resources in FB cells and its regulation by the miRNA machinery point to a central role of miRNAs in coordinating the cellular and physiological responses to nutritional starvation. In response to nutrient deprivation, downregulation of Dicer-1, Drosha, and Ago1 levels result in a general reduction of active mature miRNAs in FB cells, thus contributing to the expected decrease in the activity of growth-promoting genes (dMyc) or pathways (PI3K) and a concomitant increase in the activity of genes, such as *dp53*, that modulate the rates of glycogen and TAG catabolism.

Amino acid sensing by TOR in FB cells regulates, through Upd/JAK-STAT signaling, the rates of dILPs secretion in the insulin-producing cells (Géminard et al., 2009; Rajan and Perrimon, 2012), which in turn modulate, through the insulin-like receptor signaling pathway, fat cell mass in adult flies (adipocyte cell number and TAGs storage; DiAngelo and Birnbaum, 2009). Our study indicates that amino acid sensing by TOR also regulates Dp53 activity levels in FB cells and that Dp53 promotes, upon starvation, a functional specialization of FB cells toward the production of sugars and fatty acids to be used by the peripheral tissues. Thus, TOR and FB cells appear to play a fundamental role in coordinating the organismal response to starvation by sensing amino acid availability in the food.

EXPERIMENTAL PROCEDURES

Drosophila Genetics, Antibodies, and Constructs

Flies were raised at 25°C in standard medium (4% glucose, 55 g/l yeast, 0.65% agar, 28 g/l wheat flour, 4 ml/l propionic acid, and 1.1 g/l Nipagin). Fly stocks, mosaic analysis, constructs, antibodies, and immunohistochemistry are described in the Supplemental Experimental Procedures.

Starvation Treatments

Starvation procedures were adapted from (Rajan and Perrimon, 2012).

For starvation sensitivity assays, 15–20 (1- to 2-day-old) flies of each genotype were transferred into vials containing 2% agar and 1% sucrose. Flies were transferred to new tubes every day, and dead flies were counted. At least 100 flies per genotype were scored. Control animals were always analyzed in parallel in each experimental condition. Statistics were performed using GraphPad Prism 4.0 software, which uses the Kaplan-Meier estimator to calculate survival fractions as well as median and maximum survival values. Curves were compared using the log-rank (Mantel-Cox) test. The two-tailed p value indicates the value of the difference between the two entire survival distributions at comparison.

For starvation treatments in adults, 5- to 7-day-old flies were used and subjected to 24 hr (for glycogen and trehalose measurements and for expression analyses) or 72 hr (for TAG measurements) of starvation.

For starvation treatments in larvae, animals were synchronized in the second to third larval transition and placed 6 hr later in tubes with 2% agar 1% sucrose (starvation) or standard food (fed). After 24–48 hr, FBs were dissected and used for immunohistochemistry or RNA extraction.

Metabolic Assays

TAG, glycogen, and trehalose levels were performed as previously described (Palanker et al., 2009). Briefly, five adult males were homogenized in 200 μl of the corresponding buffers and immediately incubated at 70°C for 5 min to inactivate endogenous enzymes. For quantification of sugars in circulation, hemolymph was pooled from 40–45 adult flies to obtain 1 μl for assay, diluted 1:100, and incubated at 70°C for 5 min. For TAG assays, samples were assayed using a serum triglyceride determination kit (Sigma-Aldrich, TR0100) according to the manufacturer's protocol. For glycogen and trehalose measurements, samples were incubated with or without 1 U of Amyloglucosidase (Sigma-Aldrich, A7420, for glycogen) or with 0.05 U/ml of trehalase (Sigma-Aldrich, T8778, for trehalose) for 2 hr at 37°C and assayed using a Glucose (GO) Assay Kit (GAGO-20). Metabolite measurements were normalized to protein concentration (Bio-Rad). Five replicates for each genotype and condition were performed, and data were normalized with respect to the corresponding levels in control flies. Further details are in the Supplemental Experimental Procedures.

Quantitative RT-PCR

For the quantification of mRNA levels, total RNA was extracted using TRIzol reagent (Invitrogen) from FBs of ten larvae, abdomens of ten adult males, five decapitated adult males, or five heads, depending on the experiment. A total of 2 μg of total RNA was used as a template for cDNA synthesis using Maxima Reverse Transcriptase (Thermo Scientific). Maxima SYBR Green/ROX qPCR Master Mix (Thermo Scientific) was used, and reactions were run in a Light Cycler 480 Real Time qPCR machine (Roche). Transcript levels were normalized to tubulin. The primer pairs used are tabulated in Table S2.

Figure 6. Increased Starvation Resistance upon FB-Specific Depletion of the miRNA Machinery

Survival rates to nutrient deprivation (2% agar, 1% sucrose) of young adult flies of the genotypes $dicer^{Q1147X}$/+ (A, B, and I), *Df(miR-305)*/+ (C and D), *ppl-gal4; UAs-dcr-1*^{RNAI} (E and F), *ppl-gal4, UAS-dcr-1*^{RNAi}, *UAS-dp53*$^{H159.N}$ (G and H), $dp53^{ns}$/+ (I), and $dicer^{Q1147X}/dp53^{ns}$ compared to control flies (black lines) of the genotypes *FRT82B* ry^{506}/+ (A and B), w^{1118} (C, D, and I), and *ppl-gal4; UAS-GFP* (E–H) subjected to the same procedure. Both males (A, C, E, G, and I) and females (B, D, F, and H) are shown. See Table S1 for n, p, median, and maximum survival values. Error bars represent SEM. ***$p < 0.001$. The p value tests the null hypothesis that the survival curves are identical.

See also Figure S4 and Table S1.

For quantification of mature miRNA levels, total RNA was extracted from the abdomens of ten adult flies with TRIzol reagent (Invitrogen). A total of 10 ng of RNA was used as a template for miRNA-specific cDNA synthesis (Applied Biosystems). miRNAs was quantified using TaqMan miRNA assays (Applied Biosystems). Snor442 and U27 were used for normalization.

In all cases, three independent samples were collected from each condition and genotype, and duplicate measurements were conducted.

SUPPLEMENTAL INFORMATION

Supplemental Information includes Supplemental Experimental Procedures, four figures, and two tables and can be found with this article online at http://dx.doi.org/10.1016/j.celrep.2014.06.020.

AUTHOR CONTRIBUTIONS

L.B., A.D., and M.M. conceived and designed the experiments. L.B. and A.D. performed the experiments. L.B., A.D., and M.M. analyzed the data. M.M. wrote the paper, and all authors approved the final version of the manuscript.

ACKNOWLEDGMENTS

We thank J. Abrams, J. Colombani, S. Cohen, R. Delanue, E. Izaurralde, H. Jasper, P. Leopold, N. Perrimon, A. Teleman, J.M. Reichhart, the Bloomington Stock Center, the Developmental Studies Hybridoma Bank, and the Vienna Drosophila RNAi Center for flies and reagents; T. Yates for text editing; and H. Stocker, A. Teleman, A. Ferreira, and L. Boulan for comments on the manuscript. L.B. and A. D. are funded by a FPI predoctoral fellowship and a Juan de la Cierva postdoctoral contract, respectively, from the Spanish Ministerio de Economía y Competitividad. M.M. is an ICREA Research Professor, and this work was funded by BFU2010-21123, CSD2007-00008, and 2005 SGR 00118 grants.

Received: January 29, 2014
Revised: May 27, 2014
Accepted: June 16, 2014
Published: July 10, 2014

REFERENCES

Arrese, E.L., and Soulages, J.L. (2010). Insect fat body: energy, metabolism, and regulation. Annu. Rev. Entomol. *55*, 207–225.

Bauer, J.H., and Helfand, S.L. (2009). Sir2 and longevity: the p53 connection. Cell Cycle *8*, 1821.

Berkers, C.R., Maddocks, O.D., Cheung, E.C., Mor, I., and Vousden, K.H. (2013). Metabolic regulation by p53 family members. Cell Metab. *18*, 617–633.

Bharucha, K.N., Tarr, P., and Zipursky, S.L. (2008). A glucagon-like endocrine pathway in Drosophila modulates both lipid and carbohydrate homeostasis. J. Exp. Biol. *211*, 3103–3110.

Blandino, G., Valerio, M., Cioce, M., Mori, F., Casadei, L., Pulito, C., Sacconi, A., Biagioni, F., Cortese, G., Galanti, S., et al. (2012). Metformin elicits anticancer effects through the sequential modulation of DICER and c-MYC. Nat Commun *3*, 865.

Brand, A.H., and Perrimon, N. (1993). Targeted gene expression as a means of altering cell fates and generating dominant phenotypes. Development *118*, 401–415.

Brennecke, J., Hipfner, D.R., Stark, A., Russell, R.B., and Cohen, S.M. (2003). bantam encodes a developmentally regulated microRNA that controls cell proliferation and regulates the proapoptotic gene hid in Drosophila. Cell *113*, 25–36.

Brodsky, M.H., Nordstrom, W., Tsang, G., Kwan, E., Rubin, G.M., and Abrams, J.M. (2000). Drosophila p53 binds a damage response element at the reaper locus. Cell *101*, 103–113.

Canavoso, L.E., Jouni, Z.E., Karnas, K.J., Pennington, J.E., and Wells, M.A. (2001). Fat metabolism in insects. Annu. Rev. Nutr. *21*, 23–46.

Colombani, J., Raisin, S., Pantalacci, S., Radimerski, T., Montagne, J., and Léopold, P. (2003). A nutrient sensor mechanism controls Drosophila growth. Cell *114*, 739–749.

Demontis, F., and Perrimon, N. (2010). FOXO/4E-BP signaling in Drosophila muscles regulates organism-wide proteostasis during aging. Cell *143*, 813–825.

DiAngelo, J.R., and Birnbaum, M.J. (2009). Regulation of fat cell mass by insulin in Drosophila melanogaster. Mol. Cell. Biol. *29*, 6341–6352.

Géminard, C., Rulifson, E.J., and Léopold, P. (2009). Remote control of insulin secretion by fat cells in Drosophila. Cell Metab. *10*, 199–207.

Gibbings, D., Mostowy, S., Jay, F., Schwab, Y., Cossart, P., and Voinnet, O. (2012). Selective autophagy degrades DICER and AGO2 and regulates miRNA activity. Nat. Cell Biol. *14*, 1314–1321.

Grewal, S.S. (2009). Insulin/TOR signaling in growth and homeostasis: a view from the fly world. Int. J. Biochem. Cell Biol. *41*, 1006–1010.

Grönke, S., Mildner, A., Fellert, S., Tennagels, N., Petry, S., Müller, G., Jäckle, H., and Kühnlein, R.P. (2005). Brummer lipase is an evolutionary conserved fat storage regulator in Drosophila. Cell Metab. *1*, 323–330.

Gu, B., and Zhu, W.G. (2012). Surf the post-translational modification network of p53 regulation. Int. J. Biol. Sci. *8*, 672–684.

Hennig, K.M., and Neufeld, T.P. (2002). Inhibition of cellular growth and proliferation by dTOR overexpression in Drosophila. Genesis *34*, 107–110.

Herranz, H., Hong, X., Pérez, L., Ferreira, A., Olivieri, D., Cohen, S.M., and Milán, M. (2010). The miRNA machinery targets Mei-P26 and regulates Myc protein levels in the Drosophila wing. EMBO J. *29*, 1688–1698.

Hermeking, H. (2012). MicroRNAs in the p53 network: micromanagement of tumour suppression. Nat. Rev. Cancer *12*, 613–626.

Hietakangas, V., and Cohen, S.M. (2009). Regulation of tissue growth through nutrient sensing. Annu. Rev. Genet. *43*, 389–410.

Ho, J.J., Metcalf, J.L., Yan, M.S., Turgeon, P.J., Wang, J.J., Chalsev, M., Petruzziello-Pellegrini, T.N., Tsui, A.K., He, J.Z., Dhamko, H., et al. (2012). Functional importance of Dicer protein in the adaptive cellular response to hypoxia. J. Biol. Chem. *287*, 29003–29020.

Huntzinger, E., and Izaurralde, E. (2011). Gene silencing by microRNAs: contributions of translational repression and mRNA decay. Nat. Rev. Genet. *12*, 99–110.

Hyun, S., Lee, J.H., Jin, H., Nam, J., Namkoong, B., Lee, G., Chung, J., and Kim, V.N. (2009). Conserved MicroRNA miR-8/miR-200 and its target USH/FOG2 control growth by regulating PI3K. Cell *139*, 1096–1108.

Jiang, P., Du, W., and Yang, X. (2013). p53 and regulation of tumor metabolism. J. Carcinog. *12*, 21.

Jin, S., Martinek, S., Joo, W.S., Wortman, J.R., Mirkovic, N., Sali, A., Yandell, M.D., Pavletich, N.P., Young, M.W., and Levine, A.J. (2000). Identification and characterization of a p53 homologue in Drosophila melanogaster. Proc. Natl. Acad. Sci. USA *97*, 7301–7306.

Jones, R.G., Plas, D.R., Kubek, S., Buzzai, M., Mu, J., Xu, Y., Birnbaum, M.J., and Thompson, C.B. (2005). AMP-activated protein kinase induces a p53-dependent metabolic checkpoint. Mol. Cell *18*, 283–293.

Kim, S.K., and Rulifson, E.J. (2004). Conserved mechanisms of glucose sensing and regulation by Drosophila corpora cardiaca cells. Nature *431*, 316–320.

Kondoh, H., Lleonart, M.E., Gil, J., Wang, J., Degan, P., Peters, G., Martinez, D., Carnero, A., and Beach, D. (2005). Glycolytic enzymes can modulate cellular life span. Cancer Res. *65*, 177–185.

Kühnlein, R.P. (2012). Thematic review series: Lipid droplet synthesis and metabolism: from yeast to man. Lipid droplet-based storage fat metabolism in Drosophila. J. Lipid Res. *53*, 1430–1436.

Lane, D.P., and Verma, C. (2012). Mdm2 in evolution. Genes Cancer *3*, 320–324.

Lee, Y., Ahn, C., Han, J., Choi, H., Kim, J., Yim, J., Lee, J., Provost, P., Rådmark, O., Kim, S., and Kim, V.N. (2003). The nuclear RNase III Drosha initiates microRNA processing. Nature *425*, 415–419.

Lu, W.J., Chapo, J., Roig, I., and Abrams, J.M. (2010). Meiotic recombination provokes functional activation of the p53 regulatory network. Science *328*, 1278–1281.

Maddocks, O.D., Berkers, C.R., Mason, S.M., Zheng, L., Blyth, K., Gottlieb, E., and Vousden, K.H. (2013). Serine starvation induces stress and p53-dependent metabolic remodelling in cancer cells. Nature *493*, 542–546.

Mandal, S., Guptan, P., Owusu-Ansah, E., and Banerjee, U. (2005). Mitochondrial regulation of cell cycle progression during development as revealed by the tenured mutation in Drosophila. Dev. Cell *9*, 843–854.

Mandal, S., Freije, W.A., Guptan, P., and Banerjee, U. (2010). Metabolic control of G1-S transition: cyclin E degradation by p53-induced activation of the ubiquitin-proteasome system. J. Cell Biol. *188*, 473–479.

Ollmann, M., Young, L.M., Di Como, C.J., Karim, F., Belvin, M., Robertson, S., Whittaker, K., Demsky, M., Fisher, W.W., Buchman, A., et al. (2000). Drosophila p53 is a structural and functional homolog of the tumor suppressor p53. Cell *101*, 91–101.

Palanker, L., Tennessen, J.M., Lam, G., and Thummel, C.S. (2009). Drosophila HNF4 regulates lipid mobilization and beta-oxidation. Cell Metab. *9*, 228–239.

Puig, O., Marr, M.T., Ruhf, M.L., and Tjian, R. (2003). Control of cell number by Drosophila FOXO: downstream and feedback regulation of the insulin receptor pathway. Genes Dev. *17*, 2006–2020.

Rajan, A., and Perrimon, N. (2012). Drosophila cytokine unpaired 2 regulates physiological homeostasis by remotely controlling insulin secretion. Cell *151*, 123–137.

Ranganayakulu, G., Zhao, B., Dokidis, A., Molkentin, J.D., Olson, E.N., and Schulz, R.A. (1995). A series of mutations in the D-MEF2 transcription factor reveal multiple functions in larval and adult myogenesis in Drosophila. Dev. Biol. *171*, 169–181.

Ruby, J.G., Stark, A., Johnston, W.K., Kellis, M., Bartel, D.P., and Lai, E.C. (2007). Evolution, biogenesis, expression, and target predictions of a substantially expanded set of Drosophila microRNAs. Genome Res. *17*, 1850–1864.

Rulifson, E.J., Kim, S.K., and Nusse, R. (2002). Ablation of insulin-producing neurons in flies: growth and diabetic phenotypes. Science *296*, 1118–1120.

Scherz-Shouval, R., Weidberg, H., Gonen, C., Wilder, S., Elazar, Z., and Oren, M. (2010). p53-dependent regulation of autophagy protein LC3 supports cancer cell survival under prolonged starvation. Proc. Natl. Acad. Sci. USA *107*, 18511–18516.

Teleman, A.A., Chen, Y.W., and Cohen, S.M. (2005). 4E-BP functions as a metabolic brake used under stress conditions but not during normal growth. Genes Dev. *19*, 1844–1848.

Toledo, F., and Wahl, G.M. (2006). Regulating the p53 pathway: in vitro hypotheses, in vivo veritas. Nat. Rev. Cancer *6*, 909–923.

Ugrankar, R., Liu, Y., Provaznik, J., Schmitt, S., and Lehmann, M. (2011). Lipin is a central regulator of adipose tissue development and function in Drosophila melanogaster. Mol. Cell. Biol. *31*, 1646–1656.

Vousden, K.H., and Ryan, K.M. (2009). p53 and metabolism. Nat. Rev. Cancer *9*, 691–700.

Waskar, M., Landis, G.N., Shen, J., Curtis, C., Tozer, K., Abdueva, D., Skvortsov, D., Tavaré, S., and Tower, J. (2009). Drosophila melanogaster p53 has developmental stage-specific and sex-specific effects on adult life span indicative of sexual antagonistic pleiotropy. Aging (Albany, N.Y. Online) *1*, 903–936.

Publication (2)

"Contributions of DNA repair, cell cycle checkpoints and cell death to suppressing the DNA damage-induced tumorigenic behavior of *Drosophila* epithelial cells"

Oncogene (2014), 1–8

www.nature.com/onc

ORIGINAL ARTICLE

Contributions of DNA repair, cell cycle checkpoints and cell death to suppressing the DNA damage-induced tumorigenic behavior of *Drosophila* epithelial cells

A Dekanty[1,3,4], L Barrio[1,3] and M Milán[1,2]

When exposed to DNA-damaging agents, components of the DNA damage response (DDR) pathway trigger apoptosis, cell cycle arrest and DNA repair. Although failures in this pathway are associated with cancer development, the tumor suppressor roles of cell cycle arrest and apoptosis have recently been questioned in mouse models. Using *Drosophila* epithelial cells that are unable to activate the apoptotic program, we provide evidence that ionizing radiation (IR)-induced DNA damage elicits a tumorigenic behavior in terms of E-cadherin delocalization, cell delamination, basement membrane degradation and neoplasic overgrowth. The tumorigenic response of the tissue to IR is enhanced by depletion of *Okra/DmRAD54* or *spnA/DmRAD51*—genes required for homologous recombination (HR) repair of DNA double-strand breaks in G2—and it is independent of the activity of Lig4, a ligase required for nonhomologous end-joining repair in G1. Remarkably, depletion of *Grapes/DmChk1* or *Mei-41/dATR*—genes affecting DNA damage-induced cell cycle arrest in G2—compromised DNA repair and enhanced the tumorigenic response of the tissue to IR. On the contrary, DDR-independent lengthening of G2 had a positive impact on the dynamics of DNA repair and suppressed the tumorigenic response of the tissue to IR. Our results support a tumor suppressor role of apoptosis, DNA repair by HR and cell cycle arrest in G2 in simple epithelia subject to IR-induced DNA damage.

Oncogene advance online publication, 17 March 2014; doi:10.1038/onc.2014.42

INTRODUCTION

Cells and tissues are continuously exposed to extrinsic and intrinsic insults that generate DNA damage including ultraviolet and ionizing radiation (IR) as well as reactive oxygen species produced during normal cellular metabolism. In order to lessen the detrimental effects of DNA lesions, the conserved ataxia telangiectasia-mutated (ATM)/Chk2 and ataxia telangiectasia-related (ATR)/Chk1 kinase pathways are rapidly activated in response to DNA damage and phosphorylate numerous substrates involved in DNA repair, cell cycle arrest and/or apoptosis (reviewed in Negrini *et al.*[1]). The conserved tumor suppressor protein p53 is a major downstream effector of the DNA damage response (DDR) pathway. p53 is phosphorylated by ATM/Chk2 and has a critical role in driving cell cycle arrest or apoptosis; these processes are mediated mainly by the transcriptional upregulation of *p21* or the pro-apoptotic genes *Puma* and *Noxa*, respectively (reviewed in Lane and Levine[2]). The DDR machinery has crucial roles during development and tissue homeostasis, as mutations in DDR genes lead to developmental defects, genetic diseases, premature aging and cancer (reviewed in Halazonetis *et al.*[3] and Jackson and Bartek[4]). Mutations in DNA repair genes have been identified in hereditary cancer, whereas mutations in *p53* and *ATM* are frequently associated with sporadic (nonhereditary) cancers. It has been generally accepted that tumorigenesis is blocked by p53-mediated cell cycle arrest, apoptotic cell death and/or cellular senescence. However, new data revealed unpredicted tumor suppressor activity of p53. DNA damage-induced tumorigenesis is suppressed in mice bearing mutant forms of p53 that are unable to induce apoptosis[5,6] or both apoptosis and cell cycle arrest.[7] Furthermore, the combined loss of p53-mediated cell cycle arrest, senescence and apoptosis is not sufficient to abrogate the tumor suppression activity of p53, and mice mutant for p21 and the pro-apoptotic genes *Puma* and *Noxa* remain tumor free in contrast to p53-deficient mice.[6,8] These results indicate that the tumor suppressor activity of p53 might also rely on its capacity to coordinate DNA repair and regulate metabolism, and they question the classical contributions of cell cycle arrest and apoptosis to suppressing spontaneous tumorigenesis.

The imaginal discs of *Drosophila*, simple monolayered epithelia that grow about a thousand-fold in mass and cell number during larval development, are valuable models in which to dissect the molecular and cellular mechanisms underlying tumor initiation and progression.[9–12] *Drosophila* is a very attractive model in which to analyze the contributions of cell cycle arrest and apoptosis to suppressing DNA damage-induced tumorigenesis, as both cell proliferation and programmed cell death can be easily manipulated in a DDR-independent manner, and both DNA damage-induced cell cycle arrest and apoptosis are independently controlled by ATM and ATR and their targets (reviewed in Song[13]). Although ATM downstream targets Chk2 and Dp53 regulate the immediate apoptotic response of the tissue to IR,[14,15] cell cycle arrest in G2 is controlled by the activity of *Drosophila* ATR (dATR),[16] and its downstream target DmChk1.[17] Repair of double-strand breaks (DSBs) is mediated in G2 by an error-free

[1]Institute for Research in Biomedicine (IRB Barcelona), Barcelona, Spain and [2]Institució Catalana de Recerca i Estudis Avançats (ICREA), Barcelona, Spain. Correspondence: Professor M Milán, Department of Cell and Development Biology, Institute for Research in Biomedicine (IRB Barcelona), Baldiri Reixac, 10-12, Barcelona 08028, Spain.
E-mail: marco.milan@irbbarcelona.org
[3]These authors contributed equally to this work.
[4]Current address: Instituto de Agrobiotecnología del Litoral, Facultad de Bioquímica y Ciencias Biológicas, Universidad Nacional del Litoral, 3000 Santa Fe, Argentina.
Received 26 September 2013; revised 4 February 2014; accepted 7 February 2014

mechanism called homologous recombination (HR), and in G1 by an error-prone mechanism called nonhomologous end-joining (NHEJ). Whereas DmRAD51 and the DEAD-like helicase DmRAD54 have essential roles in HR,[18,19] NHEJ is executed by the activity of the ATP-dependent DNA ligase Lig4.[20]

Here we studied the potential protumorigenic action of IR-induced DNA damage and the contribution of cell cycle arrest, apoptosis and DNA repair to tumor progression. We first show that *Drosophila* epithelial cells subject to IR and unable to activate the apoptotic program at the level of the pro-apoptotic genes or the effector Caspases Drlce and Dcp1 present a tumorigenic behavior in terms of E-cadherin delocalization, cell delamination, cell motility, basement membrane degradation and expression of the mitogenic molecule Wingless (Wg). We also unravel a G2-specific role of cell cycle arrest and DNA repair in suppressing IR-induced tumorigenesis. Our results reinforce the suppressor activities of DNA repair, cell cycle arrest and apoptosis in IR-induced tumor initiation in simple epithelia. Whereas p53-dependent DNA repair might be sufficient to counteract the tumorigenic action of the DNA damage produced under normal physiological conditions, cell cycle arrest and apoptosis might enter into action only upon induction of nonphysiological levels of DNA damage.

RESULTS

Tumorigenic behavior of IR-induced delaminating cells

When IR-treated cells are maintained in the tissue by means of expression of the baculovirus protein P35, which binds and represses the activity of effector caspases Drlce and Dcp1 and blocks cell death,[21] or by expressing a double-stranded RNA (dsRNA) form of the effector caspase Drlce, ectopic expression of the mitogenic molecule Wg is observed (white arrows in Figures 1b–d).[22] Note that transgene expression is restricted to one compartment of the wing disc and the neighboring compartment serves as control (Figures 1b–d). Ectopic expression of Wg is dependent on the activity of the Jun N-terminal kinase (JNK) pathway, as co-expression of a dominant-negative version of *Drosophila* JNK (Basket^{DN}) together with p35 rescues Wg expression (Figure 1f). Remarkably, JNK-dependent expression of Wg also causes a clear overgrowth of the IR-treated tissue expressing p35. Thus, the p35-expressing territory (the P compartment) is enlarged when compared with the neighboring one (the A compartment), and this enlargement is fully reversed by co-expression of Basket^{DN} (Figure 1l). These observations prompted us to analyze the potential protumorigenic action of the IR treatment.

The wing primordium is a cellular monolayer that forms a two-sided epithelial sac and consists of two apposed epithelia: the main epithelium that is pseudostratified and the peripodial membrane that is squamous (Figure 1a). The apical (ap) side of both epithelia faces the lumen and the basal (bs) side is located at the periphery. We noted that the ectopic expression of Wg upon IR was restricted to small groups of delaminated cells located on the basal side of the main epithelium (Figures 1h and i), thus unraveling a neoplastic response of the tissue to this radiation. Interestingly, clones of cells mutant for the pro-apoptotic genes *hid*, *reaper* and *grim* (in *Df(H99)* clones) also delaminated upon IR and induced JNK activation, monitored by the expression of Wg (Figures 1e and j). This observation implies that delamination and JNK activation are not a consequence of entry into apoptosis. Delamination was not caused by JNK activation either as IR-treated wing discs expressing p35 and a dominant-negative version of JNK (Basket^{DN}) showed delaminated cells on the basal side of the epithelium that did not express Wg (Figure 1k).

Epithelial architecture relies on the polarization of the plasma membrane into apical and basolateral domains separated by adherens junctions, and genetic depletion of components of the Cdc42/Par6/atypical protein kinase C or Scribbled/Disc Large/Lgl polarity complexes induces a reduction in junctional DE-cadherin (DE-cad) level, cell delamination and JNK activation.[9,23–25] We then used antibodies against Atypical Protein Kinase C, Disc Large and DE-cad to view the subapical, basolateral and junctional domains, respectively, in IR-induced delaminating cells (Figure 2a). Atypical Protein Kinase C and Disc Large remained at the membrane of these cells (Figure 2b, b′). However, their overall protein levels

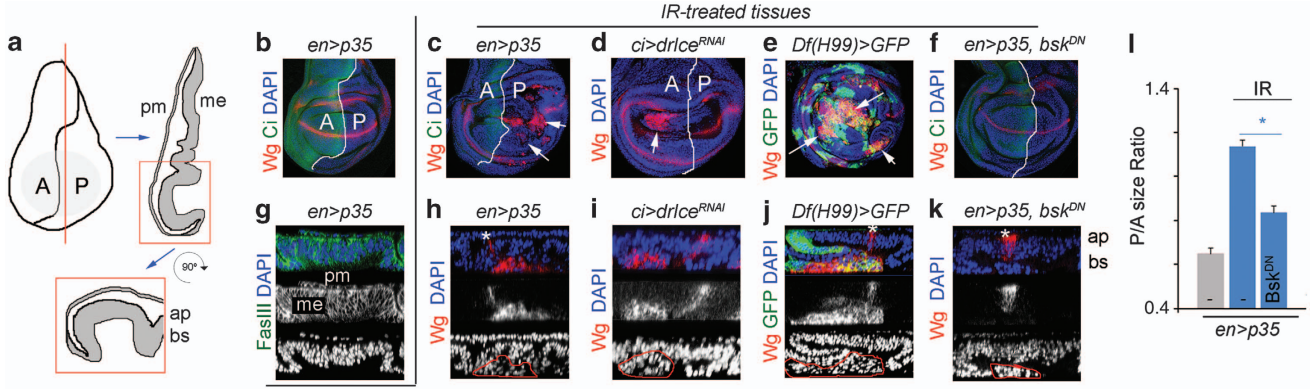

Figure 1. Cell delamination and Wg expression are not caused by entry into apoptosis. (**a**) Cartoon depicting the wing primordium (left), a cross-section along the red line (right) and a magnification of the region within the red square (bottom). Whereas the main epithelium (me) is pseudostratified, the peripodial membrane (pm) is a squamous epithelium. Anterior (A) and posterior (P) compartments, and apical (ap) and basal (bs) sides of the main epithelium are depicted. (**b**–**f**) Wing primordia from wild-type (**b**), *en-gal4; UAS-p35* (**c**), *ci-gal4; UAS- Drlce^{RNAi}* (**d**), *en-gal4; UAS-p35; UAS-bsk^{DN}* (**f**) larvae or with clones of cells mutant for *Df(H99)* and expressing green fluorescent protein (GFP; green, **e**), subject to IR 72 h before dissection and stained for Wg (red), Ci (green, **b**, **c**, **f**), and DAPI (blue). *en-gal4* (**b**, **c**, **f**) and *ci-gal4* (**d**) drive transgene expression in the posterior (P) and anterior (A) compartments, respectively. Ci labels the A compartment in **b**, **c** and **f**. White arrows in **a**–**c** point to Wg-expressing cells. (**g**–**k**) Cross-sections of wing primordia from wild-type (**g**), *en-gal4; UAS-p35* (**h**), *ci-gal4; UAS- Drlce^{RNAi}* (**i**), *en-gal4; UAS-p35; UAS-bsk^{DN}* (**k**) larvae or with clones of cells mutant for *Df(H99)* and expressing GFP (green, **j**), subject to IR 72 h before dissection and stained for Fas III (green, **g**), Wg (red, **h**–**k**) and DAPI (blue). The endogenous expression of Wg is marked by an asterisk and delaminated cells by a red line. The apical (ap) and basal (bs) sides of the epithelium are indicated. In **g**, the peripodial membrane (pm) and main epithelium (me) are indicated. (**l**) Histogram plotting the P/A size ratio of wing primordia expressing p35 and the indicated transgenes and quantified 72 h after IR treatment. Error bars represent s.e.m. $^*P < 0.001$.

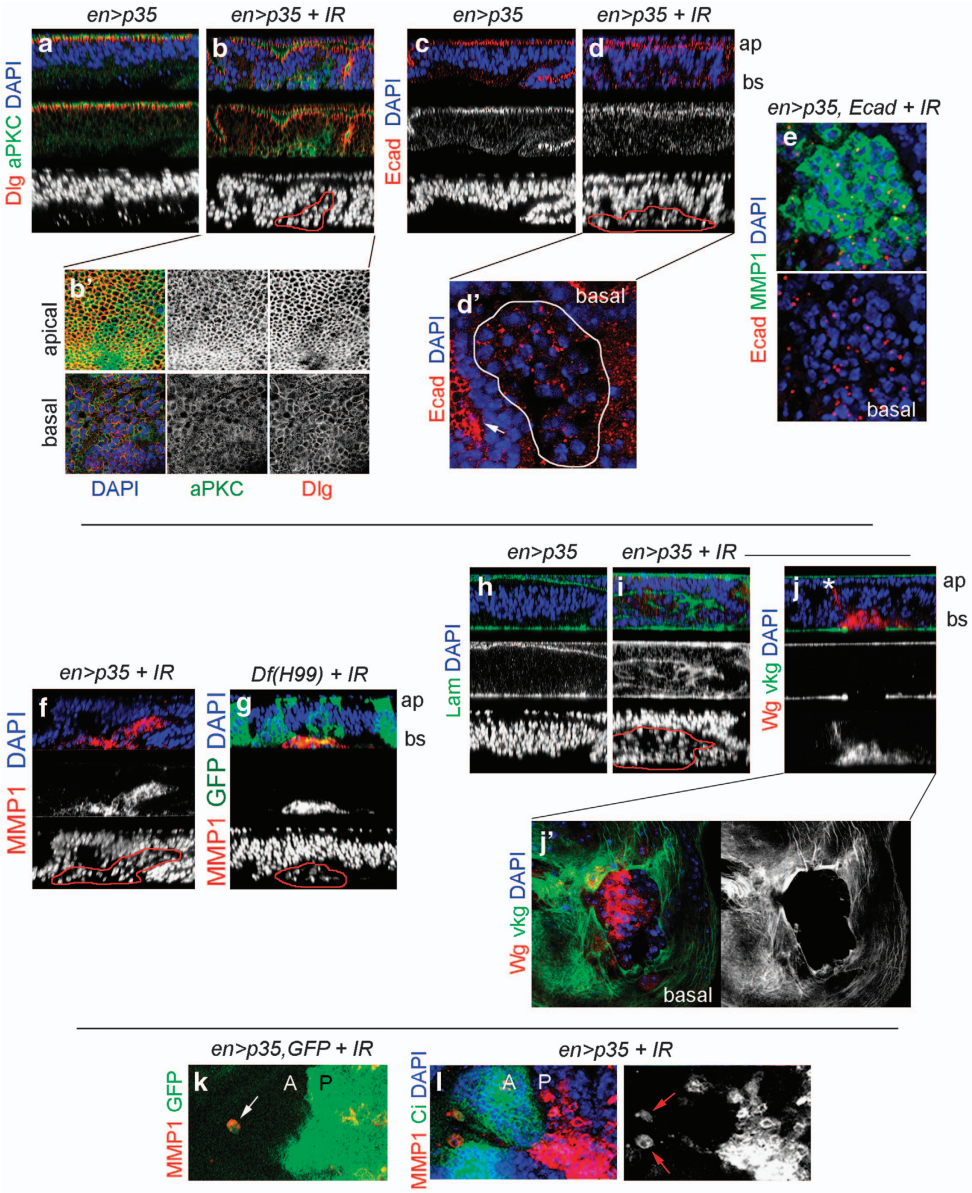

Figure 2. Tumorigenic behavior of IR-induced delaminated cells. (**a-d**) Cross-sections of the posterior compartment of wing primordia expressing the indicated transgenes under the control of the *en-gal4* driver and stained for Dlg (Disc Large; red, **a**, **b**), atypical protein kinase C (aPKC; green, **a**, **b**), E-cad (red, **c**, **d**) and DAPI (blue). In **b** and **d**, larvae were subjected to IR 72 h before dissection. Apical (ap) and basal (bs) sides of the epithelium are indicated. (**b**, **d**′) X-Y sections of the apical or basal sides of the wing epithelia are shown in **b** and **d**. In **d**′, delaminated cells are marked by a white line, and the nondelaminated tissue by an arrow. (**e**) X-Y sections of the basal side of a wing epithelium expressing the indicated transgenes, subject to IR 72 h before dissection and stained for E-cad (red), MMP1 (green) and DAPI (blue). (**f**–**j**) Cross-sections of the posterior compartment of wing primordia expressing the indicated transgenes under the control of the *en-gal4* driver (**f**, **h**–**j**) or with clones of cells mutant for *Df(H99)* and expressing green fluorescent protein (GFP; green, **g**) and stained for MMP1 (red, **f**, **g**), Wg (red, **j**), DAPI (blue), laminin-γ (labels the basement membrane (BM) in green, **h**, **i**), and *viking-GFP* (*collagen IV*, green, **j**). In **f**, **g**, **i** and **j**, larvae were subject to IR 72 h before dissection. In **j**, the endogenous expression of Wg is marked by an asterisk. Apical (ap) and basal (bs) sides of the epithelium are indicated. (**j**′) X-Y section of the basal side of the wing epithelium is shown in **j**. (**e**, **k**, **l**) X-Y sections of the basal side of wing primordia expressing the indicated transgenes, subject to IR 72 h before dissection and stained for MMP1 (red), Ci (green, **l**) and DAPI (blue). *en-gal4* drives transgene expression in the posterior (P) compartment and the anterior (A) compartment is labeled by the expression of Ci in **l**. Note in **k** and **l**, the presence of delaminated cells (arrows) originating from the P compartment and migrating toward the nearby A compartment.

were severely reduced (Figure 2b′, bottom panels), when compared with nondelaminated cells (Figure 2b′, top panels). Interestingly, DE-cad lost its tight junctional distribution, and the overall protein levels were clearly decreased in delaminated cells (Figures 2c, d and d′). This molecule was no longer detectable in most of the delaminated cells, with the exception of some small discrete puncta. Overexpression of a modified version of DE-cad (DE-cadΔCyt:α-catenin), able to rescue the adhesion properties of *E-cad*-mutant cells and unable to interfere with endogenous β-catenin signaling,[26] did not block the delamination process, and the overexpressed form of DE-cad also localized to small discrete puncta in delaminating cells (Figure 2e). Thus, dissociation

of *Drosophila* epithelial cells upon IR is not due to reduced levels of DE-cad but is most probably caused by DE-cad mis-localization. Interestingly, delaminating cells expressed Matrix Metaloproteinase 1 (MMP1; Figures 2e–g), and MMPs are known to contribute to basement membrane degradation in flies and mammals.[25,27,28] Consistently, the basement membrane, labeled with Laminin-γ or with a GFP (green fluorescent protein)-tagged protein trap in the *viking/collagen IV* gene, was disrupted in the delaminated cell population (Figures 2h–j, j′). MMP1-expressing delaminated cells also became motile and were observed in the nearby compartment (Figures 2k and l). Altogether, these results unveil a tumorigenic response of the tissue to IR upon additional blockade of the apoptotic pathway.

A tumor suppressor role of HR repair of DSBs

As entry into apoptosis is not required for IR-induced activation of JNK, we next addressed whether the induction of DSBs by IR treatment contributed to JNK activation and to the tumorigenic behavior of the tissue. The DNA damage sensor ATM recruits and phosphorylates the histone H2A variant, H2AX, to mark the sites of damage (reviewed in Srivastava *et al*.[29]). We observed elevated levels of phosphorylated H2Av (P-H2Av), the functional homolog of H2AX in *Drosophila*, in wild-type wing discs subject to IR and dissected 5 h after (Supplementary Figure S1). Overall, P-H2Av levels decreased 72 h after the IR treatment (Supplementary Figure S1). dATR/Mei-41 kinase is a conserved regulator of cellular responses to DSBs and has been reported to phosphorylate H2Av during the repair of meiotic DSBs.[30] Depletion of this kinase (by means of expression of a dsRNA form of *mei-41*) also reduced P-H2Av levels in IR-treated wing discs (Figure 3b), thus supporting a general role of Mei-41 in the repair of IR-induced DSBs. In wing discs expressing p35, the dynamics of H2Av phosphorylation upon IR were largely similar to that observed in control wing discs, with the exception of small groups of cells with elevated levels of P-H2Av up to 72 h after IR (red arrows in Figure 3a). Thus, apoptosis inhibition does not have a major impact on the dynamics of DSB repair.

In order to analyze the causal relationship between IR-induced DNA damage, monitored by P-H2Av and JNK activation, we compromised the repair of DSBs and analyzed the impact of wing discs subjected to IR and expressing p35 on JNK activation and tissue overgrowth. DSB repair is mediated by two distinct mechanisms. On one hand, an error-free mechanism, HR, executed by the activities of DmRAD51/spnA[18] and the DEAD-like helicase DmRAD54/Okra,[19] allows a damaged chromosome to be repaired using a sister chromatid available in S/G2. On the other hand, NHEJ, executed by the activity of Lig4,[20] takes place in G1 and induces error-prone repair. We then compared the contributions of these two DNA repair mechanisms with the IR-induced tumorigenic behavior of the tissue. Although depletion of DmRAD54/Okra or DmRAD51/spnA maintained the overall high levels of P-H2Av observed immediately after IR treatment during at least 72 h (Figures 3c–e and Supplementary Figure S1, compared with Figure 3a), the impact of Lig4 depletion on P-H2Av dynamics was undetectable (Figure 3f and Supplementary Figure S1). Similar results were obtained with an independent dsRNA form of DmRAD54/Okra (Supplementary Figure S3). These observations indicate that HR makes a greater contribution to DSB repair after IR treatment than NHEJ. Interestingly, the levels of JNK activation, the number of delaminating cells and the degree of tissue overgrowth induced by IR were increased in DmRAD54/Okra-depleted tissues (Figures 3g, h and l), and the resulting IR-induced tissue overgrowth was fully rescued upon depletion of the JNK pathway (Figures 3i and l). A similar impact on JNK activation was observed in DmRAD51/spnA-depleted tissues (Figure 3j and Supplementary Figure S3). JNK was not activated in untreated tissues depleted of DmRAD54/Okra or DmRAD51/spnA and expressing p35 (Supplementary Figure S2). Consistent with the observation that Lig4 had no impact on the P-H2Av dynamics of IR-treated tissues, JNK activation and the degree of tissue overgrowth induced by IR was very similar in control and *lig4*-mutant wing discs expressing p35 (Figures 3k and l). Taken together, these results support the notion that IR-induced DSBs contribute to JNK activation and reveal a tumor suppressor role of error-free HR repair of DNA DSBs.

A tumor suppressor role of cell cycle arrest in G2

The G2 cell cycle arrest induced by IR is controlled in *Drosophila* by the activity of dATR/Mei-41 (Song *et al*.[16]) and its downstream target DmChk1 (Grapes in *Drosophila*)[17] and is thought to contribute to the repair of DSBs by HR. Consistently, depletion of DmChk1/Grapes maintained the overall high levels of P-H2Av observed immediately after IR treatment during at least 72 h (Figures 4a and b, compared with Figure 3a). Interestingly, the overall levels of JNK activation and the resulting overgrowth of the DmChk1/Grapes tissue were increased when compared with control samples (Figures 4c–e). An even stronger impact on JNK activation and tissue overgrowth was observed upon depletion of dATR/Mei-41 levels (Figures 4c, d and f; expression of the JNK targeted *puc* is shown in Figure 4f), most probably because this kinase is also directly involved in DSB repair.[16] A similar enhancement of JNK activation was observed upon depletion of DmChk1/Grapes or dATR/Mei-41 with independent dsRNA forms (Supplementary Figure S3). The resulting tissue overgrowth was fully rescued upon depletion of the JNK pathway (Figures 4c and g) and JNK was not activated in untreated tissues depleted of DmChk1/Grapes or dATR/Mei-41 and expressing p35 (Supplementary Figure S2). These results unravel a tumor suppressor role of IR-induced cell cycle arrest in G2 and support the notion that this cell cycle arrest contributes to the repair of DSBs by HR.

In order to further characterize the tumor suppressor role of IR-induced cell cycle arrest in G2, we addressed whether DDR-independent lengthening of G2 contributed to HR-dependent repair of DSBs, and whether this lengthening had any impact on the level of JNK activation. Tribbles is an ubiquitin ligase that binds, ubiquitinates and degrades String, the Cdc25 *Drosophila* ortholog involved in activating Cdc2 and promoting the G2/M transition.[31–34] Tribbles overexpression in epithelial cells is well known to induce a G2 lengthening and a concomitant shortening of G1 to maintain the overall length of the cell cycle.[34] Interestingly, Tribbles overexpression in IR-treated wing discs caused a mild but reproducible reduction in the overall levels of P-H2Av (Figure 4h) and suppressed JNK activation (Figures 4i and j, compared with Figures 4d and e). Similar results were obtained upon expression of dsRNA forms of *string* or *cdc2* (Figure 4k and data not shown).

Overexpression of the CDK inhibitor Dacapo (Dap, the *Drosophila* p21/p27 ortholog), which traps the cyclin E/CDK2 complex in a stable but inactive form,[36,37] induces G1 lengthening in epithelial cells and a concomitant shortening of G2 to maintain the overall length of the cell cycle.[35] In this case, repair of IR-induced DSBs might be compromised, given that the contribution of NHEJ, which takes place in G1, to DNA repair is minor with respect to HR, which takes place in G2 (Figure 3). Consistent with this proposal, Dacapo overexpression in IR-treated tissues maintained the overall high levels of P-H2Av observed immediately after IR treatment during at least 72 h (Figures 4l and m), and increased the levels of IR-induced JNK activation (Figures 4n and o, compared with Figures 4d and e). These results reinforce the relative contributions of NHEJ and HR to the repair of IR-induced DSBs and to the suppression of IR-induced JNK activation.

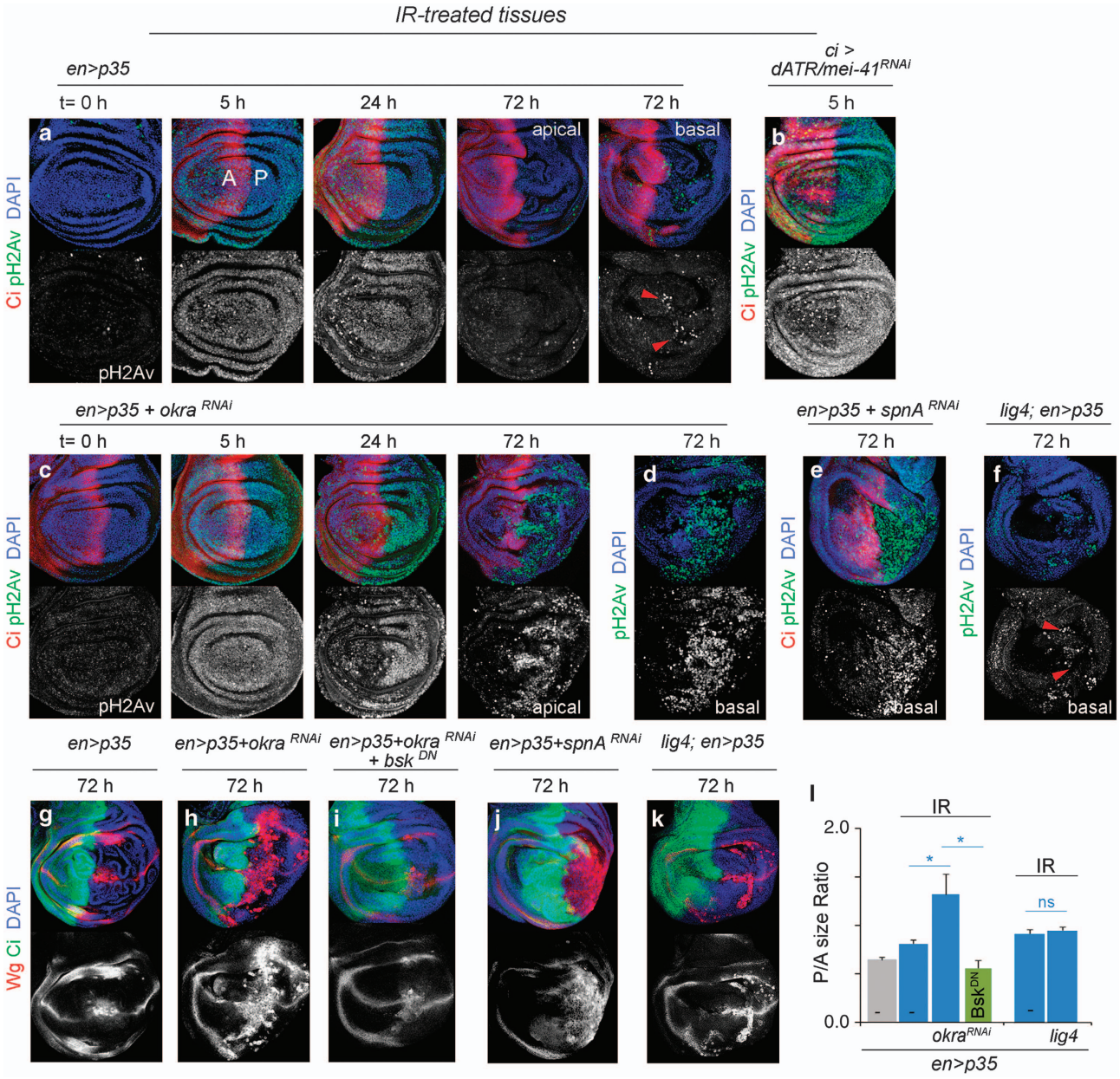

Figure 3. A tumor suppressor role of HR DNA repair. (**a**–**k**) Wing primordia expressing the indicated transgenes under the control of the *en-gal4* (**a**, **c**–**k**) or *ci-gal4* (**b**) drivers and stained for pH2Av (green or white, **a**–**f**), Wg (red, g–k), Ci (red in **a**–**c** and **e**; green in **g**–**k**) and subjected to IR at the indicated time points before dissection. *en-gal4* and *ci-gal4* drive transgene expression in the posterior (P) compartment and anterior (A) compartments, respectively. Ci expression labels the A compartment. The basal side of the epithelium is shown in panels **d**–**f**. In the other panels, the apical side is shown. Red arrowheads, in **a** and **f**, point to pH2Av-positive cells localized on the basal side of the epithelium. (**l**) Histogram plotting the P/A size ratio of wing primordia subject to IR 72 h before dissection and expressing the indicated transgenes under the control of the *en-gal4* driver. Error bars represent s.e.m. $^*P < 0.001$. NS, not statistically significant.

DISCUSSION

DNA damage-induced tumorigenesis

Here we have used the imaginal discs of *Drosophila* to revisit the contributions of DNA repair, cell cycle arrest and apoptosis in suppressing DNA damage-induced tumorigenesis. The tumorigenic behavior of the tissue to IR-induced DNA damage relies on groups of cells losing their apical-basal polarity, mislocalizing DE-cad, delaminating from the main epithelium, becoming motile, and activating the stress-responsive JNK pathway, which drives a transcriptional program that induces the expression of the mitogenic molecule Wg and MMP1. The tumorigenic response of the tissue to IR-induced DNA damage was unraveled upon inhibition of the apoptotic program at various levels, including the pro-apoptotic genes and the effector caspases. Thus, cell delamination and JNK activation is not a consequence of the entry into apoptosis. The contribution of NHEJ to the repair of IR-induced DSBs was undetectable and IR-induced JNK activation and tumorigenesis were largely unaffected by mutations in *lig4*. On the contrary, HR had a major role in the repair of these DSBs, and depletion of elements involved in HR had a major impact on the tumorigenic behavior of the tissue. Consistent with the role of HR in DSB repair, which occurs in S/G2, we unveiled a tumor suppressor role of the cell cycle arrest in G2 upon IR-induced DNA damage. Thus, defects in G2 cell cycle arrest upon IR treatment

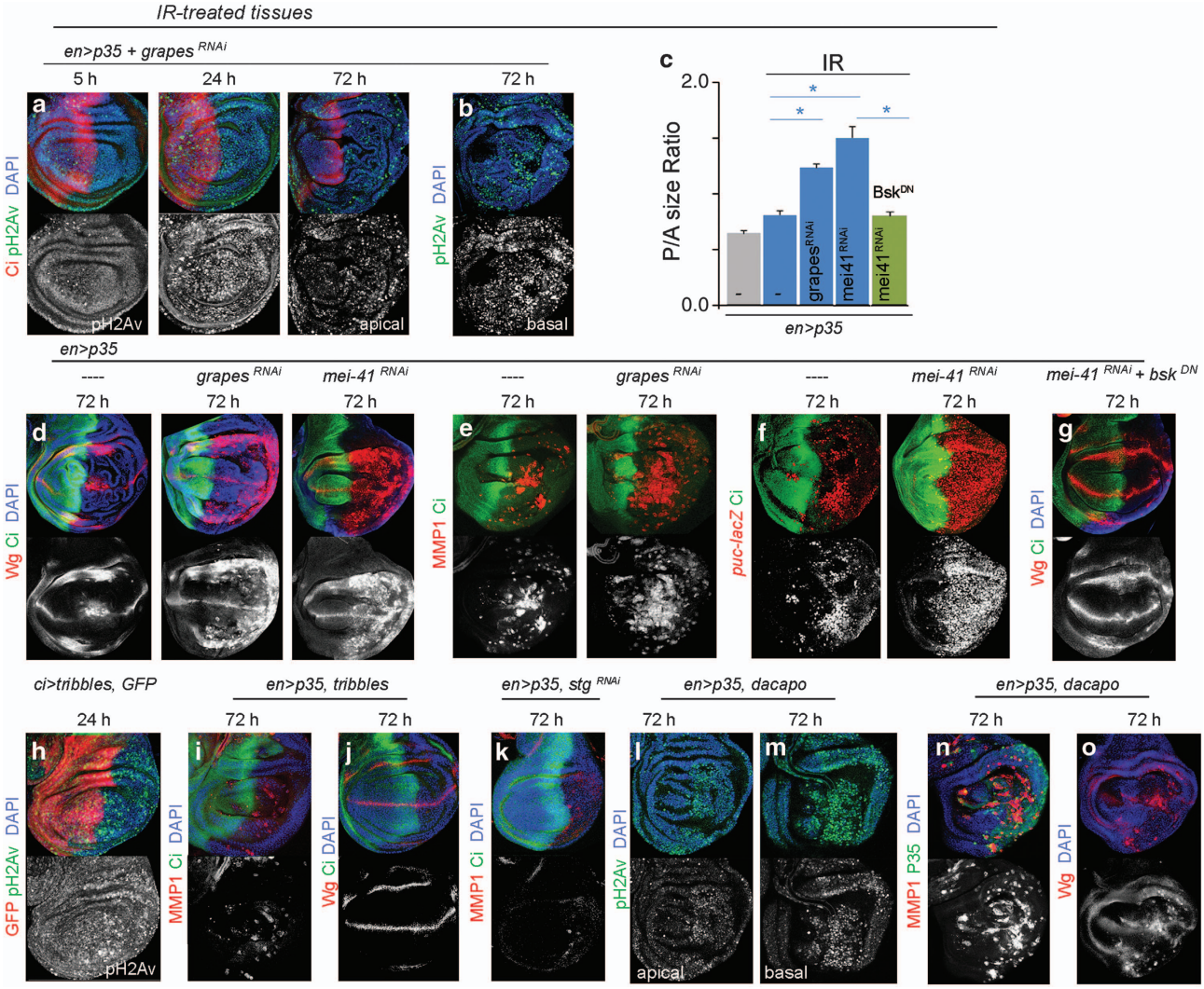

Figure 4. A tumor suppressor role of cell cycle arrest in G2. (**a**, **b**, **d**–**o**) Wing primordia expressing the indicated transgenes, stained for pH2Av (green or white, **a**, **b**, **h**, **l**, **m**), Ci (red in **a**; green in **d**–**g**, **i**–**k**), DAPI (blue in **a**, **b**, **d**, **g**–**o**), Wg (red, **d**, **g**, **j**, **o**), MMP1 (red, **e**, **i**, **k**, **n**), *puckered-lacZ* (red, **f**), green fluorescent protein (GFP; red, **h**), P35 (green in **n**) and subjected to IR 72 h before dissection. *en-gal4* and *ci-gal4* drive transgene expression in the posterior (P) compartment and anterior (A) compartment, respectively. Ci expression labels the A compartment. (**c**) Histogram plotting the P/A size ratio of wing primordia subject to IR 72 h before dissection and expressing, under the control of the *en-gal4* driver, the indicated transgenes. Error bars represent s.e.m. $*P < 0.001$.

compromised the dynamics of DNA repair and enhanced the tumorigenic response of the tissue. Remarkably, DDR-independent lengthening of G2 contributed to DNA repair and completely rescued IR-induced JNK activation. These results support the proposal that IR-induced G2 cell cycle arrest contributes to the repair of DSBs by HR. Taken together, our observations reinforce the classical contributions of apoptosis, cell cycle arrest and DNA repair to suppressing IR-induced tumorigenesis, and provide an ideal genetic experimental setup to identify new molecular elements involved in DNA damage-induced tumorigenesis.

Whereas apoptosis and cell cycle arrest have a major role in suppressing IR-induced tumorigenesis, they are dispensable for p53-dependent suppression of spontaneous tumor development. Thus, mice mutant for *p21* and the pro-apoptotic genes *Puma* and *Noxa* remain tumor free, in contrast to DDR or *p53*-mutant mice, and the combined loss of p53-mediated cell cycle arrest, senescence and apoptosis is not sufficient to abrogate the tumor suppression activity of p53.[8,38] These results imply that p53-dependent DNA repair might be sufficient to counteract the tumorigenic action of the DNA damage produced under normal physiological conditions, and cell cycle arrest and apoptosis might enter into action only upon induction of nonphysiological levels of DNA damage.

Genomic instability and tumorigenesis

We observed a temporal delay between the overall levels of H2Av phosphorylation, which mark the presence of DSBs, and the induction of JNK activity in IR-treated tissues expressing p35. Thus, JNK activation was still observed 72 h after the IR treatment, a time at which P-H2Av levels were very low. We also noted that DSBs were observed throughout the *DmRAD54/okra-*, *DmRAD51/spnA-* or *DmChk1/grapes*-depleted tissues in both delaminated and non-delaminated cells, while sustained JNK activation was restricted only to delaminated cells. These observations suggest that JNK activation is an indirect consequence of the presence of DSBs in the tissue. Impaired HR repair of DSBs, caused by *DmRAD54/okra* or *DmRAD51* depletion, enhances JNK activation in IR-treated tissues (Figures 3h and j and Supplementary Figure S3) and has been previously shown in *Drosophila* tissues to induce genome rearrangements such as deletions.[39,40] Thus, genome rearrangements, generated by imprecise repair of DSBs, might contribute to

JNK-mediated tumorigenesis of IR-treated tissues expressing p35. Consistent with this proposal, the molecular and cellular mechanisms underlying the tumor-like behavior induced by the IR treatment resemble, in a remarkable manner, those caused by chromosomal instability,[41] a type of genomic instability that refers to the high rate by which chromosome structure and number changes over time in cancer cells compared with normal cells.[1] In this scenario, sustained JNK activation is also restricted to delaminated cells, and delaminated cells are the ones with the highest levels of aneuploidy in the tissue.[41] We would like, thus, to propose that segmental aneuploidy (in the case of IR-treated tissues) or whole-chromosome aneuploidy (in the case of chromosomal instability[41]) cause an imbalance in the expression levels of a large set of genes and, this imbalance well known to cause proteotoxic and metabolic stress in human and yeast cells,[42,43] induces JNK-dependent programmed cell death. When programmed cell death is blocked, a subversive tumorigenic role of JNK is unveiled. Whether this imbalance also contributes to the role of genomic instability in human cancer remains to be elucidated.

HR repair of DSBs also has a suppressor role of spontaneous tumor development in aged adult flies. Genome rearrangements, including translocations and deletions, are the most predominant type of mutations in aged adult flies,[44] and aged flies develop tumors in proliferating tissues such as the testis and the gut.[45] Impairment of HR repair, in flies mutant for *DmBlm* (the Drosophila ortholog of Bloom (BLM) RecQ helicase involved in unwinding the DNA double helix for replication or repair[46]), increases the frequency of genome rearrangements and, most interestingly, increases the frequency of tumor development at early ages in testis and gut tissues.[47] The incidence of genomic instability and spontaneous tumorigenesis in aged adult flies is largely unaffected by mutations in *lig4*.[47] Thus, genomic instability, in the form of chromosome rearrangements, also contributes to spontaneous tumor development in proliferative tissues of aged flies. These results together with the ones presented in the present work support the proposed tumorigenic role of genomic instability in human cancer.[48]

MATERIALS AND METHODS

Drosophila strains

UAS–mei-41^{RNAi} (ID 11251* and ID 103624, Vienna Drosophila RNAi Center (VDRC), Vienna, Austria); *UAS–okra^{RNAi}* (ID 104323*, VDRC and HMS00585 TRiP); *UAS–grapes^{RNAi}* (ID 12680* and ID 110076, VDRC); *UAS-spnA^{RNAi}* (ID 13362* and ID 14021, VDRC); *UAS- bsk^{K53R}* [*UAS-bsk^{DN}* in the text]*; UAS-p35; UAS-tribbles* (a kind gift from B Edgar); *UAS-dacapo* (a kind gift from I Hariharan); *viking (collagen IV)-GFP*;[12] *Df(3 L)H99; lig4^{169}*; *puckered-lacZ*[49] are described in Flybase.; *UAS-DE-CadΔCyt:α-Catenin*.[26] Other stocks are described in Flybase. dsRNA forms used in the main figures are the ones whose IDs contain an asterisk.

Immunohistochemistry

Mouse anti-MMP1 (14A3D2, Developmental Studies Hybridoma Bank (DSHB), Iowa City, IA, USA); rabbit anti-p35 (IMG5740, IMGENEX, San Diego, CA, USA); rabbit anti-gal (Cappel, Westchester, PA, USA); rat anti-Ci (2A1, DSHB); mouse anti-Fasciclin III (7G10, DSHB); mouse anti-disc large (4F3, DSHB); mouse anti-Wg (4D4, DSHB); rat anti-E-cadherin (DCAD2, DSHB); rabbit anti-atypical protein kinase C (DSHB); rabbit anti-laminin- (ab47651, AbCam, Cambridge, MA, USA); rabbit anti-P-H2AV (Rockland, Gilbertsville, PA, USA); and rabbit anti-human cleaved caspase 3 (Cell Signaling, Danvers, MA, USA). Secondary antibodies were obtained from Molecular Probes (Eugene, OR, USA).

Quantification of tissue growth

Size of the A and P compartments in the wing primordia were measured using the Fiji Software (NIH, Bethesda, MD, USA). At least 10 wing discs per genotype and condition were scored. The average P/A ratio and the corresponding s.d. were calculated and *t*-test analysis was carried out. In each experiment, control wing primordia (expressing p35 alone and subject or not to IR) were dissected and stained and the P/A ratio quantified. All genotypes included in each histogram were analyzed in parallel.

Mosaic analysis with a repressible cell marker clones

The following genotypes were used to generate loss-of-function clones for the H99 deficiency by the mosaic analysis with a repressible cell marker (Lee and Luo, 2001)[50] technique to simultaneously express different UAS transgenes in the clones: *hs-FLP, tub-Gal4, UAS-GFP/+; FRT2A tub-Gal80/ FRT2A Df(H99)*.

IR treatments

Irradiations were carried out in an YXLON MaxiShot X-ray system at the standard dose of 40 Gy. Clones of cells mutant for the H99 deficiency (*Df (H99)*) were induced by heat shock (1 h at 37 °C) at 72 h After egg laying (AEL), larvae were irradiated 24 h after clone induction and collected for dissection 72–96 h after IR treatment.

CONFLICT OF INTEREST

The authors declare no conflict of interest.

ACKNOWLEDGEMENTS

We thank B Edgar and I Hariharan for flies and reagents, T Yates for help in editing the manuscript, and M Clemente-Ruiz for comments on the manuscript. AD is funded by a Juan de la Cierva post-doctoral contract and LB by a pre-doctoral fellowship (Ministerio de Economía y Competitividad), MM is an ICREA Research Professor and MM's laboratory was funded by Grants from the Ministerio de Economía y Competitividad (BFU2010-21123 and CSD2007-00008), the Generalitat de Catalunya (2005 SGR 00118), intramural funds and the EMBO Young Investigator Programme.

REFERENCES

1 Negrini S, Gorgoulis VG, Halazonetis TD. Genomic instability–an evolving hallmark of cancer. *Nat Rev Mol Cell Biol* 2010; **11**: 220–228.
2 Lane D, Levine A. p53 Research: the past thirty years and the next thirty years. *Cold Spring Harb Perspect Biol* 2010; **2**: a000893.
3 Halazonetis TD, Gorgoulis VG, Bartek J. An oncogene-induced DNA damage model for cancer development. *Science* 2008; **319**: 1352–1355.
4 Jackson SP, Bartek J. The DNA-damage response in human biology and disease. *Nature* 2009; **461**: 1071–1078.
5 Foster SS, De S, Johnson LK, Petrini JH, Stracker TH. Cell cycle- and DNA repair pathway-specific effects of apoptosis on tumor suppression. *Proc Natl Acad Sci USA* 2012; **109**: 9953–9958.
6 Liu G, Parant JM, Lang G, Chau P, Chavez-Reyes A, El-Naggar AK *et al.* Chromosome stability, in the absence of apoptosis, is critical for suppression of tumorigenesis in Trp53 mutant mice. *Nat Genet* 2004; **36**: 63–68.
7 Brady CA, Jiang D, Mello SS, Johnson TM, Jarvis LA, Kozak MM *et al.* Distinct p53 transcriptional programs dictate acute DNA-damage responses and tumor suppression. *Cell* 2011; **145**: 571–583.
8 Valente LJ, Gray DH, Michalak EM, Pinon-Hofbauer J, Egle A, Scott CL *et al.* p53 efficiently suppresses tumor development in the complete absence of its cell-cycle inhibitory and proapoptotic effectors p21, Puma, and Noxa. *Cell reports* 2013; **3**: 1339–1345.
9 Brumby AM, Richardson HE. Scribble mutants cooperate with oncogenic Ras or Notch to cause neoplastic overgrowth in Drosophila. *EMBO J* 2003; **22**: 5769–5779.
10 Dar AC, Das TK, Shokat KM, Cagan RL. Chemical genetic discovery of targets and anti-targets for cancer polypharmacology. *Nature* 2012; **486**: 80–84.
11 Ohsawa S, Sato Y, Enomoto M, Nakamura M, Betsumiya A, Igaki T. Mitochondrial defect drives non-autonomous tumour progression through Hippo signalling in Drosophila. *Nature* 2012; **490**: 547–551.
12 Pagliarini RA, Xu T. A genetic screen in Drosophila for metastatic behavior. *Science* 2003; **302**: 1227–1231.
13 Song YH. Drosophila melanogaster: a model for the study of DNA damage checkpoint response. *Mol Cells* 2005; **19**: 167–179.
14 Brodsky MH, Nordstrom W, Tsang G, Kwan E, Rubin GM, Abrams JM. Drosophila p53 binds a damage response element at the reaper locus. *Cell* 2000; **101**: 103–113.
15 Peters M, DeLuca C, Hirao A, Stambolic V, Potter J, Zhou L *et al.* Chk2 regulates irradiation-induced, p53-mediated apoptosis in Drosophila. *Proc Natl Acad Sci USA* 2002; **99**: 11305–11310.

16 Song YH, Mirey G, Betson M, Haber DA, Settleman J. The Drosophila ATM ortholog, dATM, mediates the response to ionizing radiation and to spontaneous DNA damage during development. *Curr Biol* 2004; **14**: 1354–1359.
17 Jaklevic BR, Su TT. Relative contribution of DNA repair, cell cycle checkpoints, and cell death to survival after DNA damage in Drosophila larvae. *Curr Biol* 2004; **14**: 23–32.
18 Staeva-Vieira E, Yoo S, Lehmann R. An essential role of DmRad51/SpnA in DNA repair and meiotic checkpoint control. *EMBO J* 2003; **22**: 5863–5874.
19 Kooistra R, Vreeken K, Zonneveld JB, de Jong A, Eeken JC, Osgood CJ *et al.* The Drosophila melanogaster RAD54 homolog, DmRAD54, is involved in the repair of radiation damage and recombination. *Mol Cell Biol* 1997; **17**: 6097–6104.
20 Romeijn RJ, Gorski MM, van Schie MA, Noordermeer JN, Mullenders LH, Ferro W *et al.* Lig4 and rad54 are required for repair of DNA double-strand breaks induced by P-element excision in Drosophila. *Genetics* 2005; **169**: 795–806.
21 Hay BA, Wolff T, Rubin GM. Expression of baculovirus P35 prevents cell death in Drosophila. *Development* 1994; **120**: 2121–2129.
22 Perez-Garijo A, Martin FA, Morata G. Caspase inhibition during apoptosis causes abnormal signalling and developmental aberrations in Drosophila. *Development* 2004; **131**: 5591–5598.
23 Warner SJ, Yashiro H, Longmore GD. The Cdc42/Par6/aPKC polarity complex regulates apoptosis-induced compensatory proliferation in epithelia. *Curr Biol* 2010; **20**: 677–686.
24 Igaki T, Pagliarini RA, Xu T. Loss of cell polarity drives tumor growth and invasion through JNK activation in Drosophila. *Curr Biol* 2006; **16**: 1139–1146.
25 Uhlirova M, Bohmann D. JNK- and Fos-regulated Mmp1 expression cooperates with Ras to induce invasive tumors in Drosophila. *EMBO J* 2006; **25**: 5294–5304.
26 Pacquelet A, Rorth P. Regulatory mechanisms required for DE-cadherin function in cell migration and other types of adhesion. *J Cell Biol* 2005; **170**: 803–812.
27 Srivastava A, Pastor-Pareja JC, Igaki T, Pagliarini R, Xu T. Basement membrane remodeling is essential for Drosophila disc eversion and tumor invasion. *Proc Natl Acad Sci USA* 2007; **104**: 2721–2726.
28 Beaucher M, Hersperger E, Page-McCaw A, Shearn A. Metastatic ability of Drosophila tumors depends on MMP activity. *Dev Biol* 2007; **303**: 625–634.
29 Srivastava N, Gochhait S, de Boer P. Bamezai RN. Role of H2AX in DNA damage response and human cancers. *Mutat Res* 2009; **681**: 180–188.
30 Joyce EF, Pedersen M, Tiong S, White-Brown SK, Paul A, Campbell SD *et al.* Drosophila ATM and ATR have distinct activities in the regulation of meiotic DNA damage and repair. *J Cell Biol* 2011; **195**: 359–367.
31 Mata J, Curado S, Ephrussi A, Rorth P. Tribbles coordinates mitosis and morphogenesis in Drosophila by regulating string/CDC25 proteolysis. *Cell* 2000; **101**: 511–522.
32 Edgar BA, O'Farrell PH. Genetic control of cell division patterns in the Drosophila embryo. *Cell* 1989; **57**: 177–187.
33 Grosshans J, Wieschaus E. A genetic link between morphogenesis and cell division during formation of the ventral furrow in Drosophila. *Cell* 2000; **101**: 523–531.
34 Seher TC, Leptin M. Tribbles a cell-cycle brake that coordinates proliferation and morphogenesis during Drosophila gastrulation. *Curr Biol* 2000; **10**: 623–629.
35 Reis T, Edgar BA. Negative regulation of dE2F1 by cyclin-dependent kinases controls cell cycle timing. *Cell* 2004; **117**: 253–264.
36 de Nooij JC, Letendre MA, Hariharan IK. A cyclin-dependent kinase inhibitor, Dacapo, is necessary for timely exit from the cell cycle during Drosophila embryogenesis. *Cell* 1996; **87**: 1237–1247.
37 Lane ME, Sauer K, Wallace K, Jan YN, Lehner CF, Vaessin H. Dacapo a cyclin-dependent kinase inhibitor, stops cell proliferation during Drosophila development. *Cell* 1996; **87**: 1225–1235.
38 Li T, Kon N, Jiang L, Tan M, Ludwig T, Zhao Y *et al.* Tumor suppression in the absence of p53-mediated cell-cycle arrest, apoptosis, and senescence. *Cell* 2012; **149**: 1269–1283.
39 McVey M, Larocque JR, Adams MD, Sekelsky JJ. Formation of deletions during double-strand break repair in Drosophila DmBlm mutants occurs after strand invasion. *Proc Natl Acad Sci USA* 2004; **101**: 15694–15699.
40 McVey M, Adams M, Staeva-Vieira E, Sekelsky JJ. Evidence for multiple cycles of strand invasion during repair of double-strand gaps in Drosophila. *Genetics* 2004; **167**: 699–705.
41 Dekanty A, Barrio L, Muzzopappa M, Auer H, Milan M. Aneuploidy-induced delaminating cells drive tumorigenesis in Drosophila epithelia. *Proc Natl Acad Sci USA* 2012; **109**: 20549–20554.
42 Oromendia AB, Dodgson SE, Amon A. Aneuploidy causes proteotoxic stress in yeast. *Genes Dev* 2012; **26**: 2696–2708.
43 Stingele S, Stoehr G, Peplowska K, Cox J, Mann M, Storchova Z. Global analysis of genome, transcriptome and proteome reveals the response to aneuploidy in human cells. *Mol Syst Biol* 2012; **8**: 608.
44 Garcia AM, Calder RB, Dolle ME, Lundell M, Kapahi P, Vijg J. Age- and temperature-dependent somatic mutation accumulation in Drosophila melanogaster. *PLoS Genet* 2010; **6**: e1000950.
45 Salomon RN, Jackson FR. Tumors of testis and midgut in aging flies. *Fly (Austin)* 2008; **2**: 265–268.
46 Kusano K, Johnson-Schlitz DM, Engels WR. Sterility of Drosophila with mutations in the Bloom syndrome gene--complementation by Ku70. *Science* 2001; **291**: 2600–2602.
47 Garcia AM, Salomon RN, Witsell A, Liepkalns J, Calder RB, Lee M *et al.* Loss of the bloom syndrome helicase increases DNA ligase 4-independent genome rearrangements and tumorigenesis in aging Drosophila. *Genome Biol* 2011; **12**: R121.
48 Hanahan D, Weinberg RA. Hallmarks of cancer: the next generation. *Cell* 2011; **144**: 646–674.
49 Martin-Blanco E, Gampel A, Ring J, Virdee K, Kirov N, Tolkovsky AM *et al.* puckered encodes a phosphatase that mediates a feedback loop regulating JNK activity during dorsal closure in Drosophila. *Genes Dev* 1998; **12**: 557–570.
50 Lee T, Luo L Mosaic analysis with a repressible cell marker (MARCM) for Drosophila neural development. *Trends Neurosci* 2001; **24**: 251–254.

Supplementary Information accompanies this paper on the Oncogene website (http://www.nature.com/onc)

Publication (3)

"Aneuploidy-induced delaminating cells drive tumorigenesis in

Drosophila epithelia"

Aneuploidy-induced delaminating cells drive tumorigenesis in *Drosophila* epithelia

Andrés Dekanty[a], Lara Barrio[a], Mariana Muzzopappa[a], Herbert Auer[a], and Marco Milán[a,b,1]

[a]Institute for Research in Biomedicine (IRB Barcelona) and [b]Institució Catalana de Recerca i Estudis Avançats (ICREA), 08028 Barcelona, Spain

Edited by Mark Groudine, Fred Hutchinson Cancer Research Center, Seattle, WA, and approved November 2, 2012 (received for review April 23, 2012)

Genomic instability has been observed in essentially all sporadic carcinomas. Here we use *Drosophila* epithelial cells to address the role of chromosomal instability in cancer development as they have proved useful for elucidating the molecular mechanisms underlying tumorigenic growth. We first show that chromosomal instability leads to an apoptotic response. Interestingly, this response is p53 independent, as opposed to mammalian cells, and depends on the activation of the c-Jun N-terminal kinase (JNK) signaling cascade. When prevented from undergoing programmed cell death (PCD), chromosomal instability induces neoplasic overgrowth. These tumor-like tissues are able to grow extensively and metastasize when transplanted into the abdomen of adult hosts. Detailed analysis of the tumors allows us to identify a delaminating cell population as the critical one in driving tumorigenesis. Cells loose their apical–basal polarity, mislocalize DE-cadherin, and delaminate from the main epithelium. A JNK-dependent transcriptional program is activated specifically in delaminating cells and drives nonautonomous tissue overgrowth, basement membrane degradation, and invasiveness. These findings unravel a general and rapid tumorigenic potential of genomic instability, as opposed to its proposed role as a source of mutability to select specific tumor-prone aneuploid cells, and open unique avenues toward the understanding of the role of genomic instability in human cancer.

Genomic instability (GI) was originally proposed to cause cancer over 100 years ago, because it was discovered in all epithelial cancers investigated (1) and found to cause abnormal and tumor-like phenotypes in developing sea urchin embryos (2). Since then, GI has been observed in essentially all sporadic carcinomas, the most common type of cancer occurring in humans and derived from putative epithelial cells. There are various forms of GI and the most common in cancer is chromosomal instability (CIN), which refers to the high rate by which chromosome structure and number changes over time in cancer cells compared with normal cells (3). Eukaryotic cells have developed quality control mechanisms, collectively called checkpoints, which ensure correct execution of cell cycle events to maintain genome stability. Three checkpoints have been thoroughly documented: the DNA damage checkpoint, which is able to block cells in G1, S, G2, or even mitosis; the DNA replication checkpoint, which monitors progression through S phase, and the spindle-assembly checkpoint (SAC), which monitors attachment of chromosomes to functional spindle microtubules, ensuring equal segregation of genomic material among daughter cells (4–6). Unfortunately, only a few lines of evidence support a potential role of CIN in tumorigenesis. CIN is not sufficient to drive tumorigenesis in *Drosophila* stem cells (7) and spontaneous tumor development in SAC mutant mice is at relatively low rates (8). Interestingly, mouse strains mutant for SAC genes activate the ataxia telangiectasia mutated (ATM)/p53 pathway and additional depletion of p53 induces tumorigenesis of mouse strains with a dysfunctional SAC (9). So far, the molecular mechanisms and cellular behaviors underlying CIN-induced tumorigenesis remain uncharacterized and perhaps the most accepted hypothesis on the role of CIN in cancer development is the one that proposes that CIN is a source of mutability that helps the tumor cell population to pass through the critical steps of tumorigenesis such as cell delamination, extravasation, and invasiveness (10). To address this further in a genetically tractable system, we have selected a group of genes involved not only in the spindle assembly checkpoint, but also in spindle assembly, chromosome condensation, and cytokinesis, whose depletion leads to CIN (7), and analyzed its impact in highly proliferative epithelial cells of *Drosophila*.

Results

CIN Leads to *Drosophila* p53-Independent Programmed Cell Death. The *Drosophila* primordia of adult wing and eye structures (the wing and eye imaginal discs) are epithelial monolayers that actively proliferate during larval development, give rise to a 1,000-fold increase in number of cells and tissue size, and have proved useful for elucidating the molecular mechanisms underlying tumorigenic growth (11, 12). To induce CIN in these cells, we have selected a group of genes whose depletion leads to CIN and analyzed its impact in highly proliferative epithelial cells of *Drosophila*. Mutations in genes involved in the spindle assembly checkpoint [*bub3* and *rough deal* (*rod*)], spindle assembly [*abnormal spindle* (*asp*)], chromatin condensation (*orc2*), and cytokinesis [*diaphanous* (*dia*)] have been shown to recapitulate the genomic defects most frequently associated with human cancer, including chromosome rearrangements and aneuploidy (7). Cytokinesis defects lead to polyploidy, which takes place in a substantial fraction of human tumors and has been proposed to constitute an important step in the development of cancer aneuploidy (13). We drove expression of dsRNA forms of these genes in the larval primordia of the adult wing and eye structures. To assess the extent of genetically induced CIN, we first quantified loss of heterozygosity (LOH) of two different genetic markers in adult tissues (see *SI Materials and Methods* for details). The first assay is based on haploinsufficiency of the *Minute* genes (14), which encode for ribosomal protein genes. Because the 65 *Minute* loci are spread throughout the euchromatic genome, reduced copy number of most large genomic regions is likely to result in the *Minute* phenotype (visualized as thin adult bristles, Fig. 1*A*). The second assay was generated in a heterozygous background for a recessive allele of the *yellow* gene, which is located on the X chromosome. LOH can be scored by analyzing *yellow* bristles in adult tissues (Fig. 1*B*). In flies expressing dsRNA forms for *asp*, *rod*, *bub3*, and *orc2*, we observed a significant increase in *yellow* and/or *Minute* LOH (Fig. 1 *A* and *B*). Because these assays rely on the ability of cells to divide, we were not able to quantify LOH in cells expressing a dsRNA form for *dia*. LOH was also analyzed in wing primordia and generated in a heterozygous background for two different transgenes located on different chromosomes (*UAS-GFP* transgene located on the second chromosome and *UAS-RFP* transgene located on the third chromosome, Fig. S1). Expression of these transgenes was driven under the control of the *en-gal4* driver and monitored in normal conditions or upon coexpression

Author contributions: A.D., L.B., and M. Milán designed research; A.D., L.B., M. Muzzopappa, and H.A. performed research; A.D., L.B., M. Muzzopappa, and M. Milán analyzed data; and M. Milán wrote the paper.

The authors declare no conflict of interest.

This article is a PNAS Direct Submission.

[1]To whom correspondence should be addressed. E-mail: marco.milan@irbbarcelona.org.

This article contains supporting information online at www.pnas.org/lookup/suppl/doi:10.1073/pnas.1206675109/-/DCSupplemental.

GENETICS

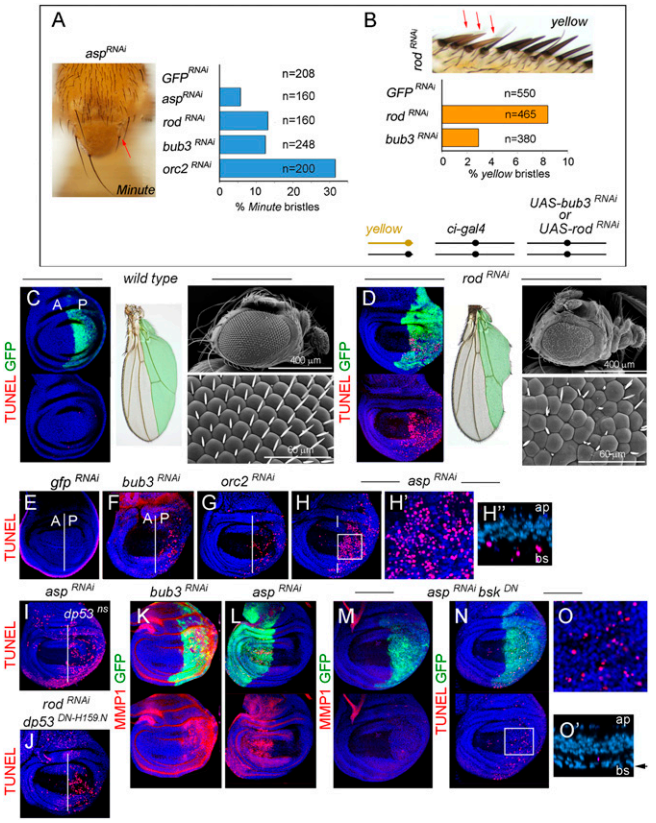

Fig. 1. Dp53-independent CIN-induced apoptosis in epithelial cells. (*A* and *B*) Loss of heterozygocity analyses of the *Minute* (*A*) and *yellow* (*B*) genes. Adult thorax with *Minute* thin bristles (*A*, red arrow) and magnification of an anterior adult wing margin with *yellow* bristles (*B*, red arrows) upon expression of asp^{RNAi} (*A*) or rod^{RNAi} (*B*) under the control of the *ci-gal4* driver, and histogram plotting the frequencies of *Minute* (*A*) and *yellow* (*B*) bristles of flies expressing GFP^{RNAi}, asp^{RNAi}, rod^{RNAi}, $bub3^{RNAi}$, or $orc2^{RNAi}$ under the control of the *ci-gal4* driver. *ci-gal4* drives expression in anterior (*A*) cells in the wing and in the whole adult thorax. Genotypes: (*A*) *+/+; ci-gal4 (II)/+; UAS-dsRNA (III)* and (*B*) *yellow/+ (I); ci-gal4 (II)/+; UAS-dsRNA (III)/+*. Only females were scored. (*C–J*) Larval wing primordia, adult wings, and eyes from individuals expressing GFP (*C* and *D*) and the indicated transgenes (*D–J*) under the control of the *en-gal4* (wings) or *ey-gal4* (eyes) drivers, and stained for GFP (green), DAPI (blue), and TUNEL staining (red). The wing primordium shown in *I* is also mutant for *dp53*. X-Y sections of the basal side of the wing epithelia are shown. *H′* shows a magnification of the squared region in *H*. *H′′* shows a cross-section of the posterior compartment. Note in *H′′* that TUNEL positive cells are located on the basal side of the epithelium. Vertical line in *E–J* depicts the boundary between anterior (A) and posterior (P) cells. (*K–O′*) Larval wing primordia from individuals expressing the indicated transgenes and GFP under the control of the *en-gal4* (*K* and *M–O′*) or *ci-gal4* (*L*) drivers, and stained for GFP (green), DAPI (blue), and MMP1 (red in *K–M*) or TUNEL staining (red in *N–O′*). X-Y sections of the basal side of the wing epithelia are shown. *O* shows a magnification of the squared region in *N*. *O′* shows a cross-section of the posterior compartment. Note in *O′* that TUNEL negative cells are located in the basal side of the epithelium. *en-gal4* drives expression in posterior (P) cells and is depicted in green in the adult wings. *ci-gal4* drives expression in anterior (A) cells. ap, apical; bs, basal.

of a dsRNA form of *rod* (Fig. S1). LOH can be scored by the loss of GFP or RFP expression within the *en-gal4* domain. In wing pirmordia expressing a dsRNA forms for *rod*, we observed a significant amount of *UAS-GFP* and/or *UAS-RFP* LOH (Fig. S1). Altogether these observations indicate that expression of these dsRNA forms was able to induce CIN in our model system (see also below).

CIN induced gross abnormalities in differentiation and tissue growth in adult wings and eyes (Fig. 1 *C* and *D* and Fig. S1) and a strong increase in the number of apoptotic cells in the larval primordia (Fig. 1 *D–H*). Apoptotic cells were located on the basal side of the wing epithelium (Fig. 1*H′′*). Mammalian cells use the ATM/p53 pathway to remove, through programmed cell death (PCD), aneuploid cells and preserve the structure and function of their genome following CIN (9, 15, 16). Surprisingly, the number of apoptotic cells observed in larval tissues subject to CIN was not significantly reduced in *Drosophila* p53 (dp53) mutant tissues or upon depletion of Dp53 activity (Fig. 1 *I* and *J* and Fig. S1). The c-Jun N-terminal kinase (JNK) pathway is involved in various stress responses in *Drosophila* tissues including DNA damage (14, 17). Interestingly, ectopic JNK activation, monitored by the expression of matrix metaloproteinase 1 (MMP1), a direct transcriptional target of dFos downstream of JNK signaling (18), was observed upon genetically induced CIN (Fig. 1 *K* and *L* and Fig. S1). MMP1 expression was completely blocked upon expression of a dominant negative version of JNK (*basket* in *Drosophila*, Fig. 1*M*) and the number of apoptotic cells was largely, but not completely rescued (Fig. 1 *N–O′*). Interestingly, we observed a large number of cells located on the basal side of the epithelium, which were nonapoptotic (compare Fig. 1 *O* and *O′* with *H* and *H′*). Altogether, these results indicate that genetically induced CIN induces, in contrast to mammalian cells, a p53-independent apoptotic response in *Drosophila* tissues, most probably to reduce the number of aneuploid cells and maintain genomic stability in the cell population. Although JNK appears to largely contribute to this apoptotic response, other stress response pathways might be involved as well.

CIN-Induced Neoplasic Tissue Growth and Host Invasiveness upon Additional Blockage of PCD. To maintain aneuploid cells in the tissue subject to CIN, apoptotic cell death was blocked or reduced by three different means. Apoptosis was first, and most generally, blocked by means of expression of the baculovirus protein p35, known to bind and repress the effector caspases DrICE and Dcp-1 (19). The DNA content profile of dissociated cells subject to CIN and expressing p35 revealed a high percentage of cells with DNA content higher than 4n (up to 41%) compared with control p35-expressing cells (Fig. 2*H* and Fig. S2). In the case of cells subject to CIN but not expressing p35, this percentage was very similar to control-expressing tissues (Fig. S2), reinforcing the role of apoptosis in eliminating aneuploid cells from the tissue. Apoptosis was also reduced in the whole larvae by halving the dose of the proapoptotic genes *hid*, *grim*, and *reaper* (in *Df(H99)*/+ animals) or blocked by mutation in the initiator caspase Dronc (in $dronc^{L29}$ animals) or in clones of cells homozygous for the *H99* deficiency. Interestingly, in all cases, a strong overgrowth was observed in the cell population subject to genetically induced CIN (labeled with p35 or GFP), compared with the neighboring wild-type tissue (not labeled) and with age-matched p35-expressing wing discs (Fig. 2 *A–G*). Similar results were obtained in adults eyes (Fig. S2). Tissues depleted of *dia* expression and expressing p35 did not grow, most probably due to defects in cytokinesis. Interestingly, larvae containing overgrown tissues kept growing for longer periods of time than GFP-expressing control larvae (Fig. S2), the resulting wing primordia were massively overgrown (Fig. 2 *I–K*) and the GFP cell population invaded the neighboring wild-type territory (labeled in red, Fig. 2 *I* and *J*). To further characterize the growth potential of the tissue subject to CIN and PCD blockade, wing tissue expressing p35, GFP, and the corresponding dsRNA transgenes was transplanted into the abdomen of adult females and maintained for a period of 20 d. Whereas p35-expressing tissue hardly grew after implantation, tissue subject to CIN and expressing p35 could grow many folds larger than the size of the implant (Fig. 2*L*) and showed disorganized tissue architecture with extensive folding (Fig. 2*M* and Fig. S2). In some cases, cells of the overgrown tissue were able to invade different organs of the host and micrometastasis of GFP-expressing cells could be found in the ovary of the adult host (Fig. 2 *N–P*).

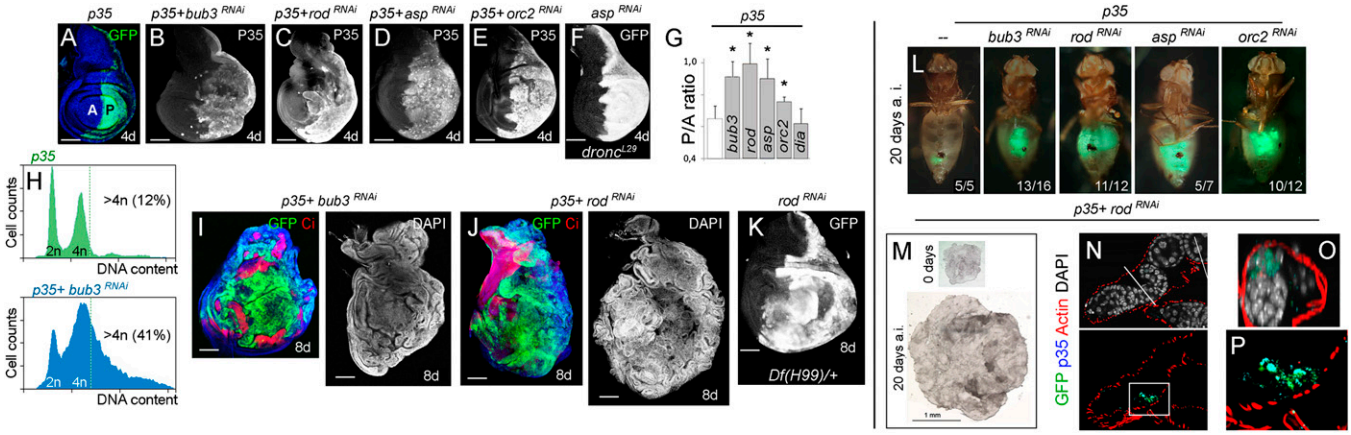

Fig. 2. CIN-induced tumor growth and tissue invasiveness upon additional blockade of programmed cell death. (*A–F* and *I–K*) Larval wing primordia from wild-type individuals (*A*) or from individuals expressing the indicated transgenes and GFP in posterior (P) cells under the control of the *en-gal4* (wings) driver and stained for GFP (green or white, *A* and *F*), P35 (*B–E*), DAPI (blue or white, *A* and *I–K*), and Ci (red, *I* and *J*) protein expression. Ci labels anterior (A) cells in *I* and *J*. Wing primordia shown in *F* and *K* are also mutant for *dronc* (*F*) or heterozygous for *Df(H99)* (*K*). (*G*) Histogram plotting the P/A size ratio of wing primordia expressing p35 and dsRNA for the indicated genes under the control of the *en-gal4* driver. Error bars represent SEM. **P* < 0.001. Larvae were 4 d old in *A–G* and 8 d old in *I–K*. (*H*) DNA content analysis by fluorescence associated cell sorter (FACS) of wing cells expressing the indicated transgenes under the control of the *ap-gal4* driver. Percentage of cells with DNA content higher than 4n is indicated. (*L*) Adult fly micrographs taken 20 d after implantation (a.i.) of GFP-labeled larval wing tissue expressing the indicated transgenes. Ratios showing the reproducibility of the phenotype are shown. (*M*) Larval wing tissue 0 and 20 d a.i. (*N–P*) GFP (green) and P35 (blue) positive cells are observed inside the host ovary stained for DAPI (gray) and actin (red). *O* is a cross-section of *N* along the white line, and *P* is a magnification of *N*.

CIN-Induced Loss of Apical–Basal Polarity and Junctional DE-Cadherin Levels. To characterize the cellular mechanisms underlying CIN-induced tumorigenesis, we carefully examined the behavior of aneuploid cells within the larval primordia. The wing primordium is a cellular monolayer that forms a two-sided epithelial sac (Fig. 3*A*). One side of this sac forms a thin squamous sheet, whereas the apposed epithelial surface (the columnar epithelium) adopts a pseudostratified columnar morphology. The apical side of both epithelia is oriented toward the lumen of the sac, whereas the basal side is the external surface. Cells subject to genetically induced CIN delaminated from the main epithelium, lost their columnar shape, and acquired a rounded and irregular form (Fig. 3 *B* and *C*). Epithelial architecture relies on the polarization of the plasma membrane into apical and basolateral domains separated by the adherens junctions. We used antibodies against atypical protein kinase C (aPKC), Disk large (Dlg), and DE-cadherin (DE-cad) to visualize the subapical, basolateral, and junctional domains, respectively. Whereas aPKC and Dlg were still observed at the membrane of delaminated cells, the overall protein levels were severely reduced (Fig. 3 *D*, *E*, *D′*, and *E′* and Fig. S3). Interestingly, DE-Cad lost its tight junctional localization and the overall protein levels were clearly reduced (Fig. 3 *F* and *G* and Fig. S3). It was no longer detectable in most of the delaminated cells with the exception of some small discrete puncta (Fig. 3 *F′* and *G′* and Fig. S3). Overexpression of a modified version of DE-cad (DE-CadΔCyt:α-catenin), able to rescue the adhesion properties of *E-cad* mutant cells and unable to interfere with endogenous β-catenin signaling (20), did not rescue the delamination process and the overexpressed form of DE-cad localized to small discrete puncta in delaminating cells (Fig. 3 *H* and *H′*). Thus, dissociation of *Drosophila* epithelial cells upon CIN is not due to reduced levels of DE-cad and is most probably a consequence of DE-cad mislocalization.

Strikingly, delaminated cells showed a high degree of aneuploidy compared with nondelaminated cells, as shown by their DNA content profile and aberrant number of chromosomes (Fig. 3 *K* and *K′* and Fig. S2). A high percentage of cells with DNA content higher than 4n was observed in the delaminated cells (up to 35%) compared with the nondelaminated ones (Fig. 3*K*). These results support the proposal that aneuploidy triggers cell delamination.

CIN-Induced JNK Activation in Delaminating Cells. Tumorigenesis is usually accompanied by disruption of the basement membrane (BM) and MMPs are well known to contribute to BM degradation both in flies and mammals (18, 21). BM was clearly disrupted in the cell population subject to CIN (labeled with laminin-γ or with a GFP-tagged protein trap in the *viking/collagen IV* gene, Figs. 3 *B*, *I*, and *J* and 4*B*) and ectopic expression of MMP1 was observed in the delaminating cell population (Figs. 3*J* and 4*B* and Fig. S4). *Mmp1* is a direct target of dFos downstream of JNK activation (18), and consistently, expressing a dominant negative version of JNK (*basket*^{DN}) blocked the ectopic expression of MMP1 (Fig. 4*E*). Expression of *puckered*, a known target of JNK signaling in *Drosophila* tissues (22), was also observed in delaminating cells (Fig. S4). The fact that MMP1 and *puckered* expression were restricted to the delaminating cell population opens the possibility of a causal relationship between JNK activation and cell delamination. However, cell delamination and E-cadherin mislocalization was not rescued upon blocking JNK activity (Fig. 4 *E–G*). These results indicate that genetically induced CIN induces delamination of epithelial cells, JNK-dependent activation of MMP1 expression, and BM disruption.

The mitogenic signaling molecule Wingless (Wg) is induced in a JNK-dependent manner by a number of insults in *Drosophila* epithelia (23–25), opening the possibility that *wg* might also be a target of JNK activity in CIN-induced delaminating cells. Indeed, ectopic expression of Wg was observed in these cells (Fig. 4 *C*, *D*, and *H* and Fig. S4) and, interestingly, expression of MMP1 and Wg were also observed in transplanted tissues subject to CIN (Fig. S2). CIN-induced Wg expression was abolished upon expression of a dominant negative version of JNK/Basket (Fig. 4*F*). Remarkably, a *wg* enhancer previously shown to drive Wg expression upon tissue injury (Fig. 4*I*) (26) was activated in cells subject to genetically induced CIN (Fig. 4*J*) and in cells expressing an activated form of JNKK (*hemipterous* in *Drosophila*, Fig. S4). We next tested whether this enhancer was absolutely required to induce JNK-dependent expression of Wg upon CIN. Luckily, the first ever identified mutation in the *wg* gene (wg^1) carries a deletion including this enhancer (Fig. 4*I*) (26, 27), and wg^1 mutant tissue did not show ectopic expression of Wg upon CIN, and the tissue was less overgrown (Fig. 4*K*). We noticed that the endogenous expression of Wg was unaffected in the wg^1 mutant condition. These results support the notion that JNK activates *wg* expression in delaminating cells and that the JNK responsive enhancer is required to induce *wg* expression upon CIN. JNK activation in CIN-

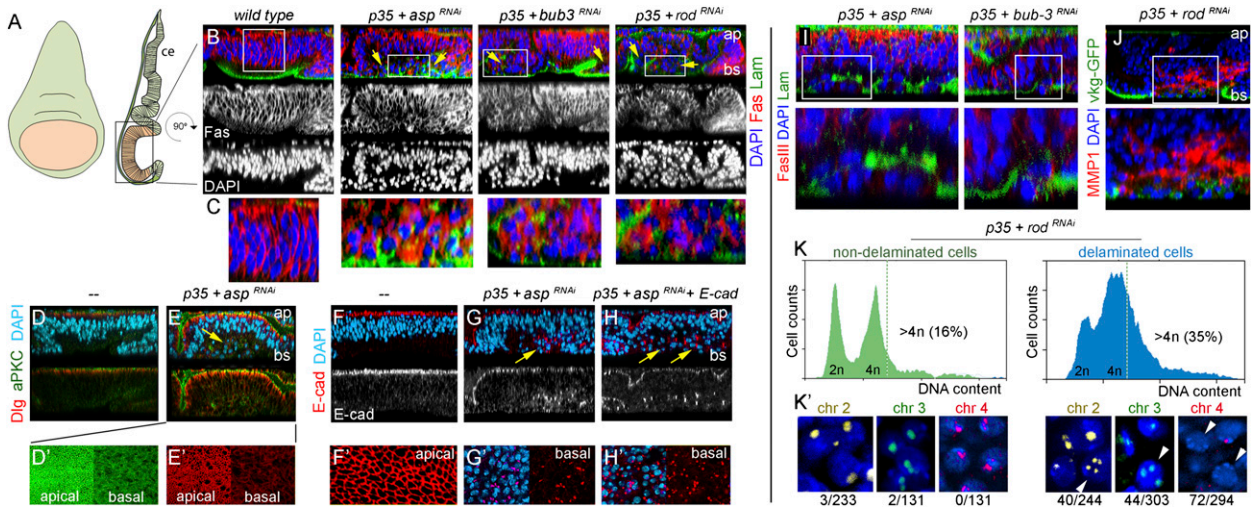

Fig. 3. CIN-induced cell delamination and BM degradation. (*A*) Cartoon depicting the columnar epithelium (ce) of the wing primordium. (*B–J*) Cross-sections of the posterior compartment of wing primordia expressing the indicated transgenes under the control of the *en-gal4* driver and stained for DAPI (blue), fasciclin III (red, *B*, *C*, and *I*), laminin-γ (labels the BM in green, *B*, *C*, and *I*), Dlg (red, *D* and *E*), aPKC (green, *D* and *E*), E-cad (red, *F–H*), and *viking-GFP* (*collagen IV*, *J*). ap, apical, and bs, basal. (*C*) Magnification of the squared regions shown in *B*. (D′–H′) X-Y sections of the apical and basal sides of the wing epithelia shown in *D–H*. Yellow arrows indicate delaminating cells. (*K* and *K′*) FACS sorted delaminated and nondelaminated cells from wing primordia expressing *p35* and a dsRNA form for *rod* under the control of the *en-gal4* driver were subject to DNA content profile analysis (*K*) and chromosome labeling with chromosome-specific probes (*K′*). In *K*, percentage of cells with DNA content higher than 4n is indicated. In *K′*, yellow arrows indicate aberrant number of chromosomes in delaminated cells. Ratios showing the number of nuclei presenting an aberrant number of chromosomes (more than two chromosomes 2 or 3 and loss of chromosome 4) are shown below each panel.

induced delaminating cells is most probably a consequence of the loss in the apical–basal polarity. Delaminating cells showed reduced aPKC protein levels, and genetic depletion of components of the Cdc42/Par6/aPKC polarity complex has been previously reported to induce JNK-dependent apoptosis and hyperplastic growth upon additional blockage of PCD (28). Similarly, CIN-induced delaminating cells showed reduced Dlg and junctional DE-cad protein levels, and genetic depletion of individual components of the Scribbled/Disk Large/Lgl polarity complex has been previously shown to induce a reduction in junctional DE-cad levels and activate the JNK pathway (18, 29, 30). JNK activation relies, in these experimental conditions, on increased endocytosis rates and on translocation of Eiger/TNF to endocytic vesicles thus leading to apoptotic JNK activation (31). Molecular mechanisms linking CIN and loss of apical–basal polarity remain to be elucidated.

Central Role of the Delaminating Cell Population in Inducing Tumorigenesis. The JNK pathway has a critical role in the tumorigenic behavior of *Drosophila* epithelial cells (18, 29–31). So far we have provided evidence that cell delamination and JNK activation correlate with high levels of aneuploidy. These results open the possibility that aneuploidy-induced JNK activation in the delaminating cell population has a critical role in organizing the hyperplastic overgrowth of the tissue. Remarkably, blocking

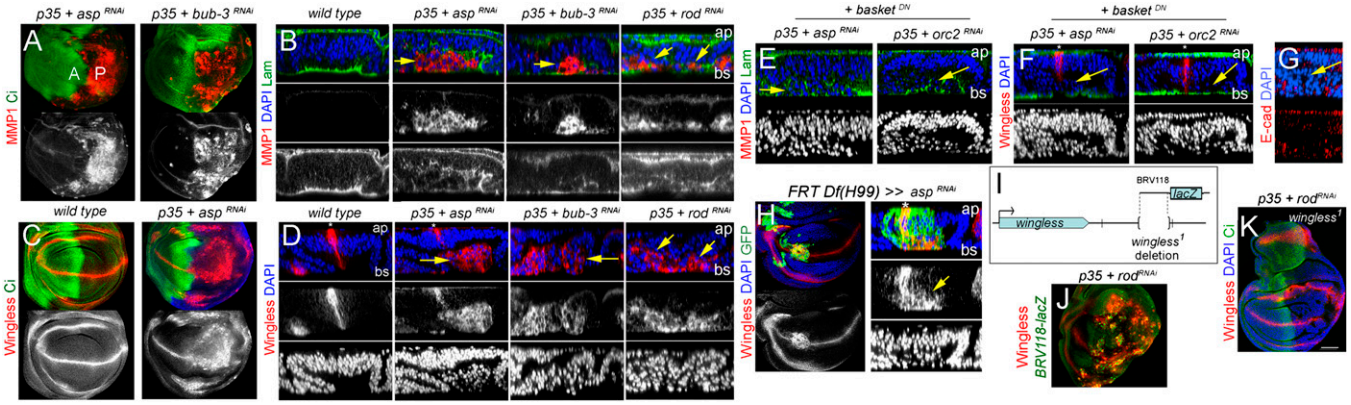

Fig. 4. CIN-induced JNK activation in delaminating cells. (*A* and *C*) Wing primordia expressing the indicated transgenes in posterior (P) cells under the control of the *en-gal4* driver, and stained for MMP1 (red, *A*), Wingless (red, *C*), and Ci (green) protein expression. Ci labels anterior (A) cells. (*B*, *D*, and *E–G*) Cross-sections of the posterior compartment of wing primordia expressing the indicated transgenes under the control of the *en-gal4* driver and stained in red for MMP1 (*B* and *E*), Wingless (*D* and *F*), or E-cadherin (*G*), in green for laminin-γ (*B*, *E*, and *F*), and in blue for DAPI. Yellow arrows indicate delaminating cells. (*H*) Wing primordium with clones of cells mutant for *Df(H99)* and expressing a dsRNA form of *asp* and GFP (green) and stained in red for Wingless and in blue for DAPI. (*Right*) Cross-section of the clone expressing Wingless. Note in this clone expression of Wg in delaminating cells (yellow arrow). (*I*) Scheme showing the genomic region of the *wingless* gene, the location of the BRV118 enhancer, and the deletion in the *wingless*^{1} mutation. (*J* and *K*) Wing primordia expressing the indicated transgenes in the posterior (P) compartment under the control of the *en-gal4* driver and stained in red for Wg, in green for *BRV118-lacZ* expression (*J*) or Ci (*K*), and in blue for DAPI (*K*). In *K*, Ci labels the anterior (A) compartment. Wing primordium shown in *K* is also mutant for *wingless*^{1}. Asterisks represent endogenous Wg expression. ap, apical; bs, basal.

JNK activity rescued the tissue overgrowth caused by CIN (Fig. 5*A*) as well as the capacity to grow extensively in allograft transplantations (Fig. 5*B*). Similarly and consistent with a role of Wg in promoting proliferative growth (32), a dsRNA form of *wg* largely rescued the tissue overgrowth (Fig. 5*C*) and the capacity of the tissue to grow extensively in allograft transplantations (Fig. 5*D*). These results support the notion that the highly aneuploid delaminating cell population has a critical role in the tumorigenic behavior of the tissue upon CIN induction. Whereas tissue hyperplasia relies on the restricted expression of Wg in this cell population, expression of MMP1 in delaminating cells degrades the underlying basement membrane thus facilitating tissue invasiveness (Fig. 5*E*). Cells subject to a high dose of ionizing radiation, known to induce aneuploidies in *Drosophila* tissues (14), or cells subject to segmental aneuploidies and maintained in the tissue by additional blockade of the apoptotic pathway, also delaminated from the main epithelium and showed MMP1 and Wingless expression (Fig. S5). These data reinforce the proposed role of aneuploidy-induced delaminated cells in driving tumorigenesis. The molecular and cellular mechanisms underlying the tumor-like behavior induced by aneuploidy upon additional blockage of PCD resemble, in a striking fashion, those caused by the cooperative action of *Ras* oncogene activation and mutations in the *scribbled* or *Discs Large* tumor suppressor genes (11, 18, 29, 30). Whereas JNK is being primarily used to remove, through PCD, cells whose genomic stability or apical–basal polarity is compromised, an additional blockade of the apoptotic pathway unravels a subversive role of JNK in driving tumorigenesis. Remarkably, JNK activation is not sufficient to drive tumorigenesis in epithelial cells even upon additional blockage of PCD, and apical–basal polarity disruption appears to play a fundamental role in this process (30). The identification of the delaminating cell population as the one with a critical role in promoting JNK-dependent deregulated growth and host invasiveness upon aneuploidy induction is consistent with these observations. In cancer development, an epithelial-to-mesenchymal transition (EMT) converts epithelial cells into migratory and invasive cells and is established as an important step in the metastatic cascade of epithelial tumors. Whether aneuploidy-induced cell delamination shares the properties of a real EMT in molecular and cell behavioral terms remains to be elucidated. However, it is interesting to note that aneuploidy-induced delaminating cells are motile (Fig. 2*C*, note isolated GFP delaminated cells far from the GFP-expressing domain) and are most probably the ones capable of invading the host.

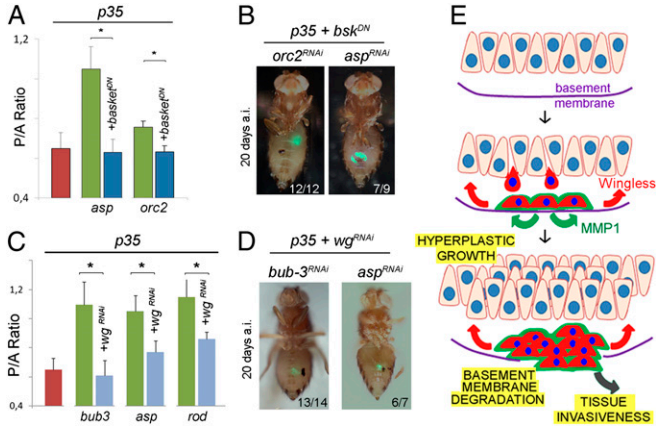

Fig. 5. A central role of the delaminating cell population in inducing tumorigenesis. (*A* and *C*) Histograms plotting the P/A size ratio of wing primordia expressing, under the control of the *en-gal4* driver, p35 alone (red bars), or p35 and dsRNA forms for *asp*, *orc2*, *bub3*, or *rod* (green and blue bars). Blue bars express also *basket-DN* (*A*) or a dsRNA form for *wingless* (*C*). Error bars represent SEM. $*P < 0.001$. (*B* and *D*) Adult fly micrographs taken 20 d after implantation (a.i.) of GFP-labeled larval wing tissue expressing the indicated transgenes. Ratios showing the reproducibility of the phenotype are shown. (*E*) Cartoon depicting CIN-induced tumorigenesis. CIN induces cell delamination of epithelial cells, and delaminating cells activate a JNK-dependent transcriptional response (dark blue nuclei) that leads to the expression of MMP1 (green) and Wingless (red) protein expression. MMP1 has an active role in degrading the basement membrane (purple), a critical step in tissue invasiveness, and Wingless contributes to the hyperplastic growth of the monolayered epithelium.

Discussion

Altogether, our results indicate that genetically induced CIN by different means leads to *Drosophila* p53 (dp53) independent apoptosis of proliferating epithelial cells, as opposed to mammalian cells (9, 15). Activation of the stress responsive JNK signaling cascade contributes to this apoptotic response and maintenance of the aneuploid cells in the tissue through additional blockage of PCD leads to tissue overgrowth and host invasiveness. This paper conducts a thorough analysis of the relationship between CIN and tumor-like growth, it provides an ideal genetic experimental setup to identify new molecular elements involved in CIN-induced tumorigenesis, and it reinforces the proposed role of programmed cell death in suppressing CIN-induced tumorigenesis.

Perhaps, the most accepted hypothesis on the role of CIN in tumorigenesis is the one that proposes that CIN is a source of mutability (e.g., loss or gain of certain chromosomes or chromosome regions carrying tumor suppressor genes or oncogenes) that helps the tumor cell population to pass through the critical steps such as cell delamination, extravasation, and invasiveness (10). Although the *Drosophila* tumor suppressor gene *l(2)gl* has been well documented to be prone to spontaneous deletions (33), overexpression of *l(2)gl* did not rescue the CIN-induced tumorigenic behavior of the tissue (Fig. S3). Amplification or deletion of other genomic regions might contribute to cell delamination and to the tumorigenic behavior of the tissue. In this context, we would like to speculate that resistance to apoptosis can also be a direct consequence of CIN (e.g., LOH of proapoptotic genes), thus contributing to the survival of aneuploid cells and to cancer development.

The identification of the delaminating cell population as the critical one in driving tumorigenesis adds another layer of complexity to our current understanding of CIN in human cancer. Whereas aneuploidy-induced delaminating cells become motile and degrade the basement membrane, supporting a cell-autonomous role of CIN in driving tissue invasiveness (10), delaminating cells play a nonautonomous role in promoting tumor growth. Wingless expression is restricted to the delaminating cell population and promotes hyperplastic growth of the nondelaminating cells. Interestingly, the nondelaminating cell population subject to CIN grows to a bigger extent than the neighboring wild-type territories (Fig. 2 *I* and *J*). Given the absolute requirement of Wingless in tumor growth (Fig. 5 *C* and *D*), these results support the proposal that low levels of aneuploidy in the nondelaminating cells might make these cells more responsive to the mitogenic action of Wingless. Whether this behavior is a consequence of LOH of genes involved in Wingless signaling requires further investigation. In addition, these observations uncover a self-reinforcement mechanism that might have implications in tumor initiation and progression in human cancer. Wingless induces hyperproliferation of signal-receiving (nondelaminating) cells, which is expected to increase aneuploidy levels and delamination rates and should lead, consequently, to a net increase in the number of signal-sending (delaminating) cells.

Besides the proposed role of CIN as a source of mutability, our results indicate that CIN also induces a general and rapid response of the tissue in terms of compromised apical–basal polarity, cell delamination, JNK activation, and basement membrane degradation, a prerequisite for tissue invasiveness. This quick response is very unlikely due to the sole accumulation of CIN-dependent oncogenic mutations and unravels, again, a subversive role of the stress-associated JNK pathway in driving tumorigenesis in *Drosophila* epithelia (11, 18, 29, 30). We support the proposal, based on work in yeast and human cells, that stress, most probably as

a result of aneuploidy-induced protein stoichiometry imbalances (34, 35), contributes to this rapid response. Further investigation is required to address whether this is the case.

Stimulation of cell death signaling by different insults and additional depletion of the activity of the apoptotic effector caspases has been previously shown to result in the production of the so-called undead cells, which express mitogenic signals that promote cell proliferation in the surrounding tissue (23, 25). Activation of the apical cell death caspase Dronc has been reported to be necessary and sufficient to drive this proliferation through a feedback mechanism that involves the activity of dp53 and the proapoptotic genes *hid* and *reaper* (Fig. S6). Interestingly, the tumorigenic response of the tissue upon CIN and additional blockage of PCD is independent of the activity of Dronc (Fig. 2*F* and Fig. S6), Dp53 (Fig. S6), and the proapoptotic genes *hid* and *reaper* (Fig. 2*K* and Fig. S6). Moreover, cells depleted for the proapoptotic genes *hid*, *grim*, and *reaper* delaminated from the main epithelium and showed Wingless expression (Fig. 4*H*), indicating that CIN-induced cell delamination and JNK activation is not a simple consequence of apoptosis induction. Although we cannot rule out a contribution of the dp53- and Dronc-dependent feedback loop in enhancing the tumorigenic response of the tissue upon CIN, our results support a rather specific oncogenic role of genomic instability in *Drosophila* epithelial cells that cannot be explained by the sole production of stress-induced undead cells.

Materials and Methods

Drosophila strains were obtained from Vienna *Drosophila* RNAi or the Bloomington Stock Center and are described in FlyBase. Antibodies were obtained from the Developmental Studies Hybridoma Bank or other private sources. These and other experimental details are described in *SI Materials and Methods*.

ACKNOWLEDGMENTS. We thank A. Bergmann, D. Bohmann, K. Golic, M. Llimargas, E. Martin-Blanco, and G. Schubiger for flies and reagents; F. Serras for technical advice in allograft experiments; C. Gonzalez for helpful discussions; and I. Hariharan, A. Nebreda, H. Richardson and two anonymous reviewers for comments on the manuscript. A.D. is funded by a Juan de la Cierva postdoctoral contract. M. Milán is an Institució Catalana de Recerca i Estudis Avançats (ICREA) research professor and this work was funded by BFU2010-21123, CSD2007-00008, and 2005 SGR 00118 and by European Molecular Biology Organization Young Investigator Programme grants.

1. von Hansemann D (1890) Ueber asymmetrische Zelltheilung in epithel Krebsen und deren biologische Bedeutung [On the asymmetrical cell division in epithelial cancers and its biological significance]. *Virchow's Arch Path Anat* 119:299. German.
2. Boveri T (1914) *Zur Frage der Entstehung Maligner Tumoren* [Origin of malignant tumors]. (Gustav Fisher, Jena), pp 1–64. German.
3. Negrini S, Gorgoulis VG, Halazonetis TD (2010) Genomic instability—an evolving hallmark of cancer. *Nat Rev Mol Cell Biol* 11(3):220–228.
4. Musacchio A, Salmon ED (2007) The spindle-assembly checkpoint in space and time. *Nat Rev Mol Cell Biol* 8(5):379–393.
5. Jackson SP, Bartek J (2009) The DNA-damage response in human biology and disease. *Nature* 461(7267):1071–1078.
6. Branzei D, Foiani M (2010) Maintaining genome stability at the replication fork. *Nat Rev Mol Cell Biol* 11(3):208–219.
7. Castellanos E, Dominguez P, Gonzalez C (2008) Centrosome dysfunction in Drosophila neural stem cells causes tumors that are not due to genome instability. *Curr Biol* 18(16):1209–1214.
8. Holland AJ, Cleveland DW (2009) Boveri revisited: Chromosomal instability, aneuploidy and tumorigenesis. *Nat Rev Mol Cell Biol* 10(7):478–487.
9. Li M, et al. (2010) The ATM-p53 pathway suppresses aneuploidy-induced tumorigenesis. *Proc Natl Acad Sci USA* 107(32):14188–14193.
10. Hanahan D, Weinberg RA (2011) Hallmarks of cancer: The next generation. *Cell* 144 (5):646–674.
11. Pagliarini RA, Xu T (2003) A genetic screen in Drosophila for metastatic behavior. *Science* 302(5648):1227–1231.
12. Brumby AM, Richardson HE (2005) Using Drosophila melanogaster to map human cancer pathways. *Nat Rev Cancer* 5(8):626–639.
13. Davoli T, de Lange T (2011) The causes and consequences of polyploidy in normal development and cancer. *Annu Rev Cell Dev Biol* 27:585–610.
14. McNamee LM, Brodsky MH (2009) p53-independent apoptosis limits DNA damage-induced aneuploidy. *Genetics* 182(2):423–435.
15. Burds AA, Lutum AS, Sorger PK (2005) Generating chromosome instability through the simultaneous deletion of Mad2 and p53. *Proc Natl Acad Sci USA* 102(32): 11296–11301.
16. Thompson SL, Compton DA (2010) Proliferation of aneuploid human cells is limited by a p53-dependent mechanism. *J Cell Biol* 188(3):369–381.
17. Brodsky MH, et al. (2000) Drosophila p53 binds a damage response element at the reaper locus. *Cell* 101(1):103–113.
18. Uhlirova M, Bohmann D (2006) JNK- and Fos-regulated Mmp1 expression cooperates with Ras to induce invasive tumors in Drosophila. *EMBO J* 25(22):5294–5304.
19. Hay BA, Wolff T, Rubin GM (1994) Expression of baculovirus P35 prevents cell death in Drosophila. *Development* 120(8):2121–2129.
20. Pacquelet A, Rørth P (2005) Regulatory mechanisms required for DE-cadherin function in cell migration and other types of adhesion. *J Cell Biol* 170(5):803–812.
21. Srivastava A, Pastor-Pareja JC, Igaki T, Pagliarini R, Xu T (2007) Basement membrane remodeling is essential for Drosophila disc eversion and tumor invasion. *Proc Natl Acad Sci USA* 104(8):2721–2726.
22. Martín-Blanco E, et al. (1998) puckered encodes a phosphatase that mediates a feedback loop regulating JNK activity during dorsal closure in Drosophila. *Genes Dev* 12(4):557–570.
23. Pérez-Garijo A, Martín FA, Morata G (2004) Caspase inhibition during apoptosis causes abnormal signalling and developmental aberrations in Drosophila. *Development* 131(22):5591–5598.
24. Smith-Bolton RK, Worley MI, Kanda H, Hariharan IK (2009) Regenerative growth in Drosophila imaginal discs is regulated by Wingless and Myc. *Dev Cell* 16(6):797–809.
25. Ryoo HD, Gorenc T, Steller H (2004) Apoptotic cells can induce compensatory cell proliferation through the JNK and the Wingless signaling pathways. *Dev Cell* 7(4): 491–501.
26. Schubiger M, Sustar A, Schubiger G (2010) Regeneration and transdetermination: The role of wingless and its regulation. *Dev Biol* 347(2):315–324.
27. Baker NE (1987) Molecular cloning of sequences from wingless, a segment polarity gene in Drosophila: The spatial distribution of a transcript in embryos. *EMBO J* 6(6): 1765–1773.
28. Warner SJ, Yashiro H, Longmore GD (2010) The Cdc42/Par6/aPKC polarity complex regulates apoptosis-induced compensatory proliferation in epithelia. *Curr Biol* 20(8): 677–686.
29. Brumby AM, Richardson HE (2003) scribble mutants cooperate with oncogenic Ras or Notch to cause neoplastic overgrowth in Drosophila. *EMBO J* 22(21):5769–5779.
30. Igaki T, Pagliarini RA, Xu T (2006) Loss of cell polarity drives tumor growth and invasion through JNK activation in Drosophila. *Curr Biol* 16(11):1139–1146.
31. Igaki T, Pastor-Pareja JC, Aonuma H, Miura M, Xu T (2009) Intrinsic tumor suppression and epithelial maintenance by endocytic activation of Eiger/TNF signaling in Drosophila. *Dev Cell* 16(3):458–465.
32. Baena-Lopez LA, Franch-Marro X, Vincent JP (2009) Wingless promotes proliferative growth in a gradient-independent manner. *Sci Signal* 2(91):ra60.
33. Green MM, Shepherd SH (1979) Genetic instability in Drosophila melanogaster: The induction of specific chromosome 2 deletions by MR elements. *Genetics* 92(3): 823–832.
34. Sheltzer JM, Torres EM, Dunham MJ, Amon A (2012) Transcriptional consequences of aneuploidy. *Proc Natl Acad Sci USA* 109(31):12644–12649.
35. Torres EM, et al. (2010) Identification of aneuploidy-tolerating mutations. *Cell* 143(1): 71–83.

Publication (4)

"Enhancer-PRE communication contributes to the expansion of gene expression domains in proliferating primordia"

Development 138, 3125-3134 (2011) doi:10.1242/dev.065599

Enhancer-PRE communication contributes to the expansion of gene expression domains in proliferating primordia

Lidia Pérez[1], Lara Barrio[1], David Cano[1], Ulla-Maj Fiuza[1], Mariana Muzzopappa[1] and Marco Milán[1,2,*]

SUMMARY

Trithorax-group and Polycomb-group proteins interact with chromosomal elements, termed PRE/TREs, to ensure stable heritable maintenance of the transcriptional state of nearby genes. Regulatory elements that bind both groups of proteins are termed maintenance elements (MEs). Some of these MEs maintain the initial activated transcriptional state of a nearby reporter gene through several rounds of mitosis during development. Here, we show that expression of *hedgehog* in the posterior compartment of the *Drosophila* wing results from the communication between a previously defined ME and a nearby cis-regulatory element termed the C enhancer. The C enhancer integrates the activities of the Notch and Hedgehog signalling pathways and, from the early wing primordium stage, drives expression to a thin stripe in the posterior compartment that corresponds to the dorsal-ventral compartment boundary. The ME maintains the initial activated transcriptional state conferred by the C enhancer and contributes to the expansion, by growth, of its expression domain throughout the posterior compartment. Communication between the ME and the C enhancer also contributes to repression of gene expression in anterior cells. Most interestingly, we present evidence that enhancers and MEs of different genes are interchangeable modules whose communication is involved in restricting and expanding the domains of gene expression. Our results emphasize the modular role of MEs in regulation of gene expression within growing tissues.

KEY WORDS: *hedgehog*, Epigenetic inheritance, Maintenance element, Notch, Ci, *Drosophila*

INTRODUCTION

Gene expression is generally governed by cis-regulatory elements that integrate cell-type and temporal information to generate accurate and stereotyped patterns of expression in space and time (Levine, 2010). One class of regulatory modules is embryonic enhancers, which drive gene expression as a result of transcription factor binding at the enhancer sequence. Very frequently, these transcription factors are only transiently expressed during development and the gene expression state of their target genes is maintained by the Polycomb group (PcG) and the Trithorax group (TrxG) of proteins. These form the basis of a cellular memory system that maintains the transcriptional state of the target genes heritable during development (for reviews, see Muller and Kassis, 2006; Schwartz and Pirrotta, 2007). The genes controlled by the PcG/TrxG system have PcG and TrxG response elements (PRE/TREs), to which these proteins bind and keep the gene either permanently repressed (PcG) or active (TrxG). In order to reflect the dual function of these regulatory elements that bind both groups of proteins, PRE/TREs are termed maintenance elements (MEs) (Brock and van Lohuizen, 2001). Some of these elements have been shown to maintain the initial activated transcriptional state of a nearby reporter gene through several rounds of mitosis during development (Cavalli and Paro, 1998). This is the case for *Drosophila* Hedgehog (Hh), a signalling molecule expressed in the posterior (P) compartment of all limb primordia and involved in anterior-posterior axis formation (Basler and Struhl, 1994; Tabata et al., 1992). An ME situated upstream of the *hh* transcription start site is able to maintain Gal4-driven *lacZ* reporter gene expression through several rounds of mitosis (Bejarano and Milan, 2009; Maurange and Paro, 2002).

Both genetic and epigenetic mechanisms are involved in regulation of *hh* expression in the *Drosophila* wing (Fig. 1A). The transcription factor Ci is expressed in the anterior (A) compartment, where it is required to repress *hh* expression (Apidianakis et al., 2001; Bejarano et al., 2007; Méthot and Basler, 1999), and the homeodomain proteins Engrailed (En) and Invected are expressed in the posterior (P) compartment, where they are required to repress Ci expression (Eaton and Kornberg, 1990) and relieve Ci-mediated repression of *hh* (Bejarano and Milan, 2009). PcG proteins help to maintain the repression of *hh* expression in A cells whereas TrxG proteins contribute to maintaining the expression of *hh* in P cells (Bejarano and Milan, 2009; Chanas and Maschat, 2005). Notch activity at the dorsal-ventral (DV) compartment boundary has also been reported to participate in the regulation of *hh* expression; however, the mechanistic basis behind this is uncertain (Bejarano and Milan, 2009). Although communication between the *hh*-ME and those cis-enhancers that integrate positional information conferred by the activities of Ci, En and Notch has been proposed as a way to initiate and maintain the transcriptional state of *hh* in P cells, the identity of these enhancers and the proposed communication remain elusive.

Here, we have isolated a 4.3-kb cis-regulatory region that recapitulates *hh* expression in the P compartment of the wing primordium. This fragment includes the previously defined *hh*-ME and a nearby enhancer (termed C enhancer) that responds to En, Ci and Notch and drives gene expression to a thin stripe in the P compartment that corresponds to the DV compartment boundary. We present evidence that the ME maintains the initial transcriptional

[1]Institute for Research in Biomedicine (IRB Barcelona), Baldiri Reixac, 10-12, 08028 Barcelona, Spain. [2]ICREA, Baldiri Reixac, 10-12, 08028 Barcelona, Spain.

*Author for correspondence (marco.milan@irbbarcelona.org)

Accepted 12 May 2011

activated state conferred by the C enhancer and contributes to expansion, by growth, of the expression domain throughout the P compartment. Communication between the ME and the C enhancer also contributes to repression of gene expression in A cells. Most importantly, we show that enhancers and MEs of different genes are interchangeable modules whose communication is involved in the expansion and repression of gene expression in the *Drosophila* wing. These results emphasize the modular role of MEs in regulating gene expression within growing tissues.

MATERIALS AND METHODS

Drosophila strains

Df(2R)en[E] deletes both *engrailed* and *invected* (Gustavson et al., 1996); *Su(z)2$^{1b.7}$* (Wu and Howe, 1995); *UAS-Ci^{Cell}* [Ci^{Cell}, a truncation of Ci at amino acid residue 975 that behaves as a constitutive transcriptional repressor (Méthot and Basler, 1999)]; *vg-BE-Gal4* (Williams et al., 1994); *UAS-N^{dsRNA}* (Presente et al., 2002); *ap^{gal4}*, *brm^{2} trx^{E2}*, *gro^{E48}*, *UAS-en*, *UAS-lacZ*, *UAS-GFP*, *UAS-N^{INTRA}* and *hh^{P30}* (*hh-lacZ* in the text) are described in FlyBase.

Antibodies

Rat anti-Ci (Motzny and Holmgren, 1995), rabbit anti-βGal (Cappel), rabbit anti-GFP (Upstate), mouse anti-Ptc [Apa 1 (Capdevila et al., 1994)], mouse anti-En [4D9 (Patel et al., 1989)], mouse anti-Wg [4D4 (Brook and Cohen, 1996)], mouse anti-Notch [C458.2H (Diederich et al., 1994)], mouse anti-Cut (2B10) and rabbit anti-βGal (40-1A) are described in the Developmental Studies Hybridoma Bank.

Genetic mosaics

The following *Drosophila* genotypes were used to generate loss-of-function clones (Xu and Rubin, 1993):

hs-FLP; *FRT42B Df(2R)en^{E} Su(Z)2^{1b-7} / FRT42B Ubi.GFP*; *hh-lacZ/+*;

hs-FLP; *FRT42B Df(2R)en^{E} Su(Z)2^{1b-7} / FRT42B Ubi.GFP; ABC-lacZ/+*.

Clone induction by heat-shock was carried out 2-4 days before wing disc dissection.

Molecular characterization of the Mrt allele of *hh*

A collection of primers were used to amplify and sequence the whole 4.3-kb genomic region upstream of the *hh* transcription start site from wild-type and *hh^{Mrt}* homozygous larvae. Primers (5′-3′) used to amplify the region containing the deletion in the *hh^{Mrt}* allele were:

Hh-3Kb-Top: GGCGTCTCCGTCTGCTTTTAATTTC;

Hh-3Kb-Bot: ATACGAACCATTTTAGCTGCCATTA.

The *hh^{Mrt}* deletion maps to the following BDGP Release 5/dm3 assembly coordinates: chr3R: 18970938-18970961.

Reporter constructs of *hh*

Reporter genes were built from the *hs43-nuc-lacZ* vector, which contains the minimal (TATA box) promoter from the *hsp43* gene (Estella et al., 2008). The A, B and C modules spanning the 4.3-kb genomic region upstream of the *hh-RB* transcription start site (according to FlyBase), and excluding the *hh* promoter, map to the following FlyBase sequence locations:

ABC (from position –4428 to –61 bp upstream of the *hh-RB* transcription start site): BDGP Release 5/dm3 assembly, coordinates: chr3R: 18967689-18972117;

A (–2265 to –105 bp): chr3R:18967689-18969849;

B (–2996 to –2340): chr3R:18969924-18970580;

C (–4265 to –3214 bp): chr3R:18970798-18971949.

The predicted *hh* promoter maps to the following FlyBase sequence location: chr3R: 18967584-18967675.

For *ABC-lacZ* and *ABC^{Mrt}-lacZ*, a 4.3-kb fragment upstream of the *hh* transcription start site was amplified by PCR from genomic DNA from wild-type and *hh^{Mrt}* homozygous larvae using the following primers (5′-3′):

ModABC-Fwd: ACACGCACACACACACTATCGCCTCGAGTTC;

ModABC-Rev: TAAGTAATCTTGGGAAATATACATAAG.

The corresponding PCR products were cloned into the pTZ57R vector (Fermentas), then excised from this vector using *Xba*I and *Bam*HI and subsequently cloned via the *Spe*I and *Bam*HI sites into the pHs43n-nuc-*lacZ* vector.

For *A-lacZ*, *B-lacZ*, *C-lacZ* and *C^{Mrt}-lacZ*, in order to amplify by PCR the A, B and C modules from genomic DNA of wild-type or *hh^{Mrt}* homozygous larvae, the following primers (5′-3′) were used:

ModA-Fwd: GGAATTCACACGCACACACACACTATC;

ModA-Rev: ATTTGCGGCCGCTTTTAACTCTTTTCTGTATT;

ModB-Fwd: GGAATTCACTATATGATCAACGAAAAG;

ModB-Rev: ATTTGCGGCCGCACATAAAATACTTGCAGCCA;

ModC-Fwd: GGGGTACCAAGTCTTTTGTTTTGGCTGC;

ModC-Rev: TTGCGGCCGCTTAATTTTTTTTTCCATCGA.

PCR fragments containing modules A and B were digested with *Eco*RI and *Not*I, the fragment containing the module C was digested with *Kpn*I and *Not*I, and subsequently cloned into the pHs43n-nuc-*lacZ* vector (Estella et al., 2008).

For *AB-lacZ* and *BC-lacZ*, module AB was amplified by PCR from genomic DNA of wild-type larvae using ModA-Fwd and ModB-Rev primers and module BC was amplified by PCR using ModB-Fwd and ModC-Rev primers. Both fragments were digested with *Eco*RI and *Not*I and cloned into the pHs43n-nuc-*lacZ* vector.

For A*C-lacZ* and *AC^{Mrt}-lacZ*, module C was amplified by PCR from genomic DNA of wild-type and *hh^{Mrt}* homozygous larvae with the following primers (5′-3′):

ModAC-Fwd: ATTTGCGGCCGCAAGTCTTTTGTTTTGGCTGC;

ModAC-Rev: TTGGATCCTTAATTTTTTTTTCCATCGA.

The fragment was digested with *Not*I and *Bam*HI and cloned downstream of ModA in the pHs43n-nuc-*lacZ* vector.

For *AλC-lacZ*, a 650-bp fragment from Lambda (λ) Phage was amplified by PCR with the following primers (5′-3′):

Lambda-Fwd:
ATAAGACTAGCGGCCGCATGAAATAAGAGTAGCCT;

Lambda-Rev: ATAAGAATGCGGCCGCTAGCAACTGGAAATCATT.

The fragment was digested with *Not*I and cloned in the *Not*I site of ModAC in the pHs43n-nuc-*lacZ* vector.

For *ACB-lacZ*, module AC was amplified by PCR from *AC-lacZ* with the following primers (5′-3′):

ModA-Fwd: GGAATTCACACGCACACACACACTATC;

ModC-ERI-Rev: TTGGATCCTTAATTTTTTTTTCCATCGA.

The PCR product was digested with *Eco*RI and cloned upstream of ModB in the pHs43n*lacZ* vector.

For *A-vgBE-lacZ*, module A was digested from the *ModA-lacZ* with *Eco*RI and *Not*I; vgBE was digested from *vgBE-lacZ* with *Not*I and B*am*HI. Both fragments were ligated into the pHs43n*lacZ* vector digested *Eco*RI and *Bam*HI.

For *iab-7-BC-lacZ*, the iab-7 PRE region (chr3R:12725498-12726604) regulating *Abd-B* was amplified by PCR with the following primers (5′-3′):

iab-7-Fwd: GATGCTATCGCGTTGATTGT;

iab-7-Rev: CGAGTTTCGGTCGCTGACGTC.

The 1120-bp PCR fragment was cloned in the pCR-XL-TOPO vector (Invitrogen), then excised from this vector with *Eco*RI and cloned upstream of module BC in the pHs43n-nuc-*lacZ* vector.

FlyBase coordinates of PCR primers are described in Table S1B in the supplementary material.

Reporter constructs of *vg*

Reporter genes were built from the *hs43-nuc-lacZ* vector, which contains the minimal (TATA box) promoter from the *hsp43* gene (Estella et al., 2008). The *vgBE-lacZ* reporter was generated by amplifying the vestigial BE region (Kim et al., 1995) by PCR from genomic DNA (chr2R:8776380- 8777133) from wild-type larvae, using the following primers (5′-3′):

vgBE Fwd GGGCAACGCGGCCGCGAATTCCGCAACTCAAT-GTTG G;

vgBE Rev CTTTGGGATCCGAATTCAGCTCCCTGGTTTATCTGC.

The vgBE PCR product was digested with *Not*I/*Bam*HI and cloned into the pHs43n-*lacZ* vector.

The *vgPRE-lacZ* reporter was made by amplifying the predicted PRE region of *vestigial* (chr2R:8793522- 8790996) by PCR using the following primers (5′-3′):

vgPRE Fwd ATTTGGATCCCTATGTCGATTAAAATGTTTGTAATGG;
vgPRE Rev TCATCAGGATCCGAACCTTGCAACCTTATGCCC.

The vgPRE PCR product was digested with *Bam*HI and introduced into the pHs43n-*lacZ* vector.

The *vgBE-PRE2-lacZ* reporter was generated by introducing the vgPRE PCR product (digested with *Bam*HI) into the *Bam*HI site of the pHs43n-vgBE-*lacZ* construct.

The vgBE (Kim et al., 1995) and vgPRE (Schuettengruber et al., 2007) regions map to the following FlyBase sequence locations:

vgBE: chr2R: 8776380-8777132;
vgPRE: chr2R: 8790966-8793542.

FlyBase coordinates of PCR primers are described in Table S1B in the supplementary material.

Bioinformatic identification of Ci and Su(H) motifs

With the predictive models published in the literature for Su(H) and Ci/Gli consensus binding sites (Bailey and Posakony, 1995; Kinzler and Vogelstein, 1990; Lecourtois and Schweisguth, 1995), we used the MatScan program (Blanco et al., 2006) to obtain a list of putative Ci and Su(H) binding sites (up to two changes in the consensus) on the C module of *hh* (BDGP Release 5/dm3 assembly, coordinates: chr3R:18970798-18971949). We filtered out the predictions that were not conserved in at least five species (including *Drosophila pseudoobscura* or more distant species) in the multiple alignments of Drosophilids (UCSC Conservation track) (Fujita et al., 2011).

RESULTS

ABC, a 4.3-kb region that recapitulates the expression of *hh* in *Drosophila* tissues

We used a transgenic reporter gene assay to search for *hh* cis-regulatory elements that are active in the wing disc. A 4.3-kb region from position –4428 to –61 bp upstream of the *hh* transcription initiation site, which we named ABC (Fig. 1B), drove *lacZ* reporter expression in a pattern that reproduced the *hh* expression pattern in the wing imaginal disc and in the embryonic ectoderm [Fig. 1C; data not shown; number of independent lines analysed (*n*)=16]. We observed that *lacZ* expression was more robust in the distal portion of the wing disc, the presumptive wing pouch (encircled region in Fig. 1C). We next tested whether the ABC region integrates the genetic and epigenetic mechanisms involved in the regulation of endogenous *hh* (Fig. 1A) (Bejarano and Milan, 2009). En and Invected are expressed in the P compartment where they are required to repress Ci expression (Eaton and Kornberg, 1990) and relieve Ci-mediated repression of endogenous *hh* (Bejarano and Milan, 2009). Consistent with that, expression of a truncated form of Ci that behaves as a constitutive transcriptional repressor (Ci^{Cell}) (Méthot and Basler, 1999) reduced ABC expression in P cells (compare Fig. 1D and 1E). PcG genes are involved in repression of *hh* in the A compartment (Randsholt et al., 2000) and, as shown in Fig. 1F, clones of cells located in the A compartment and mutant for the PcG gene *Suppressor 2 of zeste* [*Su(z)2*] showed ectopic expression of *hh*. In these clones, expression of the ABC reporter was also induced

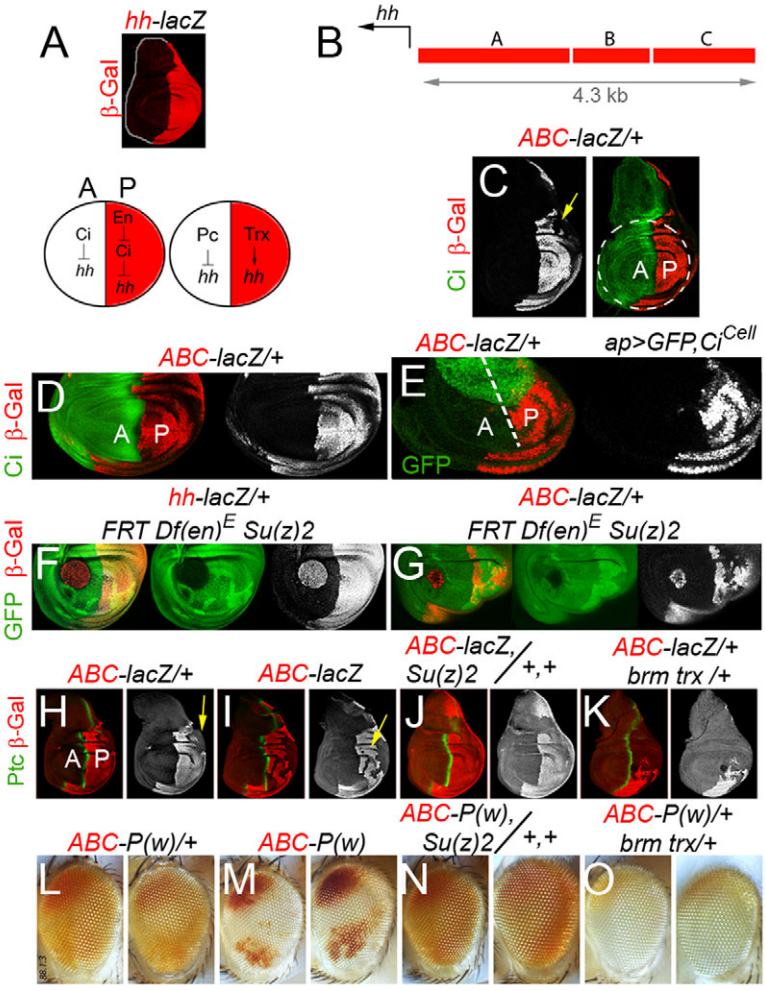

Fig. 1. ABC recapitulates the expression pattern of *hh* in the wing disc and behaves as a PcG response element (PRE) in *Drosophila* wing discs and adult eyes. (**A**) Top: Wing discs carrying the *hh-lacZ* enhancer trap labelled to visualize β-gal protein expression. Bottom: Schematic of the genetic and epigenetic mechanisms involved in the regulation of *hh* expression in the wing primordium. White, anterior compartment; red, posterior compartment. (**B**) Genomic organization of the *hh* locus where the 4.3-kb-long genomic region (ABC) upstream of the *hh* transcription start site is depicted in red. (**C-G**) Wing discs carrying the *ABC-lacZ* reporter construct (C-E,G) or the *hh-lacZ* enhancer trap (F) and labelled to visualize in green Ci (C,D) or GFP (E,F,G) and in red or white β-gal protein expression. In E, Ci^{cell} and GFP were expressed under the control of the *ap-gal4* driver and the anterior-posterior (AP) compartment boundary is depicted by a dashed line. In F and G, clones of cells mutant for $Df(en)^E$ and the *PcG* gene *Su(z)2*, and labelled by the absence of GFP are shown. In C, the yellow arrow points to a group of cells not expressing *lacZ* in the posterior compartment and the wing pouch is encircled. (**H-O**) Transgenic reporter assays for PRE function and expression in the wing disc. Wing discs (H-K) or adult eyes (L-O) of transgenic flies carrying a *lacZ* and a *mini-white* reporter construct containing the ABC region of *hh* [*ABC-lacZ* or *ABC-P(w)*] show expression of *lacZ* in the posterior (P) compartment of the wing (H-K), variegation (H,L, in adult eyes), pairing-sensitive silencing (I,M, in adult eyes), loss of silencing in the *PcG* mutant background *Su(z)2*/+ (J,N) and reduced activation in the *trxG* mutant background *brm trx*/+ (K,O). Wing discs shown in H-K were labelled to visualize Ptc (green) and β-gal (red and white) protein expression. Yellow arrows in H,I point to groups of cells not expressing *lacZ* in the posterior compartment of wing discs. A, anterior; P, posterior.

(Fig. 1G). Note that these clones were also mutant for a deficiency covering both *en* and *invected* [*Df(en)*^{E}], as these two genes are de-repressed in anterior *Su(z)2* mutant clones [data not shown, see also Busturia and Morata (Busturia and Morata, 1988)] and are able to induce de novo expression of *hh* when ectopically expressed in A cells (Tabata et al., 1992).

The ABC cis-regulatory element contains the previously described *hh*-ME (Maurange and Paro, 2002). Consistent with this, *ABC-lacZ* expression in the P compartment was frequently repressed or variegated, with some groups of cells losing *lacZ* expression (Fig. 1C,H, yellow arrows). The *mini-white* reporter gene used to identify transgenic animals also showed a large degree of variegation in adult eyes (Fig. 1L; see Table S1 in the supplementary material). The ABC element showed pairing-sensitive silencing in the expression of the *lacZ* reporter in wing cells (Fig. 1I, yellow arrows) and of *mini-white* in adult eyes (Fig. 1M; see Table S1 in the supplementary material). Thus, *lacZ* expression or eye colour of individuals homozygous for the transgene was usually more variegated than in heterozygous animals. Both types of variegation were also sensitive to a reduction in the doses of the PcG gene *Su(z)2* and the TrxG genes *brahma* and *trithorax*. Expression of the corresponding reporters was less variegated in wing discs and adult eyes of *Su(z)2/+* animals (Fig. 1J,N), and was largely reduced in *brahma trithorax* double heterozygous animals (Fig. 1K,O). Together, these results indicate that the ABC region integrates the genetic and epigenetic mechanisms involved in the regulation of *hh*. Other cis-regulatory regions might also be involved in the control of endogenous expression of this gene, as the *ABC* fragment drove variegated expression of *lacZ* in the P compartment and this expression was sensitive to changes in the doses of PcG and TrxG genes whereas a *hh-lacZ* enhancer trap drove robust expression in all P cells and this expression was not sensitive to changes in the doses of PcG and TrxG genes (data not shown).

Distinct functional modules within the ABC cis-regulatory element

On the basis of sequence conservation with other *Drosophila* species (Vista Genome Browser, data not shown), we subdivided the 4.3-kb region upstream of the *hh* transcription start site in three fragments (A, B and C) (Fig. 1B) and generated reporter constructs carrying them. The A fragment drove some expression of *lacZ* in a patchy manner in wing discs, thereby indicating that it contains some wing enhancers (Fig. 2A, *n*=8). Most interestingly, A drove expression of *lacZ* and *mini-white* in a variegated manner in wing discs and adult eyes (Fig. 2A,E; see Table S1 in the supplementary

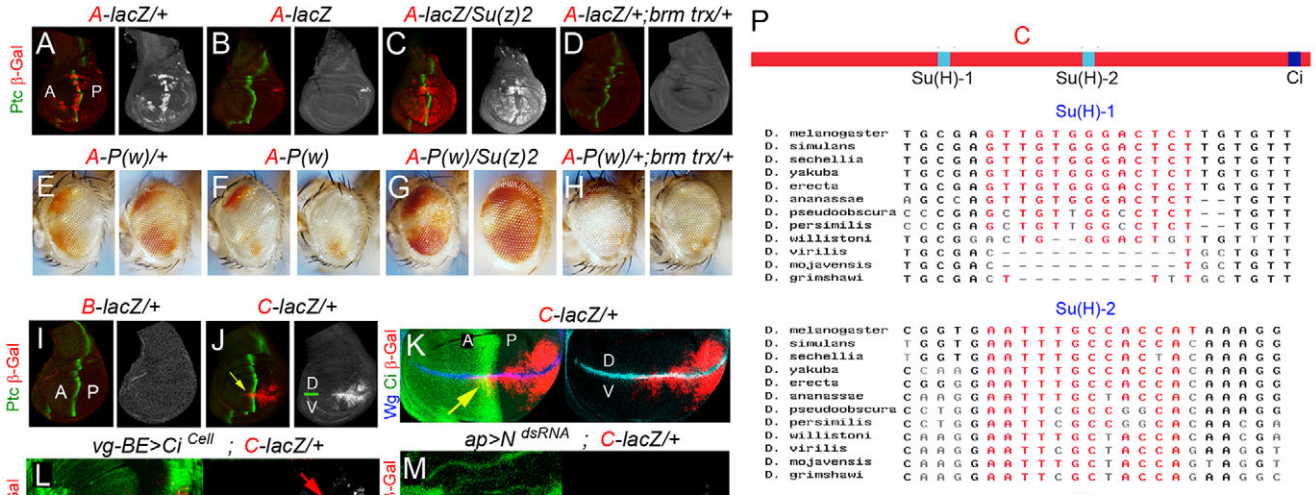

Fig. 2. Dissection of ABC. (**A-H**) Transgenic reporter assays for PcG response element (PRE) function and expression in the wing disc. Wing discs (A-D) or adult eyes (E-H) of transgenic flies carrying a *lacZ* and a *mini-white* reporter construct containing the A region of *hh* [*A-lacZ* or *A-P(w)*] show variegation (A,E), pairing-sensitive silencing (B,F), loss of silencing in a *PcG* mutant background [*Su(z)2*, C,G] and reduced activation in a *trxG* mutant background (*brm trx*, D,H). Wing discs shown in A-D were labelled to visualize Ptc (green) and β-gal (red or white) protein expression. (**I-O**) Wing discs carrying the *B-lacZ* (I) or the *C-lacZ* (J-O) reporter constructs were labelled to visualize in green Ptc (I,J), Ci (K,L,N), Notch (M), or Wg (O) protein expression, in red or white β-gal protein expression and in blue Wg (K). Yellow arrows in J and K indicate *lacZ* expression in anterior cells. In L and N, *Ci*^{Cell} was expressed under the control of the *vg-BE-gal4* (L) or *ap-gal4* (N) drivers. Note loss of *C-lacZ* expression (red or white) in those cells expressing Ci^{Cell} (green). Red arrow in L points to the loss of C-*lacZ* expression in those cells expressing high levels of Ci^{Cell} in the posterior compartment. In M and O, *N*^{dsRNA} (M) or *N*^{INTRA} (O) were expressed under the control of the *ap-gal4* driver. Note that *N*^{dsRNA}-induced loss of Notch protein (green) and C-*lacZ* expression in dorsal (D) cells. Expression of *N*^{INTRA} in the D compartment induced expression of Wg (green) in the anterior (A) and posterior (P) compartments and expression of C-*lacZ* (red or white) mainly in the P compartment. (**P**) Conserved consensus binding sites (red letters) of Su(H) and Ci transcription factors are found in the C module of the *hh* gene. Coordinates of the sites (BDGP Release 5/dm3 assembly) in the *Drosophila melanogaster* genome are: Su(H)-1: chr3R: 18971144-18971156; Su(H)-2: chr3R: 18971421-18971433; Ci: chr3R: 18971833-18971941.

material). Expression of both reporters showed pairing-sensitive silencing (Fig. 2B,F; see Table S1 in the supplementary material) and was modulated by changes in the doses of PcG (Fig. 2C,G) and TrxG genes (Fig. 2D,H). These results indicate that the 2.1-kb long A fragment behaves as a PRE. Consistent with these data, chromatin immunoprecipitation (ChIP) on chip assays to map the chromosomal distribution of Gaf (Trl – FlyBase), Pho, PhoL (Phol – FlyBase) and Dsp1, four DNA-binding proteins thought to be involved in PcG recruitment, identified this region as a potential PRE (Schuettengruber et al., 2009).

The reporter constructs carrying the B or C fragments did not show variegation in adult eyes (see Table S1 in the supplementary material) and expression of *mini-white* was unaffected by changes in the doses of PcG or TrxG genes (data not shown). In wing discs, the B fragment did not drive expression of *lacZ* (Fig. 2I, n=8), whereas the C fragment drove expression in a posterior wedge straddling the DV compartment boundary (Fig. 2J,K, n=5). Some expression in anterior cells abutting the AP and DV compartment boundaries was observed in *C-lacZ* wing discs (Fig. 2J,K, yellow arrows). As the Notch signalling pathway is activated at the DV boundary (Irvine and Vogt, 1997), we examined whether *C-lacZ* expression depends on the activity of Notch. For this purpose, we analysed the effects on reporter expression after blocking or activating this pathway. Expression of a dsRNA form of Notch (N^{dsRNA}) in dorsal cells induced a cell-autonomous loss of *C-lacZ* expression (Fig. 2M), and expression of a dominant active form of Notch (N^{intra}) in the same cells led to an expansion of *C-lacZ* expression throughout the D compartment (Fig. 2O). We analysed next the role of Ci in regulating the expression of *C-lacZ*. A repressor form of Ci (Ci^{Cell}) induced a cell-autonomous loss of *C-lacZ* expression (Fig. 2L,N). Ectopic expression of Engrailed in anterior cells is known to repress *ci* expression (Eaton and

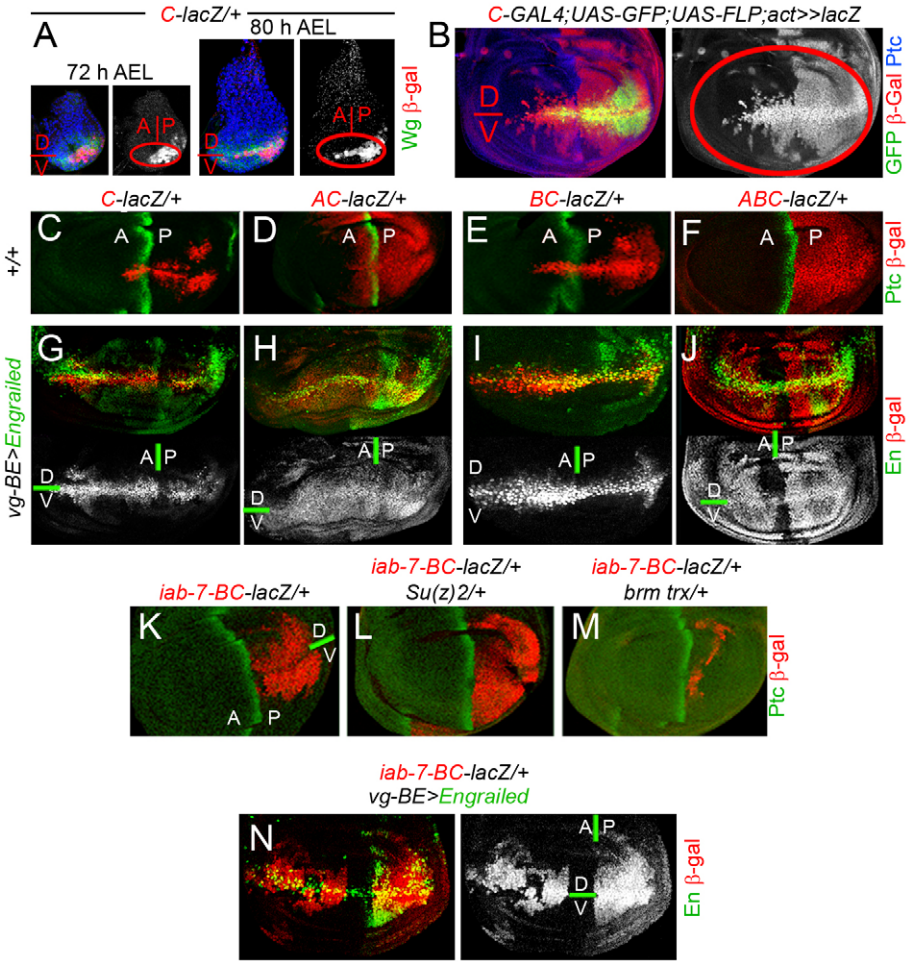

Fig. 3. Epigenetic maintenance of gene expression. (**A**) Early (left) and mid (right) third instar wing discs carrying the *C-lacZ* reporter construct and labelled to visualize Wingless (Wg, green) and β-gal (red or white) protein expression. (**B**) Late third instar wing disc in which all the cells that have ever activated the C-enhancer are labelled by the expression of β-gal (red or white, see text for details), and expression of the C-enhancer is visualized by the expression of GFP (green). The anterior-posterior (AP) boundary is labelled by the expression of Ptc protein (blue) and the dorsal-ventral (DV) boundary is labelled. The presumptive wing pouch is encircled in A and B. (**C-J**) Wing discs carrying the following reporter constructs: *C-lacZ* (C,G), *AC-lacZ* (D,H), *BC-lacZ* (E,I) and *ABC-lacZ* (F,J) were labelled to visualize in green Patched (Ptc, C-F) or Engrailed (En, G-J) and β-gal (red or white) protein expression. In G-J, Engrailed was expressed under the control of the *vg(BE)-gal4* driver. (**K-N**) Wing discs carrying a reporter construct containing the *iab-7* PcG response element (PRE) and the B and C elements of *hh* (*iab-7-BC-lacZ*) were labelled to visualize in green Patched (Ptc, K-M) or Engrailed (En, N) and β-gal (red or white) protein expression. Wing discs in L and M were heterozygous for the *PcG* mutant *Su(z)2* (L) or for the *trxG* mutants *trx* and *brm* (M). In N, Engrailed was expressed under the control of the *vg(BE)-gal4* driver. The anterior (A), posterior (P), dorsal (D) and ventral (V) compartments are labelled in most figure panels. Note that in G-J and N, as previously reported (Crickmore et al., 2009; Garaulet et al., 2008; Tabata et al., 1995), exogenous En was able to induce a reduction in the endogenous levels of En expression in P cells.

Kornberg, 1990) and we showed that it induced the expression of *C-lacZ* along the anterior DV boundary (Fig. 3G). Together, these results indicate that the C fragment integrates the activities of the Notch pathway and the Ci^{rep}. Interestingly, canonical binding sites for Ci and the transcriptional factor Su(H) are found in this fragment (Fig. 2P) and chromatin-binding assays identified this region as a binding domain for Ci^{rep}, Su(H) and Notch (Biehs et al., 2010) (S. Bray, personal communication).

Enhancer-PRE communication mediates epigenetic inheritance of gene expression

The results above indicate that C contains the enhancers that drive expression to a posterior wedge straddling the DV compartment boundary whereas A behaves as a PRE. This PRE has been reported to be able to maintain Gal4-driven *lacZ* reporter gene expression through several rounds of mitosis (Bejarano and Milan, 2009; Maurange and Paro, 2002). It is known that most wing pouch cells are progenies of the cells determined at the DV boundary at early larval stages (Klein, 2001). Thus, we hypothesized that transcription of *hh* is activated, through the C enhancer, in boundary cells during early larval development. The active transcriptional state should then be inherited, by the activity of the *hh*-PRE, to daughter cells after mitosis. This should result in expression of the gene in all wing pouch cells. We undertook the following experimental approaches to evaluate this hypothesis. First, we examined the expression induced by C during wing development. In early wing primordia, C drove *lacZ* expression to a posterior wedge straddling the DV boundary; this posterior wedge occupies a large fraction of the wing pouch and this fraction was reduced as the wing disc grew in size (Fig. 3A). This comparison suggests that cells lose *lacZ* expression as they are displaced out of the C domain by growth of the disc and that most of the wing pouch cells in the posterior compartment are born in the C domain. To verify that this is indeed the case, we lineage-tagged cells born in the C-expressing region using C-Gal4 to direct expression of FLP recombinase. In larvae carrying C-Gal4, UAS-GFP, UAS-FLP and act5c>sto*P*>*lacZ*, FLP recombinase is expressed in cells expressing C-Gal4 and mediates excision of the flip-out 'stop' cassette from the inactive reporter construct to generate an active act5c>*lacZ* transgene (Struhl and Basler, 1993). After excision of the cassette, reporter gene expression is regulated by the actin promoter and is clonally inherited in all the progeny of *C-Gal4*-expressing cells in which the recombination event took place. In *C-Gal4*, *UAS-GFP*, *UAS-FLP*, *act5c>stoP>lacZ* wing discs, expression of *lacZ* was expanded throughout most of the posterior wing pouch (Fig. 3B, compare with the activity of the C-enhancer in mature wing primordia labelled by the expression GFP). These results indicate that most of the wing pouch cells in the posterior compartment are born in the C domain.

We next analysed the capacity of A, as an ME, to mediate epigenetic inheritance of C-induced expression and to expand, by growth, the expression domain of C throughout the posterior wing pouch. The combination of A and C was able to expand the expression domain of C throughout the most distal part of the wing disc (compare Fig. 3C and 3D, *n*=4), and in the presence of the B fragment this expansion took place only in P cells (compare Fig. 3E and 3F, see below, *n*=16). Interestingly, *iab-7*, a well characterized ME of *Abdominal B* (*Abd-B*) (Hagstrom et al., 1997; Mishra et al., 2001), in combination with B and C (in *iab-7-BC-lacZ* wing discs), also expanded the expression domain throughout the most distal part of the P compartment (Fig. 3K, *n*=3) and this expansion depended on the doses of PcG and TrxG genes (Fig. 3L,M). We also tested the capacity of A and *iab-7* to mediate epigenetic inheritance of C-induced expression upon ectopic expression of En in the anterior compartment. Ectopic expression of En along the DV compartment boundary (with the *vg-BE-gal4* driver) induced expression of *C-lacZ* or *BC-lacZ* only in those anterior cells with high levels of En protein (Fig. 3G,I). By contrast, this expression was maintained throughout the wing pouch in the absence of detectable levels of En when the constructs also carried the A fragment or the *iab-7* PRE (e.g. *AC-lacZ*, *ABC-lacZ* or *iab-7-BC-lacZ*, Fig. 3H,J,N). Note, as shown in Fig. 6C, that most of the wing pouch cells were born in the *vg-BE* domain. Together, these results indicate that communication between a PRE (A) and the enhancers located in the C module drive sustained expression throughout the posterior wing pouch.

Enhancer-PRE communication mediates repression of gene expression

Whereas the ABC domain of *hh* drove restricted and sustained expression of *lacZ* in the posterior compartment of the developing wing (Fig. 1), the absence of the B fragment (in *AC-lacZ* reporter constructs) failed to repress *lacZ* expression in anterior cells close to the AP boundary (Fig. 4A, white arrow). In order to address the role of B in mediating repression in the anterior compartment, we combined it with other modules and analysed the resulting expression patterns. B in combination with A was indistinguishable

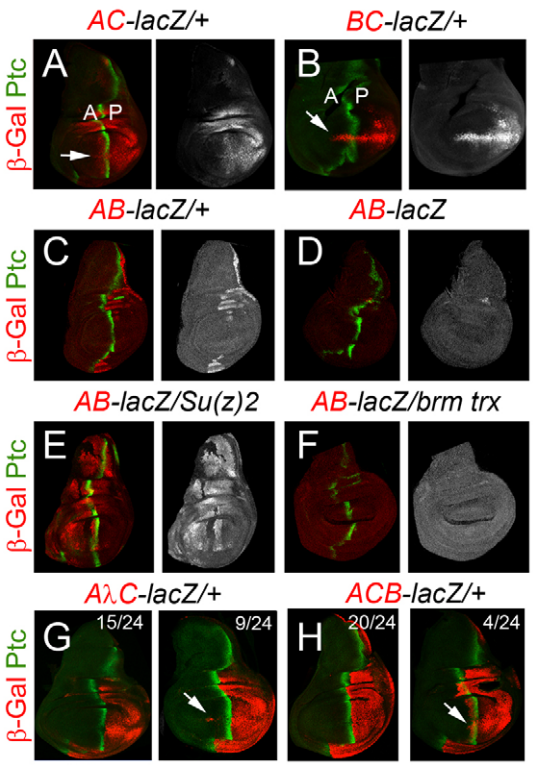

Fig. 4. Repression in the anterior compartment. (**A-H**) Wing discs carrying the following reporter constructs: *AC-lacZ* (A), *BC-lacZ* (B), *AB-lacZ* (C-F), *AλC-lacZ* (G), *ACB-lacZ* (H) were labelled to visualize in green Patched (Ptc) and in red or white β-gal protein expression. *AB* showed variegated *lacZ* expression (C), pairing-sensitive silencing (D), loss of silencing in a *PcG* mutant background (E) and reduced activation in a *trxG* mutant background (F). In A and B, the anterior (A) and posterior (P) compartments are labelled and white arrows point to the expression of β-gal in the anterior compartment. In G and H, the ratio of wing discs with or without ectopic expression of *lacZ* in the anterior compartment (white arrows) is shown.

from A alone (compare Fig. 2A-D and Fig. 4C-F) and the resulting construct, AB, drove expression of *lacZ* and *mini-white* in a variegated manner in wing discs and adult eyes (Fig. 4C, *n*=2; data not shown; see Table S1 in the supplementary material). Reporter expression driven by AB showed pairing-sensitive silencing in wing and eye tissues (Fig. 4D and data not shown; see Table S1 in the supplementary material) and this expression was modulated by changes in the doses of PcG and TrxG genes (Fig. 4E,F; data not shown). Thus, the features of A as a PRE were not visibly affected by the presence of B. Similarly, B in combination with C was indistinguishable from C alone (compare Fig. 4B and Fig. 2J) and the resulting construct, BC, drove expression in a posterior wedge straddling the DV compartment boundary (*n*=5). Some anterior cells expressed *lacZ*, as observed with the C alone (Fig. 4B, white arrow). All together, these results indicate that B participates in mediating repression of *lacZ* in anterior cells receiving the Hh signal only in the presence of both A and C fragments (Fig. 1C). Interestingly, an ACB fragment, where the order of the A, B and C fragments was altered, drove restricted and sustained expression of *lacZ* in the posterior compartment (Fig. 4H, *n*=20/24), suggesting that B contains those enhancers that respond, in the presence of A and C, to the mechanisms involved in the repression of anterior *hh* expression. However, a chimeric A-λ-C fragment, in which the B element was substituted by an heterologous DNA fragment (the λ phage) of the same size (600 bp), also gave similar results in terms of restricted and sustained expression of *lacZ* in all P cells (Fig. 4G, *n*=15/24), suggesting that B also serves as a scaffold in mediating communication between the A and C modules. Thus, B plays a dual and redundant role in the repression of *hh* expression in A cells. Interestingly, we noticed that some wing discs carrying the *ACB-lacZ* or *AλC-lacZ* reporters showed some *lacZ* expression in the anterior compartment (Fig. 4G, *n*=9/24, and Fig. 4H, *n*=4/24, white arrows), suggesting that the dual role of the B fragment confers robustness to the repression of gene expression in anterior cells.

It has been reported that the *hh* gain-of-function allele *Moonrat* (hh^{Mrt}) results in de-repression of *hh* in anterior cells located at the DV boundary (Fig. 5E,F) and causes duplication of anterior structures (Fig. 5A,B) (de Celis and Ruiz-Gomez, 1995; Felsenfeld and Kennison, 1995). The adult wing phenotype is enhanced when halving the doses of *ci* (Fig. 5C) or *groucho* (Fig. 5D), a transcriptional co-repressor involved in repression of *hh* in anterior cells (Apidianakis et al., 2001; Bejarano et al., 2007). We sequenced the ABC domain of hh^{Mrt} homozygous larvae and a small deletion of 24 bp, a highly conserved region among *Drosophila* species (Fig. 5H), was identified in C (Fig. 5G). Interestingly, the ABC domain containing the Mrt deletion (ABC^{Mrt}) drove expression of *lacZ* to some anterior cells located at the DV boundary (Fig. 5H, *n*=16), and this anterior expression was largely increased when halving the doses of *groucho* (Fig. 5I). Intriguingly, the C^{Mrt} mutant module drove expression of *lacZ* to a similar domain as the wild-type C module (Fig. 5J, *n*=3). Although the role of this fragment in mediating anterior repression of gene expression remains to be further characterized, these results indicate that the deletion in C contributes to the Mrt phenotype and reinforce the proposal that communication between A and C mediate repression of *hh* in anterior cells.

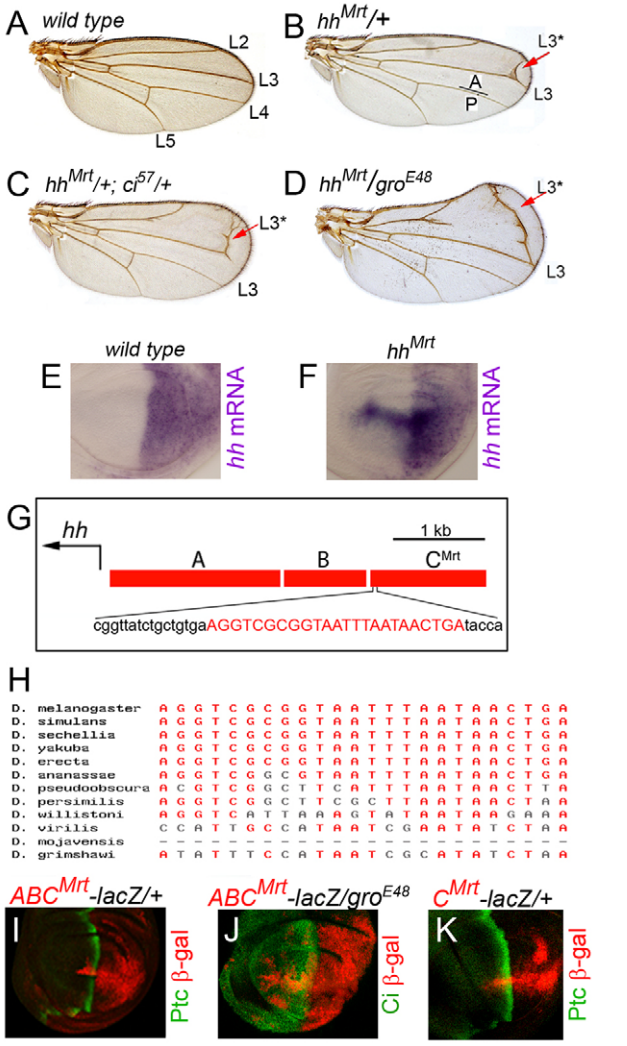

Fig. 5. Molecular characterization of the *Moonrat* allele of *hh*. (**A-D**) Cuticle preparation of wild-type (A), hh^{Mrt}/+ (B), hh^{Mrt}/+; ci^{57}/+ (C) and hh^{Mrt} /gro^{E48} (D) adult wings. Longitudinal veins L1-L5 are shown and ectopic veins L3 (L3*) are indicated by a red arrow. (**E**,**F**) Wild-type (E) and hh^{Mrt} (F) wing discs labelled to visualize expression of *hh* mRNA in purple. (**G**) Genomic organization of the *hh* locus with the deleted nucleotides found in hh^{Mrt} homozygous larvae shown as capital red letters. (**H**) Conservation among *Drosophila* species of the 24 bp deletion found in hh^{Mrt} flies. (**I-K**) Wing discs carrying the following reporter constructs: ABC^{Mrt}-*lacZ* (I,J) and C^{Mrt}-*lacZ* (K) were labelled to visualize in green Patched (Ptc, I,K) or Ci (J) and in red β-gal protein expression. The wing disc shown in J is also heterozygous for gro^{E48}.

Enhancer-PRE communication mediates epigenetic inheritance of gene expression: is this a general mechanism?

Our results indicate that communication between a PRE (A) and the enhancers located in the C fragment that respond to Ci^{rep} and Notch drive sustained expression of *hh* throughout the posterior wing pouch. We then questioned how generally this mechanism is used in development. *vestigial* (*vg*), a gene required for growth and cell survival of wing cells, is expressed in the wing pouch in a graded manner at both sides of the DV boundary (Fig. 6A) (Kim et al., 1996). *vg* expression is regulated by the combined activities of the Notch pathway and the Wingless signalling molecule. The so-called boundary enhancer (vg-BE, located in the second intron of *vg*, Fig. 6K) drives expression to the DV boundary (Fig. 6B, *n*=8) and responds to the activity of Notch (Kim et al., 1996), whereas the quadrant enhancer (vg-QE, located in the fourth intron, Fig. 6K) drives expression in non-boundary cells and responds to the activity of Wingless, a signalling molecule expressed at the DV boundary.

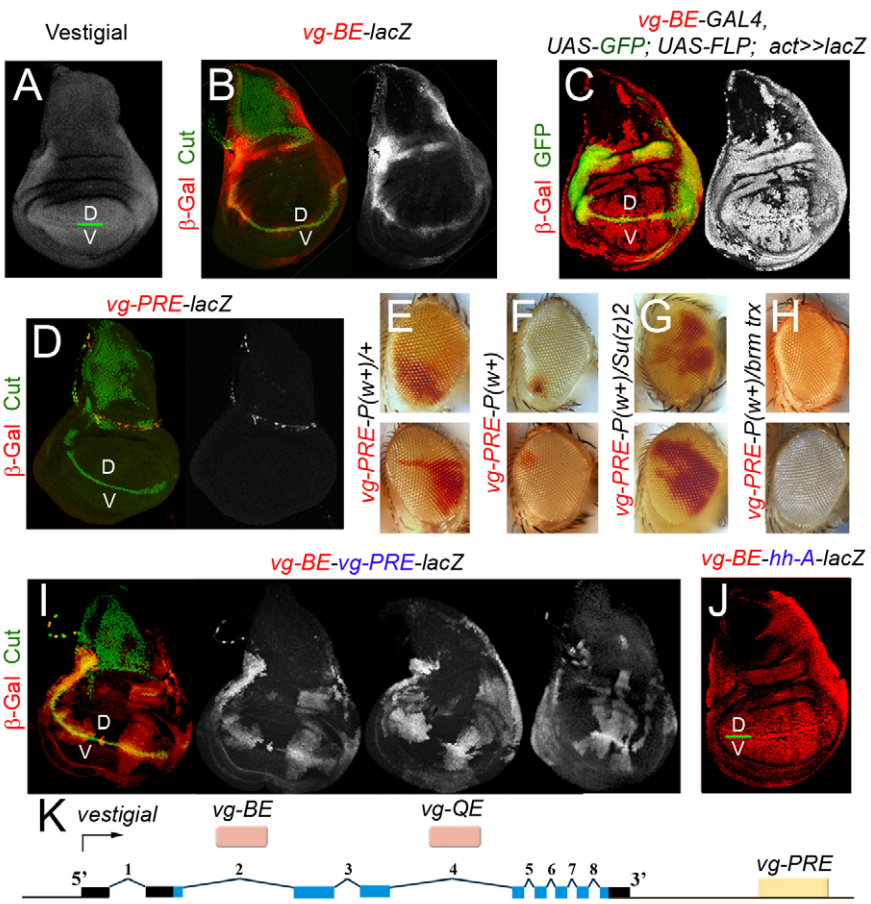

Fig. 6. Enhancer-PcG response element (PRE) interaction: a general mechanism? (**A**,**B**,**D**,**I**,**J**) Wing discs labelled to visualize Vestigial protein expression in white (A) or carrying the following reporter constructs: *vg-BE-lacZ* (B), *vg-PRE-lacZ* (D), *vg-BE-vg-PRE-lacZ* (I), *vg-BE-hh-A-lacZ* (J), were labelled to visualize in green Cut (B,D,I) and β-gal (red or white) protein expression. (**C**) Late third instar wing disc in which all the cells that have ever activated the vg-BE enhancer are labelled by the expression of β-gal (red or white, see text for details) and expression of the vg-BE enhancer is visualized by the expression of GFP (green). Dorsal (D) and ventral (V) compartments are labelled in all wing discs. (**E-H**) Transgenic reporter assays for PRE function in adult eyes. Adult eyes of transgenic flies carrying a *mini-white* reporter construct containing the PRE region of *vg* [*vg-PRE-P(w+)*] show variegation (E), pairing-sensitive silencing (F), loss of silencing in a *PcG* mutant background [*Su(z)2*, G] and reduced activation in a *trxG* mutant background (*brm trx*, H). (**K**) Genomic organization of the *vg* locus where the PRE, boundary enhancer (BE) and quadrant enhancer (QE) are depicted. Blue and black boxes represent coding and non-coding exons, respectively.

Intriguingly, *vg* can be expressed in the wing pouch in the absence of Wingless protein at the DV boundary or in cells lacking the Wingless receptor (Piddini and Vincent, 2009). These surprising results suggest that *vg* expression in the wing pouch is not only regulated by Wingless but also by other redundant mechanisms. Interestingly, genome wide bioinformatic prediction of PRE/TREs identified one potential PRE in the *vg* locus that was confirmed by ChIP as a PcG binding site in S2 cells (Ringrose et al., 2003). In transgenic assays, this PRE caused variegation and pairing sensitive silencing of a *mini-white* gene in adult eyes (Fig. 6E,F; see Table S1 in the supplementary material) (see also Lee et al., 2005). We then addressed whether communication between this PRE and the vg-BE contributes to expansion of the expression domain of *vg* at both sides of the DV boundary in a similar manner to *hh*. Again, we undertook the following experimental approaches to evaluate this hypothesis. First, we lineage-tagged cells born in the vg-BE-expressing region using vg-BE-Gal4 to direct expression of FLP in larvae carrying the act5c>sto*P*>*lacZ* cassette (Struhl and Basler, 1993). In these wing discs, expression of *lacZ* was expanded throughout most of the wing disc (Fig. 6C) (see also Vegh and Basler, 2003), indicating that most of the wing disc cells are born in the vg-BE domain. Next we analysed the capacity of the potential vg-PRE to mediate epigenetic inheritance of vg-BE-induced expression and to expand, by growth, the expression domain of vg-BE throughout the wing disc. vg-PRE did not drive expression of *lacZ* in wing disc cells (Fig. 6D, *n*=10) and induced, as previously reported (Lee et al., 2005), variegation of the *mini-white* gene in adult eyes (Fig. 6E; see Table S1 in the supplementary material), showed pairing-sensitive silencing (Fig. 6F; see Table S1 in the supplementary material) and was modulated by changes in the doses of PcG (Fig. 6G) and TrxG genes (Fig. 6H). Interestingly, the combination in cis of vg-PRE with vg-BE drove expression of *lacZ* reporter not only in DV boundary cells but also at both sides of the DV boundary in a variegated manner (Fig. 6I, *n*=4), indicating that the presence of the vg-PRE was able to induce expansion of the expression domain of vg-BE at both sides of the DV boundary. A second PRE located in the *vg* promoter region was identified by ChIP on chip assays as an enrichment site in PcG proteins (Schuettengruber et al., 2007). However, this PRE was not able to induce expansion of the expression domain of vg-BE at both sides of the DV boundary (data not shown).

Finally, we analysed whether enhancers and PREs from different genes were interchangeable and worked in a modular manner. For this purpose, we combined in cis vg-BE with the hh-PRE (the A module) and analysed the resulting expression pattern. Interestingly, the expression domain of vg-BE was expanded throughout the wing pouch in the presence of the A module of *hh* (Fig. 6J, *n*=5). This observation together with the fact that the PRE of Abd-B (*iab-7*) was able to expand the expression domain of the C enhancer of *hh* when located in cis (Fig. 3K,L) strongly suggest that enhancers and PREs are interchangeable modules whose communication contributes to the expansion of gene expression in growing tissues.

DISCUSSION

Bithorax (*BX-C*) and *Antennapedia* homeotic gene complexes determine the segmental identity of the fly along the anterior-posterior axis and functional analysis of the >300-kb cis-regulatory

region of the *BX-C* complex has been very illustrative with regard to understanding the modular role of enhancers and MEs in the initiation and maintenance of expression of the three BX-C homeotic genes *Ubx*, *abd-A* and *Abd-B* along the anterior-posterior axis of the fly embryo (for a review, see Maeda and Karch, 2006). Here, we provide evidence that communication between enhancers and MEs are also involved in the initiation and maintenance of gene expression within the growing primordium of the fly wing. Functional analysis of the 4.3-kb cis-regulatory region upstream of *hh* has been very illustrative in this regard (Fig. 7). We have identified a cis-regulatory element (termed C) that contains the enhancers that respond to the activity of the repressor form of Ci (Ci^{rep}) (see also Biehs et al., 2010) and the Su(H) transcription factors, and initiates gene expression, from the early wing primordium stage, in a posterior wedge that corresponds to the DV compartment boundary (Fig. 7A). Transcriptional activation is maintained by the activity of a previously identified ME in cis and is expanded, by tissue growth, throughout the posterior compartment (Fig. 7B). This expansion depends on the activity of PcG and TrxG genes, as changes in the doses of these genes modulate the capacity of the ME to maintain the expression in posterior cells. We underscored a dual role of a fragment of 600 bp located between the C enhancer and the ME in mediating repression of gene expression in anterior cells.

Interestingly, repression and expansion of gene expression can also be mediated by the presence of the ME of *Abd-B* in cis with the C element. This observation thus reinforces the proposal that enhancer-ME communication mediates repression and epigenetic inheritance of gene expression (Muller and Kassis, 2006) and that MEs are interchangeable modules (Americo et al., 2002; Chiang et al., 1995; Kozma et al., 2008). It is interesting to note in this context that enhancer-PRE communication appears to contribute to the expansion of the expression domains of other developmental genes, such as *vg*, and that these enhancers also behave as interchangeable modules. Thus, communication between the vg-BE enhancer, which responds to the activity of Su(H) and is expressed in cells at the DV boundary, and a vg-PRE is able to expand, to some extent, the expression to wing pouch cells. This expansion can be also mediated by the presence of the *hh*-ME when in cis with vg-BE. Hence, on the basis of our findings we propose that enhancer-ME communication is a general mechanism at work in highly proliferative tissues that contributes to the expansion of the expression domains of developmental genes.

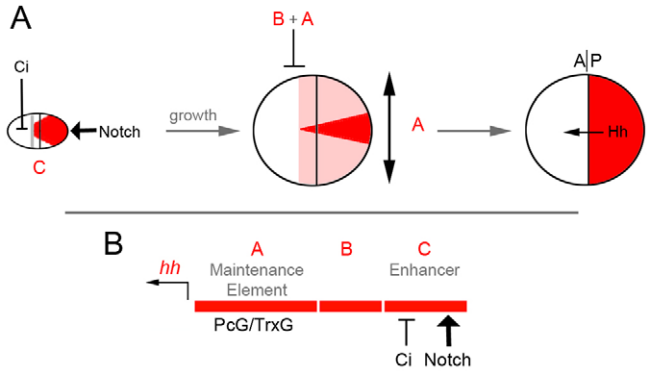

Fig. 7. Enhancer-PcG response element (PRE) communication contributes to *hh* expression in the *Drosophila* wing. (**A**) The combined activities of Ci in anterior cells and Notch in cells along the dorsal-ventral (DV) compartment boundary act through the hh-C Enhancer and result in the initial induction of gene expression to a posterior wedge straddling the DV boundary. Note expression in anterior cells abutting the anterior-posterior (AP) compartment boundary (A/P). Communication between the hh-C Enhancer and the hh-A maintenance element contributes to the expansion, through growth, of gene expression in the posterior compartment and to the repression of gene expression in the anterior compartment. The hh-B element plays a dual role in the repression of gene expression in anterior cells. As a consequence, expression of *hh* (red) is restricted to the posterior compartment. (**B**) Genomic organization of the *hh* locus in which the ABC upstream region of the *hh* transcription start site is depicted in red and the different molecules acting on the hh-A maintenance element (PcG and TrxG protein) and the hh-C Enhancer (Ci and Notch) are shown.

Acknowledgements
We thank M. L. Espinás, C. Estella, R. Holmgren, P. Ingham, R. Mann, J. Müller, the Bloomington Stock Center and the Developmental Studies Hybridoma Bank for flies and reagents, S. Bray for sharing unpublished data and Ainoa Olza for the generation of transgenic flies. We also thank K. Basler, G. Cavalli, H. Herranz, L. Ringrose and three anonymous reviewers for comments on the manuscript, T. Yates for help in preparing the manuscript and E. Blanco for the bioinformatics analysis. L.B. was funded by a pre-doctoral fellowship (Ministerio de Educación y Ciencia), M. Milán is an ICREA Research Professor and M. Milán's laboratory was funded by Grants from the Dirección General de Investigación Científica y Técnica (BFU2007-64127/BMC), the Generalitat de Catalunya (2005 SGR 00118), intramural funds and the EMBO Young Investigator Programme.

Competing interests statement
The authors declare no competing financial interests.

Supplementary material
Supplementary material for this article is available at
http://dev.biologists.org/lookup/suppl/doi:10.1242/dev.065599/-/DC1

References

Americo, J., Whiteley, M., Brown, J. L., Fujioka, M., Jaynes, J. B. and Kassis, J. A. (2002). A complex array of DNA-binding proteins required for pairing-sensitive silencing by a polycomb group response element from the Drosophila engrailed gene. *Genetics* **160**, 1561-1571.
Apidianakis, Y., Grbavec, D., Stifani, S. and Delidakis, C. (2001). Groucho mediates a Ci-independent mechanism of hedgehog repression in the anterior wing pouch. *Development* **128**, 4361-4370.
Bailey, A. M. and Posakony, J. W. (1995). Suppressor of Hairless directly activates transcription of *Enhancer of split* Complex genes in response to Notch receptor activity. *Genes Dev.* **9**, 2609-2622.
Basler, K. and Struhl, G. (1994). Compartment boundaries and the control of *Drosophila* limb pattern by *hedgehog* protein. *Nature* **368**, 208-214.
Bejarano, F. and Milan, M. (2009). Genetic and epigenetic mechanisms regulating hedgehog expression in the Drosophila wing. *Dev. Biol.* **327**, 508-515.
Bejarano, F., Perez, L., Apidianakis, Y., Delidakis, C. and Milan, M. (2007). Hedgehog restricts its expression domain in the Drosophila wing. *EMBO Rep.* **8**, 778-783.
Biehs, B., Kechris, K., Liu, S. and Kornberg, T. B. (2010). Hedgehog targets in the Drosophila embryo and the mechanisms that generate tissue-specific outputs of Hedgehog signaling. *Development* **137**, 3887-3898.
Blanco, E., Messeguer, X., Smith, T. F. and Guigo, R. (2006). Transcription factor map alignment of promoter regions. *PLoS Comput. Biol.* **2**, e49.
Brock, H. W. and van Lohuizen, M. (2001). The Polycomb group-no longer an exclusive club? *Curr. Opin. Genet. Dev.* **11**, 175-181.
Brook, W. J. and Cohen, S. M. (1996). Antagonistic interactions between Wingless and Decapentaplegic responsible for dorsal-ventral pattern in the Drosophila leg. *Science* **273**, 1373-1377.
Busturia, A. and Morata, G. (1988). Ectopic expression of homeotic genes caused by the elimination of the Polycomb gene in Drosophila imaginal epidermis. *Development* **104**, 713-720.
Capdevila, J., Estrada, M. P., Sánchez-Herrero, E. and Guerrero, I. (1994). The *Drosophila* segment polarity gene *patched* interacts with *decapentaplegic* in wing development. *EMBO J.* **13**, 71-82.
Cavalli, G. and Paro, R. (1998). The Drosophila Fab-7 chromosomal element conveys epigenetic inheritance during mitosis and meiosis. *Cell* **93**, 505-518.
Chanas, G. and Maschat, F. (2005). Tissue specificity of hedgehog repression by the Polycomb group during Drosophila melanogaster development. *Mech. Dev.* **122**, 975-987.

Chiang, A., O'Connor, M. B., Paro, R., Simon, J. and Bender, W. (1995). Discrete Polycomb-binding sites in each parasegmental domain of the bithorax complex. *Development* **121**, 1681-1689.
Crickmore, M. A., Ranade, V. and Mann, R. S. (2009). Regulation of Ubx expression by epigenetic enhancer silencing in response to Ubx levels and genetic variation. *PLoS Genet.* **5**, e1000633.
de Celis, J. F. and Ruiz-Gomez, M. (1995). *groucho* and *hedgehog* regulate *engrailed* expression in the anterior compartment of the *Drosophila* wing. *Development* **121**, 3467-3476.
Diederich, R. J., Matsuno, K., Hing, H. and Artavanis-Tsakonas, S. (1994). Cytosolic interaction between deltex and Notch ankyrin repeats implicates deltex in the Notch signalling pathway. *Development* **120**, 473-481.
Eaton, S. and Kornberg, T. (1990). Repression of ci-D in posterior compartments of *Drosophila* by *engrailed*. *Genes Dev.* **4**, 1068-1077.
Estella, C., McKay, D. J. and Mann, R. S. (2008). Molecular integration of wingless, decapentaplegic, and autoregulatory inputs into Distalless during Drosophila leg development. *Dev. Cell* **14**, 86-96.
Felsenfeld, A. L. and Kennison, J. A. (1995). Positional signaling by hedgehog in Drosophila imaginal disc development. *Development* **121**, 1-10.
Fujita, P. A., Rhead, B., Zweig, A. S., Hinrichs, A. S., Karolchik, D., Cline, M. S., Goldman, M., Barber, G. P., Clawson, H., Coelho, A. et al. (2011). The UCSC Genome Browser database: update 2011. *Nucleic Acids Res.* **39**, D876-D882.
Garaulet, D. L., Foronda, D., Calleja, M. and Sanchez-Herrero, E. (2008). Polycomb-dependent Ultrabithorax Hox gene silencing induced by high Ultrabithorax levels in Drosophila. *Development* **135**, 3219-3228.
Gustavson, E., Goldsborough, A. S., Ali, Z. and Kornberg, T. B. (1996). The Drosophila *engrailed* and *invected* genes: partners in regulation, expression and function. *Genetics* **142**, 893-906.
Hagstrom, K., Muller, M. and Schedl, P. (1997). A Polycomb and GAGA dependent silencer adjoins the Fab-7 boundary in the Drosophila bithorax complex. *Genetics* **146**, 1365-1380.
Irvine, K. D. and Vogt, T. F. (1997). Dorsal-ventral signaling in limb development. *Curr. Opin. Cell Biol.* **9**, 867-876.
Kim, J., Irvine, K. D. and Carroll, S. B. (1995). Cell recognition, signal induction and symmetrical gene activation at the dorsal/ventral boundary of the developing Drosophila wing. *Cell* **82**, 795-802.
Kim, J., Sebring, A., Esch, J. J., Kraus, M. E., Vorwerk, K., Magee, J. and Carroll, S. B. (1996). Integration of positional signals and regulation of wing formation by *Drosophila vestigial* gene. *Nature* **382**, 133-138.
Kinzler, K. W. and Vogelstein, B. (1990). The GLI gene encodes a nuclear protein which binds specific sequences in the human genome. *Mol. Cell. Biol.* **10**, 634-642.
Klein, T. (2001). Wing disc development in the fly: the early stages. *Curr. Opin. Genet. Dev.* **11**, 470-475.
Kozma, G., Bender, W. and Sipos, L. (2008). Replacement of a Drosophila Polycomb response element core, and in situ analysis of its DNA motifs. *Mol. Genet. Genomics* **279**, 595-603.
Lecourtois, M. and Schweisguth, F. (1995). The neurogenic Suppressor of Hairless DNA-binding protein mediates the transcriptional activation of the *Enhancer of split* complex genes triggered by Notch signaling. *Genes Dev.* **9**, 2598-2608.
Lee, N., Maurange, C., Ringrose, L. and Paro, R. (2005). Suppression of Polycomb group proteins by JNK signalling induces transdetermination in Drosophila imaginal discs. *Nature* **438**, 234-237.
Levine, M. (2010). Transcriptional enhancers in animal development and evolution. *Curr. Biol.* **20**, R754-R763.
Maeda, R. K. and Karch, F. (2006). The ABC of the BX-C: the bithorax complex explained. *Development* **133**, 1413-1422.
Maurange, C. and Paro, R. (2002). A cellular memory module conveys epigenetic inheritance of hedgehog expression during Drosophila wing imaginal disc development. *Genes Dev.* **16**, 2672-2683.
Méthot, N. and Basler, K. (1999). Hedgehog controls limb development by regulating the activities of distinct transcriptional activator and repressor forms of Cubitus interruptus. *Cell* **96**, 819-831.
Mishra, R. K., Mihaly, J., Barges, S., Spierer, A., Karch, F., Hagstrom, K., Schweinsberg, S. E. and Schedl, P. (2001). The iab-7 polycomb response element maps to a nucleosome-free region of chromatin and requires both GAGA and pleiohomeotic for silencing activity. *Mol. Cell. Biol.* **21**, 1311-1318.
Motzny, C. K. and Holmgren, R. A. (1995). The *Drosophila* cubitus interruptus protein and its role in *wingless* and *hedgehog* signal transduction pathways. *Mech. Dev.* **52**, 137-150.
Muller, J. and Kassis, J. A. (2006). Polycomb response elements and targeting of Polycomb group proteins in Drosophila. *Curr. Opin. Genet. Dev.* **16**, 476-484.
Patel, N. H., Martin-Blanco, E., Coleman, K. G., Poole, S. J., Ellis, M. C., Kornberg, T. B. and Goodman, C. S. (1989). Expression of *engrailed* proteins in arthropods, annelids, and chordates. *Cell* **58**, 955-968.
Piddini, E. and Vincent, J. P. (2009). Interpretation of the wingless gradient requires signaling-induced self-inhibition. *Cell* **136**, 296-307.
Presente, A., Shaw, S., Nye, J. S. and Andres, A. J. (2002). Transgene-mediated RNA interference defines a novel role for notch in chemosensory startle behavior. *Genesis* **34**, 165-169.
Randsholt, N. B., Maschat, F. and Santamaria, P. (2000). polyhomeotic controls engrailed expression and the hedgehog signaling pathway in imaginal discs. *Mech. Dev.* **95**, 89-99.
Ringrose, L., Rehmsmeier, M., Dura, J. M. and Paro, R. (2003). Genome-wide prediction of Polycomb/Trithorax response elements in Drosophila melanogaster. *Dev. Cell* **5**, 759-771.
Schuettengruber, B., Chourrout, D., Vervoort, M., Leblanc, B. and Cavalli, G. (2007). Genome regulation by polycomb and trithorax proteins. *Cell* **128**, 735-745.
Schuettengruber, B., Ganapathi, M., Leblanc, B., Portoso, M., Jaschek, R., Tolhuis, B., van Lohuizen, M., Tanay, A. and Cavalli, G. (2009). Functional anatomy of polycomb and trithorax chromatin landscapes in Drosophila embryos. *PLoS Biol.* **7**, e13.
Schwartz, Y. B. and Pirrotta, V. (2007). Polycomb silencing mechanisms and the management of genomic programmes. *Nat. Rev. Genet.* **8**, 9-22.
Struhl, G. and Basler, K. (1993). Organizing activity of *wingless* protein in Drosophila. *Cell* **72**, 527-540.
Tabata, T., Eaton, S. and Kornberg, T. B. (1992). The *Drosophila hedgehog* gene is expressed specifically in posterior compartment cells and is a target of *engrailed* regulation. *Genes Dev.* **6**, 2635-2645.
Tabata, T., Schwartz, C., Gustavson, E., Ali, Z. and Kornberg, T. B. (1995). Creating a Drosophila wing de novo: the role of *engrailed* and the compartment border hypothesis. *Development* **121**, 3359-3369.
Vegh, M. and Basler, K. (2003). A genetic screen for hedgehog targets involved in the maintenance of the Drosophila anteroposterior compartment boundary. *Genetics* **163**, 1427-1438.
Williams, J. A., Paddock, S. W., Vorwerk, K. and Carroll, S. B. (1994). Organization of wing formation and induction of a wing-patterning gene at the dorsal/ventral compartment boundary. *Nature* **368**, 299-305.
Wu, C. T. and Howe, M. (1995). A genetic analysis of the Suppressor 2 of zeste complex of Drosophila melanogaster. *Genetics* **140**, 139-181.
Xu, T. and Rubin, G. M. (1993). Analysis of genetic mosaics in developing and adult *Drosophila* tissues. *Development* **117**, 1223-1237.